NASA Reference Publication 1405

Second International Microgravity Laboratory (IML–2) Final Report

R.S. Snyder, Compiler

July 1997

NASA Reference Publication 1405

Second International Microgravity Laboratory (IML–2) Final Report

R.S. Snyder, Compiler
Marshall Space Flight Center • MSFC, Alabama

National Aeronautics and Space Administration
Marshall Space Flight Center • MSFC, Alabama 35812

July 1997

CONTENTS

Foreword.....1

IML-2 Configuration.....2

Large Isothermal Furnace (LIF) Highlights.....5

Liquid Phase Sintering in a Microgravity Environment.....6

Mixing of a Melt of a Multicomponent Compound Semiconductor.....8

Effect of Weightlessness on Microstructure and Strength of Ordered TiAl Intermetallic Alloys.....10

Electromagnetic Containerless Processing Facility (TEMPUS) Highlights.....12

Containerless Processing in Space: The TEMPUS Team Results.....13

Bubble, Drop, and Particle Unit (BDPU) Highlights.....20

Bubble Migration, Coalescence, and Interaction with the Solidification Front.....22

Thermocapillary Migration and Interactions of Bubbles and Drops.....24

Bubble Behavior under Low Gravity.....26

Interfacial Phenomena in Multilayered Fluid Systems.....28

Thermocapillary Convection in a Multilayer System.....30

Nucleation, Bubble Growth, Interfacial Phenomena, Evaporation, and Condensation Kinetics.....32

Dynamics of Liquids in Edges and Corners.....34

CONTENTS

Critical Point Facility (CPF) Highlights.....36

Critical Phenomena in SF_6 Observed under Reduced Gravity.....38

Summary of Results from the Adiabatic Fast Equilibration (AFEQ) and Thermal Equilibration Bis (TEQB) Experiments.....40

Density Equilibration Time Scale.....42

Heat Transport and Density Fluctuations in a Critical Fluid.....44

Microgravity Environment and Countermeasures.....46

Space Acceleration Measurement System (SAMS) and Orbital Acceleration Research Experiment (OARE).....48

Quasi-Steady Acceleration Measurement (QSAM).....50

Vibration Isolation Box Experiment System (VIBES) Highlights.....47

Influence of G-Jitter on Convection and Diffusion.....52

Thermally Driven Flow Experiments (TDFU).....54

Advanced Protein Crystallization Facility (APCF) Highlights.....56

The Crystallization of Apocrustacyanin C_1.....60

Crystallization of Collagenase and Photoreaction Center under Microgravity.....62

Crystallization of Rhodopsin in Microgravity.....64

Crystallization of RNA Molecules.....66

Studies of Lysozyme Protein Crystal Perfection from Microgravity Crystallization.....68

Crystallization of Octarellins and Copper Oxalate.....70

Microgravity Effects on Macromolecule and Virus Crystallization.....72

CONTENTS

Advanced Protein Crystallization Facility (APCF) (cont.)

Crystal Growth of Ribonuclease S....76

Crystallization of Ribosomal Particles in Space....78

Crystallization of Bacteriorhodopsin....80

Free Flow Electrophoresis Unit (FFEU) Highlights....82

Applications of Continuous Flow Electrophoresis to Rat Anterior Pituitary Particles (Hymer, Part 1)....84

Feeding Frequency Affects Cultured Rat Pituitary Cells in Low-Gravity (Hymer, Part 2)....86

Separation of a Nematode C. *elagans* Chromosome DNA by FFEU....88

Experiments of Separating Animal Cell Culturing Solution in High Concentration in Microgravity....90

Applied Research on Separation Methods Using Space Electrophoresis (RAMSES) Highlights....92

Purification of Biological Molecules by Continuous-Flow Electrophoresis in a Microgravity Environment....94

Electrohydrodynamic Sample Distortion During Electrophoresis....96

Slow Rotating Centrifuge Microscope (NIZEMI) Materials Science Experiment Highlights.... 93

Convective Stability of Solidification Fronts (Moni)....98

Aquatic Animal Experiment Unit (AAEU) Highlights....100

Mechanism of Vestibular Adaptation of Fish under Microgravity....102

Early Development of a Gravity-Receptor Organ in Microgravity....104

Fertilization and Embryonic Development of Japanese Newt in Space....106

Mating Behavior of the Fish (Medaka) and Development of their Eggs in Space....108

CONTENTS

Biorack (BR) Highlights.....110

Activation Signals of T Lymphocytes in Microgravity (Adhesion).....116

Movements and Interactions of Lymphocytes in Microgravity (Motion).....119

Effect of Microgravity on Cellular Activation in Lymphocytes: Protein Kinase C Signal Transduction (Phorbol) and Cytokine Synthesis (Cytokine).....122

Cell Microenvironment and Membrane Signal Transduction in Microgravity (Signal).....124

Effect of Stirring and Mixing in a Bioreactor Experiment in Microgravity (Bioreactor).....126

Biological Investigations of Animal Multi-Cell Aggregates Reconstituted under Microgravity Conditions (Aggregates).....128

Replication of Cell Growth and Differentiation by Microgravity: Retinoic Acid-Induced Cell Differentiation (Mouse).....130

The Sea Urchin Larva, A Suitable Model for Biomineralization Studies in Space (Urchin).....132

The Effect of Microgravity and Varying Periods of 1-g Exposure on Growth, Mineralization, and Resorption in Isolated Fetal Mouse Long Bones (Bones).....134

Investigation of the Mechanisms Involved in the Effects of Space Microgravity on *Drosophila* Development, Behavior, and Aging (Drosophila).....136

The Role of Gravity in the Establishment of the Dorso-Ventral Axis in the Amphibian Embryo (Eggs).....138

Regulation of Cell Differentiation by Gravity in the Lentil Root (Lentil).....140

Root Orientation, Growth Regulation, Adaptation, and Agravitropic Behavior of Genetically Transformed Roots (Transform).....142

Plant Growth and Random Walk (Random).....144

Dosimetric Mapping in Biorack (Dosimetry).....146

The Influence of Microgravity on Repair of Radiation-Induced DNA Damage in Bacteria and Human Fibroblasts (Repair & Kinetcs).....148

CONTENTS

Slow Rotating Centrifuge Microscope (NIZEMI) Life Sciences Highlights.....151

Gravisensitivity and Gravi(Geo)taxis of the Slime Mold *Physarum polycephalum* (Slime Mold).....154

Influence of Accelerations on the Spatial Orientation of *Loxodes* and *Paramecium* (Loxodes).....156

Gravitaxis in the Flagellate *Euglena gracilis* is Controlled by an Active Gravireceptor (Euglena).....158

Effects of Micro-g on *Aurelia* Ephyra Behavior and Development (Jellyfish).....160

Chara Rhizoids: Studies during a Long Period of Microgravity (Chara).....162

Graviresponse of Cress Roots under Varying Gravitational Forces below Earth Acceleration (1-g) (Cress).....164

Thermoelectric Incubator (TEI) and Cell Culture Kits (CCK) Highlights.....166

Gravity and the Stability of the Differentiated State of Plant Somatic Embryos.....168

Microgravity Effects on the Growth and Function of Rat Normal Osteoblasts.....170

Differentiation of *Dictyostelium discoideum* in Space.....172

Extended Duration Orbiter Medical Project (EDOMP) Highlights.....174

Lower Body Negative Pressure (LBNP): Countermeasure Investigation for Reducing Postflight Orthostatic Intolerance.....176

Airborne Microbiological Contamination.....178

Spinal Changes in Microgravity (SCM) Highlights.....180

Spinal Changes in Microgravity.....182

Performance Assessment Workstation (PAWS) Highlights.....181

Microgravity Effects on Standardized Cognitive Performance Measures.....186

CONTENTS

Real-Time Radiation Monitoring Device (RRMD) Highlights.....188

Measurement of LET Distribution and Dose Equivalent
on Board the Space Shuttle STS-65 (IML-2) (RRMD, Part 1).....189

Effect of Microgravity on DNA Repair of *Deinoccus Radiodurans* (RRMD, Part 2).....191

IML-2 Results Summary.....193

Foreword

This report contains a brief summary of the mission science accomplished aboard the Second International Microgravity Laboratory Mission (IML-2). The IML-2 mission, managed by the National Aeronautics and Space Administration's (NASA's) Marshall Space Flight Center (MSFC) in Huntsville, Alabama, laid the groundwork for broader international partnerships and scientific alliances that are continuing in current global space science endeavors. Five other space agencies joined NASA on this mission: the Canadian Space Agency (CSA), the European Space Agency (ESA), the French Space Agency (CNES), the German Space Agency (DARA), and the National Space Development Agency of Japan (NASDA).Through the mission's global approach to space science, the international partners shared the costs of developing equipment and supporting investigators for the mission. During the mission, hundreds of scientists and engineers from countries represented by theses agencies conducted operations from the MSFC Payload Operations Control Center (POCC), where they coordinated their experiments with colleagues, communicated with the space crew performing experiment operations, and sometimes commanded their experiment equipment.

For IML-2, microgravity and life sciences investigations were completed inside Spacelab, a special laboratory that fits in the Space Shuttle payload bay. The IML-2 mission objective was to conduct microgravity and life sciences investigations that require the unique low-gravity environment created inside an orbiting space laboratory free-falling around Earth. Microgravity science and life sciences are exciting areas of research because discoveries in these fields have the potential to greatly enhance the quality of life on Earth through applications and spin-offs. Spacelab was an ideal laboratory for these experiments because it provided proven support hardware, was staffed by trained crew, and could return samples and data for immediate analysis.

The IML-2 Mission was launched aboard the Space Shuttle *Columbia* (STS-65) on July 8, 1994 at 11:43 a.m. Central Daylight Time from the John F. Kennedy Space Center (KSC). The Shuttle altitude was 160 nautical miles (296 kilometers), the orbital path was circular, and the inclination was 28.5 degrees. A special gravity-gradient attitude enhanced the Spacelab's low-gravity environment. The seven IML-2 crew members were Col. Robert D. Cabana (Commander), Lt. Col. James Donald Halsell, Jr. (Pilot), Lt. Col. Carl E. Walz (Flight Engineer), Richard J. Hieb (Payload Commander), Dr. Leroy Chiao (Mission Specialist), Dr. Donald A. Thomas (Mission Specialist), and Dr. Chiaki Mukai (Payload Specialist). Dr. Jean-Jacques Favier, the Alternate Payload Specialist, worked in the ground control center and helped coordinate activities with the crew in space.

Experiment operations were conducted 24-hours around the clock for 14 days from Spacelab activation at Mission Elapsed Time (MET) 00/04:32 until Spacelab deactivation at 13/21:00 MET. The mission was extended an extra day, which allowed some samples and specimens to be exposed to microgravity for an additional day. The Space Shuttle landed on July 23, 5:39 p.m. CDT, (14/17:56 MET) at KSC and investigators immediately began experiment analysis of samples and data. Some investigators are still continuing to analyze the volumes of data obtained during this successful mission. This report highlights the major findings obtained to date.

Dr. Robert Snyder
IML-2 Mission Scientist

Mr. Lanny Upton
IML-2 Mission Manager

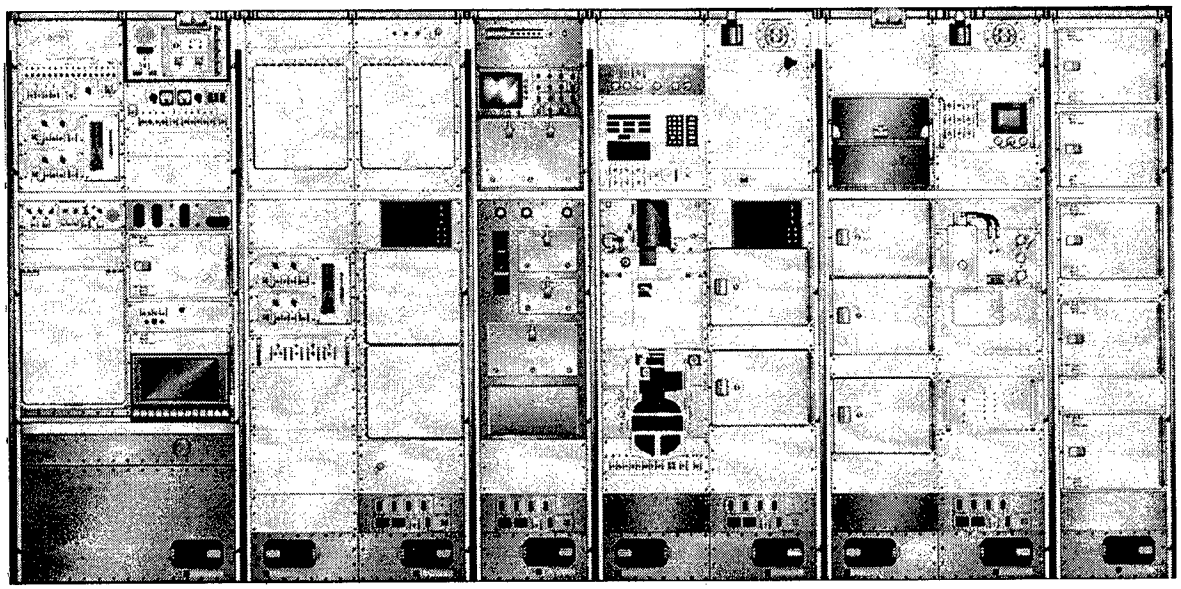

Rack 2 *Rack 4* *Rack 6* *Rack 8* *Rack 10* *Rack 12*

IML-2 CONFIGURATION

The IML-2 mission used a pressurized Spacelab module. Most facilities were mounted in 12 racks in the laboratory module. One experiment facility and other support equipment and samples were in the middeck, which was connected to Spacelab by a tunnel.

Rack 2 Spacelab Control Center

This the computer center was for managing data and for operating laboratory systems and certain experiments. The crew carried out some activities, while computers performed others automatically.

Rack 4 Standard Spacelab Subsystems

This support equipment included a water pump that supported experiments, video recorders that supported payload data, and an experiment heat exchanger.

Rack 6

Applied Research on Separation Methods Using Electrophoresis (RAMSES): This electrophoresis unit used electrical fields to separate biological materials into their individual components and studied the electrophoresis process in low gravity.

Rack 8

Bubble, Drop, and Particle Unit (BDPU): This facility contained special optical diagnostics, cameras, and sensors for studying fluid behavior in microgravity.

Rack 10

Electromagnetic Containerless Processing Facility (TEMPUS): This electromagnetic device positioned metal alloys so that they did not touch container walls and melted samples in an ultra-pure environment.

Rack 12 & 11 Experiment Stowage Racks

Experiment equipment and samples were stored in these racks.

Rack 9

Biostack (BSK): Sealed detectors were used to determine the effects of cosmic radiation on biological samples.

Critical Point Facility (CPF): This temperature-controlled facility supported the investigation of fluids at critical phase transitions from liquids to gases.

Life Sciences Laboratory Equipment (LSLE) Freezer and Biorack Cooler: These facilities freeze and refrigerate perishable samples to preserve them for postflight analysis.

Rack 7

Large Isothermal Furnace (LIF): This furnace melted and uniformly mixed compounds and then solidified the samples.

Slow Rotating Centrifuge Microscope (NIZEMI): A centrifuge with a microscope and macroscope was used to observe the movement and behavior of organisms at various gravity levels and for monitoring the solidification of materials.

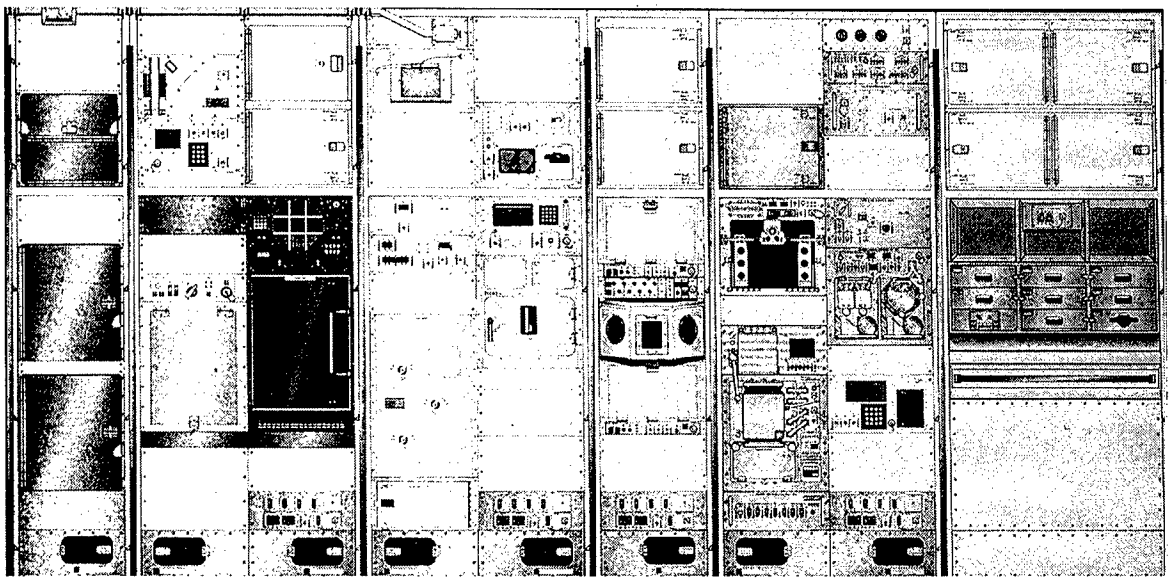

Rack 11 *Rack 9* *Rack 7* *Rack 5* *Rack 3* *Rack 1*

Rack 5

Biorack (BR): This facility supported investigations into the effects of microgravity and cosmic radiation on cells, tissues, plants, bacteria, small animals, and other biological samples. The IML-2 Biorack system contained two incubators and a glovebox.

Rack 3

Vibration Isolation Box Experiment System (VIBES): Experiments were contained in a box made of special materials designed to reduce the effects of accelerations; they measured accelerations caused by crew movements and other equipment operations in Spacelab.

Thermoelectric Incubator (TEI)/Cell Culture Kit (CCK): This general-purpose incubator provided a temperature-and humidity-controlled environment for cultures of mammal and plant cells.

Free Flow Electrophoresis Unit (FFEU): This unit used an electric field to separate a different set of biological samples than RAMSES.

Real-Time Radiation Monitoring Device (RRMD): The instrument actively measured the high-energy cosmic radiation that entered Spacelab on orbit and recorded the radiation's impact on biological materials.

Aquatic Animal Experiment Unit (AAEU): This facility provided life support for newts and fish. Investigators studied spawning, fertilization, embryology, and behavior of these animals in microgravity.

Quasi-Steady Acceleration Measurement (Q-SAM): Four rotating and three stationary sensors measured low-frequency accelerations within Spacelab.

Rack 1 Workbench

In this area, crewmembers recorded data in their logs or carried out general activities. The workbench included stowage containers, tools, and small equipment.

Center Aisle (not shown in illustration)

Space Acceleration Measurement System (SAMS): This electronics package with remote accelerometers was placed in three locations in Spacelab.

Extended Duration Orbiter Medical Project (EDOMP): These investigations were designed to maintain and evaluate crew health and safety on long-duration Shuttle missions.

Spinal Changes in Microgravity (SCM): This study included cameras that recorded stereophotographs of the spine and ultrasound equipment that imaged vertebral spacing and other data related to spinal and neurosensory system changes induced by microgravity.

Middeck (not shown in illustration)

Advanced Protein Crystallization Facility (APCF): This facility provided a temperature-controlled environment for growing a variety of protein crystals using three different processes and a video recording device.

LARGE ISOTHERMAL FURNACE (LIF)

INVESTIGATIONS	PRINCIPAL INVESTIGATORS	RESULTS HIGHLIGHTS
Liquid Phase Sintering in a Microgravity Environment	Dr. R.M. German The Pennsylvania State University, University Park Pennsylvania, United States	Microstructural features were created that have never before been seen in tungsten-heavy alloys. Microgravity had a drastic impact on the samples' microstructural development.
Mixing of a Melt of a Multicomponent Compound Semiconductor	Dr. A. Hirata Waseda University Tokyo, Japan	Samples were successfully processed in microgravity. Space-grown samples of In-Sb were almost spherical. Samples of In-GaSb-Sb were round, not quite spherical.
Effect of Weightlessness on Microstructure and Strength of Ordered TiAl Intermetallic Alloys	Dr. A. Sato National Research Institute for Metals Tokyo, Japan	TiB_2 particles were uniformly distributed in the alloy solidified in microgravity. Microgravity enhanced the uniformity of the microstructure.

Liquid Phase Sintering in a Microgravity Environment

Dr. R.M. German, The Pennsylvania State University, University Park, Pennsylvania, United States

When a density difference exists between the solid and liquid phase in liquid-phase sintering of powdered metal components, several undesirable phenomena occur. First, the solid phase settles to the bottom of the component, leaving a liquid-rich area at the top. This segregation produces anisotropic mechanical properties along the height of the sample. Second, the excess liquid that is present causes non-uniform dimensional changes. This imposes a severe physical barrier on the composition and size of components needed for advanced materials applications.

The objective of this experiment was to obtain fundamental knowledge about the microstructural development of liquid-phase sintered materials. This includes the study of grain growth mechanisms, the role of coalescence in microstructural evolution, the role of volume fraction in a microgravity environment, and the mathematical modeling of these concepts. Tungsten-nickel-iron was selected as the desired alloy system because a significant amount of data has been accumulated on them, they are easy to process, and they have an ideal microstructure that eliminates many second-phase formations that occur in more complex system. These alloys also have important industrial applications such as in armor penetrators, radiation containment, and cladding for corrosive environments.

The alloys are ideal for studying the effects of microgravity because the liquid and solid phases in this system have a density difference of almost 9 g/cm^3. Therefore, any gravitational effects are exaggerated compared to other liquid-phase sintering systems.

Flight Activities

Five different alloy compositions, ranging from 78 wt.% to 98 wt.% tungsten in 5 wt.% increments, with the remainder being nickel and iron in a 7 to 3 ratio, were selected for processing. Each sample, which was a cylinder 10 mm in diameter and 10 mm in height, was placed in a alumina crucible. The crucibles fit inside a cartridge that was loaded in the Large Isothermal Furnace (LIF). During the flight, the samples were sintered for 1, 15, and 120 min at a temperature of 1500 °C. Sensors measured temperature and time.

Highlights

- Microstructural features were created that have never before been seen in tungsten-heavy alloys.
- Microgravity had a drastic impact on the samples' microstructural development.

Postflight Analysis

After the flight, the samples were flown to Japan for removal from the cartridge. Then they were hand carried to our laboratory in the United States. Before destructive evaluation, the samples were extracted, labeled, and photographed, and we measured their physical dimensions to obtain data for developing a mathematical model on densification and shape distortion. The physical density of the samples was obtained using both a helium pycometer and water immersion.

The samples were then taken to NASA's Lewis Research Center in Ohio, where they were readied for metallurgical examination using traditional sectioning, mounting, and polishing techniques. The samples were interference layered so that they could be viewed using traditional bright-field optical microscopy.

Every sample contained microstructural anomalies that had never before been observed in samples sintered under equivalent terrestrial conditions. The frequency and magnitude of these anomalies is larger in samples containing lower volume fractions of tungsten. In the sample consisting of 78 wt.% tungsten that was

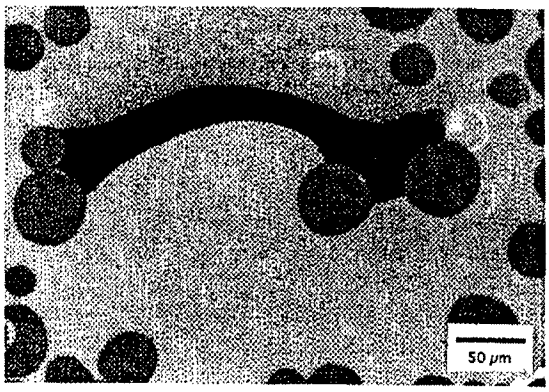

Figure 1: Dog bone-shaped pore

processed for 120 min, the extended sintering time and low-volume fraction of the solid did not causes the solid and liquid phases to segregate as they do when processed on the ground. Under terrestrial conditions, a persistent liquid system would normally sinter to 100% of theoretical density, thereby eliminating all pores. However, because no buoyancy forces exist in microgravity, gas pores are stable and become a discrete phase within the microstructure. The lack of gravity produced anomalous pore morphologies. Micrographs of this sample show pores with distorted shapes that connect to adjacent tungsten grains; liquid also intrudes into the pores.

The sample with 78 wt.% tungsten processed for 1 min had many of the same microstructural anomalies as well as some additional ones. The samples were processed during a time when no forces caused by Shuttle accelerations would affect them. Therefore, it appears that these equilibrium microstructural features are stable in the microgravity environment. The cause of their formation is unknown.

Conclusion

Microgravity had a drastic impact on the microstructural development of the samples. Features were observed that have never been seen before, despite the fact that tungsten-nickel-iron heavy alloys are well characterized metallurgically. New scientific explanations are needed to describe the formation of the anomalies, but specific observations can be made about the microstructures. First, gas-filled pores appear to be a stable, discrete phase in microgravity liquid-phase sintered materials. These pores undergo coalescence as they become very large compared to the scale of the microstructure.

The lack of gravity also produced very unusual pore morphologies (See Figure 1). Pore shape is probably influenced by attachment to tungsten grains. We are in the process of reconstructing the three-dimensional microstructure of these samples. In microgravity, the pores are highly distorted and only spheroidize after long sintering times. There are many unanswered questions. We are dissecting the samples layer by layer and using image analysis equipment to electronically reconstruct the microstructure. We may fly more samples on an upcoming mission to provide information on the effect of surface energy, solid content, etc., on microstructural development in microgravity. More samples will be processed during the Materials Science Laboratory mission scheduled for 1997.

References

German, R.M., "Microstructure of the gravitationally settled region in a liquid phase sintered dilute tungsten heavy alloy," *Metallurgical and Materials Transactions,* vol. 26A, pp. 279-288, (1995).

German, R.M., "Space study of gravitational role in liquid phase sintering," *Industrial Heating,* vol. 62, no. 2, pp. 52-54, (1995).

Raman, R. and German, R.M., "A mathematical model for gravity-induced distortion during liquid phase sintering," *Metallurgical and Materials Transactions,* vol. 26A, pp. 653-659 (1995).

Heaney, D.F., German, R.M., and Ahn, I.S., "The gravitational effects on low solid volume liquid phase sintering," *Journal of Materials Science,* in press.

German, R.M., Iacocca, R.G., Johnson, J.L., Liu, Y., and Upadhyaya, A., "Liquid-phase sintering under microgravity conditions," *Journal of Metals,* vol. 47, no. 8, pp. 46-48 (1995).

Mixing of a Melt of a Multicomponent Compound Semiconductor

Dr. A. Hirata, Waseda University, Tokyo, Japan

With recent developments in the electronics industry, high-quality compound semiconductors are in demand as device materials. Since convection caused by density differences and sedimentation are small in microgravity, it should be possible to create high-quality alloys and compound semiconductors composed of multiple components with different densities, with atomic level uniformity and without any segregation. However, the molecular diffusion rates are so small that it takes a long time for uniform mixing of the melt. Therefore, it is very difficult to obtain high-quality materials with completely uniform mixing compositions in time-limited experiments in microgravity.

One objective of this investigation was to develop a new technique for the uniform mixing of compound semiconductors composed of multiple components of different densities. We used gravity segregation caused by Marangoni convection (interfacial tension-gradient-driven convection) that occurs because of a concentration difference on the free interface of a melt. We wanted to clarify real Marangoni convection induced by a concentration gradient without any gravity convection, to obtain the counter molecular diffusivity of molten compound semiconductors and to compare mixing by Marangoni convection with mixing only by molecular diffusion.

Flight Activities

The samples were divided into 2 groups: M-1, M-2, M-3, and M-3', concerned with Marangoni convection induced by a concentration gradient on the free interface of a melt and D-1 and D-2, which investigated the role of molecular diffusion without a free interface. Marangoni convection is induced by an interfacial tension gradient caused by a temperature and/or concentration gradient at the free interface. In this experiment, the samples were melted under uniform temperature conditions with the Large Isothermal Furnace (LIF).

Highlights

- Samples were successfully processed in microgravity.
- Space-grown samples of In-Sb were almost spherical.
- Samples of In-GaSb-Sb were round, not quite spherical.

The samples had three different compositional ratios. One group was In-Sb, which corresponds to In_1-xGaxSb of X=0 (M-1 and D-1). The other was made of an In-GaSb-Sb sandwich structure to become $In_{0.5}$ $Ga_{0.5}$ Sb (M-3, M-3') and $In_{0.3}$ $Ga_{0.7}$ Sb (M-2 and D-2). The initial size of samples in the M-series was 12.8 mm in diameter and 7.0 mm in length, with a cylindrical configuration. D-series samples were 11.5 mm in diameter; the length was 10.5 mm in D-1 and 18.1 mm in D-2.

Postflight Analysis

We evaluated the shape of the crystal, the size of crystal particulate, and the effect of Marangoni convection and molecular diffusion on the mixing process. Transparent X-ray images were taken from the outside of quartz sample cartridges. The shape of the M-1 sample was almost spherical except for a few areas. Since respective melting points of In and Sb was 156 and 630 °C, these two materials should have completely melted like a ball by approaching 733 °C, the maximum temperature. When the temperature decreased to 525 °C, the In-Sb melt started to solidify from outside the melt ball toward its inside because of the temperature gradient caused by the connective heat transfer. This means that the melt was confined by a solid shell which appeared in the first stage of solidification. Since the density of solid InSb is 5.78 g/cm^3 smaller than 6.32 g/cm^3 of the In-Sb melt, the volume expansion caused by solidification becomes about 1.1 times. An excessive

In-Sb melt in the solid sphere was spouted out, and several solid projections were formed.

The M-2 sample was roughly round although it was not a complete sphere. The Sb side was in a semi-spherical shape of a smaller diameter compared to the In side. The M-3 and M-3' samples were rounder than M-2. As the Ga compositional ratios of M-2 and M-3 are 0.3 and 0.5, respectively, the initial thickness of the GaSb crystal was 4.88 mm in M-2 and 3.50 mm in M-3. Part of the GaSb in M-2 may not have dissolved completely.

The cylindrical crucible determined the shape of the D-1 and D-2 samples. In the D-1 sample, a part of InSb protruded from the crucible because of the solidification expansion. The D-2 sample was confined completely in the BN crucible by using a carbon spring at the end of the sample.

For the space-grown samples, both M-1 and D-1 were mixed uniformly. Diffusion interfered with even mixing in the D-2 sample, while the M-2 space-grown sample was mixed well by convection. The detailed analysis of M-2, M-3, and M-3' are in progress.

Conclusion

Samples composed of In-Sb (M-1, D-1) and In-GaSb-Sb (M-2, M-3, M-3', D-2) were melted and cooled rapidly under 1-g and microgravity. For the In-Sb system, the M-1 sample was almost spherical, and both M-1 and D-1 were mixed because of long dissolution times. On the other hand, for the D-1 samples grown on the ground, In concentration increased downward because of gravity segregation.

For the space-grown In-GaSb-Sb samples, all the M samples became round although they were not completely spherical. The shape of the Sb side was shrunken compared with that of the In side. The concentration distribution of D-2 samples grown in space was not uniform because of diffusion.

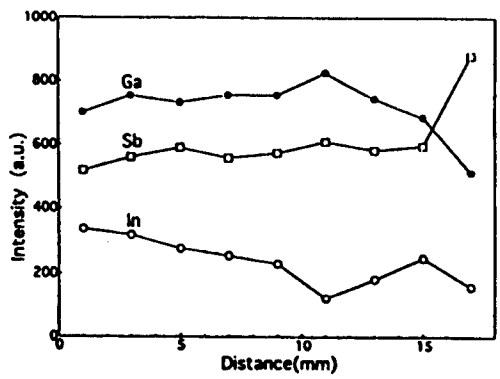

Figure 1: Concentration distribution at the center in the cut surface of the D-2 space-grown sample

Effect of Weightlessness on Microstructure and Strength of Ordered TiAl Intermetallic Alloys

Dr. A. Sato, National Research Institute for Metals, Tokyo, Japan

The intermetallic alloys based on γ-titanium aluminide with an $L1_0$ structure have a high specific strength at high temperatures and good oxidation resistance, so they have potential for use as high-temperature structural components in jet engine turbines. However, the mechanical properties of the alloys are very sensitive to the microstructure, and microstructure control is a key to improving the required properties. Directional solidification as well as single crystallization using the liquid/solid phase transformation are two of the methods to make the alloy stronger at high temperatures. The microstructure control using the solid/solid phase transformation is very important to strengthen the alloys as well, since the alloys are transformed from the hcp α-Ti phase to the ordered face centered tetragonal γ-TiAl phase during cooling.

Another method to further strengthen the alloys is particle dispersive strengthening. On Earth, however, it is not so easy to disperse the particles uniformly within the matrix by conventional metallurgy. Since heat convection is negligibly and it is possible to disperse solid species uniformly in a liquid phase in microgravity, novel microstructures that strengthen the materials may be formed by melting and solidification.

The objectives of this study were to examine the microstructure evolution that occurred during solidification under microgravity in the alloys based on γ-TiAl with and without TiB_2 particles and to understand (1) the effect of thermal convection on crystal grain morphology, (2) the effect of gravity on distribution of ceramic particles, and (3) the role of ceramic particles in liquid/solid and solid/solid phase transformations. The mechanical properties of these alloys were examined and correlated with the microstructure.

Highlights

- TiB_2 particles were uniformly distributed in the alloy solidified in microgravity.
- Microgravity enhanced the uniformity of the microstructure.

Flight Activities

The alloys were the binary Ti-48 at.% Al and one with 5 vol. % of TiB_2 ceramic particles. The density of each binary alloy and the particle itself is approximately 3.8 and 4.5 g/cm^3, respectively. The 18 mm in diameter and 25 mm in length samples were put into the CaO crucible, which was placed in the Large Isothermal Furnace (LIF). The temperature profile was specifically designed to heat up to 1530 °C, which is high enough to melt the binary alloy (T_m : ~ 1480 °C) but below the melting temperature of TiB_2 (T_m : ~ 3000 °C), held there for a few minutes, followed by cooling at 10 °C/min under pressure.

Postflight Analysis

When we compared the macrostructures of these alloys with those of the ground experiment, it was evident that regardless of the level of gravity the binary alloy exhibits a columnar grain structure, whereas the alloy with TiB_2 particles shows an equiaxed grain structure with an average grain size much smaller than that of the binary alloy. There was not much difference in the grain structure of each alloy formed under different gravity, suggesting that heat convection does not greatly influence the nucleation and growth of the primary phase during solidification. Gravity significantly affects the distribution of the shrinkage voids; the microgravity samples have voids in the middle of the sample, whereas normal gravity samples have the voids at the tops of the samples.

The microstructures of the flight samples near the outer surfaces have the columnar grain structures in which the lamellae are clearly visible in the binary alloy. Lamellar grains with an average diameter of 200 μm are observed in

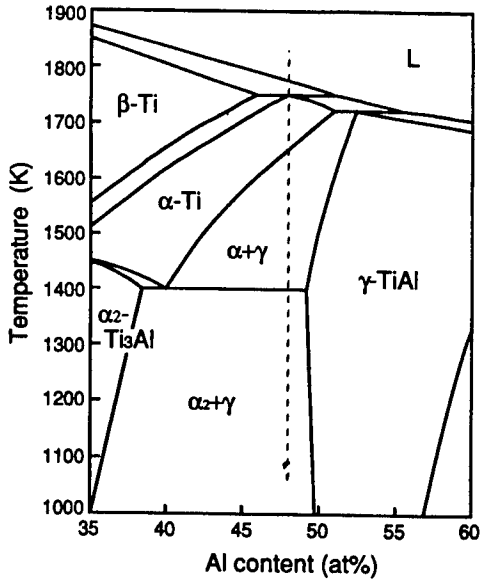

Figure 1: The binary Ti-Al phase diagram near the equiatomic composition (the broken line represents the solidification path of the alloy studied).

the alloy with TiB_2 particles. The particles were agglomerated to each other and made a network at the lamellar grain boundaries. However, unlike the morphology of the sample solidified under normal gravity, no segregated distribution of the particles was observed in the sample solidified in microgravity. The hardness measurements near the bottom edge of the samples revealed not much difference in hardness between the binary samples solidified under different gravity. However, because of the higher density of the particles at the bottom of the samples solidified under normal gravity, the ground samples show higher hardness than the microgravity samples. These results indicate that the microgravity environment makes it possible to distribute the different density particles uniformly within the matrix phase.

The present results demonstrate that the particles act as a nucleation site for the primary phase in solidification in microgravity, since the grain morphology changes from columnar in the binary alloy to equiaxed in the alloy with TiB_2 particles. In addition, the particles could also play an important role in the nucleation site for the precipitation of the solid phase. The lamellar orientation changes where the particles are agglomerated continuously but does not change where they are isolated.

From the present experiments, we found that the most remarkable effect of gravity on the microstructure evolution is the distribution morphology of the particles. Besides this, the microgravity environment does not appear to affect the formation of the microstructures. From a macroscopic viewpoint, this may be right, but as far as the microscopic level is concerned, the microstructure evolution is significantly influenced by the level of gravity. Therefore, the microgravity environment could be useful to produce the columnar-grained materials with particles uniformly distributed within the grains by directional solidification.

	HARDNESS (GPa)	
GRAVITY	TiAl	TiAl/TiB_2
μg	2.31	2.67
1-g	2.25	2.84*

*the hardness value obtained from the bottom of the sample.

Table 1: The hardness value of the alloys with and without TiB_2 particles near the surface of the specimens solidified under both μ-g and 1-g.

Conclusion

Microstructure evolution of the alloys based on TiAl with and without TiB_2 particles during solidification under both microgravity and normal gravity was examined. The binary alloy exhibits a columnar grain structure from the outer surface to the center of the specimen, whereas the alloy with TiB_2 particles shows a large, equiaxed grain structure. The cavities caused by solidification shrinkage are enclosed in the middle of the specimen solidified under microgravity. The TiB_2 particles are uniformly distributed in the alloy solidified under microgravity, whereas they are segregated at the bottom of the specimen under normal gravity. The particles act as nucleation sites of not only the primary β-phase in the liquid phase but also the α-phase precipitation in the β-phase, and the role of the particle in phase transformations is sensitive to its size and distribution morphology.

References

Takeyama, M. and Kikuchi, M., *J. Japan Soc. Heat Treatment*, vol. 34, no. 4, p. 179, (1994).

ELECTROMAGNETIC CONTAINERLESS PROCESSING FACILITY (TEMPUS)

INVESTIGATIONS	PRINCIPAL INVESTIGATORS	RESULTS HIGHLIGHTS
Containerless Processing in Space: The TEMPUS Team Results	Dr. I. Egry DLR, Institute for Space Simulation, Cologne, Germany	First successful attempt to electromagnetically levitate samples in microgravity.
Effect of Nucleation by Containerless Processing	Dr. R. Bayuzick Vanderbilt University, Nashville, Tennessee, United States	Achieved 48 h of levitation time. Melted and heated Zr up to 2000 °C and subsequent under-cooling by $\triangle T = 160$ °C.
Thermodynamic and Glass Formation of Undercooled Metallic Melts	Dr. H. Fecht University of Augsburg Augsburg, Germany	Measured specific heat of NiNb and ZrNi in the undercooled state.
Alloy Undercooling Experiments	Dr. M. Flemings Massachusetts Institute of Technology, Cambridge, Massachusetts, United States	Measured surface tension of Au, AuCu, and ZrNi.
Non-Equilibrium Solidification of Deeply Undercooled Melts	Dr. D.M. Herlach DLR, Institute for Space Simulation, Cologne, Germany	
Thermophysical Properties of Metallic Glasses and Undercooled Alloys	Dr. W. Johnson California Institute of Technology, Pasadena, California, United States	
Measurement of the Viscosity and Surface Tension of Under-cooled Metallic Melts and Supporting MHD Calculations	Dr. J. Szekely Massachusetts Institute of Technology, Cambridge, Massachusetts, United States	
Structure and Solidification of Deeply Undercooled Melts of Quasicrystal-Forming Alloys	Dr. K. Urban Institute for Solid State Physics Research Center, Julich, Germany	

Containerless Processing in Space: The TEMPUS Team Results

Dr. I. Egry, DLR Institute for Space Simulation, Cologne, Germany

Containerless processing provides a pure environment for processing high-temperature, highly reactive materials. It is particularly well suited for acquiring the metastable state of an undercooled melt. In the absence of container walls, the nucleation rate is greatly reduced, and deep undercoolings are possible. Electromagnetic levitation is especially suitable for the study of metallic melts. It allows high temperatures, up to 2600 °C, the levitation of bulk samples of a few grams, and the maintenance of their undercooled state for an extended period, up to hours. When used in 1-g, high electromagnetic fields deform the shape of molten samples and induce turbulent currents inside the sample. The fields are so strong that the samples must be cooled convectively using a high-purity inert gas, like He or Ar. All these drawbacks are avoided if electromagnetic levitation is performed in microgravity.

IML-2 was the first flight of the TEMPUS containerless processing facility. TEMPUS is an electromagnetic levitation facility designed to operate under microgravity conditions. It melts and undercools metallic samples of 8 mm diameter, with no contact to a crucible. Thus, experiments on nucleation statistics, non-equilibrium solidification, and measurements of thermophysical properties are possible.

A team of 8 Principal Investigators (listed in Table 1) from the United States and Germany performed 26 experiments on liquid metals and alloys. The experiments were grouped into 3 classes: nucleation (Bayuzick, Flemings, Herlach, and Urban), specific heat (Fecht and Johnson), and surface tension (Egry and Szekely). Twenty-two samples of different compositions were processed, including pure metals, such as Au, Ni, Zr, and eutectic alloys, such as NiNb and ZrNi. In addition, the solidification of quasicrystal forming alloys (AlCuFe and AlCuCo) was studied. The specific heat and surface tension of a number of samples was measured.

Highlights

- First successful attempt to electromagnetically levitate samples in microgravity.
- Achieved 48 h of levitation time.
- Melted and heated Zr up to 2000 °C and subsequent undercooling by $\Delta T = 160$ °C.
- Measured specific heat of NiNb and ZrNi in the undercooled state.
- Measured surface tension of Au, AuCu, and ZrNi.

Flight Activities

The TEMPUS facility fit in a single Spacelab rack. In microgravity, the fields did not have to produce a lifting force; restoring forces were only required to counteract the effect of the random g-jitter and residual accelerations. TEMPUS provided stable sample positioning against 10^{-2} g, reducing the power absorbed in the sample by a factor of 100, compared to the 1-g case. TEMPUS used a quadrupole field for positioning, which is established by two sets of parallel coils of identical dimensions. An additional heating coil produced a high heating efficiency with only small forces. For the observation of sample behavior, two video cameras recorded images of the top and side of the sample. Both video cameras operated in a high-speed mode, with sampling rates set from 60 Hz to 480 Hz.

A number of pyrometers measured temperature. One major difficulty in the temperature measurement of liquid high temperature melts is their high evaporation rate. Evaporating atoms can contaminate the optical path between pyrometers and targets, leading to erroneous temperature readings. To avoid this, each experiment had its own evaporation shield that was automatically put into place before or during processing. Since evaporation problems might still

Principal Investigator	Experiment Class	Experiment Title
Dr. R. Bayuzick Vanderbilt University, Nashville, Tennessee, United States	A: Nucleation	Effects of Nucleation by Containerless Processing
Dr. I. Egry DLR, Institute for Space Simulation, Cologne, Germany	C: Surface Tension	Viscosity and Surface Tension of Undercooled Metallic Melts
Dr. H. Fecht University of Augsburg, Augsburg, Germany	B: Specific Heat	Thermodynamics and Glass Formation of Undercooled Metallic Melts
Dr. M. Flemings Massachusetts Institute of Technology, Cambridge, Massachusetts, United States	A: Nucleation	Alloy Undercooling Experiments
Dr. D.M. Herlach DLR , Institute for Space Simulation, Cologne, Germany	A: Nucleation	Non-Equilibrium Solidification of Deeply Undercooled Melts
Dr. W. Johnson California Institute of Technology, Pasadena, California, United States	B: Specific Heat	Thermophysical Properties of Metallic Glasses and Undercooled Alloys
Dr. J. Szekely Massachusetts Institute of Technology, Cambridge, Massachusetts, United States	C: Surface Tension	Measurement of the Viscosity and Surface Tension of Undercooled Metallic Melts and Supporting MHD Calculations
Dr. K. Urban Institute for Solid State Physics Research Center, Julich, Germany	A: Nucleation	Structure and Solidification of Deeply Undercooled Melts of Quasicrystal-Forming Alloys

Table 1: TEMPUS Principal Investigators. Experiments are discussed by class.

effect the optical systems (pyrometers and video) and also the levitation coils, investigators prioritized the sequence of experiments based on the evaporation rates of the different samples and the sticking properties of the layers deposited on the coils.

The science teams combined their efforts and resources to maximize the science output of the mission. They shared samples and performed different experiment classes on the same sample. During the mission, this spirit of cooperation became vital to overcome difficulties encountered on the maiden TEMPUS flight. All the samples were heavily contaminated. This was obvious from their appearance on the video pictures: oxide particles or even a closed oxide layer on the surface were clearly visible. Sample stability was also a problem. The radial translation oscillations of the liquid samples had a larger amplitude than anticipated. In addition, all samples were positioned off-center with respect to the center of the sample cage, leaving only a little space for sample excursions

Sample Composition (at%)	Experiment Time (hh:mm)	Experiment Class	Results	Remarks
W	03:08	N/A	calibration	confirmed premission data
$Al_{60}Cu_{34}Fe_6$	01:57	A	hit cage in 4th cycle, 1 melting cycle	microstructural analysis
Au	01:32	C	hit cage in 9th cycle, 6 melting cycles	surface tension and viscosity
$Au_{56}Cu_{44}$	00:15	C	hit cage after 3 cycles	surface tension and viscosity
$Zr_{76}Ni_{24}$	01:53	B	hit cage after 13 cycles	specific heat
$Ni_{79}Si_{21}$	02:01	A	not melted because of heavy rotations	none
$Zr_{76}Ni_{24}$	06:20	B	hit cage after 17 cycles	specific heat
$Ni_{86}Sn_{14}$	00:36	A	4 melting cycles	10 K undercooling, micro-structural study
$Ni_{86}Sn_{14}$	00:22	A	hit cage after 3 cycles	microstructural study
Cu	00:20	C	hit cage in 1st cycle	none
$Zr_{78}Co_{22}$	02:31	B	nominal run	specific heat
$Ni_{60}Nb_{40}$	03:25	B	exceed max. time	specific heat
$Zr_{64}Ni_{36}$	01:37	C	replaced AuCu	specific heat
$Al_{67}Cu_{21}Co_{12}$	01:59	A	hit cage after 6 cycles, 1 melting cycle	microstructural analysis
$Zr_{64}Ni_{36}$	01:37	C	replaced by AuCu	surface tension, viscosity, dynamic nucleation
$Ni_{79}Si_{21}$	03:28	A	2 melting cycles	10 K undercooling, mi-crostructural analysis
$Ni_{60}Nb_{40}$	03:28	B	nominal run	specific heat, 50 °C under-cooling, metastable phase formation
Zr	00:09	A	sample hit cage in solid state	none
$Ni_{79}Si_{21}$	00:10	C	hit cage in 1st cycle	viscosity
$Ni_{81}Sn_{19}$	00:29	A	2 melting cycles	10 K undercooling
$Al_{65}Cu_{25}Co_{10}$	00:42	A	hit cage after 1st cycle	slight undercooling
Zr	00:10	A	sample hit cage after 1st cycle	160 K undercooling, heat fusion
$Ni_{99.4}Cl_{0.6}$	00:52	A	telescience; sample hit cage after 2 cycles; severe contamination	microstructural analysis, growth velocity
$Fe_{75}Ni_{25}$	00:16	A	hit cage 1st cycle	none
Ni	04:33	A and C	2 melting cycles; contamination	none
Total	48:00			

Table 2: TEMPUS experiment sequence as flown during IML-2

to one side of the cage. As the amplitude of these oscillations increased, the sample stuck to the cage and was no longer available for further experiments. Despite these problems, TEMPUS operated for the entire mission, about 200 h. Of course, the planned experiment sequence could not be maintained, and massive replanning was necessary. The experiments performed in the mission are shown in Table 2. The experiments are discussed by classes, rather than by investigation.

Class A: Undercooling Experiments

These experiments were concerned with nucleation and growth phenomena from the undercooled melt. They suffered most severely from the contamination. The impurities served as heterogeneous nucleation sites, and only very small undercoolings could be obtained, with the exception of Zr.

Bayuzick had planned to perform a statistical study on the nucleation behavior of Zr and ZrNi alloy. Unfortunately, only one undercooling cycle could be obtained on Zr. The sample was heated up to 2000 °C and undercooled. No statistical analysis was possible, but some data were collected.

Investigators Herlach and Flemings wanted to measure growth velocities as a function of undercooling and produce metastable solid states by solidification of deeply undercooled metallic melts. NiSn alloys of two different compositions and alloys Fe-Ni, Ni-Si, Ni-C were chosen. None of these samples could be undercooled, and hence no results are available.

Urban's experiments intended to study the undercoolability and solidification behavior of melts of quasicrystal-forming alloys. Experiments were performed on melts of Al-Cu-Fe and Al-Cu-Co. Al-Cu-Fe forms a stable icosahedral quasicrystalline phase (I-phase), and Al-Cu-Co forms a stable decagonal quasicrystal phase (D-phase). During ground-based research, samples of these alloys were successfully undercooled in an electromagnetic levitation facility. The space experiments aimed to investigate the maximum undercoolability of these melts under improved purity conditions. Urban also wanted to study the impact of reduced convection and

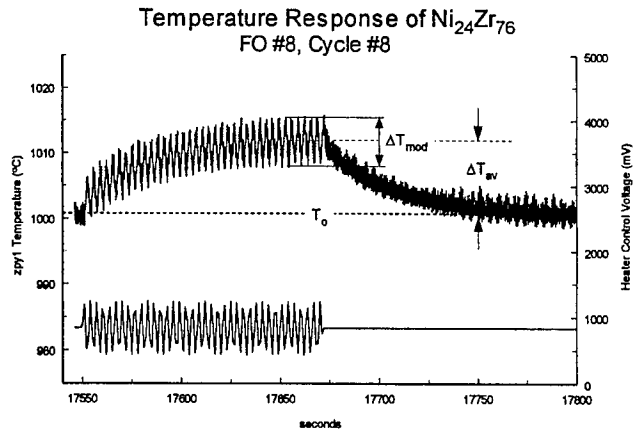

Figure 1: Temperature response (upper curve) of a $Ni_{24}Zr_{76}$ sample to a modulation of the heat input (lower curve)

fluid flow on the microstructure of the solidified samples.

The microstructural analysis of the $Al_{60}Cu_{34}Fe_6$ specimen, which did not significantly undercool in the TEMPUS, showed two different phase selection sequences. The primary solidification of λ-$Al_{13}Fe_4$, which is followed by the formation of the I-phase and several low-temperature phases, was observed. The same phase selection sequences were also observed as the specimen solidified on Earth from a melt that was not significantly undercooled. However, the flight sample showed the primary formation of CsCl-type β-phase again followed by the solidification of the I-phase and several low-temperature phases. On Earth, this phase selection sequence was only observed in Al-Cu-Fe samples with a higher Fe content. This result might be interpreted as a local enrichment of the melt with Fe, which is facilitated by reduced convection and fluid flow during the microgravity experiment.

For the $Al_{65}Cu_{25}Co_{10}$ flight sample, a small undercooling of about 40 K was achieved in TEMPUS. This undercooling was sufficient to obtain the primary formation of D-phase. The formation of the CsCl-type β-phase, which solidifies under equilibrium conditions at the liquidus temperature of the alloy, was bypassed. The primarily solidified D-phase formed large rod-like structures. These rods were surrounded

by several low-temperature phases that formed later during the cooling. Large pores were observed between the rods. The high porosity resulted in an increase of the sample diameter from 8 mm to 9.3 mm after processing. This was the first observation of such a porous morphology, and further investigations are needed to understand the reason for this effect.

Class B: Specific Heat Measurement

The experiments in this class were concerned with the measurement of the specific heat of a number of glass-forming alloys. The method used was developed by Johnson and Fecht. It is a variant of non-contact a.c. calorimetry, normally used in low-temperature physics; this method is applicable in the undercooled state, too. Fecht selected Zr-alloys of eutectic compositions: $Zr_{78}Co_{22}$, $Zr_{64}Ni_{36}$, $Zr_{76}Fe_{24}$. These alloys are good glass-formers, and one objective was to study the anomaly of the specific heat near the glass transition. Because of contamination problems, the undercooling did not approach the glass transition temperature. Nevertheless, the a.c. calorimeter method worked perfectly in the melt, and specific heat data near these alloys' melting points were obtained. The specific heat as a function of temperature was determined (Table 3). The melting enthalpy was determined from the length of the recalescence plateau as $\triangle H_f$ = 14.7 kJ/mol.

T (K)	c_p(J/Kmol)
1485	43.4 ± 2.0
1433	43.5 ± 2.0
1313	43.4 ± 1.5
1284	44.5 ± 1.0
1253	45.7 ± 1.2

Table 3: Fecht's calculations of specific heat of $Zr_{64}Ni_{36}$

Johnson's investigations used the same method, but he selected different alloys: NiNb of eutectic composition and a Zr24Ni-alloy, which is also an eutectic and a good glass former. Table 4 gives the specific heat of this alloy.

T (K)	c_p (J/(K mol))
1160	49.9
1248	46.0
1295	45.2

Table 4: Johnson's calculation of specific heat for $Zr_{76}Ni_{24}$

The experiment with NiNb was particularly successful. It was processed in the molten state for more than 3 h, and an undercooling of

$$\triangle T = 50 \text{ K}$$

was obtained, providing a wealth of specific heat data on this alloy, shown in Table 5. In addition, when the sample finally solidified, it solidified in a metastable phase, the existence of which was presumed but never proven before.

	c_p (J/(K mol))
1466	**48.8**
1477	**47.6**
1498	**47.9**
1527	**47.2**
1559	**47.3**
1606	**47.1**

Table 5: Johnson's calculations of specific heat for $Ni_{60}Nb_{40}$

Class C: Surface Tension and Viscosity

These experiments used the oscillating drop technique to measure surface tension and viscosity. In microgravity, the liquid samples perform oscillations around their spherical equilibrium shape, and a formula of Rayleigh and Kelvin can be used to relate frequency and damping of the oscillations to surface tension and viscosity. On Earth, corrections have to be made for external forces, namely gravity and the electromagnetic field. The corrections have been calculated to be on the order of 5-10% but need experimental verification.

For TEMPUS, experiments on the noble metals Au, Cu, its alloy AuCu, and Ni were planned by

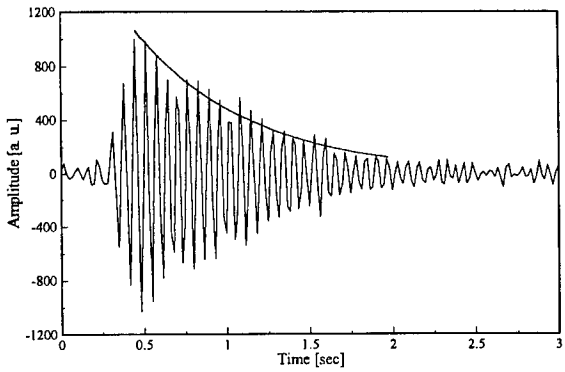

Figure 2: Damped shape oscillations of a $Au_{56}Cu_{44}$ sample.

Egry and Szekely. The experiments on Au and AuCu were performed successfully; no data points could be taken on the copper sample, and nickel was not processed. Instead an additional run was performed on Fecht's ZrNi sample.

For the runs, the heater was turned on for approximately 90 seconds to melt the sample and was run at a minimum value during the cooling phase, which took about 3 min. At the beginning of the cooling phase, a short heating pulse was applied to excite oscillations. Two video cameras recorded the sample oscillations, providing an axial and a radial view. The area of visible cross section is analyzed for each frame, and its variations yields the required time-dependent signal for each oscillation. The new data from IML-2 and from ground-based experiments differ by 5% but show excellent agreement if the latter are corrected for the effect of external forces. The results of the surface tension measurements on IML-2 can be summarized by the following equations:

$$\sigma_{Au}(T°C) = 1.15 - 0.14(T-1064) N/m$$

For $Au_{56}Cu_{44}$, a composition at which this alloy melts congruently, we obtain

$$\sigma_{AuCu}(T°C) = 1.21 - 0.15(T-910) N/m$$

For ZrNi at the eutectic composition $Zr_{36}Ni_{64}$, the result is

$$\sigma_{ZrNi}(T°C) = 1.55 + 0.08 (T - 1010) N/m$$

The experiments on ZrNi yielded an unexpected result: the pulses used to excite the oscillations occurred when there was already a slight undercooling. In each cycle, the appearance of these heating pulses and the onset of nucleation coincide, indicating that the heating pulses may have triggered nucleation. Also, the undercooling with the excitation pulses was reproducibly $\triangle T = 40$ K, whereas during free cooling in the class B experiment on the same sample, an undercooling of $\triangle T = 70$ K was obtained. This phenomenon may be attributed to dynamic nucleation.

We also attempted to determine the viscosity from the damping of the oscillations. After comparing ground and flight data, we concluded that the damping of the oscillations cannot be attributed to viscosity alone, and other damping mechanisms must be present.

Conclusion

After the flight, all the samples were examined for contaminants by Auger, XPS, and electron microscopy. Finding the source and reason for contamination was essential to assuring a successful reflight of TEMPUS in which investigators can obtain data in the deeply undercooled regime.

All samples investigated had foreign particles on the surfaces. These particles included alumina and silica in addition to pieces of many other sample materials loaded in the TEMPUS. Each sample showed evidence of wear tracks on the surface except for those stuck to the cages. All samples had evidence of surface contamination by carbon, oxygen, and in many cases fluorine. Particles of alumina most certainly originated from the sample pedestal. The samples and sample holders were abraded by mutual contact. During transport, launch, and landing this abrasion resulted in particulate material generation. In the TEMPUS facility, these particulates floated around the chamber and resulted in subsequent cross-contamination of all the samples examined.

We conclude that the sample holder and cage system used on IML-2 was the primary cause of

sample contamination. A new sample holder has been designed that not only shields the coils effectively from evaporation but is also free from other contamination problems.

The loss of samples because of stability and alignment in the sample cage was also evaluated. This has been minimized by careful design of the leads and by introducing additional intentional asymmetries that cancel the original ones. The coil design has also been improved by doubling the radial force at the expense of the heating efficiency. By solving these problems, the investigator team is confident that better scientific results, especially in the undercooled regime, will be obtained during a TEMPUS reflight on the Microgravity Science Laboratory mission.

References

Piller, J., Knauf, R., Preu, P., Lohoefer, G., Herlach, D.M., "Electromagnetic positioning and inductive heating under microg-g," *Sixth European Symposium on Materials Sciences and Microgravity Conditions,* Bordeaux, pp. 437-444, (1986).

Lohoefer, G., Neuhaus, P., and Egry, I.,"TEMPUS -- a facility for measuring the thermophysical properties of undercooled liquid metals," *High Temperature - High Pressure*, vol. 23, pp. 333-342, (1991).

Holland-Moritz, D., Herlach, D.M., and Urban, K., "Observation of the Undercoolability of Quasicrystal forming alloys by electromagnetic levitation," *Phys. Rev. Lett.,* vol. 71, pp. 1196-1199, (1993).

Eckler, K. and Herlach, D.M., "Measurements of dendrite growth velocities in undercooled pure Ni-melts: Some new results," *Mat. Sci. Eng.,* vol. A178, p. 5, (1994).

Fecht, H. and Johnson, W., A conceptual approach for non-contact calorimetry in space," *Rev. Sci. Instr.*, vol. 62, pp. 1299-1303, (1991).

Egry, I, Lohoefer, G., Jacobs, G., "Surface Tension Measurements on ground and in space," *Phys. Rev. Letters,* pp. 4043-4046, (1995).

Bratz, A. and Egry, I., "Surface oscillations of electromagnetically levitated viscous metal droplet," *J. Fluid Mech.,* vol. 298, pp. 347-359, (1995).

Schwartz, E., Saerland, S., Szekely, J., and Egry, I., "On the shape of levitated liquid metal droplets in electromagnetic levitation experiments," *Containerless Processing: Techniques and Applications,* Hofmeister, W. and Schifman, R., eds, TMS Warrendale, pp 57-64, (1993).

Chalmers, B., "Dynamic nucleation," in *Liquids: Structure, Properties, Solid Interactions,* Hughes, T., ed., Elevier, pp 308-325, (1965).

Morton, C.W., Hofmeister, W.H., Bayuzick, R.J., and Robinson, M.B., "A statistical approach to understanding nucleation phenomena," *NATO Advanced Workshop on Undercooling,* Il' Ciocco, Italy, June 1993, *Mat. Sci. and Eng.,* vol. A178, (April 1994).

Wu, Y., Piccone, T.J., Shiohara, Y., and Flemings, M.C., "Dendrite growth of an undercooled Nickel-Tin alloy: Part III," *Metall. Trans.,* vol. 19A, pp. 1109-1119, (1988).

BUBBLE, DROP, AND PARTICLE UNIT (BDPU)

INVESTIGATIONS	PRINCIPAL INVESTIGATORS	RESULTS HIGHLIGHTS
Bubble Migration, Coalescence, and Interaction with the Solidification Front	Prof. R. Monti University of Napoli Napoli, Italy Dr. R. Fortezza MARS Center Napoli, Italy	Surfactant strongly affected the migration of bubbles in a liquid matrix formed by melted paraffin, preventing the development of the surface tension gradient. Further investigations need to study the interaction between planar and non-planar fronts with gas bubbles in low-gravity.
Thermocapillary Migration and Interactions of Bubbles and Drops	Dr. R.S. Subramanian Clarkson University Potsdam, New York United States	Confirmed the predictions of models for the migration velocities of bubbles and drops. Made unique observations of interactions between a small and large drop.
Bubble Behavior under Low Gravity	Dr. A. Viviani Seconda Università di Napoli Aversa, Italy	Achieved a milestone in thermocapillary research. First demonstration of thermocapillary migration of bubbles from hot to cold liquids.
Interfacial Phenomena in Multilayered Fluid Systems	Dr. J.N. Koster and Dr. S. Biringen, University of Colorado at Boulder Colorado, United States	Completed ground-based and theoretical research. Obtained a better understanding of the physics of coupling between convecting immiscible liquid layers. Need to verify pure thermocapillary case with flight experiment.

INVESTIGATIONS	PRINCIPAL INVESTIGATORS	RESULTS HIGHLIGHTS
Thermocapillary Convection in a Multilayer System	Dr. J.C. Legros and Dr. Ph. Georis, Universite Libre de Bruxelles, Brussels, Belgium	Built a mechanically stable, three-layer system that could be applicable for encapsulated floating zone crystal growth. Confirmed theoretical and numerical predictions, including that the heat diffusivity ratio of the liquids is the relevant parameter for the description of thermocapillary instability in multilayer systems.
Nucleation, Bubble Growth, Interfacial Phenomena, Evaporation, and Condensation Kinetics	Dr. J. Straub Technical University of Munich Munich, Germany	First measurements of the growth and collapse of bubbles in a homogenous supersaturated and subcooled liquid in microgravity over long periods, up to 300 sec. Determined the evaporation and condensation coefficients: $1{:}10^{-4}$ and $1{:}10^{-3}$ for R11.
Dynamics of Liquids in Edges and Corners	Dr. D. Langbein ZARM, University of Bremen, Bremen, Germany	Data revealed the dependence of the fluid-solid contact angle on temperature. Results posed questions regarding the role of hysteresis in critical-wetting phenomena.

Bubble Migration, Coalescence, and Interaction with the Solidification Front

Prof. R. Monti, University of Napoli, Napoli, Italy, and Dr. R. Fortezza, MARS Center, Napoli, Italy

The objective of this experiment was to investigate the motion of bubbles/drops induced by interfacial tension gradients (Marangoni migration) inside a liquid matrix and their interaction with solidification/melting fronts. The Test Cell was filled with a low-temperature melting material in which some bubbles of different dimensions had been preformed. The material selected was a paraffin wax: tetracosane, with a melting point of Tm=51 °C.

The most important aspects of this experiment are the understanding of the Marangoni migration for drops/bubbles and the study of the interaction between a moving solidification/melting front with bubbles and drops of different diameters. The results obtained from this experiment would have been used to update and to improve the theoretical/numerical models. The characterization of the interaction between the phase change interface and the inclusions is of great importance in all the problems of separation/segregation of materials during the solidification of melt (alloys, crystals, glasses, etc.).

Other experiments on liquid metals were carried out during the previous missions using different materials and gases. Inhomogeneities have been observed in the samples that represent a clear indication of segregation and migration effects during the melting phase, which are studied by this experiment.

Flight Activities

A failure occurred in the Test Container, interrupting the first run. About 30 min after the melting phase, while the tetracosane block was melted for a length of about 1 cm at each side, a leakage was detected at the level of first containment. The scientific team, located in the MARS Telescience Control Room monitored and evaluated the failure and relevant effects. Postflight analysis demonstrated that the problem was caused by an internal compensation pipe exhibiting a loss in the thermal insulation. The heating power was not sufficient to reach the melting point so that a solid material avoided the compensation of the pressure inside the fluid cell that was increased due to solid expansion during melting.

Highlights

- Surfactant strongly affected the migration of bubbles in a liquid matrix formed by melted paraffin, preventing the development of the surface tension gradient.
- Further investigations need to study the interaction between planar and non-planar fronts with gas bubbles in low-gravity.

Thanks to effective team work, it was quickly demonstrated that the failure was not dangerous for the Spacelab or for the BDPU, and some experimental results were achieved during a new experiment run on the following day. Designing the new run was facilitated by the teams remote location in the MARS facility where computer facilities were available to perform simulations to design the new experimental run and the whole science team could work together.

During the first part of the run, the results gained demonstrated a good matching between the experimental results and the real-time on-line numerical code, running in parallel and acquiring directly the boundary conditions from the facility (See Figure 1). This code was based on a finite difference technique and on the enthalpy method; a grid of 30x30x30 points was enough to simulate accurately the temperature distribution of the complete test cell in real time.

The distortion of the thermal field due to heat loss through the sapphire windows was validated by a comparison with previous ground tests. The solid-liquid interface was deformed

according to the simulation, and the investigators knew the thermal field inside the test cell and the temperature gradient at which the bubbles would have been immersed. Finally a good agreement was obtained between the experimental values measured by some thermocouples inserted along the walls of the test cell and the numerical results computed in the correspondent node of the computational domain.

Postflight Analysis

The large leakage during the first run drastically affected the experiment. A large amount of air penetrated into the fluid cell, limiting the observation of bubbles and drops in the liquid matrix; a large area of the front window was covered by solidified tetracosane; therefore the postflight analysis was limited to the observation of some bubbles through the part of the window not affected by the leakage. As planned, the sample was melted and some bubbles were released from the solid tetracosane sample, but no migration was observed despite of the large temperature gradient. Even if not expected, this result showed that thermocapillary migration as calculated in literature (e.g. the Young, Goldstein and Block paper), does not take into account the presence of very small amounts of surfactants. Another important aspect is that the leakage caused some pollution that strongly affected the purity of the liquid matrix, and then the surface tension gradient was reduced. In any case, additional purification processes (zone refining) are required for future experiments to minimize these effects.

The numerous bubbles inside the fluid matrix influenced the study of the interaction between inclusions and the solidification front. Under ideal conditions, small bubbles interacting with a planar solid-liquid front do not disturb the temperature distribution. The large amount of air modified the temperature distribution so that the advancing front was far from the planar shape, hiding bubbles close to the interface and preventing detailed study. Finally, some coalescence phenomena were observed during the run; the results show that these phenomena are very fast in such a viscous liquid (Pr=42), and their analysis requires high-speed cameras, which were not installed on BDPU.

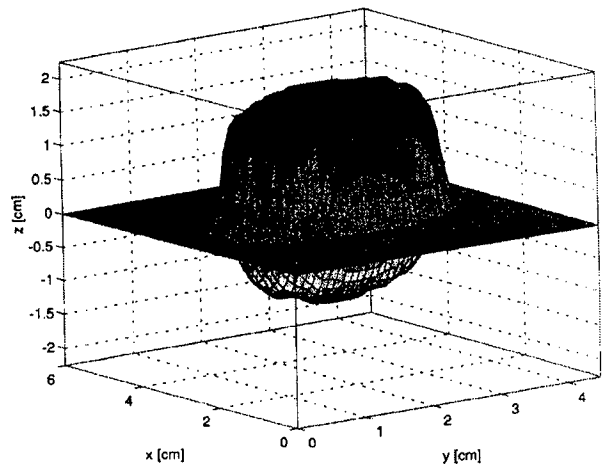

Figure 1: Tetraconsane solid surface

Conclusion

The experiment was affected by a failure in the test container that strongly limited the scientific results. Thanks to the team effort that allowed us to perform another run, some scientific results were obtained. The migration of bubbles in a liquid matrix formed by a melted paraffin is strongly affected by surfactant that prevent the surface tension gradient from being developed. This is a very important point that should be considered in most solidification processes (e.g., shaped casting, weldments, continuous casting, etc.). These processes involve alloys, relatively rich in solute, that are not completely degassified. These alloys in turn, solidify at solidification rates and thermal gradients that cause the interface not to be planar. Therefore, further investigations are strongly required on the interaction between planar and non-planar fronts with gas bubbles in a low-gravity environment.

References

Monti, R., Cavaliere, F., Desiderio, G., Fortezza, R., "INEX-MAN: An Italian facility for an interactive experiment on Marangoni migration," *7th Annual Symposium on Microgravity Science and Space Processing*, (1993).

Monti, R., Castagnolo, D., Cavaliere, F., Desiderio, G., Evangelista, G., Fortezza, R., Sacerdoti, F.M., "User support to AFPM Fluid Science Experiment during the D-2 Mission," *44th Congress of the International Astronautical Federation*, (1993).

Thermocapillary Migration and Interactions of Bubbles and Drops

Dr. R.S. Subramanian, Clarkson University, Potsdam, New York, United States

Thermocapillary migration is important for the processing of materials in reduced gravity aboard spacecraft as well as in separation processes that might be conceived for recycling life-sustaining substances such as water and oxygen in long-duration space excursions. The action of Earth's gravitational field makes it difficult to experimentally study purely thermocapillary migration, so experiments are conducted in space. The objective of this experiment was to measure the speed and shape of isolated gas bubbles and isolated liquid drops in a suitable continuous phase resulting from the action of an applied temperature gradient. A secondary objective was to make similar measurements on interacting pairs of bubbles and pairs of drops.

Flight Activities

Experiments were performed in a Dow-Corning silicone oil of a nominal viscosity of 50 centistokes. The bubbles were air, while the drops were Fluorinert FC-75. The Bubble, Drop, and Particle Unit (BDPU) provided power, optical diagnostics and illumination, imaging facilities, including a video and a motion picture camera, and other support services.

The experiments were carried out in two suitable test cells measuring 45 x 45 x 60 mm that the payload specialist inserted in the BDPU. Subsequently, we controlled the experiment from the ground, sending software commands to operate the experiment and record the video and data that were received on the ground. Our experiment lasted 3 periods between 10 and 12 h each, including setup and planning. We recorded data for about 6 h.

Conceptually, the experiments were simple. Within a test cell filled with liquid and mounted in the facility, a temperature gradient was established, and a bubble or a drop was injected. The subsequent motion of the object was recorded on videotape for later analysis on the ground as well as on cine film on board the Shuttle. When a bubble or drop reached the hot wall, it was extracted and another was injected.

Highlights

- Confirmed the predictions of models for the migration velocities of bubbles and drops.
- Made unique observations of interactions between a small and large drop.

Air bubbles were observed during one time period, and liquid drops were studied during the other two. A total of 22 bubbles and 98 drops were recorded on videotape, and 16 of the bubbles and 65 of the drops on cine film. Both media were analyzed frame by frame for the size and position of the objects.

Postflight Analysis

Data on air bubbles were obtained in two temperature gradients, and data on liquid drops were obtained in four temperature gradients. We observed from the data that the bubbles and drops were spherical to within the uncertainty of the diameter measurements made. From the video recordings, data on the velocities were obtained for the entire traverse of the object from its injection location to the heated wall.

We used the images of the interior of the test cell to obtain data on the migration velocity as a function of size and the applied temperature gradient. The data were converted to scaled form by dividing the velocity by the prediction from a linear model and plotted against the Marangoni number which signifies the relative importance of convective energy transport when compared to conduction. The Reynolds number was less than or equal to 2.2 for the bubble experiments and less than or equal to 0.85 for the drop experiments. Therefore, inertial effects were small.

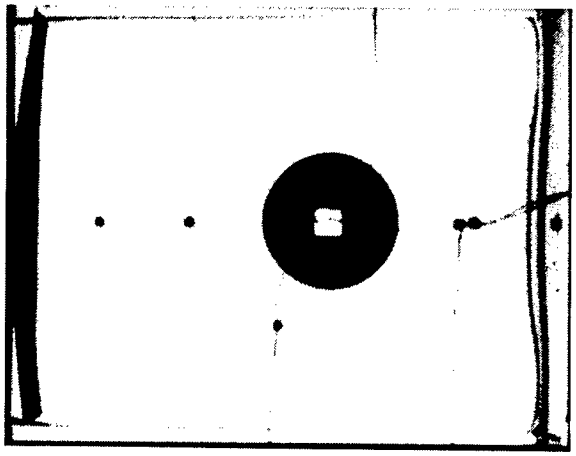

Figure 1: IML-2 investigators gathered data primarily on the motion of single bubbles or drops in a temperature gradient, such as this air bubble in silicone oil. Future investigations will expand this data by providing information on the interactions between pairs of drops and pairs of bubbles.

Predictions are available in the case of gas bubbles, and it was found that the scaled velocity decreases with increasing Marangoni number as expected, even though there were quantitative discrepancies. The scaled velocity also appeared to approach a theoretical asymptote predicted in the limit of large values of the Marangoni number for Stokes motion. Drop data, scaled in a similar manner, were similar to bubble data.

Results from a preliminary experiment on a pair of drops revealed the remarkable feature that a small drop, which leads a large drop in a temperature gradient, can significantly retard the motion of the large, trailing drop while itself moving as though it is virtually unaffected by the presence of the large drop. It is conjectured that this is caused by the long thermal wake behind the leading bubble in which the temperature gradient is weakened. The fluid in the wake wraps around the trailing drop reducing the temperature gradient on its surface, and therefore the driving force for motion.

Conclusion

The results for the migration velocity of air bubbles qualitatively confirm the trend predicted by a theoretical model, but there are quantitative discrepancies. The data for drops display similar trends.

Results on an interacting pair demonstrate the remarkable feature that a small leading drop, which itself appears unaffected in its motion, can significantly influence the motion of a larger trailing drop almost twice its diameter. It is conjectured that this is a consequence of the thermal wake behind the leading drop, but more experiments are needed to confirm this hypothesis.

References

Balasubramaniam, R, Lacy, C.E., Wozniak, G., and Subramanian, R.S., "Thermocapillary migration of bubbles and drops at moderate values of the Marangoni number in reduced gravity," *Physics of Fluids*, vol. 8, no. 4, pp. 872-880, (1996).

Balasubramaniam, R. and Subramanian, R.S., "Thermocapillary bubble migration -- thermal boundary layers for large Marangoni numbers," *Int. J. Multiphase Flow*, vol. 22, no. 3, pp. 593-612, (1996).

Subramanian, R.S., "Motion of drops and bubbles in reduced gravity," *I & E C Res.*, vol. 34, pp. 3411-3416, (1995)

Wei, H. and Subramanian, R.S., "Interactions between a pair of bubbles under isothermal conditions and in the presence of a downward temperature gradient," *Physics of Fluids*, vol. A6., no. 9, pp. 2971-2978, (1994).

Subramanian, R.S., "The motion of bubbles and drops in reduced gravity," *Transport Processes in Bubbles, Drops, and Particles*, Chhabra, R. and De Kee, D., eds., Hemisphere, New York, pp. 1-41, (1992).

Bubble Behavior under Low Gravity

Dr. A. Viviani, Seconda Università di Napoli, Aversa, Italy

This experiment revealed a new kind of thermocapillary migration that was predicted by the investigator. This phenomena was not expected based on prior experiments. The experiment demonstrated that in some saturated aqueous solutions of long-chain alcohols (such as normal heptanol), dependence on the temperature of the surface tension at the interface with air causes bubbles to migrate from the hot side to the cold one, the latter now being the pole of minimum surface tension. This is very relevant to applications of space material sciences since that behavior of the interface tension with respect to the temperature is the same behavior exhibited at high (1000 - 1500 °C) temperatures by a wide class of materials of high technological interest.

Highlights

- Achieved a milestone in thermocapillary research.
- First demonstration of thermocapillary migration of bubbles from hot to cold liquids.

Flight Activities

The diagram of the surface tension versus the temperature of normal heptyl alcohol shows a parabolic behavior with a minimum around 40 °C in the case of thermodynamic equilibrium (i.e., each point of the diagram is obtained by measuring the surface tension at the interface between the solution and air with the solution saturated at the given temperature).

In the experimental configuration, a linear temperature distribution (i.e., a constant thermal gradient) was imposed along the test cell (6 cm in length); this means the liquid, as an isolated system, is not in thermodynamic equilibrium. We discovered that the position of minimum of the surface tension is not at 40 °C. In fact, the bubbles injected did not stop in the corresponding position in the cell; they moved toward the coldest temperature, even though their non-linear velocity of approach to the cold wall seemed to slow down to rest at a temperature around 10 °C. Because the operative temperatures of the cell are in the range of 10-90 °C, the bubble may have stopped around 10 °C. It may have been disturbed by the distortion in the thermal field that occurred near the surrounding wall and/or of the extraction net of the cell. In that zone, the Point Diffraction Interferometer (PDI) images show a disturbance in the imposed thermal gradient, with an unforeseen light gradient in a direction perpendicular to the imposed one.

The deceleration of the bubbles is a fact that demonstrates the non-linear dependence of the surface tension on the temperature; a deeper analysis will try to extrapolate the derivative of the surface tension on the temperature in each point of the cell, starting from the numerical predictions that were performed before the experiment.

The coalescence of more bubbles was observed in the last part of the experiment. A large bubble was injected some seconds later than a smaller one; as predicted by theory, the bigger bubble was faster than the smaller, the former reaching the latter to coalesce after a few instants of touching.

Postflight Analysis

Several thermal gradients were imposed along the cell during the experiment, and for each of them, bubbles of different diameters were injected. A quantitative analysis of bubble speed has to be performed by the integrated use of the Man Machine Interface/House Keeping (MMI/HK) data and the video (interferometer and cine-camera) images.

The velocities of the bubbles will be compared with the numerical predictions, even though the surface tension diagram in the experiment configuration appeared to be different from the theoretical static measurements. For this reason,

an analysis of the experimental liquid will be performed to evaluate the effective saturation of the solution at different temperatures, since a loss of saturation can affect the surface tension diagram in an unpredictable way.

Moreover, because of some imprecision in the injection system, accurate measurements of the real bubble diameters will be performed. Then, by the use of the MMI/HK data in which the exact thermal situation will be acquired, the velocity of each bubble will be related to the relevant influencing parameters.

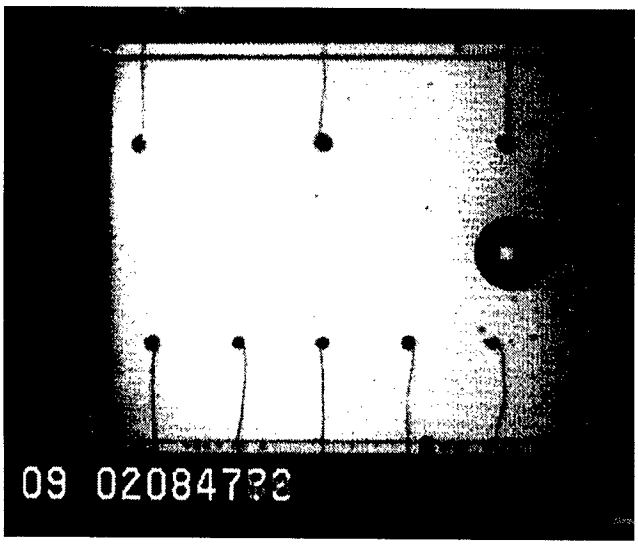

Figure 1: IML-2 investigators gathered data primarily on the motion of single bubbles or drops in a temperature gradient, such as the bubble shown here. This experiment provided new data on the dependence on the temperature of the surface tension at the liquid-bubble interface. It revealed the first evidence for the existence of liquids in which thermocapillary migration of bubbles occurs from a hot liquid toward a colder one.

Conclusion

This experiment is a milestone in the field of thermocapillary (or Marangoni) bubble migration (i.e., the motion of bubbles in a liquid subjected to a thermal gradient because of the dependence on the temperature of the surface tension at the liquid-bubble interface). For the very first time, the existence of liquids in which thermocapillary migration of bubbles occurs from the hot liquid toward the colder one was shown, as opposed to the classical Marangoni migration in which bubbles move from a colder liquid to the hot one.

References

Golia, C., Viviani, A., and Fortezza, R., "Bubbles and drops behavior under low-gravity - A space experiment for the IML-2 mission." *VIIIth European Symp. on Materials and Fluid Sciences in Microgravity,* Bruxelles (Belgium), ESA-SP-333, pp. 211-216, ESA Publications Division, ESTEC, Noordwijk, The Netherlands, (1992).

Golia, C., Viviani, A., and Diurno, W., "Finite elements solution for thermocapillary motion of bubbles at high Reynolds number," *International Congress on Numerical Methods in Engineering and Applied Sciences,* Conception, Chile, (1992).

Viviani, A., Golia, C., and Diurno, W., "Numerical simulation of the IML-2 Italian Experiment on thermocapillary bubbles migration," *44th International Astronautical Federation Congress,* Graz, Austria, Paper No. IAF93-J.3.282, (1993).

Golia, C., Viviani, A., and Cioffi, M., "Thermocapillary bubble migration in confined medium," *45th International Astronautical Federation Congress,* Jerusalem, Israel, Paper No. IAF-94J.5.262, (1994).

Interfacial Phenomena in Multilayered Fluid Systems

Dr. J.N. Koster and Dr. S. Biringen, University of Colorado at Boulder, Colorado, United States

This project dealt with (1) a systematic ground-based study of convective flow in two immiscible liquid layers, with horizontal as well as vertical temperature gradients, (2) a study of pure interface-tension-driven flow in 3 liquid layers separated by 2 parallel interfaces subject to parallel temperature gradients.

The results were expected to significantly advance our knowledge in the areas of surface-tension-driven convection, natural convection, and Rayleigh-Bénard convection (and combinations of these) as applied to multilayered fluid systems. Of particular scientific interest are the coupling mechanisms between adjacent fluid layers and subsequently knowledge of how to control fluid flows in interior liquid layers. These scientific results find direct applications in fields related to encapsulated float zone processing and LEC. Float zone processes are commercial techniques that are used to grow crystals. It is thought that if such processes can be done in space, these processes might result in crystals with relatively fewer imperfections.

Flight Activities

During the opening of the curtains that separated the three immiscible layers, the layers became unstable, and the layered fluid system broke down to form an encapsulated drop.

Postflight Analysis

Since the experiment did not provide valuable data, the postflight analysis was geared toward analysis of the failure. A reflight of an improved test cell was not approved.

Conclusion

The ground-based and theoretical research has been completed and the physics of the coupling between convecting immiscible layers are now better understood. The pure thermocapillary case lacks experimental verification because the IML-2 experiment did not succeed.

Highlights

- Completed ground-based and theoretical research.
- Obtained a better understanding of the physics of coupling between convecting immiscible liquid layers.
- Need to verify pure thermocapillary case with flight experiment.

References

Prakash, A. and Koster, J.N., "Steady natural convection in a two-layer system of immiscible liquids," *Int. J. Heat Mass Transfer,* in press 1997.

Prakash, A. and Koster, J.N., "Steady Rayleigh-Bénard convection in a two-layer system of immiscible liquids," *J. Heat Transfer,* vol. 118, no. 2, pp. 366-373, (1996).

Prakash, A. and Koster, J.N., "Steady thermocapillary convection in a GaAs melt encapsulated by molten B_2O_3," *J. Material Synthesis and Processing,* vol. 4, no. 1, pp. 43-50, (1996).

Koster, J.N. and Nguyen, K.Y., "Steady natural convection in double layer of immiscible liquids with density inversion," *Int. J. Heat Mass Transfer,* vol. 39, pp. 467-478, (1996).

Schmitt, T., Koster J.N., and Hamacher, H., "Particle design for displacement tracking velocimetry," *Measurement Science and Technology,* vol. 6, pp. 682-689, (1995).

Peltier, L.J., Biringen, S., and Farhangnia, M., "Numerical simulation of time-dependent thermocapillary convection in multiple fluid layers," *J. Thermophysics and Heat Transf.,* vol. 9, pp. 702-707, (1995).

Prakash, A., and Koster, J.N., "Convection in multiple layers of immiscible liquids in a shallow cavity - Part I: steady natural convection," *Int. J. Multiphase Flow,* vol. 20, no. 2, pp. 383-396, (1994).

Prakash, A. and Koster, J.N., "Convection in multiple layers of immiscible liquids in a shallow cavity - Part II: Steady thermocapillary convection," *Int. J. Multiphase Flow,* vol. 20, no. 2, pp. 397-414, (1994).

Prakash, A. and Koster, J.N., "Thermocapillary convection in three immiscible liquid layers," *Microgravity Q,* vol. 4, no. 1, pp. 47-54, (1994).

Burkersroda, C.V., Prakash, A., and Koster, J.N., "Interfacial tension between fluorinerts and silicone oils," *Microgravity Q.,* vol. 4, no. 2, pp. 93-99, (1994).

Tong, W. and Koster, J.N., "Penetrative convection in sublayer of water including density inversion," *Wärme-und Stoffübertragung,* vol. 29, pp. 37-49, (1993).

Prakesh, A. and Koster, J.N., "Natural and thermocapillary convection in three layers," *European Journal of Mechanics B/Fluids,* vol. 12, no. 5, pp. 635-655, (1993).

Tong, W. and Koster J.N. "Density inversion effect on transient natural convection in a rectangular enclosure," *Int. J. Heat Mass Transfer,* vol. 37, no. 6, pp. 927-938, (1993).

Tong, W. and Koster, J.N., "Natural convection of water in a rectangular cavity including density inversion," *Int. J. Heat Fluid Flow,* vol. 14, no. 4, pp. 366-375, (1993).

Doi, T. and Koster, J.N., "Thermocapillary convection in two immiscible liquid layers with free surface," *Physics of Fluids A: Fluid Dynamics,* vol. 5, no. 8, pp. 1914-1927, (1993).

Tong, W. and Koster, J.N., "Coupling of natural convection flow across a vertical density inversion interface," *Wärme-und Stoffübertragung,* vol. 28, pp. 471-479, (1993).

Prakesh, A., Fujita, D., and Koster, J.N., "Surface tension and buoyancy effects on a free-free layer," *European Journal of Mechanics B/Fluids,* vol. 12, no. 1, pp. 15-29, (1993).

Fontaine, J.P., Koster, J.N., and Sani, R.L., "Thermocapillary effects in a shallow cavity filled with high Prandtl number fluids," *Ann. Chim. Fr.,* vol. 17, pp. 377-388, (1992).

Thermocapillary Convection in a Multilayer System

Dr. J.C. Legros and Dr. Ph. Georis, Universite Libre de Bruxelles, Brussels, Belgium

We studied the thermocapillary flow arising in a symmetrical three-layer system heated perpendicular to the free interfaces. The objective was to obtain a quantitative description of the thermocapillary instability in a three-layer system to verify the theoretical and numerical models and to derive concrete knowledge of the thermocapillary mechanism at liquid/liquid interfaces. This knowledge can be used for the development of a float zone encapsulation technique for growing improved crystals in microgravity.

Highlights

- Built a mechanically stable, three-layer system that could be applicable for encapsulated floating zone crystal growth.
- Confirmed theoretical and numerical predictions, including that the heat diffusivity ratio of the liquids is the relevant parameter for the description of thermocapillary instability in multilayer systems.

Flight Activities

The symmetrical 3-layer system was made up of 2 layers of Fluorinert FC70, which sandwiched 1 layer of silicone oil 10 cSt. Fluorinert and silicone are almost perfectly immiscible and form an interface that is not sensitive to contamination, qualities that make them ideal for this experiment. The layers were 50 mm wide, 35 mm deep, and 8 mm thick.

On the ground, the layers were separated by two thin stainless steel foils that were retracted during the microgravity experiment (curtain retraction). The mechanical stability of the layers in microgravity relied on a knife edge coated with Teflon on the FC70 side. After curtain retraction, an increasing temperature difference between the two flanges was applied step by step. Steady gradient periods were used for the observation of the convective flow with the light sheet located in different positions.

The three-layer system was inside a test container in the Bubble, Drop, and Particle Unit (BDPU), which supported the experiment. Eight thermistors provided the temperature profile inside the layers and on the cold and the hot flange side. To visualize fluid flow, a laser light plane parallel to the longest side of the layers illuminated the tracer particles in suspension within the liquid. The light plane was translated, allowing the visualization of flow at different locations in the test container. During the phases of transient heating, the light sheet was located 10 mm from the front wall of the test container. During the phases of steady temperature gradients, the light sheet was positioned at 4 mm, 8 mm, and 20 mm from the front wall; this allowed the observation of the three-dimensional structure of the convective flow. The video sequences were sent to the ground in real time for investigators to review or was recorded on board. The video sequences were digitized and analyzed using digital particle image velocimetry software. The analysis provided a 46x22 array of velocity vectors. Typical computation time for 1 vector is less than 10 ms. Some of the images were of poor quality, so the velocity fields were time averaged. Part of the noise in the velocity field may be removed using a low-pass spatial filter.

The total experiment run time was 6 h, which was not long enough to achieve all our objectives because the fluid system could not reach steady thermal conditions at each experiment step. The thermal relaxation time of the system is $\tau=h^2/k \sim 1800$ s. Since at least 4 τ are required to reach a true steady state, the critical temperature gradient cannot be determined accurately in just 6 h. Despite this limitation inherent to most space experiments, valuable data on the mechanical stability and the thermocapillary instability of such systems was obtained.

Postflight Analysis

Ground-based experiments on pure thermocapillary instability in multilayer systems are impossible. Therefore, ground-based research is limited to theoretical and numerical modeling. Space is the only place where these experiments are possible. The linear stability analysis is used to determine the theoretical critical temperature difference for the onset of convection. The space experiment was not long enough to determine the critical temperature difference for the onset of convection. However, transient convection was observed during the thermal overshoot at the beginning of the heating phase. The first organized convective pattern was observed at t~2750 s ($\Delta T \sim 3.8$ °C). There was no video picture for 850 s < t < 2750 s, so convection may have started before t = 2750 s. The convection was clearly driven by the hot interface in agreement with the theoretical prediction. The cold layer was almost at rest, although the cold interface was not immobile. The convective pattern did not reach a steady state, and a true critical point cannot be determined in transient conditions.

Conclusion

This experiment provided the first data on pure thermocapillary instability in a multilayer system. The concept used to build the three-layer system in microgravity proved very efficient. The critical temperature difference has been determined approximately and is compatible with the predictions of the linear stability analysis.

The convective patterns observed during the first stage of the experiment were compared to the ones obtained by two-dimensional simulation. This result is important because it confirms that the physical description of the liquid-liquid thermocapillary convection used in the mathematical modeling is correct. In particular, the interfacial deformation does not seem to play an active role in the thermocapillary instability in multilayer systems in microgravity. For larger temperature differences, the convective pattern becomes strongly three-dimensional and cannot be analyzed. The magnitude of the velocities measured are significantly larger than the values obtained by numerical simulations. Further analysis on enlarged cine camera film sequences will help us understand the reasons for this discrepancy.

A similar experiment was flown on the Life and Microgravity Sciences mission in 1996. This last experiment, which was performed with a different couple of liquids has permitted us to observe oscillatory thermocapillary convection in a multilayer system. These new data will nicely complete the results of the IML-2 mission. Next, we will propose an investigation that uses a configuration similar to one that would be practical for encapsulated crystal growth: a liquid column encapsulated by another one and submitted to radial heat flux.

We would like to acknowledge that this text presents results of the Belgian program on Interuniversity Pole of Attraction initiated by the Belgian State Federal Service of Scientific Technical and Cultural affairs. The Prodex program of ESA has supported the preparation of this microgravity experiment.

References

Martinez, I. and Croll, A., "Liquid bridges and floating zones," *Fluid Physics Lecture Notes of Summer Schools,* Verlarde, M.G. and Christov, C.I., eds, *World Scientific,* (1994).

Dupont, O., Hennenberg, M., and Legros, J.C., "Onset of the non oscillatory Marangoni-Benard Instability under microgravity conditions: experimental and theoretical results," *J. Heat & Mass Transfer,* (1992), vol. 35, 12, pp. 3237-3244, (1992).

Johnson, E.S., "Liquid encapsulated floating zone melting of GaAs," *Journal of Crystal Growth,* p 30, (1975).

Georis, Ph., *Contribution a l'etude des instabilities de Marangoni-Benard et Rayleigh-Benard pour les systemes multicouches*, Phd Thesis, Universite Libre de Bruxelles, (1994).

Georis, Ph., Hennenbeg, M, Simanovskii, I.B., Nepomniaschy, A., Wertgeim, I.I., and Legros, J.C., "Thermocapillary convection in a multilayer system," *Phys. Fluids A,* vol., p. 5, (1993).

Nucleation, Bubble Growth, Interfacial Phenomena, Evaporation, and Condensation Kinetics

Dr. J. Straub, Technical University of Munich, Munich, Germany

The evaporation and condensation process is important for many technical applications in chemical engineering and power conversion. For example, the boiling mechanism, which is governed by the evaporation and condensation process, is an efficient method for heat transfer. A better understanding of these processes is needed for applications in microgravity and in Earth's gravitational field.

To increase our understanding of evaporation and condensation, this experiment focused on bubble dynamics (vapor bubble growth and vapor bubble collapse) in a supersaturated and subcooled liquid with an initial uniform temperature. Microgravity conditions allow the production of large bubbles that are not removed from the location of nucleation by buoyancy forces. Furthermore, the temperature field around the bubble is not disturbed by buoyancy-induced convection. In addition to obtaining data on bubble dynamics, we also wanted to compare experiment results with analytical and numerical models for bubble growth and collapse governed by heat conduction and to apply the kinetic theory for evaporation and condensation and calculate the accommodation coefficients based on this theory.

Flight Activities

The experiment was conducted in the Bubble, Drop, and Particle Unit (BDPU), a multi-user facility for fluid physics experiments in space. The pressure of an isothermal liquid was reduced below the saturation pressure of the liquid to achieve an isothermal supersaturated liquid. The test liquid (Freon R11) was placed inside a test container that fit in the BDPU. A spot heater produced a short heating pulse, which generated bubbles in the liquid. In the absence of gravity, the bubbles remain at the place of nucleation and grow in an undisturbed temperature field.

Highlights

- First measurements of the growth and collapse of bubbles in a homogenous supersaturated and subcooled liquid in microgravity over long periods, up to 300 sec.
- Determined the evaporation and condensation coefficients: $1{:}10^{-4}$ and $1{:}10^{-3}$ for R11.

Eight thermistors placed in the liquid measured temperature. The driving force for bubble growth (evaporation) and bubble shrinkage (condensation) in the supersaturated and subcooled liquid is the temperature difference between the liquid vapor interface and the surrounding liquid. Heat conduction is responsible for the transport of the latent heat needed for evaporation and condensation. The bubble growth rates can be calculated with a numerical model based on the conservation equations for the liquid around the growing vapor bubbles.

We made the first observations of bubble growth over a long period, up to 300 sec. The experiments were performed at 6 different fluid temperatures (30, 40, 50, 60, 70, and 85 °C). At each temperature, we completed 3 to 7 experiment runs at various supersaturation pressures ranging from 50 to 300 mbar, resulting in a total of 32 runs. We observed the runs on real-time video and began analysis with computers. We were able to optimize parameters by sending commands from Earth to the BDPU. We studied the influence of supersaturation on bubble growth and subcooling on bubble collapse, as well as the impact of absolute temperature level.

Postflight Analysis

The data, especially the cine films and video tapes, contain excellent material for the analysis of bubble growth. The quantitative evaluation is being done picture by picture with a digital image processing system. This is very time consuming, so analysis is still in progress.

One interesting phenomenon that we observed during several runs was the coalescence of

vapor bubbles. After coalescence, the resulting vapor bubble oscillates with a certain frequency. New bubbles are generated at the first retraction of the large oscillating vapor bubble.

We calculated the variation of the evaporation and condensation coefficient during bubble growth. The evaporation coefficient is nearly equal to the condensation coefficient. Preliminary results indicated that the coefficients for different vapor bubbles lie between $1{:}10^{-4}$ and $1{:}10^{-3}$. The largest uncertainty is caused by the calculation of the liquid temperature at the bubble surface.

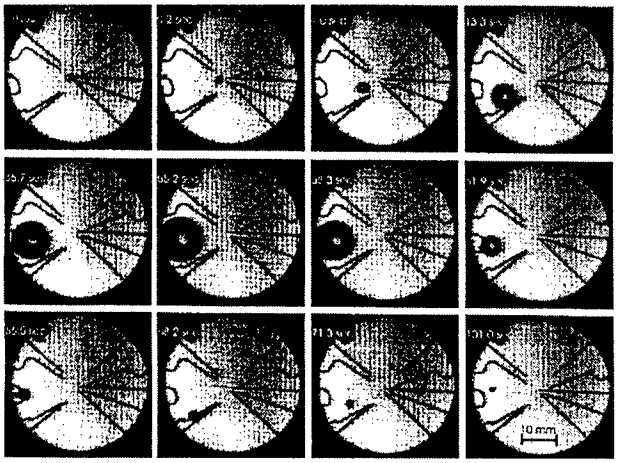

Figure 1: Growing vapor bubble under microgravity, T_l = 29.7 °C, Δp_{sat} = 60 mbar

Conclusion

This series of experiments provided data about the growth and shrinkage of free vapor bubbles in an homogenous supersaturated and subcooled liquid in microgravity. For the first time, the growth and collapse of bubbles was observed over long periods, up to 300 sec. The bubble growth rates in R11 were determined at various liquid temperature levels and supersaturation values.

The measured curves for vapor bubble growth are in good agreement with our numerical simulation. The numerical model for heat-conduction-controlled bubble growth is based on the energy balance. The model takes into account the displacement of the liquid during bubble growth. Using the numerical code, we also calculated the temperature at the bubble interface and the evaporation and condensation coefficients.

The IML-2 data were used to design more experiments that were conducted over an even longer time period on the Life and Microgravity Mission in 1996. These experiments used the refrigerant R123 to study the influence of inert gas on evaporation and condensation kinetics.

References

Straub, J., Picker, G., Steinbichler, M., Winter, J., and Zell, M., "Heat transfer and various modes of bubble dynamics on a small hemispherical heater under microgravity and 1-g condition," *Eurotherm Seminar No. 48: "Pool Boiling,"* Paderborn, Germany, September 1996.

Straub, J., Picker, G., Winter, J., and Zell, M., "Effective cooling of electronic components by boiling phase transition in microgravity," *47th International Astronautical Congress*, Beijing, October 1996.

Straub, J., Winter, J., Picker, G., Zell, M., "Study of vapor bubble growth in supersaturated liquid," *Proc. of the 30th National Heat Transfer Conference*, Portland, Oregon, USA, Sadhal, S.S., *et al.*, eds, vol. 3. New York: ASME, HDT, vol. 305, pp. 29-37, (1995).

Matsumoto, M., Yasuoka, K., Kataoka, Y., "Molecular simulation of evaporation and condensation at the liquid vapor interface," *Proc. 14th Japan Symp. on Thermophysical Properties*, Japan, pp. 143-146, (1993).

Pound, G.M. "Selected Values of Evaporation and Condensation Coefficients for Simple Substances," *J.Phys. Chem. Ref. Data*, vol. 1, no. 1, pp. 135-146, (1972).

Dynamics of Liquids in Edges and Corners

Dr. D. Langbein, ZARM, University of Bremen, Bremen, Germany

In microgravity, the configuration of a fluid interface is dictated solely by the container shape and the fluid-solid contact angle. Thus by a judicious selection of each, one might be able to control the location of the bulk fluid. Such information is valuable for in-space fluid separation processes, liquid fuel/oxygen storage and transport, fluid waste management, passive thermal systems such as heat pipes, and fluids and materials experiment design.

This experiment probed the particular behavior of capillary surfaces in containers of irregular cross section. Temperature control was used to vary the fluid-solid contact angle, a questionable thermodynamic parameter of the system, small changes in which can dramatically influence the configuration, stability, and flow of a capillary surface. A liquid penetrates into a solid wedge if the sum of the fluid-solid contact angle and half the dihedral angle of the wedge is smaller than a right angle (Case 1). If the mentioned sum exceeds a right angle, the liquid instead is pushed out of the wedge (Case 2). Container shapes, test fluid, and temperature ranges were selected for observing both local changes in interface curvature as well as a global change in fluid orientation because of the above critical-wetting phenomenon.

Flight Activities

Four cylindrical vessels of rhombic cross section were fabricated out of fused silica (quartz). The test cells were made as large as the Bubble, Drop, and Particle Unit (BDPU) would allow. This was to minimize the effects of surface roughness, contamination, etc., on the anticipated motion of the free surface. The test fluid was a fused silica index of refraction-matched liquid (code 50350). The interior surfaces of the test cells were coated with FC-724, a surface modifier that was used to establish the desired wetting conditions in the cells.

Highlights

- Data revealed the dependence of the fluid-solid contact angle on temperature.
- Results posed questions regarding the role of hysteresis in critical-wetting phenomena.

The BDPU provided power for heating and fluid transfer, background illumination, temperature measurement, cine camera photography and commanding. The module was inserted into the core of the BDPU. The module was complete with rhombic test cells, onboard fluid reservoirs and fill apparatus for the charging of the test cells, and resistance heaters and temperature probes for thermal control.

During the flight, the cells were partially filled via four independent fill ports. The temperature was then cycled from 20 to 80 °C in increments of 20 °C, requiring approximately 20 to 30 min per incremental increase. Though the originally planned peak temperature was 80 °C, the system temperature was further increased to 95 °C. The cooling steps followed similarly with the surface shapes being recorded on cine film after each step. The change in curvature of the interface from the initial ambient condition to the final ambient condition is most easily observed and is attributable to the effects of contact angle hysteresis. Even in reprint, the interfaces can be clearly distinguished, leaving no need for post-flight image enhancement.

The BDPU and test container operated perfectly from the fill to the photography to the temperature commanding and control. It was actually possible to increase the temperature beyond what was originally planned. The freedom of complete commanding from the ground made operations efficient. The high-quality images from the cine films were readily digitized for postflight analysis.

Postflight Analysis

Analyses were performed for Cases 1 and 2. The former requires solution of the dynamical flow equations while the latter requires geometric considerations in addition to a stability analysis. Both provide valuable insight into the variety of fluid interfacial behavior possible over a wide range of temperatures.

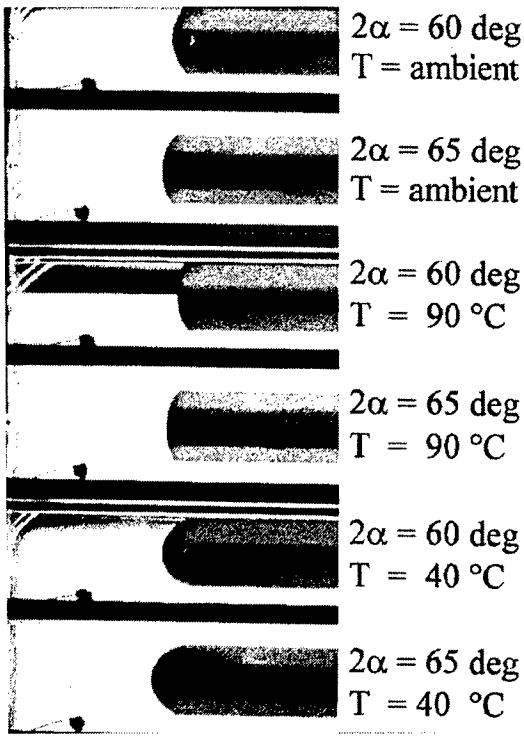

Figure 1: Development of the liquid surface in rhombic prims with dihedral angles 2 α = 60 deg and 65 deg during heating up and cooling down

The surfaces resulting in Case 2 are portions of spherical surfaces. It is this feature of the surfaces achieved on orbit that allowed for their easy characterization. By knowing the radius of curvature of the surfaces from the film records, the angle of intersection of the surface and the wall in the plane of the photographs could be transformed simply to give the contact angle for the particular cell at temperature.

The experiment hardware performed beyond what was expected, and fluid interfaces could be readily digitized postflight to show the dependence of the interface curvature on temperature. For each of the containers, surfaces were observed that did not satisfy the classic equations for the prediction of interface shape (with constant contact angle boundary condition). This is explained by the presence of contact angle hysteresis arising from expansion and contraction of the liquid during the heating and cooling steps of the test procedure. More importantly, surfaces exceeding the critical surface curvature required for critical wetting were measured, yet no wetting was observed. These findings are indeed curious and pose key questions concerning the role of hysteresis for this critical-wetting phenomena.

The stability of such surfaces was determined numerically, and it is shown that stability is enhanced (reduced) when a surface is in its advancing (receding) state. The analysis shows complete instability as the critical wetting condition is reached. The solutions indicate a square root dependence of the capillary rise rate on time, which is corroborated by drop tower tests. The analysis clearly shows that infinite time is necessary for surfaces to reorient at the critical-wetting transition.

Conclusion

Because of its relevance to applications and interest to scientists, research will continue on related topics concerning the behavior of fluid interfaces in containers of irregular geometries. These results and future experiments will provide knowledge about the nature of fluids in partially fluid filled containers possessing interior corners. Since such surfaces arise in many contexts, particularly in space fluids systems, much predictive capability has been added to our fundamental understanding of capillary surfaces and flows.

References

Langbein, D., "Liquid surfaces in polyhedral containers," *Robert Finn Conference Proceedings,* Concus, P. and Lancaster, L., eds., International Press, Cambridge, pp. 168-173, (1994).

Langbein, D., "Liquid surfaces in polyhedral containers," *Microgravity sci. technology*, VIII, pp. 148-154, (1995).

Langbein, D. and Weislogel, M.M., "Capillary driven flows in corners," (in preparation).

CRITICAL POINT FACILITY (CPF)

INVESTIGATIONS	PRINCIPAL INVESTIGATORS	RESULTS HIGHLIGHTS
Critical Phenomena in SF_6 Observed under Reduced Gravity	Dr. D. Beysens Commissariat à l'Energie Atomique, Grenoble, France	First observation that thermalization by Piston Effect is dramatically disturbed by buoyancy-driven convection. First observation of two different regimes of phase separation in the same sample. Measurement of the state variables (P,ρ,T) and the key parameters $(\partial\rho/\partial T)_s$ and $(\partial T/\partial P)_s$.
Summary of Results from the Adiabatic Fast Equilibration (AFEQ) and Thermal Equilibration Bis (TEQB) Experiments	Dr. R.A. Ferrell University of Maryland College Park, Maryland United States	Measured the adiabatic response of fluid to a heat pulse and the late stages of density equilibrium. First measurements of the isothermal increase of the density of a near-critical sample as a function of the applied electric field.

INVESTIGATION	PRINCIPAL INVESTIGATORS	RESULTS HIGHLIGHTS
Density Equilibration Time Scale	Dr. H. Klein DLR , Institute for Space Simulation, Cologne, Germany	The piston effect alone does not lead to short equilibration times. The times necessary for the sample to become homogeneous scale with the correlation length. Balloelectricity and surface tension convection have major influence on bubble and droplet distributions in phase separating fluids.
Heat Transport and Density Fluctuations in a Critical Fluid	Dr. A.C. Michels University of Amsterdam Amsterdam, The Netherlands	Isentropic heating offers a powerful tool for assessing equations of state in the vicinity of the critical point. Evaluation of the density fluctuations obtained by light-scattering measurements is promising.

Critical Phenomena in SF_6 Observed under Reduced Gravity

Dr. D. Beysens, Commissariat à l'Energie Atomique, Grenoble, France

Thermalization of dense, pure fluids classically involves the mechanisms of convection, diffusion, and radiation. Recently, the understanding of thermal equilibration of a pure fluid near its gas-liquid critical point has evidenced a fourth mechanism, the so-called "Piston Effect" (PE). Although it is also present in an ideal gas, it is emphasized near the Critical Point where the compressibility of a fluid diverges. When a homogeneous bulk fluid enclosed in a sample cell is suddenly heated from one wall, a hot, diffusive thermal boundary layer forms at the wall-fluid interface. Due to the high compressibility of the bulk, the fluid layer expands and acts as a piston, generating an acoustic wave that propagates in the bulk and is reflected on the second wall enclosing the fluid. Thermal conversion of this pressure and density rise is, in turn, able to heat the fluid in an adiabatic way.

Another kind of experiments was carried out: *phase transition* experiments, which typically consist in quenching a sample from an initial state (temperature T_i) to another state (temperature T_f) where it is not stable and where the process of phase separation occurs. Such a process is characterized by a pattern of gas and liquid droplets that apparently evolve according to quite complex behavior on Earth. When gravity is suppressed, one expects only two simple growth laws. The goal of the experiment was to observe these two growth laws in the same sample by using different thermal quench depths.

Flight Activities

This experiment in the Critical Point Facility (CPF) studied thermalization plus phase transition kinetics in sulfur hexafluoride (SF_6) near its critical point. A weak acceleration was given by the rotation of the Shuttle during key events. *Thermalization* of off-critical fluids has been studied by using samples of cylindrical shape (11.9 mm diameter, 6.79 mm height) filled with SF_6 at off-critical density $\rho = 1.27\ \rho_c$. Radial walls were made of CuBe, whereas the sample was closed at the bottom and the top by sapphire windows. The sample was mounted in one arm of a Twymann-Green interferometer, with interference fringes that permit the detection and analysis of density variations of the fluid.

Highlights

- First observation that thermalization by Piston Effect is dramatically disturbed by buoyancy-driven convection.
- First observation of two different regimes of phase separation in the same sample.
- Measurement of the state variables (P,ρ,T) and the key parameters $(\partial\rho/\partial T)_s$ and $(\partial T/\partial P)_s$.

Three thermistors recorded the temperature at three different points of the sample. One of them, TH1, was situated in the middle of the sample and could be heated to perform an energy pulse within the fluid. The second thermistor, TH2, was nearly half the distance between the source and the wall, and TH3 was near the sample wall. A pressure transducer was integrated into the sample wall for measurements of pressure variations. During acquisition sequences, temperature measurements were sampled at a frequency of 1 Hz, while pressure was detected at 20 Hz, and video images recorded at 30 Hz.

The first part of this experiment was concerned with the study of the two basic mechanisms of heat transfer in a supercritical fluid under reduced gravity: thermal diffusion and adiabatic compression (Piston Effect). In a second part, the same study was carried out when exposed to micro-accelerations. This study is of interest in view of understanding the storage of propellants in space vehicles and satellites, where fluids are often stored in a supercritical state at large, "liquid-like" densities.

Concerning the *phase separation* experiment, the cell, filled at the precise, slightly off-critical density $\rho = 1.0065\rho_c$ was set in a high-precision thermostat having a temperature stability within 100 μK and a minimum temperature stepping of 0.1 mK. Temperature quenches were performed at a mean rate of 0.2 mK/s. The cell was illuminated by a parallel white light beam. A plane of order 0.1 mm fluid thickness was imaged on a CCD video camera and a photographic camera. Laser light-scattering measurements (turbidity, light scattered at 22° and at 90°) were used to determine the coexistence temperature T_{cx}. We found T_{cx} = 45.53260 °C, with $T_c - T_{cx}$ = 14 μK. Four quenches were performed between 50 μK and 1.66 mK below T_c.

Figure 1: Convection of a hot boundary layer as induced by the Shuttle rotation. Thermalization by Piston Effect is dramatically disturbed.

Postflight Analysis

Thermalization experiment: Temperature measurements at different locations inside the cell volume evidenced the spatially homogeneous PE heating mechanism. Comparison of experimental curves with a numerical simulation permitted recovery of the main features of the heat transfer processes involved. Both calculations of density variations from fringe shift and pressure measurements confirmed the isentropic character of PE heating.

Phase separation experiment: We observed that the cell is not homogenous when the initial temperature T_i of the quench is nearer to the coexistence than 1 mK. The density gradient is due to the heat flow that insures thermal regulation; this minute thermal gradient in the cell induces a density gradient near the coexistence temperature. In spite of the gradient, we observed the 2 expected growth regimes in $t^{1/3}$ and t^1 and estimated to 32% ±6% the value of the crossover volume fraction between the growth laws.

Conclusion

The process of adiabatic heating of compressible fluids (Piston Effect) has been evidenced in SF_6 at off-critical density. The temperature response of the fluid to an internal heat pulse has been recorded at two different points inside the sample. The (spatially) homogeneous temperature rise outside an expanding boundary layer has been confirmed, where the fluid behaves according to a given equation of state. The isentropic character of the PE was confirmed by calculations from both the pressure and density data.

Studies of the behavior of fluids with stratified density under accelerations of order 10^{-2}-g have confirmed the unstable character of those fluids. PE dynamics are strongly suppressed by buoyancy-driven convection.

Phase separation kinetics have been studied in a sample filled at slightly off-critical density. For the first time, two growth laws depending on the temperature quench depth (a slow growth according to time$^{1/3}$ and fast growth whose rate is proportional to time) have been observed in the same sample.

References

Fröhlich,T., Guenoun, P., Bonetti, M., Perrot, F., Beysens, D., Garrabos, Y., Le Neindre, B., and Bravais, P., "Adiabatic versus conductive heat transfer in off-critical SF_6 in absence of convection," *Phys. Rev.*, vol. E54, p. 1544, (1996).

Nikolaev, V.S.,Beysens, D., and Guenoun, P., "New hydrodynamic mechanism for drop coarsening," *Phys. Rev. Lett.*, vol. 76, p. 3144, (1996).

Summary of Results from the Adiabatic Fast Equilibration (AFEQ) and Thermal Equilibration Bis (TEQB) Experiments

Dr. R.A. Ferrell, University of Maryland, College Park, Maryland, United States

The critical point of a fluid marks the endpoint of the liquid-vapor coexistence curve in the pressure-temperature plane and is uniquely characterized by a critical temperature T_c, critical density ρ_c and critical pressure P_c. For SF_6, the critical point occurs at $T_c = 318.59$ K, $P_c = 3.76$ Mpa, and $\rho_c = 0.73$ g/cc. Many of the fluid properties exhibit singular behavior at the critical point. For example, the specific heats at constant volume c_v and constant pressure c_p, the isothermal compressibility K_T, and thermal conductivity are all diverging quantities. Close to T_c, the high compressibility leads to density stratification in Earth's gravitational field. For a fluid such as SF_6, the density stratification becomes significant within 30 mK of T_c.

Flight Activities

The experiments were performed using the Critical Point Facility (CPF) and ran sequentially and successfully for nearly 7 days. In the AFEQ experiment, we studied the effects of electric fields and heat pulses on a SF_6 fluid sample above and below the critical temperature T_c. The TEQB experiment measured the time constant for thermal diffusion above T_c. By performing the experiments in a low-gravity environment, we were able to make measurements and observations which are impossible to do in the presence of Earth's gravity.

Heat was applied to fluid contained in two cells: the AFEQ IF cell and the TEQB IF cell. All sample cells were filled to within 0.3% of the critical density with 99.999% pure SF_6. The sample cells were imaged by a CCD camera and real-time video. Commands from the ground to CPF were used to turn the voltage or current on and off, take high-resolution still photographs, and change the setpoint of the thermostat.

Highlights

- Measured the adiabatic response of fluid to a heat pulse and the late stages of density equilibrium.
- First measurements of the isothermal increase of the density of a near-critical sample as a function of the applied electric field.

At a given setpoint temperature, the long-term temperature stability was better than 0.1 mK. Changes in the fluid density distribution were measured by monitoring changes in the interferometric fringe pattern, which sensed changes in the optical path length.

Postflight Analysis

Our objective was to quantitatively test the theory of fast adiabatic equilibration, using interferometry to measure the fluid response after a "strong" heat pulse (enough heat to raise the reduced temperature of the fluid by 50%). By applying a short-duration-current pulse to the resistance wire in the fluid, we raised the temperature of the fluid relative to the boundaries and then measured the response. We expected to observe an instantaneous fringe shift twice as large in the 2-mm-thick section of the fluid than in the 1-mm-thick section, with the 2 shifts tending toward equality on the scale at the adiabatically sped-up time t_c.

There was not an instantaneous fringe shift that occurred on the same time scale as the duration of the heat pulse. We believe that this was because of strong local heating, which took the fluid near the heating wire far from the critical region. Because of the strong non-linearity near the wire, the AFEQ strong-heat-pulse data does not appear to be amenable to analytic calculations. There may be some interesting physics because of the non-linearity, but more theoretical work is needed.

Electrostriction is the deformation of a fluid or solid in the presence of an electric field. Near a

critical point, the electrostriction effect becomes more pronounced because the isothermal compressibility diverges. To our knowledge, these are the first measurements of electrostriction near a critical point.

The adiabatic response of the fluid to a heat pulse and the late stages of density equilibration were measured. (The measured time constant for thermal diffusion in a 1-mm-thick sample ranged from 200 s to 5,500 s at temperatures ranging from T_c +200 mK down to T_c+3.4 mK and is consistent with pervious light scattering measurements.) We also measured the isothermal increase of the density of a near-critical sample as a function of the applied electric field. In agreement with theory, this electrostriction effect exhibits the same divergence near the critical point as that of the isothermal compressibility. As expected, turning on the electric field in the presence of density gradients can induce flow within the fluid, in a way analogous to turning on gravity. The electric field was generated by applying 500 V to a fine wire passing through the critical fluid. Many observations were made in the two-phase region as we studied the effects of various heat pulses and an electric field on the fluid. Both visual and interferometer images of the sample cells were obtained by means of video downlink.

Conclusion

The electrostriction effect in a near-critical fluid does become more pronounced as the critical point is approached because of diverging compressibility. The increase in density associated with the electrostriction effect near the wire is slow to develop because of the long thermal diffusion times encountered near the critical point. The density increase near the wire has been measured interferometrically and agrees with theory. Many of our observations of electric field effects in the fluid are analogous to a gravitational force directed radially toward the wire.

The time constant for late-stage equilibration has been measured very close to the critical point. We have analyzed our results in terms of a tilt function, which is a sum of normal modes decaying exponentially in time. The measured time constant is in excellent agreement with a semi-empirical expression that is expected to be valid near the critical point. The values inferred for the thermal diffusivity of SF_6 are found to be consistent with light scattering measurements made by others and extend the measured values of D one decade closer to the critical point than previous measurements. (See Figure 1.)

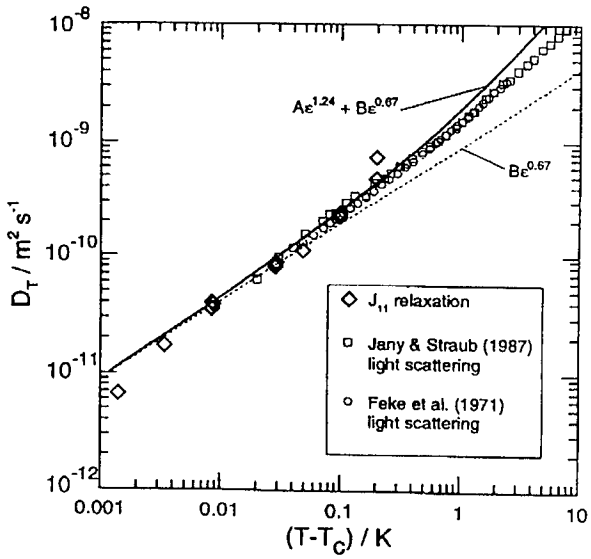

Figure 1: Experimental and calculated values of the thermal diffusivity D_T. The present measurements were derived from the time constants τ_{11} associated with the slowest mode. Within T_c + 100 mK, our measurements are consistent with previous dynamic light scattering determinations of D_T. The measurement at T_c + 1.4 mK is low by a factor of 1.7.

References

Zimmerli, G., Wilkinson, R.A., Hao, H., Ferrell, R.A., Moldover, M.R., "Electric field effects in a near-critical fluid in microgravity," *Proc. of the 30th 1995 National heat Transfer Conference,* vol. 3, ASME, (1995).

Wilkinson, R.A., Zimmerli, G., Hao, H., Ferrell, R.A., Johnson, W.L., and Gammon, R.W., "Late stages of thermal equilibration of a near-critical fluid in microgravity," *Proc. of the 30th 1995 National Heat Transfer Conference,* vol. 3, ASME, p. 127, (1995).

Onuki, A., Hao, H., and Ferrell, R.A., "Fast adiabatic equilibrium in a single-component fluid near the liquid-vapor critical point," *Phys. Rev. A.*, vol. 41, p. 2256, (1990).

Ferrell, R.A. and Hao, H., "Adiabatic temperature changes in a one-component fluid near the liquid-vapor critical point," *Physica A*, vol. 197, p. 23, (1993).

Density Equilibration Time Scale

Dr. H. Klein, DLR, Institute for Space Simulation, Cologne, Germany

Equilibrium in fluids implies that temperature and density are homogeneous throughout. Recent experiments have lead to the hypothesis that in a gas/liquid system, any local change of temperature will propagate very quickly through the system, especially near the critical point. The rational behind this hypothesis is that heating or cooling the sample causes the fluid layer adjacent to the container walls to expand or contract, respectively. The related changes of volume propagate through the sample like sound waves, thereby changing the temperature of the sample by adiabatic heating or cooling, respectively, in a very short time (Piston Effect). This experiment studies the hypothesis that in a near-critical fluid, thermal equilibration is fast and density equilibration is slow.

Flight Activities

Sulfur hexafluoride (SF_6) of critical density was used. Three different temperature/time profiles were applied to generate non-equilibrium states. Laser beam attenuation was used to probe the deviations from the equilibrium states. In the two-phase regime below the critical temperature, the laser beam was bent at the gas/liquid interfaces so that the beam no longer impinged on the detector. Changes of the distribution of the gaseous and liquid phases and changes of the gas/liquid interfaces were observed by video.

The experiment used the Critical Point Facility (CPF), which comprises a high precision thermostat, a device for laser beam attenuation measurements, and an optical image recording unit including video recording. The sample volume was a cylindrical shape, 10 mm in internal diameter and 5 mm in internal thickness. The sample cell was mounted in the CPF thermostat.

Three experimental runs differing in the starting conditions gave insight into the equilibration process in near-critical fluids. Run 1 started with homogeneous density distribution. Temperatures were above the critical. For each of the applied temperature changes during Run 1, an almost immediate response of the laser beam attenuation was observed. This response was larger the closer the sample temperature was to the critical point. This behavior agrees with the Piston Effect. However, thermal equilibrium was not reached completely even during the periods specifically provided for equilibration. Deviations were found between the experimental and the theoretical values of laser beam attenuation.

In Run 2 and Run 3, the equilibration process included both thermal equilibration and mass diffusion. In both runs the sample was brought from a gas/liquid state below the critical temperature to a homogeneous state above the critical temperature. [T_c + 1K in Run 2, T_c + (0.06 $\pm$ 0.04) K in Run 3] Either transition implied the dissolution of macroscopic density inhomogeneities. These inhomogeneities caused strong scattering of the laser beam transmitted through the sample. Consequently, the experimental values of the transmitted laser beam intensity, I/I_o, were small compared with the theoretical values. With homogenization at temperatures above the critical temperature, the value of I/I_o gradually reached the order of magnitude of the respective equilibrium value. The relaxation time of density equilibration was about 1 h in Run 2 and about 5.5 h in Run 3. This finding indicates that density equilibration in fluids is a long-lasting process with relaxation times increasing toward the critical point.

Highlights

- The piston effect alone does not lead to short equilibration times.
- The times necessary for the sample to become homogeneous scale with the correlation length.
- Balloelectricity and surface tension convection have major influence on bubble and droplet distributions in phase separating fluids.

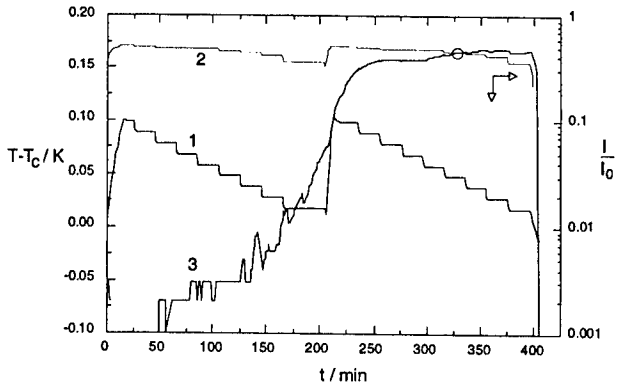

Figure 1: Three curves related to experimental Run 3 (experiment temperatures T, T_c-1K<T<T_c+ O.1K)
Curve 1: Temperature/time profile.
Curve 2: Experimental I/I_0 versus time curve.
Curve 3: Equilibrium I/I_0 versus time curve calculated from equation (3) with the same parameters used in Run 1. Circle indicates point of merging of the experimental and theoretical curve.

Postflight Analysis

The measured and the calculated equilibrium curve of laser beam attenuation versus time differ. The Piston Effect caused an almost immediate response of the sample to any of the applied temperature changes but did not lead to correspondingly short equilibration times.

Equilibration times after heating the sample from the two-phase to the one-phase region suggest scaling properties of the density equilibration time. New experiments are necessary to broaden the experimental basis of this supposition.

Optical observations of the gas/liquid phase transition indicate that the distribution of the gaseous and liquid phase is mainly determined by interfacial effects, e.g., wetting and surface tension convection. Reluctant coalescence of bubbles and droplets is attributed to the balloelectrical effect. Again, equilibration is found to be a process of long duration.

Conclusion

From Run 1, we conclude that within 1 K above the critical temperature, time periods of 16.5 min and 10 min, respectively, are not long enough for the sample to reach equilibrium. We conclude that the Piston Effect alone does not lead to an equilibrium state. Other effects that are yet to be discovered must explain the equilibration process in homogeneous near-critical samples.

From Run 2 and Run 3, we conclude that the relaxation time of density inhomogeneities scales with the correlation length $\xi \sim (T - T_c)^{-\nu}$ with $\nu = 0.63$, similar to the relaxation time caused by thermal diffusivity. From the video observations we conclude that the gas/liquid configuration and its development after cooling from above to below the critical temperature are mainly determined by interfacial effects. These include wetting, surface tension convection, and electrical charging due to balloelectricity.

References

Ikier, C., Klein, H., and Woermann, D., "Optical observation of the gas/liquid phase transition in near-critical SF_6 under reduced gravity," to be published in *J.Colloid Interface Science*, vol. 178, p. 368, (1995).

Ikier, C., Klein, H., and Woermann, D., "Density equilibration in a near-critical fluid under reduced gravity, *Ber. Bunsenges. Phys. Chem.*, vol. 100, p. 1308, (1996).

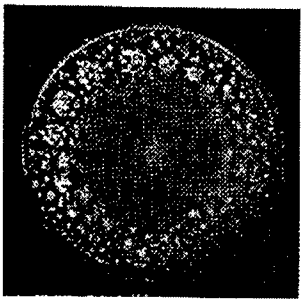

Figure 2: Snapshot during cooling of near-critical SF_6 at reduced gravity, 70 mK below, 10 min after crossing the critical temperature from above. Bubbles appear as bright spots, form clusters, and arrange in a quasi-regular pattern due to interfacial effects. It takes the small bubbles hours to gather in a single large bubble suspended in the co-existing liquid phase.

Heat Transport and Density Fluctuations in a Critical Fluid

Dr. A.C. Michels, University of Amsterdam, Amsterdam, The Netherlands

Near the gas-liquid critical point, fluid systems exhibit a number of very striking features. Of these, perhaps the most prominent is the divergence of the isothermal compressibility, K_T, at the critical point; many of the exciting phenomena that can be observed in critical fluids are directly related to this. The density of a critical fluid becomes drastically sensitive to small disturbances. Microscopically, large density fluctuations occur spontaneously. The occurrence of large density fluctuations causes the phenomenon of critical opalescence, i.e., the strong scattering of light incident on a critical fluid. Light scattering may be used to study critical phenomena in a non-invasive way.

This experiment studies the transfer of heat and density fluctuations inside a critical fluid in the absence of gravity. On Earth, gravity-induced effects, such as convection and density stratification, hamper the measurements of these and other transport properties of critical fluids. Therefore, microgravity conditions sustained over prolonged periods are imperative to examine conclusively the behavior of critical fluids.

Flight Activities

The core of the Critical Point Facility (CPF) is a thermostat into which experiment cells are inserted. The thermostat provides extremely precise temperature stability on the order of 30 μK/h with spatial gradients of less than 10 μK/cm. The CPF is also equipped with optical and electronic interfaces that enable the stimulation and observation of the test fluid.

Our test cell consisted of 2 interconnected cylindrical chambers with a total volume of approximately 6 cm^3. The larger chamber accommodated a mirror that formed a part of an interferometer (IF) system, while the smaller chamber enabled light-scattering (LS) measurements at discrete angles between 22 and 90 degrees [referred to as the wide angle light scattering (WALS)] and continuously over a range of 0 to 30 degrees [small angle light scattering (SALS)], with the 0 angle serving for turbidity measurement. Direct visualization (VIS) of the sample in the smaller chamber was also available.

Highlights

- Isentropic heating offers a powerful tool for assessing equations of state in the vicinity of the critical point.
- Evaluation of the density fluctuations obtained by light-scattering measurements is promising.

Experiments were performed in the temperature range 2500 to 1 mK above the critical point, where simultaneous density and temperature measurements are conducted during a number of transient heating runs. The interferometer was used to determine density changes in the fluid and trace the evolution of boundary layers following heat pulses. Several high sensitivity (μK) temperature sensors (thermistors) were used to measure temperature changes of the test cell, one of which measured the temperature of the bulk of the fluid. Light scattering signals were collected using fiber-optic guides and transmitted to a photomultiplier tube.

The sample was first heated to $T-T_c \sim 2500$ mK (48 °C), and time was allowed for it to become homogeneous. It was then cooled down in steps to 1000, 300, 100, 50 and finally 15 mK above T_c. At T_c + 15 mK, a slow cooling ramp was initialized, ending a few mK below T_c when phase separation was confirmed. The sample was again homogenized at $T-T_c \sim 2500$ mK and cooled down, in steps, to 2000, 1500, and 800 mK above T_c and then, in ramps, to 450, 150, 50, 30, 10, 5, 2, and 1 mK above T_c. Finally, the sample was heated slowly to T_c + 100 mK to check for hysteresis effects.

After each change in temperature, various waiting periods were used in an attempt to obtain, as closely as possible, thermodynamic equilibrium.

The evidence of the IF images shows that equilibrium was never reached but that with specific precautions a steady state could be achieved, i.e., at $T-T_c = 50$ mK after 5 h.

Postflight Analysis

There are three distinct issues addressed in our work: the adiabatic effect, thermal diffusivity, and density fluctuations. An assessment of theoretical work has been made that confirms the profound role of the adiabatic mechanism for the uniform heating of the critical fluid. The experimentally determined adiabatic temperature rise displays a behavior in line with the theoretical predictions, supporting in this way the idea of a crossover region in the adiabatic equilibration time scale, as T_c is approached. Because of the observed adiabatic effect, a new way for assessing thermodynamic properties in the critical region was found, based on the experimental determination of the adiabatic thermal expansion coefficient.

The WALS measurements have been calibrated for stray light and fiber efficiency and show a remarkably high consistency. The discrepancy between theory and experiment close to T_c originates from not incorporating the multiple scattering and attenuation effects. As an initial result, it proves the outstanding performance of the experiment configuration of the WALS. To extract a correlation between K_T and ξ, or even an exact determination of the two with respect to the distance to the critical point, a more thorough investigation including the aforementioned effects is needed. Nevertheless, results look very promising. Unfortunately, the SALS data including turbidity measurements are not suitable for analysis.

Conclusion

In general, the results of our measurements show clearly that diffusive heat transfer slows down dramatically as the critical point is approached and that only a thin boundary layer adjacent to the heater is influenced directly by thermal conduction. Furthermore, a fast thermalization takes place uniformly throughout the sample with essentially no effect on existing temperature and density gradients. Results from analysis of this isentropic compressive heating mechanism are excellent and thereby offer a powerful tool to test experimentally equations of state in the vicinity of the critical point. We are still trying to determine the thermal diffusivity by conducting a detailed study of the fast video images. Also, the preliminary evaluation of the density fluctuations obtained from light scattering measurements is promising.

References

Wakeham, W.A., Trusler, J.P.M., de Bruijn, R., van Diest, R.J.J., and Michels, A.C., "Heat transport near the critical region of a pure fluid in microgravity," in *Proceedings of the Second European Symposium on Fluids in Space,* Naples, Italy, p. 21, (1996).

de Bruijn, R., van Diest, R.J.J., Karapantsios, T.D., Michels, A.C., Wakeham, W.A., and Trusler, J.P.M., "Heat transfer in pure critical fluids surrounded by finitely conducting boundaries in microgravity," submitted to *Physica A,* (1996).

Ferrell, R.A. and Hao, H., "Adiabatic temperature changes in a one-component fluid near the liquid-vapor critical point," *Physica A,* vol. 197, p. 23, (1993).

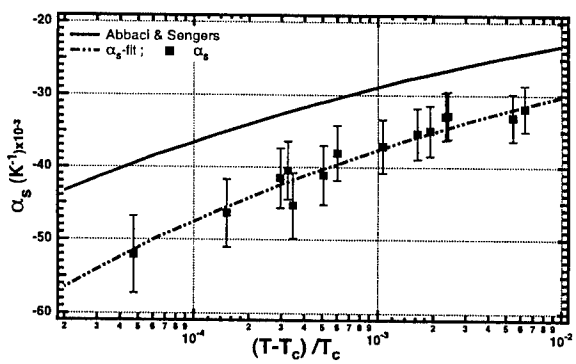

Figures 1 & 2: Comparison between predictions and experiments as regards the adiabatic thermal expansion coefficient (above). Light- scattering intensity at different discrete angles versus reduced temperature compared to theory (below).

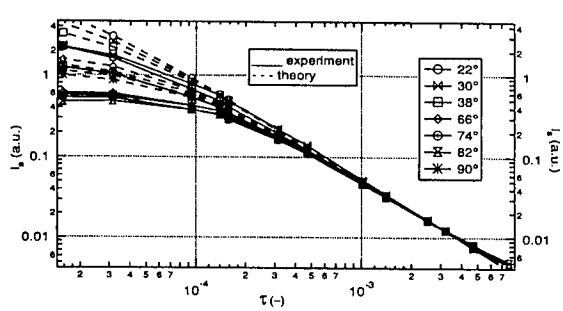

MICROGRAVITY ENVIRONMENT AND COUNTERMEASURES

INVESTIGATIONS	PRINCIPAL INVESTIGATORS	RESULTS HIGHLIGHTS
Space Acceleration Measurement System (SAMS) and Orbital Acceleration Research Experiment (OARE)	Mr. R. DeLombard NASA Lewis Research Center Cleveland, Ohio, United States	Established a network to disseminate microgravity data to investigators. Recorded accelerations that helped investigators analyze their data.
Quasi-Steady Acceleration Measurement (QSAM)	Dr. H. Hamacher DLR, Institute for Space Simulation, Cologne, Germany	Obtained data on accelerations in the g-jitter range. Demonstrated the role of micro-gravity measurement for controlling payload and facility operations.

VIBRATION ISOLATION BOX EXPERIMENT SYSTEM (VIBES)

INVESTIGATIONS	PRINCIPAL INVESTIGATORS	RESULTS HIGHLIGHTS
Influence of G-Jitter on Convection and Diffusion	Dr. H. Azuma National Aerospace Laboratory Chohu-shi, Japan	Observed enhanced diffusion caused by g-jitter. Recorded data indicating that convection caused g-jitter.
Thermally Driven Flow Experiments (TDFU)	Dr. M. Furukawa NASDA Tsukuba Space Center Ibaraki, Japan	Demonstrated a new type of thermal accumulator for two-phase fluid loop systems. Conducted experiments in liquid/vapor phase separation, liquid positioning, and liquid transfer.

Space Acceleration Measurement System (SAMS) and Orbital Acceleration Research Experiment (OARE)

Mr. R. DeLombard, NASA Lewis Research Center, Cleveland, Ohio, United States

Microgravity instruments measured the accelerations and vibrations to which science experiments were exposed. The data were processed and presented to the principal investigators in a variety of formats to aid their assessment of the microgravity environment during their experiment operations. Numerous activities, including crew movements, and equipment operations, are of interest to the low-gravity community. Disturbances which are common to Orbiter missions were also apparent, including the Ku-band antenna dither, orbital maneuvering system and primary reaction control system firings, and attitude changes.

Flight Activities

The OARE and SAMS measured the low-gravity environment. The OARE instrument measures low-level accelerations in the frequency range below 1 Hz down to essentially steady-state. It is mounted near the center of mass of the Orbiter vehicle in the payload bay. The SAMS units have the capability of measuring low-level accelerations from 0.01 Hz up to 100 Hz. The SAMS sensors are mounted in or near the science experiment equipment inside Spacelab.

Postflight Analysis

The seven member crew worked on a dual shift schedule. Because of this schedule, the variation in the microgravity environment between the crew sleep and awake periods that is seen in data from single shift missions is not seen. OARE measured a relatively constant level of disturbance for the extent of the mission in this low-frequency region. When the crew were in the flight deck, SAMS data show the environment is fairly quiet across the frequency range

Highlights

- Established a network to disseminate microgravity data to investigators.
- Recorded accelerations that helped investigators analyze their data.

of interest (100 Hz) compared with a nominal level of crew activity. When a crew member was exercising on the bicycle ergometer, SAMS data show an excitation of 1.2 and 2.4 Hz frequencies. These frequencies correspond to the pedaling and body motion frequencies of the crew member. On MET day 8, experiment operations required a crew member to mix experiment components. In live video of these activities, the crew member both vigorously shook a sample "up and down" and swung the sample around, making full circles with his arm. Investigation of the SAMS data collected during this time indicates clear oscillations in the X_0 (Figure 1) and Z_0 axes. The data suggest about 7 to 8 circles were made in about 10 sec in the XZ-plane. The swinging frequency suggested by the SAMS data correlates well with the recorded video of this event.

The Electromagnetic Containerless Processing Facility (TEMPUS) contained a motor-driven water pump with a rotational speed of about 4800 rpm. This resulted in a strong frequency component at 80 Hz in the SAMS data, Figure 2.

As on prior Spacelab module missions, refrigerator/freezer units were flown to support life sciences experiments. A strong 22.5 Hz signal and upper harmonics of this frequency, Figure 2, are typical of refrigerator/freezer compressor cycling seen before on STS-47. It is believed that this signal is related to the Life Sciences Laboratory Equipment (LSLE) refrigerator/freezer in the Spacelab module.

Conclusion

The data and information about the microgravity environment of IML-2 was acquired for the purpose of disseminating it among the principal

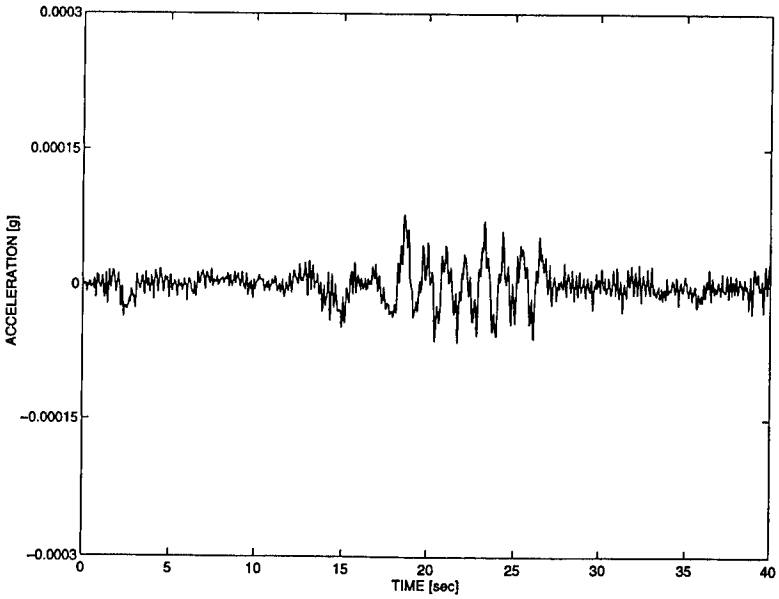

Figure 1: SAMS data reveal oscillations that occurred when a crew member was swinging an experiment sample in circles (X_0 axis).

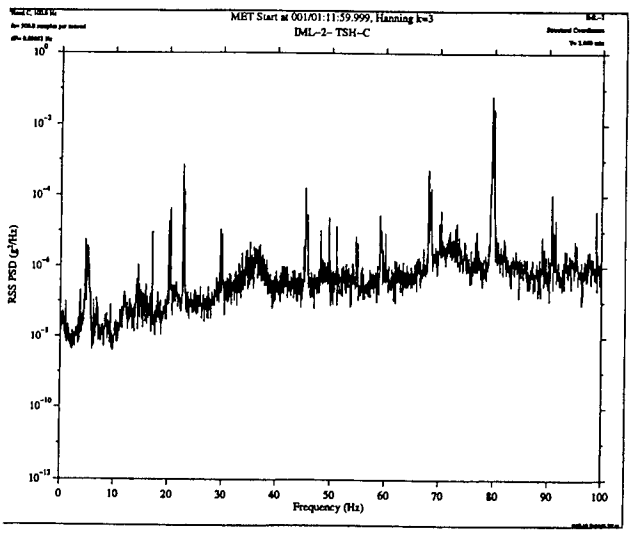

Figure 2: Power spectral density plot showing disturbance frequencies (17, 22.5, 45, 67.5, and 80 Hz.)

investigators and other participants of the mission. Accordingly, CD-ROM's containing the SAMS data have been developed and supplied to the principal investigators. The SAMS and OARE data have also been made available through a network file server which is accessible worldwide. The server address is:

beech.lerc.nasa.gov.

A mission summary report about the microgravity environment was written, published and distributed to the principal investigators. Unique requests from principal investigators have been received and processed, and results have been provided to the principal investigators.

References

Rogers, M. J. B. and DeLombard, R., "Summary report of mission acceleration measurements for STS-65," *NASA Technical Memorandum*, 106871 (1995).

Matisak, B., French, L., Rogers, M.J.B., Destro-Sidik, K., DeLombard, R., and Wagar, W.O., "Results of the quasi-steady acceleration environment from the STS-62 and STS-65 missions," *AIAA95-0691*, (1995).

Quasi-Steady Acceleration Measurement (QSAM)

Dr. H. Hamacher, DLR, Institute for Space Simulation, Cologne, Germany

The residual acceleration of a space laboratory is a perturbation to experiments intended to be executed under weightlessness. Detailed knowledge of microgravity is therefore indispensable for the analysis of the experiment results. Measurements of the residual acceleration are required at various locations in the spacecraft. According to the spectral sensitivity of experiments, frequencies from static (0 Hz) to high-frequency contributions on the order of 100 Hz must be detected. The low-amplitude levels of static and quasi-static accelerations (typically 1 μg and below) require inflight sensor calibration. The Quasi-Steady Acceleration Measurement system (QSAM), is an instrument especially designed to detect acceleration in the entire range between 0 and 50 Hz. Continuous sensor calibration is achieved by signal modulation. The IML-2 mission was the first in-orbit test of QSAM. Data analysis started on the ground during the mission. Postflight analyses concentrated mainly on investigations of characteristic perturbation patterns like those induced by the Life Science Laboratory Equipment (LSLE) refrigerator/freezer and the oscillations of samples in the TEMPUS facility. In addition to the results published, a video was prepared that shows onboard scenes superimposed with synchronized accelerations.

Flight Activities

The QSAM system is designed to detect the low-frequency and g-jitter range. This is achieved by two different types of sensor packages: flipping sensors to detect the low-frequency acceleration and a tri-axial fixed package for the g-jitter range. The flipping sensors detect the components between 0 Hz and 0.02 Hz. Continuous suppression of bias and noise is accomplished by signal modulation as the result of flipping. The g-jitter is detected by conventional fixed sensors.

Highlights

- Obtained data on accelerations in the g-jitter range.
- Demonstrated the role of microgravity measurement for controlling payload and facility operations.

Postflight Analysis

Strong periodic disturbing phases were noticed during the entire mission and occurred about two times per hour. It turned out that the source was a freezer in the Life Science Laboratory Equipment (LSLE) located on the QSAM side of the aisle. The contour plot of the power density spectrum indicates a pronounced excitation of 22 Hz and 44 Hz, which is the fundamental frequency of the QSAM Rack and the first harmonic, respectively. There was no way to reduce the disturbance level. But QSAM inflight measurements allowed the prediction of on/off times of the LSLE, which helped to optimize the experiment operation in some cases.

Experiments of the Electromagnetic Containerless Processing Facility (TEMPUS) occasionally suffered from strong, unintended oscillations of the sample perpendicular to the longitudinal axis of the coil system. In some cases, the molten sample hit the cage. One of the potential causes was a high susceptibility of the levitation system to residual accelerations of the TEMPUS rack. First analyses were done on the basis of the QSAM data during the mission to support trouble-shooting activities. A clear correlation between the QSAM quick-look data and the sample oscillation, however, could not be found during the mission.

Detailed analyses started after the mission in collaboration with the DLR Microgravity User Support Center (MUSC) and the Payload Element Developer, Daimler Benz Aerospace Dornier. The TEMPUS sample/coil system is a very weakly damped oscillator with a resonance frequency in the XY-plane between 1 and 2 Hz and a transient time of about 30 sec. For the frequency range of interest, QSAM data are an

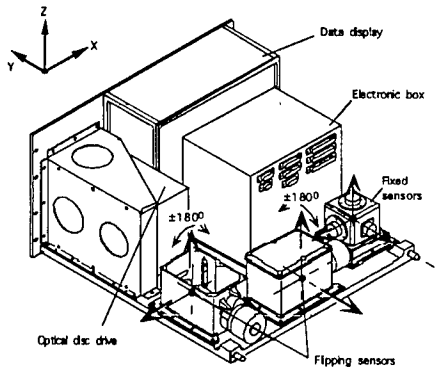

Figure 1: QSAM hardware (back view). The low-frequency acceleration vector is detected by the two flipping sensor packages, the g-jitter range by the tri-axial fixed sensor package.

appropriate basis for the analysis, even though the QSAM accelerometers were located some 3 m away from TEMPUS. We also made use of SAMS data measured in the TEMPUS rack. Single spectral lines were analyzed between 1 and 2 Hz for the events when the sample hit the cage. The analysis period was 1 min before the event. We found strong phase distortions in all events. The phase variations during the analysis interval are higher than 180° in both directions. Hence, there is little evidence that the contact was caused by acceleration. This is true more or less for all other events studied.

Impulses by the Orbiter primary thruster firings have been analyzed to investigate the low-frequencies of the Orbiter/Spacelab system. The most dominant frequencies were up to 6 Hz. This range is of special importance to the design of microgravity isolation mounts and levitation devices. Similar investigations have been done for the D-1 and D-2 Missions and were compared with IML-2 data. There is essentially little variation in that range from mission to mission.

Conclusion

The IML-1 mission was the first flight of the QSAM system. The QSAM data and the SAMS measurements gave a detailed picture of the residual acceleration of the Spacelab Module, especially in the g-jitter range. The significance of microgravity measurements to support experimenters was confirmed. The IML-2 mission demonstrated the unique role of microgravity measurement for controlling payload and facility operations. The significance of this aspect increases with the complexity of the system. Real-time data transmission to the ground for processing will be important for the space station.

The analysis of low-frequency data is continuing. We plan to fly QSAM on the Russian free-flying capsule FOTON-11 and the U.S. Microgravity Science Laboratory in 1997.

References

Hamacher, H., "Spacecraft low frequency acceleration," *Journal on Spacecraft and Rockets*, vol. 32, pp. 324-327, (1995).

Krueder, J., *Microgravity conditions of Spacelab, a case study based on the IML-2 mission*, Diploma Thesis, Technical University of Munich, Dpt. of Aeronautics and Astronautics, 155 pages in German, (1995).

Hamacher, H., Bluemel, U., and Jilg, R., "Spacelab's microgravity environment -- a characterization based on D-1 and D-2 data," *9th European Symp. Gravity-Dependent Phenomena in Physical Sciences*, Berlin, pp. 343-344, (1995).

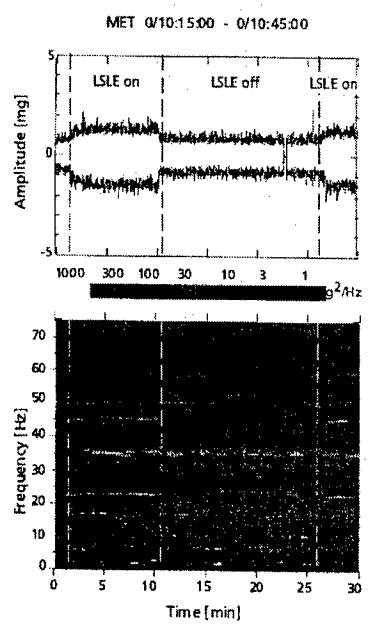

Figure 2 :Disturbances caused by the freezer of LSLE. Top: Peak value representation (Δt = 1 sec, bandwidth 50 Hz). Bottom: power spectral density

Influence of G-Jitter on Convection and Diffusion

Dr. H. Azuma, National Aerospace Laboratory, Chohu-shi, Japan

In the Space Shuttle, there is a small amount of stationary residual gravity caused by such factors as air drag g-jitter, mechanical operations, and crew activities. This residual gravity has some effect on flow and convection even if they are small. To know the effects is of great importance in the fields of fluid physics and materials processing.

The objective of this experiment was to measure the effect of g-jitter and residual gravity on diffusion and natural convection and to estimate the induced convective flow caused by g-jitter and residual gravity by measuring diffusion. A rectangular container (7 cm x 8 cm x 2 cm) that was filled with water, phenolphtalein 0.0035% (1.1 x 10-4 mol/ l), ethanol (7.0%) and salt (0.02 mol/l) was set in the Vibration Isolation Box System (VIBES) aboard the Shuttle.

Flight Activities

During the flight, this experiment was completed for 2 different cases: Case 1 with the box isolated from Shuttle vibrations by the VIBES and Case 2 (1 day after the first experiment) with the box locked in place and Shuttle vibrations directly translated to the experimental container. Two sets of three-axis accelerometers were set inside and outside the VIBES.

A thermal gradient was gradually formed up to ~70 °C with a direct current 5 mA being applied between the cathode and the anode for 5 sec every 5 min to enable the dye color. A video camera recorded diffusion of the color. The experiments went smoothly, but a bubble (1/8 of 10 mm dia.) was found in the left-upper corner of the container (opposite the heated wall). The averaged value of g-jitter measured in Case 2 was larger than in Case 1.

Highlights

- Observed enhanced diffusion caused by g-jitter.
- Recorded data indicating that convection caused g-jitter.

Postflight Analysis

Color diffusion was measured after image processing of the video. Diffusion of OH- was measured by using the fact that phenolphtalein changes color between pH 8 and pH 10. Diffusion occurred 20% faster rate than the rate that was theoretically predicted. This means that the apparent diffusion coefficient of OH- was D*~2D in the first experiment and D*~3D in the second, where D is diffusion coefficient of OH-.

The effect of the thermal gradient is thought to be negligible because this experiment was conducted just after the heating of the wall and before a clear thermal gradient was formed. In Case 2 where the g-jitter was stronger, the diffusion was faster than in Case 1. These facts indicate that some convection was caused by g-jitter.

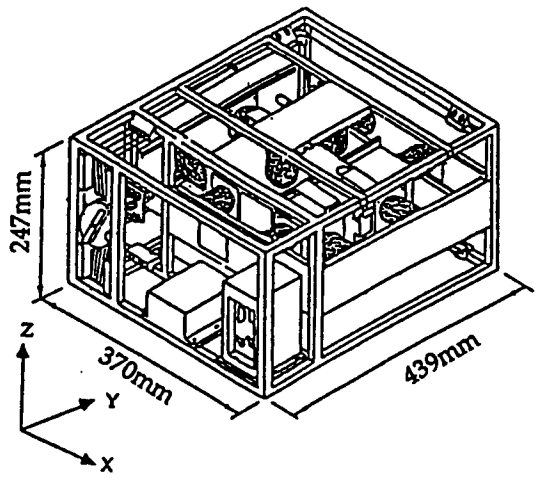

Figure 1: Vibration Isolation Box (VIBES)

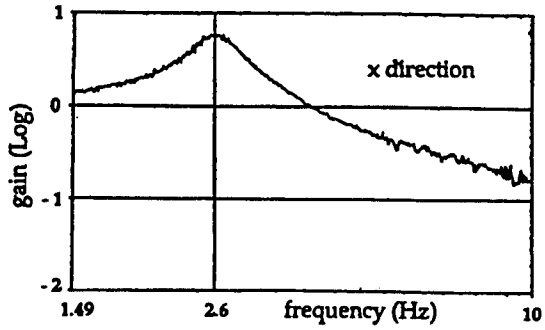

Figure 2: Transmissibility of VIBES (Case 1)

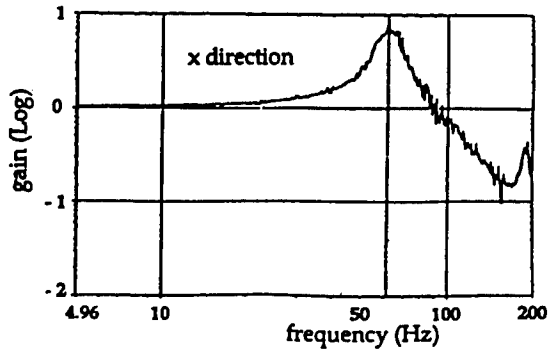

Figure 3: Transmissibility of VIBES (Case 2)

Diffusion after 1200 sec was also measured to find convection caused by any residual gravity. We tried to detect it by the deflection of color distribution. This, however, failed because we could not obtain a clear distribution of color by image processing and the direction of convection was thought to be reversed to the one expected from the direction of gravity and the thermal gradient. Comparison of the color distributions between Case 1 and Case 2 showed that the diffusion rate in the second case was faster than in the first.

Conclusion

Enhancement of diffusion caused by g-jitter was observed. In Case 1, where the VIBES was in operation, the apparent diffusion coefficient D* was D* = 2D. In Case 2, where the VIBES was locked, D* = 3D. This indicates that some kind of convection caused by g-jitter exists, although the exact mechanism is unclear. In the longer experiment with a thermal gradient, a faster diffusion rate was observed in the second case than in the first.

References

Atkins, P.W.,*Physical Chemistry*, 2nd edition (in Japanese), Tokyo Kagaku Dohjin.

Walter, H.W., ed., *Fluid Sciences and Material Sciences in Space*, Springer-Verlag.

Otto, G.H. and Frohberg, G., "Droplet dissolution kinetics in the miscibility gap of Ga-Hg: comparison of microgravity results with a computer simulation," *ESA SP-256*, (1987).

Thermally Driven Flow Experiments (TDFU)

Dr. M. Furukawa, NASDA Tsukuba Space Center, Ibaraki, Japan

For heat transport technology, two-phase fluid loops are generally used instead of single-phase loops. Accumulators are then indispensable to any loop system, but two-phase ones are quite different from single-phase ones. Two-phase accumulators are not mere reservoirs but should act as pressure regulators to control the loop temperature. Vented gas pressurant accumulators are unsuitable for long-term missions because the pressurant will be depleted. For this reason, bellows/diaphragm accumulators of nonvented gas pressurant have been developed since the early stage of research. Such electromechanical accumulators have, nevertheless, potential problems associated with reliability and weight. Thermal accumulators are therefore preferable in space applications.

Our concept is based upon the use of thermally driven flows and upon applications of capillary forces. Evaporative/condensing vapor flows, resulting from heating/cooling of wetted surfaces or of thin liquid films, usually generate such streams. For two-liquid surfaces opened to vapor space, separated from each other but internally connected, the liquid transfer between the two is generally possible by the vapor pressure increase/decrease. Evaporation and condensation are then used for such pressure changes. This is the operating principle of a new type of thermal accumulator that we devised.

Flight Activities

The Thermally Driven Flow Unit (TDFU) demonstrated liquid/vapor phase separation, liquid positioning, and liquid transfer in space. A major part of the TDFU is composed of 2 rectangular-solid copper vessels, named 1 and 2, connected with a rectangular copper duct forming a flow passage between the vessels. Each vessel has a polycarbonate window for observing liquid behaviors and consists of 2 portions: (1) a vapor space enclosed with grooved surfaces from 3 sides except top, bottom, and face; and (2) specially devised wedge-shaped liquid traps, here called tapered cores. The grooved surfaces are suitably finished for evaporative liquid supply at heating and for condensed liquid removal at cooling, while the cores serve liquid/vapor phase separation and liquid positioning. Principal functions of the TDFU depend on capillary forces acting in orbit as well as on the ground. About 10 cm^3 of distilled water are charged in the vessels as the working fluid. Both heating and cooling are by Peltier elements, placed in a matrix on the back side of the vapor space. In our experiments, one vessel is heated while another is cooled, and the liquid transfer from the heated vessel to the cooled one is observed because of a resultant vapor pressure difference.

Highlights

- Demonstrated a new type of thermal accumulator for two-phase fluid loop systems.
- Conducted experiments in liquid/vapor phase separation, liquid positioning, and liquid transfer.

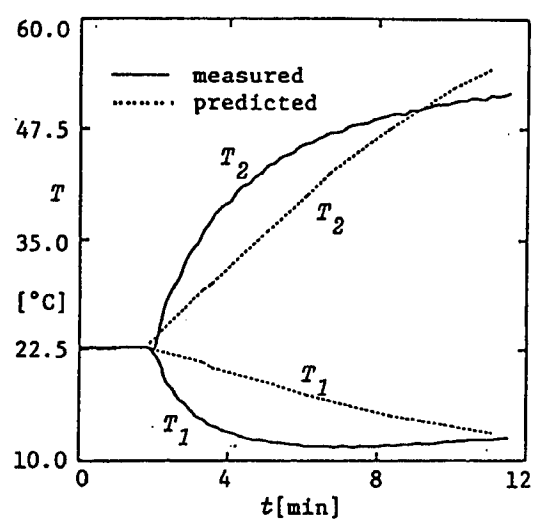

Figure 1: TDFU vessel temperature for Case 1

To examine the influences of oscillatory disturbances on thermally driven flows, the TDFU was installed in a vibration isolation box, VIBES. If VIBES is turned on, vibrations of higher frequencies than 3 Hz are then cut off; if VIBES is not activated, no vibrations are isolated. The following experiments were each done 3 times:

- Case 1: heating Vessel 2 and cooling Vessel 1 for 10 min under vibration-permitted conditions on MET-3,
- Case 2: again, heating Vessel 2 and cooling Vessel 1 for 11 min and then, conversely cooling Vessel 2 and heating Vessel 1 for 7 min. under vibration-isolated conditions on the same day,
- Case 3 -- heating/cooling in the same way as in Case 2 for 20 min and then for 10 min on MET day 11.

In any experiment (Cases 1 - 3), irrespective of imposed vibrations, the followings were visually confirmed: liquid/vapor phase separation, liquid positioning in the cores, and liquid transfer from a heated vessel to a cooled one.

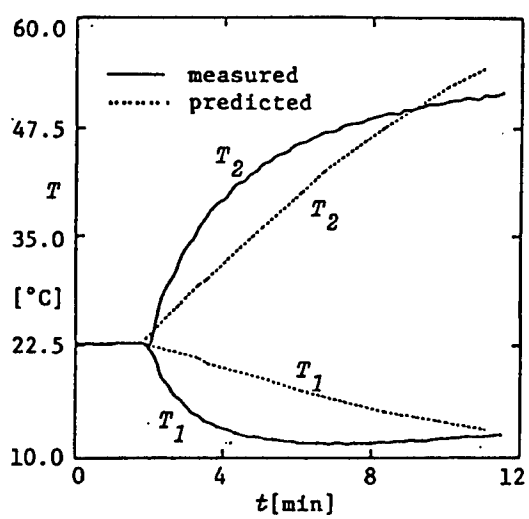

Figure 2: TDFU vessel temperatures for Case 2

Real-time video revealed liquid transfer caused by thermally driven flows. For Case 1 and 2, liquids cannot be found in the innermost (#1) core of Vessel 1 because some bubbles blocked the flow passage. For Case 3, all the bubbles were finally expelled, and all the liquid levels became quite even in each vessel.

Postflight Analysis

Liquid travel distances observed in Cases 1 - 3 were almost the same as our estimated mathematical predictions. A 30-node model was then prepared for TDFU temperature predictions. Data showed no thermal problems. Measured vibrational environments were in 10^{-4} g. The capacities of the batteries were 2.69 A·h at initial charge and 2.09 A·h at total discharge. The remaining capacities are hence 0.60 A·h, which make 18-min experiments possible.

Experiment results show that the observed liquid travel distance was what was theoretically estimated and that the measured vessel temperatures were similar to predicted ones. We conclude that thermally driven flows are instrumental for fluid management in microgravity.

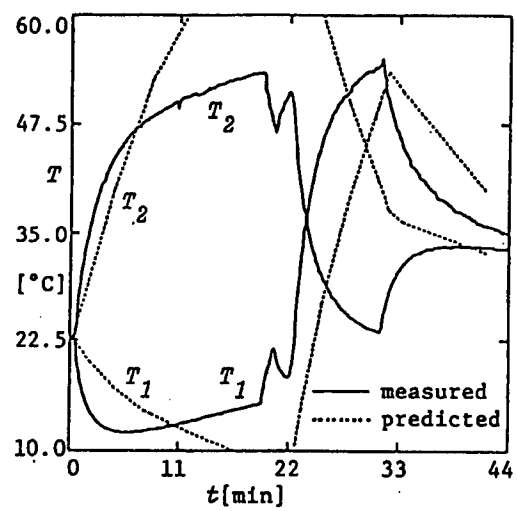

Figure 3: TDFU vessel temperature for Case 3

Conclusion

Thermally driven flow experiments on board the Space Shuttle were completed successfully, and the results demonstrated the feasibility of a newly devised type of thermal accumulator for two-phase fluid loop use.

ADVANCED PROTEIN CRYSTALLIZATION FACILITY (APCF)

INVESTIGATIONS	PRINCIPAL INVESTIGATORS	RESULTS HIGHLIGHTS
The Crystallization of Apocrustacyanin C_1	Dr. N.E. Chayen Blackett Laboratory Imperial College of Science, Technology and Medicine London, United Kingdom	Space crystals were larger and of better quality than most of those grown on the ground. CCD images of the crystal growth during the flight display a motion of the crystals within the hanging drop (attributed to Marangoni convection effects) and provide the first evidence for depletion zones around the growing crystals, as would be expected in a microgravity environment.
Crystallization of Collagenase and Photoreaction Center under Microgravity	Dr. I. Broutin, Dr. M. Ries, and Dr. A. Ducruix, LEBS, CNRS, Gif sur Yvette, France	Collagenase space-grown crystals recorded on the wiggler beam line of LURE had stronger intensities and signal to noise ratio than ground controls. PRC space-grown crystals diffracted far less than ground crystals, probably because of aging of the protein. APCF was a versatile facility allowing good experimental control.
Crystallization of Rhodopsin in Microgravity	Dr. W. J. de Grip University of Nijmegen Nijmegen, The Netherlands	Microgravity seemed to enhance rhodospin crystallization. Longer growing periods (>1 month) are needed to obtain crystals suitable for X-ray diffraction.

INVESTIGATORS	PRINCIPAL INVESTIGATORS	RESULTS HIGHLIGHTS
Crystallization of RNA Molecules	Dr. V.A. Erdmann and S. Lorenz Institut für Biochemie, Freie Universität Berlin, Berlin, Germany	Space crystals were about 3 times larger in volume than ground grown crystals. The amount of crystals grown in space were lower than in the ground control experiments.
Studies of Lysozyme Protein Crystal Perfection from Microgravity Crystallization	Dr. J. R. Helliwell University of Manchester Manchester, United Kingdom	Rocking width data showed microgravity-grown crystals displayed intensity levels three to four times that of their Earth-grown counterparts. Large perfect regions were visible within the microgravity grown crystals while Earth controls had a crumbly network.
Crystallization of Octarellins and Copper Oxalate	Dr. J. Martial Université de Liège Belgique (U.Lg.), Brussels, Belgium Dr. L. Wyns Université de Bruxelles Brussels, Belgium	Obtained first crystals for a *de novo* protein of the size of Octarellin. Small crystals were obtained, which allowed us to finally approach the conditions required for crystallizing these artificial proteins.

ADVANCED PROTEIN CRYSTALLIZATION FACILITY (APCF)

INVESTIGATIONS	PRINCIPAL INVESTIGATORS	RESULTS HIGHLIGHTS
Microgravity Effects on Macromolecule and Virus Crystallization	Dr. A. McPherson University of California Riverside, California United States	Observed alterations in the average or maximum size of crystals. Crystals grown in space had morphological modifications. Changes in the diffraction properties were observed.
Crystal Growth of Ribonuclease S	Dr. L. Sjolin Chalmers University of Technology and Göteborg University, Göteborg, Sweden	Crystals grown in microgravity had increased perfection, as measured by reduced mosaicity, and concordance, as measured by the agreement between diffraction data sets. Space-grown crystals had more uniform morphologies than Earth-grown crystals.

INVESTIGATIONS	PRINCIPAL INVESTIGATORS	RESULTS HIGHLIGHTS
Crystallization of Ribosomal Particles in Space	Dr. A. Yonath Max-Planck-Laboratory for Ribosomal Structure Hamburg, Germany	Grew crystals that had more isotropic shapes, which had never been observed on Earth. Growth of crystals without seeding indicated potential of microgravity.
Crystallization of Bacteriorhodopsin	Dr. G. Wagner Justus-Liebig University of Giessen, Giessen, Germany	Crystals were grown using two different techniques and varying ingredients. Crystals grown with liquid-liquid diffusion had sharp edges, smooth faces, and increased sizes, up to 200 μm in length. Adding benzamidine hydrochloride to crystals grown with liquid-liquid diffusion resulted in crystals with improved compact alignment of the crystalline filaments, increased crystal size, and higher resolution X-ray diffraction data.

The Crystallization of Apocrustacyanin C_1

Dr. N.E. Chayen, Blackett Laboratory, Imperial College of Science, Technology and Medicine, London, United Kingdom

The blue cryptic coloration of the lobster carapace is provided by the astaxanthin [3,3'-dihydroxy-β, β–carotene-4,4'-dione] binding protein, α–crustacyanin. The native carotenoprotein is an aggregate of 16 apoprotein units of about 20 kDa, one astaxanthin molecule being bound per apoprotein monomer. Both types of apoprotein are members of the lipocalin family of small hydrophobic ligand-binding proteins.

Extensive crystallization experiments have so far failed to yield well-ordered crystals of the carotenoprotein α-crustacyanin. An improvement in molecular ordering has, for some proteins, been achieved by carrying out crystallization under microgravity. This has been attributed to lack of sedimentation and convection in microgravity. In prior experiments, larger crystals of the oligomeric α–crustacyanin than have so far been obtained terrestrially have been grown under microgravity conditions, but no visible X-ray diffraction was obtained from these crystals (Zagalsky, *et al*, 1995). Crystals of type I subunit C_2 diffracting to 2.2Å have been attained terrestrially. More recently the major subunit, C_1 has also been crystallized.

Flight Activities

Crystallization took place in the vapor diffusion reactors of the Advanced Protein Crystallization Facility (APCF). Eight reactors were used in microgravity while eight identical reactors acted as ground controls. The protein solution (50 µl) was held in a closed glass cylindrical tube that could be raised to expose the protein drop to the interior of the chamber, thereby activating the crystallization process.

The experiments commenced in orbit 10 days following loading of the reactors and 16 days following the preparation of the apoprotein. Ground controls containing solutions identical to those in microgravity were activated (i.e., the protein drops became exposed to the reservoir blocks) at the same time as those aboard the Shuttle. On the ground, the drops were oriented as sitting drops. Crystallization proceeded for 12.5 days at 20 °C ±1 °C; deactivation of the corresponding (ground and flight) experiments was performed 24 h before landing. In two of the reactors the crystal growth was monitored by CCD observation at time intervals throughout the experiment.

Highlights

- Space crystals were larger and of better quality than most of those grown on the ground.
- CCD images of the crystal growth during the flight display a motion of the crystals within the hanging drop (attributed to Marangoni convection effects) and provide the first evidence for depletion zones around the growing crystals, as would be expected in a microgravity environment.

Postflight Analysis

Following landing, the APCF reactors were transported at 20 °C ± 1 °C to our laboratory where analyses were performed. Three of the ground control reactors (1.8 M, 1.85 M, and 1.95 M ammonium sulfate, respectively) reactivated soon after deactivation because of movement of the syringe holding the drop, probably resulting from air pressure in the leak-tight reactors. (In microgravity the reactors were clamped on activation/deactivation). As a consequence the drops in these chambers were exposed to the reservoir blocks for a prolonged period. A further ground control (1.9 M ammonium sulfate), giving poor-quality crystals, reactivated in transport before analysis. The largest crystal from each reactor was mounted in glass Lindemann tubes and X-ray diffraction data were collected.

In microgravity, crystals of apocrustacyanin C_1 were obtained in 7 of the 8 reactors with reservoir ammonium sulfate concentrations of

1.85 M, 1.9 M (x3), 1.95 M, and 2.0 M (x2), respectively; no crystals were obtained in the reactor containing 1.8 M ammonium sulfate. The crystals were single and rod-shaped with dimensions of 0.5-1.0 mm x 0.05-0.2 mm x 0.05-0.2 mm and diffracted to between 2.3Å and 3.2Å. The best crystals were formed, reproducibly, in the (triplicate) reactors containing 1.9 M ammonium sulfate. Microgravity conditions did not eliminate growth of crystals adhering to the wall of the glass piston holding the drop; these crystals were of inferior morphology to those in the bulk solution.

Crystals were likewise formed in 7 of the 8 ground controls (1.85-2.0 M ammonium sulfate) but were generally of poor morphology and size. In the four ground controls that did not function properly the crystals had a better chance to grow as they had more time in contact with the reservoir blocks compared to the other reactors. In spite of this apparent advantage, the crystals were of poor quality. Only 1 crystal (0.75x0.25x0.1 mm), harvested from 1 of the 3 reactors containing 1.9 M ammonium sulfate, was suitable for X-ray diffraction analysis; data from this crystal was collected to a resolution of 2.3Å, similar to that given by crystals grown in microgravity using the same ammonium sulfate concentration in the reservoir. The crystals exhibit the same symmetry ($P2_12_12_1$; cell dimensions: a= 42.0 Å, b= 81.9 Å, c= 110.9 Å) as crystals grown in the laboratory in hanging and sitting drops.

It is still not established whether the optimum terrestrial conditions for crystallization of proteins are also optimal for crystallization under microgravity. Prior experiments using the batch method for the crystallization of hen egg white lysozyme suggested that the optimal protein concentration for growth in microgravity is higher than that on Earth. Another study implied that the enzyme reverse transcriptase required a higher concentration of precipitant for crystallization in microgravity (Chayen, 1995). In the present crystallization at fixed protein concentration, there appears to be no shift in the optimal concentration of precipitant between ground and microgravity experiments, with the best crystals grown from 1.9M ammonium sulfate in both environments. Moreover, the same form of crystal is produced in microgravity, ground controls, and in the laboratory, contrary to a number of cases where a different crystal form was obtained in microgravity.

Conclusion

Even though a single ground control crystal diffracted to as high a resolution as those grown under microgravity, statistically the microgravity grown crystals were superior when comparing the same conditions and using identical apparatus. (Chayen, *et al.*, 1996) Crystals of apocrustacyanin grown on the ground under containerless conditions gave better crystals than those grown in contact with a surface (Chayen, 1996), but their quality was not better than the microgravity-grown crystals.

The crystals in the reactors that were monitored by CCD observation displayed a motion within the hanging drop that is attributed to Marangoni convection effects. The images also indicate the presence of depletion zones, i.e., solution regions that are depleted of the protein. The effect of depletion zones around growing crystals, especially in microgravity, has been discussed by several researchers, but the presence of "halos" observed in the CCD images from the IML-2 flight provides, for the first time, evidence for the depletion zone around the growing crystals as is expected in a microgravity environment (Chayen, *et al.*, 1997).

References

Chayen, N.E., "Microgravity protein crystallization aboard the Photon satellite," *J. Cryst. Growth,* vol. 153, pp. 175-179, (1995).

Chayen, N.E., Gordon, E.J., and Zagalsky, P.E., "The crystallization of apocrustacyanin C_1 on the International Microgravity Laboratory (IML-2) Mission," *Acta Cryst. D,* vol. 52, pp. 156-159, (1996a).

Chayen, N.E., Snell, E.H., Helliwell, J.R., and Zagalsky, P.F., "CCD video observation of microgravity crystallization: apocrustacyanin C_1, *J. Cryst. Growth,* vol. 171, no 1/2, (1997).

Zagalsky, P.F., Wright, C.E., and Parsons, M., "Crystallization of α-crustacyanin, the lobster carapace astaxanthin - protein: results from Eureca," *Adv. Space Research,* vol. 16, pp. 91-94, (1995).

Chayen, N.E., "A novel technique for containerless protein crystallisation," *Protein Engineering,* vol. 10, pp. 927-929, (1996).

Crystallization of Collagenase and Photoreaction Center under Microgravity

Dr. I. Broutin, Dr. M. Ries, and Dr. A. Ducruix, LEBS, CNRS, Gif sur Yvette, France

While X-ray methods are at this time the most suitable techniques for the determination of the three-dimensional structure of biological macromolecules, production of crystals diffracting at high resolution remains a difficult step. Because of the multi-parametric aspect of protein crystallization, accurate control of each parameter is required to monitor reproducibility of the crystallization process.

This experiment aimed to quantify the influence of microgravity on nucleation rate, potential improvement of diffraction, and potential improvement of mosaicity with two well-characterized proteins (collagenase and photoreaction center, PRC) that have been studied in our laboratory for several years. Well characterized means that the protein has been properly defined from a biochemical point of view (purity, ion-spray mass spectrometry) and from a physical chemistry point of view (solubility diagram, X-ray structure). It is thus possible to make a calibration of the X-ray properties of Earth-grown crystals to compare them to space-grown crystals.

Flight Activities

The crystals were grown in the Advanced Protein Crystallization Facility (APCF). Nine days prior to launch, all reactors were filled. We used 5 hanging drop cells of 80 µl for HL and 5 dialysis cells of 200 µl for PRC. Temperature of experiments was 20 °C. Samples were handed over to the investigator 3 days after landing.

Postflight Analysis

Crystals were mounted in glass capillaries and submitted to X-ray radiation for diffraction limits and for mosaicity measurements.

Highlights

- Collagenase space-grown crystals recorded on the wiggler beam line of LURE had stronger intensities and signal to noise ratio than ground controls.
- PRC space-grown crystals diffracted far less than ground crystals, probably because of aging of the protein.
- APCF was a versatile facility allowing good experimental control.

The number and size of collagenase crystals grown in space are similar to ground experiments within the range of reproducibility. Crystals suitable for X-ray analysis were recorded from 2 of the 5 reactors. The 5 largest were mounted for X-ray analysis.

Crystals hl128 a, b, c, and d were obtained from reactor 128 with 15 mg/ml protein, 1.24M ammonium sulfate (pH 7.2 -> 6.1) and sursaturation of 11. Crystal hl129e grew from 10 mg/ml protein, 1.39M ammonium sulfate (pH 7.2 -> 5.6) and a sursaturation of 12. Solubility value was reached at the end of the experiment. Crystals hl128 a, b, c and hl129e were analyzed at LURE using the wiggler beam line. The largest one (hl129e), which also was diffracted the best, was fully recorded to obtain a complete data set comparable to our best ground data set (hlmarkII). Three others, hl128a, b and c were also X-ray recorded at the wiggler beam line, but they were only analyzed on 2 portions of the reciprocal space, separated by 90°. A synchrotron beam shut down occurred while recording crystal hl128c, so we completed the X-ray analysis in our laboratory, also using an image plate detector but a rotating anode source. Crystal hl128c decayed very rapidly, so only the 20° recorded at LURE were kept for analysis. Crystal hl128d was fully recorded in our laboratory. As the quality of a data set depends to a large degree on the intensity of the source, to be able to judge the quality of hl128d data set, we also report the analysis of the best data set obtained in our laboratory with a collagenase crystal (hlraxis).

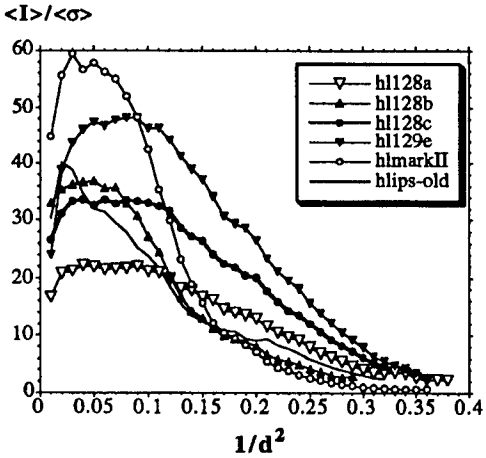

comparison of <I>/<σ> for data sets recorded using a synchrotron source

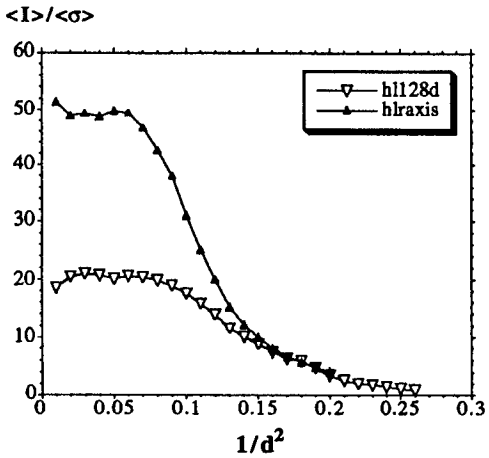

comparison of <I>/<σ> for data sets recorded using a rotating anode source

Results for PRC were not as satisfying as for collagenase because of aging of the protein, stored in a dilute state at 20 °C before launch. As experiments were optimized by diluting concentrated stock protein solution stored at 4 °C, this parameter could not be optimized before launch because of a time shortage. Thus only one FID reactor, used with dialysis membrane, yielded crystals usable for X-ray diffraction. They were subjected to synchrotron X-ray radiation. All of them diffracted far less than ground crystals, and thus X-ray data were not recorded.

Conclusion

With some minor improvements, the APCF will be one of the best devices allowing scientists to perform well-controlled experiments, versatile with respect to techniques and volumes, with controlled and recorded temperature,and with the possibility of observation.

The hanging drop reactor has to be improved for pH shifts and observation. The failure of the PRC crystallization underlines the crucial step of optimizing crystallization with flight-identical reactors. No conclusion regarding nucleation or crystal size and quality can be drawn from the PRC experiments. Concerning collagenase, the number and size of crystals are similar to the ground experiment within the range of reproducibility in the APCF hanging drop reactor.

All space crystals recorded on the wiggler beam line of LURE have stronger intensities and intensity over signal values than any other collagenase crystals already tested, in the resolution range above 3Å. (See figures.) Before we can correlate this benefit to microgravity, we have to make sure that it is not linked to the new image plate detector of LURE. This will be done soon. In parallel, the structure refinement will be repeated using the hl129e data set to visualize the effect in the real space (electron density) of the improvement of the data set.

References

Broutin, I., Arnoux, B., Riche, C., Lecroisey, A., Keil, B., Pascard, C., and Ducruix, A., "1.8 Å structure of hypoderma lineatum collagenase: a member of the serine proteinase family," *Acta Cryst.*, vol. D52, pp., 380-392, (1996).

Fourme, R., Ducruix, A, Rieskautt, M., and Capelle, B., "The perfection of protein crystals probed by direct recording of Bragg reflection profiles with a quasi-planar X-ray wave," *Journal of Synchrotron Radiation,* vol. 2, pp. 136-142, (1995).

Broutin, I., Mérigeau, K., and Ducruix, A., *J. Cryst. Growth,* article accepted for publication in 1997.

Crystallization of Rhodopsin in Microgravity

Dr. W. J. de Grip, University of Nijmegen, Nijmegen, The Netherlands

Rhodopsin is the light-sensitive protein (visual pigment) of the rod cell in the vertebrate retina. This experiment examined the crystallization and structure of the visual pigment rhodopsin. The high-resolution structure of this protein is unknown, which seriously hampers studies of the signal transduction mechanism on a molecular level. Better insight will increase our basic knowledge of this protein and may have medical and pharmacological applications.

To understand receptor properties and signal-transduction mechanism of this membrane protein family on a molecular level, detailed knowledge of the three-dimensional structure is essential. Since these proteins are too large (40 to 70 kD) to allow structure analysis by NMR techniques, crystallization with high-resolution analysis by X-ray diffraction is the only feasible approach. This requires relatively large amounts of purified protein, and bovine rhodopsin is the only representative of this receptor family that can be isolated and purified from its native source in sufficient quantities for this purpose. The amino acid sequence of bovine rhodopsin was elucidated a decade ago, and very recently a low-resolution projection structure obtained from two-dimensional crystals has been reported. However, a detailed three-dimensional structure is still not available.

We have obtained crystals of rhodopsin (40 kD) in our laboratory using the sitting-drop vapor diffusion technique, but so far they were too small or unordered to provide any diffraction information. A major problem with crystallization of membrane proteins is their amphipathic character, requiring detergents and detergent phaseshift modifiers, and their relatively low polar surface area prohibits extensive strong protein-protein interactions. We have investigated many parameters to produce optimal conditions (protein concentration, type and concentration of detergents, type and concentration of precipitant, buffer, pH, temperature, lipids, stabilizing or micelle-modifying additives).

Highlights

- Microgravity seemed to enhance rhodospin crystallization.
- Longer growing periods (>1 month) are needed to obtain crystals suitable for X-ray diffraction.

Evidence is accumulating that microgravity not only could be beneficial to protein crystallization in that larger size or better ordered crystals can be obtained than at 1-g, but also that diffractable crystals are generated of proteins that on Earth only give low-order or microcrystals. The latter condition prevails for rhodopsin.

Flight Activities

We tested seven different crystallization conditions, selected from trial on Earth, which generated small crystals of various shapes. Special precautions were taken to ensure that light with wavelengths below 630 nm, for which rhodopsin is very sensitive, could not enter the reactor. The APCF reactors were fitted with long-pass filters (690 nm cut-off) to ensure that the rhodopsin was not exposed to any damaging light during handling of the reactors.

Although none of the reactors produced crystals of sufficient size to attempt X-ray diffraction, in four of the reactors more and/or larger structures were observed than in the ground control. The small size could be caused by the relatively short incubation times, since in terrestrial trials crystals need from 4 to 12 weeks to grow to their final size.

Postflight Analysis

Screening for crystal formation was done microscopically in red light (Schott long-pass filter RG645) using shape and birefringence as criteria to identify crystals. Mother liquor and crystalline structures were screened for the presence

and quantity of intact protein by immunoblot analysis using specific antibodies.

Three of the seven reactors produced results not very different from the ground controls in that no or very few crystalline structures were found. This is probably because of the relatively short incubation times, as these conditions on Earth usually require more than 3 weeks to produce crystals. The other four flight reactors performed better than their controls, generating more and/or larger structures. In two flight reactors, a respectable number of small needles together with some larger structures were obtained, while the ground controls only produced a few needle-like structures. However, none of the reactors produced crystals of sufficient size to attempt X-ray diffraction (this would require a minimal size of 50 to 100 μm in all dimensions).

We have tried to assess packing and order of the small needles obtained using microspectrophotometry, but this approach was not yet successful. Analysis by X-ray diffraction has not been attempted in view of the small size of the crystals. As far as we could determine, there was no sign of spectral deterioration of the samples, indicating that the precautions taken to prevent light damage had worked perfectly.

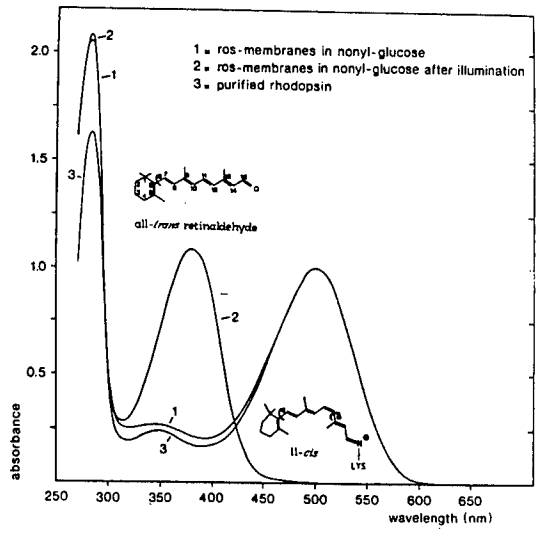

Figure 1: Absorbance spectrum of detergent-solubilized photoreceptor membranes before (1) and after (2) illumination (2 min, 20 °C) and of purified rhodopsin (3)

Conclusion

Microgravity seems to have a positive effect on the rhodopsin crystallization process. The fact that we could not yet produce crystals with diffraction potential might be because of the relative short crystallization times available in space. One option to explore further is to try more extended crystallization time periods (> 1 month). Another option to explore further is based on the recent observation that the optimal crystallization conditions in microgravity might slightly differ from those on Earth. This would prompt crystallization trials in microgravity using a range of conditions close to the optimal ones found at 1-g.

Crystallization of RNA Molecules

Dr. V.A. Erdmann and S. Lorenz, Institut für Biochemie, Freie Universität Berlin, Berlin, Germany

Since RNA molecules participate in a large number of biological functions, it is not surprising that they are essential for living cells. The human cells contain more than 100,000 different RNA molecules, but very little is known about their structure. There is currently not enough information to establish general structural rules for RNA molecules (Moras, *et. al.*).

A better knowledge of the structure and function of RNA molecules is also necessary for the development of RNA technologies, which are key technologies influencing the areas of biotechnology and medicine in the future. Our model compound for the IML-2-mission was the ribosomal 5S rRNA from the thermophilic eubacterium *Thermus flavus* and the chemically synthesized domain A of this molecule.
5S rRNA is an essential part of the large ribosomal subunit. It is 120 nucleotides long. Reconstitution experiments have shown that ribosomes without 5S rRNAs are inactive in protein biosynthesis. Earlier crystallization experiments on the ground and in space involving nearly 20 different 5S rRNA species have shown that so far the 5S rRNA from *Thermus flavus* is best suited for this purpose. The best crystals obtained in the laboratory exhibited a resolution of 8 Å by X-ray analysis (Lorenz, *et. al.*).

Parallel to the crystallization experiments with the whole 5S rRNA, we used the chemically synthesized domain A of *Thermus flavus* 5S rRNA for similar experiments. Our crystals from this RNA, produced on Earth, gave us a resolution up to 2.3 Å (Lorenz, *et al.* and Betzel, *et. al.*). Domain A is a dodecamer double helix with 12 base pairs.

Flight Activities

The crystallization of the ribosomal 5S rRNA from *Thermus flavus* took place in the micro-

Highlights

- Space crystals were about 3 times larger in volume than ground grown crystals.
- The amount of crystals grown in space were lower than in the ground control experiments.

dialysis reactor (MD) of the Advanced Protein Crystallization Facilities (APCF).

Four MD-reactors with a probe volume of 15 µl were used for the space experiment under microgravity. The 5S rRNA-fragment (Domain A) was crystallized in space in 2 hanging drop reactors with a drop volume of 6 µl and a reservoir volume of about 500 µl. Ten days after filling the reactors with the probes and the reservoirs (6 days 4 °C, 4 days 20 °C), the APCF reactors were activated in space and were operated for 16 days at 20 °C. The deactivation of the reactors was carried out about 24 h before landing. For both cases (the 5S rRNA and the 5S rRNA fragment), nearly identical control experiments were performed on the ground.

Postflight Activities

After landing at KSC the reactors were photographed at KSC and transferred at 20 °C to our laboratory. After further photographing the amount and sizes of the crystals were determined. In the microgravity experiments with the whole 5S rRNA, we observed crystals in 3 of 4 MD-reactors. In the ground control experiments all 4 MD-reactors contained crystals (See Table 1).

Microgravity conditions did not eliminate the growth of the crystals on the wall and on the membrane of the MD reactors. Nevertheless it was easy to harvest the 5S rRNA crystals for the X-ray studies. The 5S rRNA fragment which was crystallized in the 8 µl hanging drop reactors gave in both cases, in space and on ground very small crystals (less than 0.1 mm in length). They were too small for X-ray studies.

The 5S rRNA space crystals, mounted in thin walled glass capillaries were analyzed 7 weeks after deactivation with the synchrotron beamline X11 at the Deutsche Synchrotron (DESY) in Hamburg /Germany. The resolution of the space crystals was between 15 and 20 Å. The resolution of the ground crystals, analyzed 4 weeks after deactivation was between 14 and 18 Å.

Precipitant Ammonium-Sulfate (AS)	**Space**	**Ground**
45% AS	no crystals	4 crystals up to 0.2 mm
50% AS	3 crystals 0.3-0.4 mm	10 crystals up to 0.2 mm
55% AS	1 crystal 0.3 mm	about 20 crystals up to 0.2 mm
60% AS	3 crystals 0.3 mm	more than 20 crystals < 0.1 mm

Table 1: Amount and sizes of 5S rRNA Thermus flavus crystals yielded in the APCF-MD-reactors from the space- and ground-control experiments.

Conclusion

For the crystallization of 5S rRNA *Thermus flavus,* a higher concentration of precipitant is necessary than in the ground controls. The number of crystals grown in space under the same conditions is significantly lower, but the sizes of them are significantly larger. The resolution of the crystals grown in space was not better than on the ground, although they are larger in size. One of the reasons for that could be the long time between crystallization and X-ray measurements.

References:

Moras, D., "Crystal structures of tRNA's," *Landolt-Börnstein New Series 1b, Nucleic Acids,* Saenger, W., ed., Springer Verlag Berlin, Heidelberg und New York, pp. 1-30, (1989).

Lorenz, S., Betzel, Ch., Raderschall, E., Dauter, Z., Wilson, K.S., and Erdmann, V.A., "Crystallization and preliminary diffraction studies of 5S rRNA from the thermophilic bacterium *Thermus flavus,*" *J. Mol. Biol.,* vol. 219, pp. 399-402, (1991).

Lorenz, S. Fürste, J.P., Bald, R., Zhang, M., Raderschall, E., Betzel, Ch., Dauter, Z., Wilson, K.S., and Erdmann, V.A., "Crystallization and preliminary diffraction studies of the chemically synthesized domain A of *Thermus flavus* 5S rRNA: an RNA dodecamer double helix," *Acta Cryst.*, vol. D 49, pp. 418-420, (1993).

Betzel, Ch., Lorenz, S., Fürste, J.P., Bald, R., Zhang, M., Schneider, Th.R., Wilson, K.S., and Erdmann, V.A., "Crystal structure of domain A of *Thermus flavus* 5S rRNA and the contribution of water molecules to it's structure," *FEBS Letters*, vol. 351, pp. 159-164, (1994).

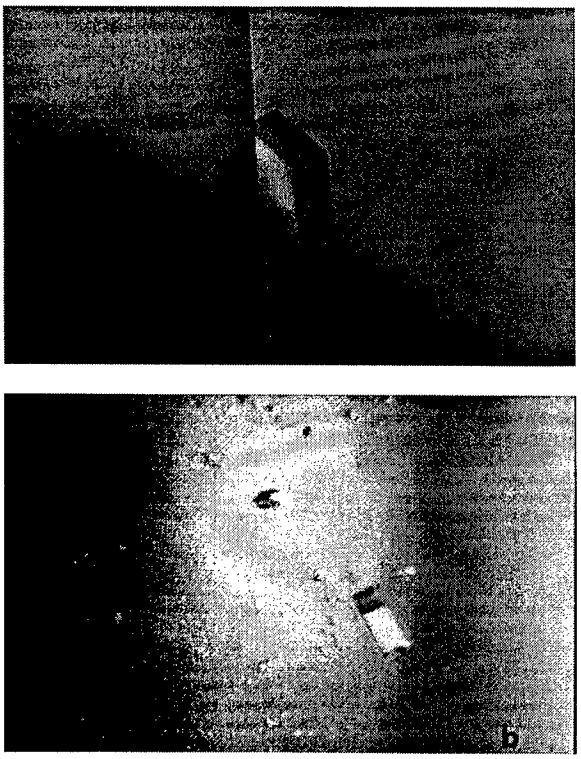

Figure 1: Crystals of 5S rRNA Thermus flavus grown under the same conditions in APCF- MD-reactors in space (a) and grown on Earth (b). The magnifications of both pictures are identical. (length of the crystals: space 0.40 mm; ground 0.18 mm).

Studies of Lysozyme Protein Crystal Perfection from Microgravity Crystallization

Dr. J. R. Helliwell, University of Manchester, Manchester, United Kingdom

This experiment studied the effects of microgravity, in terms of perfection, on crystallization of a well-studied test case protein, chicken egg white lysozyme. Perfection and crystal quality were assessed using high-angular-resolution rocking width techniques and X-ray topography.

Highlights

- Rocking width data showed microgravity-grown crystals displayed intensity levels three to four times that of their Earth-grown counterparts.
- Large perfect regions were visible within the microgravity-grown crystals while Earth controls had a crumbly network.

Flight Activities

For crystallization, 15.8 mg of chicken egg white lysozyme was dissolved in 0.188 ml 0.04M salt pH 4, 7 acetate buffer. Crystallization took place in the Advanced Protein Crystallization Facility (APCF) using the dialysis method. Control experiments were also performed on Earth. The crystallization was monitored by CCD video observation during the flight.

Postflight Analysis

Crystals were analyzed 3 months after the flight on the Laue beamline (BL3) of the European Synchrotron Radiation Facility (ESRF). The crystals were further analyzed some 6 months after the first flight on the joint Swiss-Norwegian beamline at the ESRF with a fine stepsize (0.001 degree) diffractometer with a highly collimated monochromatic beam of 1 Å wavelength. High-resolution rocking widths were measured. The instrument resolution function was calculated to be 0.00195 degrees (at 0 degree scattering angle). X-ray topographic measurements were made at the Brookhaven National Synchrotron Light Source (NSLS), station X26-C, 1 year after the mission.

Data collection on the Laue beamline highlighted problems with handling large size crystals grown on the microgravity mission (2.4 mm length at maximum). Ordinary glass capillaries of suitable diameter proved too fragile to be useful, and quartz glass was substituted instead for the monochromatic measurements.

The monochromatic data collection gave microgravity rocking widths of 0.0017 degrees at minimum compared with 0.0067 degrees for Earth-grown controls. It was noticed that the decrease in rocking width is proportional to the increase in peak height of the reflection (Figure 1). After corrections for illuminated volume the microgravity crystals displayed peak intensity levels three to four times that of the Earth-grown controls. It was possible to find significant reflections for the microgravity-grown case at 1.2 Å resolution.

Topographic studies revealed large perfect regions visible within the microgravity-grown crystals (Figure 2). In comparison, the ground controls appeared to have a crumbly network of dislocations. CCD video observation of the crystal provided useful information on the growth showing that there were periods when growth stopped and then restarted. The reasons for this are unknown. The CCD images also showed some slight motion (200 micron) of crystals at varying times during the mission. The reasons for that are not known.

Conclusion

Both fine angle resolution mosaicity and X-ray topography measurements can help crystal growers obtain the best possible growth conditions for macromolecular crystals. In addition, these results set a benchmark against which both Earth-grown and microgravity-grown crystals can be judged.

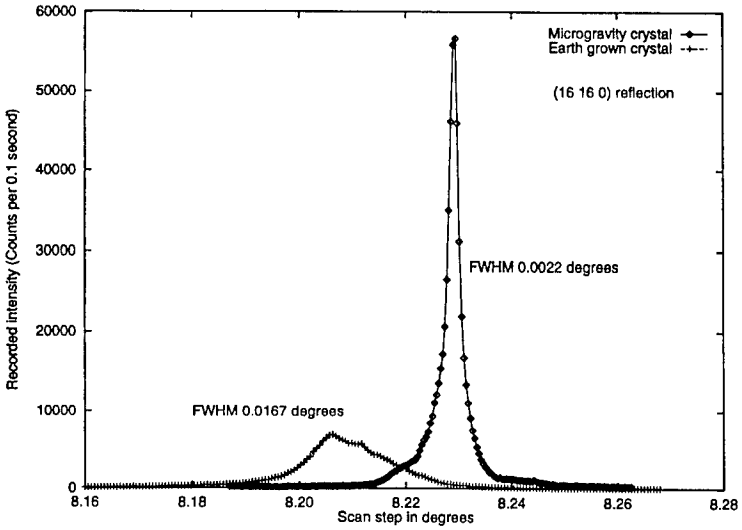

Figure 1: Rocking curves for the (16 16 0) reflection for microgravity versus Earth-grown lysozyme crystals.

Figure 2: X-ray topograph of a microgravity-grown lysozyme crystal.

References

Helliwell, J.R., "Protein crystal perfection and the nature of radiation damage," *J. Cryst. Growth*, vol. 90, pp. 259-272. (1988).

Snell, E.H., Weisgerber, S., Helliwell, J.R., Weckert, E., Holzer, K., and Schroer, K., "Improvements in lysozyme protein crystal perfection through microgravity growth," *Acta Cryst.*, vol. D51, pp. 1099-1102. (1995).

Helliwell, J.R., Snell, E.H., and Weisgerber, S., "An investigation of the perfection of lysozyme protein crystals in microgravity (Spacehab-1 and IML-2) and on earth," *Proceedings of the 1995 microgravity meeting*, Berlin, Ratke, L., Walter, H., and Feuerbacher, B., eds., pp. 155-177, Springer Verlag Lecture notes in Physics, (1996).

Stojanoff, V., Siddons, D.P., Snell, E.H., and Helliwell, J.R., "X-ray topography; An old technique with a new application," Synchrotron Radiation News, vol. 9, pp. 25-26, (1996).

Crystallization of Octarellins and Copper Oxalate

Dr. J. Martial, Université de Liège Belgique (U.Lg.), Brussels, Belgium and Dr. L. Wyns, Unversité de Bruxelles, Brussels, Belgium

In the context of the protein *de nova* design, our Protein Engineering group has synthesized and partially structurally characterized the first *de nova* protein, named Octarellin, designed on basis of alpha/beta-barrel structure. This artificial polypeptide presents a high percentage of stable secondary structures and a partially compact fold. In line with the iterative approach, implying repeated cycles of design and rigorous experimental characterizations of the *de nova* polypeptides, we have already redesigned and produced a second generation of Octarellin (Octarellin II). The solubility and the stability of this new artificial protein seem to be higher than those of Octarellin I. The determination of the Octarellin three-dimensional structure is crucial for the continuation of our project and for all applications which should be derived from it. No *de nova* designed protein with the size of Octarellin has ever been crystallized. The Octarellin structure cannot be analyzed by NMR because of its size and symmetry. The only way to unambiguously elucidate its three-dimensional structure is by X-ray diffraction.

Flight Activities

The design, synthesis, and purification of Octarellins were performed at Liège in Dr. Martial's laboratory (50 mg of both Octarellin at least 95% pure). Preliminary crystallization assays on Earth were performed in the laboratory of Dr. Lode Wyns (V.U.B., Brussels). Based on this screening, various conditions were selected for producing crystals in the Advanced Protein Crystallization Facility in space. Octarellin III and Thermotoga TIM crystals were grown using the hanging drop method. Octarellin II, Human TIM, and Mutant Human TIM were grown using the dialysis method.

Highlights

- Obtained first crystals for a *de novo* protein of the size of Octarellin.
- Small crystals were obtained, which allowed us to finally approach the conditions required for crystallizing these artificial proteins.

Postflight Analysis

Needle-shaped microcrystals were obtained of Octarellin II in both the ground-control experiment and the flight experiment. In addition, 3 small crystals (about 10 microns in size) grew in the Earth-based reactors. They were analyzed and surprisingly diffracted to below 3 Å and were quite resistant to radiation damage. With these crystals 70° of data were collected. Octarellin III did not produce any crystals on Earth or in space.

Thermotoga TIM produced many regular small crystals in the space reactor that were almost the same size as those seen in the ground-control hanging drop and dialysis reactors. Both space- and Earth-grown crystals were subjected to X-ray diffraction. The Earth-grown crystals diffracted to a resolution below 2.3 Å and the space-grown crystals diffracted to 3 Å. These crystals were very sensitive to radiation damage; after 1 exposure of 5 sec, the diffraction decreased to 3 Å and below. As a result, only a partial data set was collected.

For Human TIM, very tiny needle-shaped crystals were formed on Earth and in space, and these crystals were unsuitable for data collection. For Mutant Human TIM, very tiny, irregular crystals were obtained both on Earth and in space; these crystals were also unsuitable for data analysis.

After the flight, we kept the reactors at 20 °C for 4 weeks. This resulted in a small increase in size. We will use these crystals as microseeds in future seeding experiments, which will hopefully lead to crystals suitable for X-ray data collection.

REACTOR	EXPERIMENT CONDITIONS	RESULTS
Hanging Drop Reactors		
Reactor 15	8% PEG 6 K; 100 mM Tris-HCL, pH 8.5; 350 µl/block; vol. of Octarellin sample: 30 µl (Octarellin II: 5 mg/ml)	Observed a slight precipitation and aggregation in this reactor
Reactor 102	8% PEG 6 K; 100 mM Tris-HCl, pH 8.5; 1.5 M Lithium Sulfate; 350 µl/block; vol. of Octarellin sample: 30 µl (Octarellin II: 5 mg/ml).	Observed a few tiny microcrystals, which did not show a drastic increase in size after keeping the reactor on Earth for another 4 weeks.
Reactor 22	8% PEG 6K; 100 mM Carodylate, pH 6.5; 1M Lithium Chloride; vol. of Octarellin sample: 30 µl (Octarellin II: 5 mg/ml).	Observed the best crystals shaped in 2 morphological forms: needle-shaped crystals and round crystals. Both types of crystals were too small for X-ray diffraction.
Reactor 124	5% PEG 6K; 100 mM Na-Acetate; pH 4.6; 1 M Lithium Chloride; 350 µl/block; vol. of Octarellin sample: 30 µl (Octarellin II: 5 mg/ml.	Produced a few small microcrystals with the same shape as crystals in Reactor 22.
Dialysis Reactors	(The 2 conditions used for dialysis are identical to the ones used in Hanging Drop Reactors 15 and 102.)	
Reactor 110	8% PEG 6K; 100 mM Tris-HCL, pH 8.5; Reservoir chamber: 350 µl; vol. of Octarellin sample: 67 µl (Octarellin II: 5 mg/ml).	Observed very tiny microcrystals.
Reactor 122	8% PEG 6 K; 100 mM Tris-HCl, pH 8.5; 1.5 M Lithium Sulfate; Reservoir chamber: 350 µl; vol. of Octarellin sample 67 µl (Octarellin II: 5 mg/ml).	Observed very tiny microcrystals.

Conclusion

Our results are very encouraging since small crystals were obtained in space, which allowed us to finally approach the conditions required for crystallizing these artificial proteins. Most remarkably, it was the first time that crystals were obtained for a *de nova* protein the size of Octarellin. We are looking forward to the performing a follow-up investigation of this exciting first experiment.

Microgravity Effects on Macromolecule and Virus Crystallization

Dr. A. McPherson, University of California, Riverside, California, United States

Experiments on macromolecular crystal growth in microgravity have now been carried out for more than 10 years using a variety of different techniques and instruments. A number of reports for specific proteins or viruses have been quite favorable and encouraging. In other cases, often not described in the literature, the results have not differed significantly from those seen on Earth. A continuing question, therefore, is which kinds or classes of macromolecules and crystals are most likely to benefit from the microgravity experience and what aspects of the process are important for obtaining optimal results.

Flight Activities

Before and during the mission, Advanced Protein Crystallization Facility (APCF) cells equivalent to those used in the actual space experiment were loaded with identical macromolecule samples and precipitants, and parallel experiments were conducted. Liquid-liquid diffusion trials carried out in a 1-g environment, however, suffer many problems that are absent in microgravity. They are rather poor controls for the microgravity experiments. For canavalin, TYMV, and STMV, the results obtained on the ground using the APCF cells were markedly inferior to those obtained in the actual space experiment.

Two T=1 and one T=3 plant viruses and a protein were crystallized in microgravity. The method employed was liquid-liquid diffusion (free interface diffusion) in the APCF. The volume of all protein chambers was 470 µl and that of the precipitant chambers 590 µl. The diffusion cell was activated 3.5 h after a microgravity environment was achieved, and the crystals grew until the cells were deactivated approximately 12.5 days later.

Highlights

- Observed alterations in the average or maximum size of crystals.
- Crystals grown in space had morphological modifications.
- Changes in the diffraction properties were observed.

The macromolecule samples used in these experiments include

(1) Canavalin: the major storage protein (vicilin) of the jack bean [*Canavalia ensiformis*].

(2) Satellite Tobacco Mosaic Virus (STMV): The plant satellite virus STMV has as its master virus Tobacco Mosaic Virus (TMV).

(3) Satellite Panicum Mosaic Virus (SPMV): The second plant satellite virus SPMV has as its master virus Panicum Mosaic Virus (PMV).

(4) Turnip Yellow Mosaic Virus (TYMV): One of the most thoroughly and earliest studied virus known is TYMV isolated for these experiments from infected Chinese cabbage.

Postflight Analysis

After sample unloading, we immediately examined and photographed the crystals. The 15 crystallization cells were returned to our laboratories. In assessing the quality of crystals grown in microgravity, X-ray diffraction results were compared with the best that had previously been obtained for any of the corresponding crystals grown in the conventional laboratory. For both the rhombohedral and hexagonal canavalin crystals and for TYMV crystals, the sizes of Earth-grown crystals were comparable or even larger than those grown in microgravity. For cubic STMV, this was not possible, because the microgravity-grown crystals were more than an

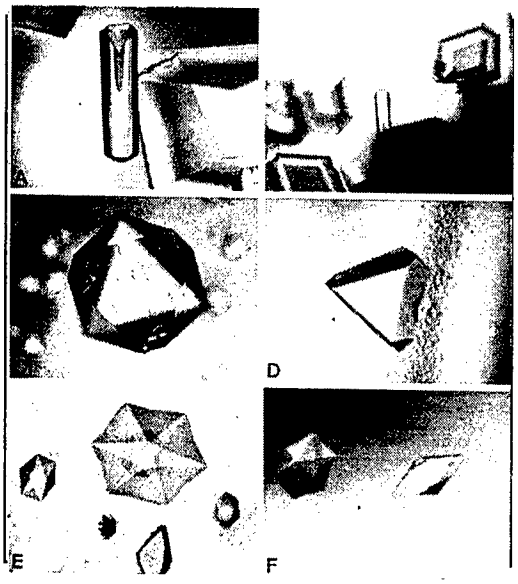

Figure 1: Crystals of proteins and viruses grown by liquid-liquid diffusion on IML-2. In A *and* B *are seen both rhombohedral and hexagonal crystals of the plant seed protein canavalin. The rhombohedral crystals are up to 1 mm on an edge, as are the lengths of the hexagonal prisms. The latter are characterized by a deep occlusion along the central axis not seen in crystals grown in a conventional laboratory. In* C *and* D *are two examples of the unusually large cubic crystals of STMV, more than 30 times the size of similar crystals grown on Earth. The STMV crystal in* D *can be seen nucleated from the surface of the quartz cell. The background of microcrystals seen in* C *are believed to have appeared after reentry from space. In* E *are crystals of TYMV displaying the unique, multifaceted forms observed only in these microgravity- grown crystals. In* F *are seen additional hexagonal bipyramidal crystals of TYMV in the APCF cell. The magnification of all photos is X40 .*

order of magnitude larger than any previously obtained on Earth.

Both rhombohedral and hexagonal canavalin crystals of large size (edges greater than 1 mm in length) were grown in large numbers (on the order of 100) in cells 208, 210, and 228. Generally both rhombohedral and hexagonal crystals were seen together, coexisting in the same cells. This is unusual in the laboratory but not unheard of. It was not seen in any of the control or optimization experiments conducted on Earth with identical protein samples.

Both the rhombohedral and hexagonal crystals were of uniformly high visual quality. The definition of edges was particularly striking for the hexagonal crystals and both forms were generally free of obvious defects, cracks, macrosteps, striations, or other imperfections. This increase in visual perfection is consistent with what we reported for canavalin crystals in previous microgravity experiments. The size distribution was excellent, with many large crystals, but none were of exceptional size that exceeded the largest obtained over the past 20 years in ground laboratories.

A striking morphological difference between hexagonal canavalin crystals grown in microgravity and on Earth was obvious, however. This was the extraordinary cusp, or occlusion, seen along the central prismatic axis of these crystals. The long, deep central cusp seen in this example was uniformly present in almost all of the hexagonal canavalin crystals grown on the mission.

X-ray diffraction analysis of the microgravity-grown canavalin crystals, both the rhombohedral and the hexagonal form, were both surprising and encouraging. We had previously grown canavalin crystals in space on numerous missions using a vapor diffusion technique. Large rhombohedral crystals were frequently grown in these experiments. When analyzed by X-ray diffraction, they demonstrated a significant improvement in signal-to-noise over the entire resolution range, but no clear improvement in the ultimate resolution of the diffraction pattern.

The results from IML-2, however, were quite different. Comparative Wilson plots of intensity, (I/σ) versus $\sin^2\theta/\lambda^2$ for 6 rhombohedral crystals chosen at random, demonstrated a marked improvement compared with the best data we had in hand from Earth-grown crystals, indeed, those that we used to actually refine the structure of rhombohedral canavalin. Even more striking, an appreciable extension of the resolution of the diffraction pattern was clearly evident for the crystals grown in microgravity.

The cubic crystal form of STMV generally grows to limited size in the laboratory, seldom if

Sample	Reactor #	Precipitant Connector	Concentration Reservoir	Results
TYMV 15 mg/ml	205	0.8 M $(NH_4)_2PO_4$	1.0M $(NH_4)_2PO_4$	many large crystals
TYMV 15 mg/ml	207	0.8M $(NH_4)_2PO_4$	1.2M $(NH_4)_2PO_4$	microcrystals
TYMV 15 mg/ml	222	0.8M $(NH_4)_2PO_4$	1.5M $(NH_4)_2PO_4$	many small crystals
SPMV 20 mg/ml	204	12% PEG 8000	12% PEG 8000	microcrystals
SPMV 24 mg/ml	206	15% PEG 8000	15% PEG 8000	microcrystals
STMV 24 mg/ml	223	14% sat'd $(NH_4)_2SO_4$	25% sat'd $(NH_4)_2SO_4$	6 large crystals
STMV 24 mg/ml	224	14% sat'd $(NH_4)_2SO_4$	30% sat'd $(NH_4)_2SO_4$	precipitate
STMV 24 mg/ml	227	14% sat'd $(NH_4)_2SO_4$	20% sat'd $(NH_4)_2SO_4$	several large crystals
Hexagonal Canavalin 22 mg/ml	208	1.5 x DPBS	2.0 x DPBS	15 large crystals
Hexagonal Canavalin 22 mg/ml	210	1.5 x DPBS	2.0 x DPBS	many medium crystals
Rhombohedral Canavalin 16 mg/ml	228	1.5 x DPBS	2.0 x DPBS	many medium crystals
Cytochrome c, 30 mg/ml	201	2.8 M $(NH_4)_2SO_4$	2.8 M $(NH_4)_2SO_4$	many large needles
Cytochrome c, 30 mg/ml	202	2.8 M $(NH_4)_2SO_4$	2.8 M $(NH_4)_2SO_4$	many large needles
Cytochrome c, 30 mg/ml	203	2.5 M $(NH_4)_2SO_4$	2.5 M $(NH_4)_2SO_4$	1 large crystal
Cytochrome c, 30 mg/ml	229	2.5 M $(NH_4)_2SO_4$	2.5 M $(NH_4)_2SO_4$	microcrystals & small clusters

ever exceeding 0.4 mm on an edge, and diffracts to only a low resolution of 6-8 Å. This is in striking contrast to the orthorhombic and monoclinic forms, which grow very large and diffract to 2.3 Å resolution in the laboratory.

Upon removing the crystallization cells from the APCF for photography, we immediately noticed, without visual aids, the extraordinarily large, octahedral habit, cubic crystals growing in cells 223 and 227. There were 15 of these crystals, and all had nucleated on the faces or in the edges and corners of the crystallization cells. The crystals had maximum linear dimensions greater than 1.5 mm and were, in the best cases, more than 30 times the volume of the largest cubic STMV crystals grown on Earth.

Whether from size alone or from some enhancement of the internal order, the resolution of the diffraction pattern of these crystals was extended significantly and to a limit of approximately 4 Å resolution versus 6 Å resolution for the best Earth-grown crystals. There is again an improvement of the I/σ ratio over the entire resolution range.

Crystals of TYMV can be readily grown in the laboratory to sizes greater than 1 mm on an edge. From synchrotron data to 3.2 Å resolution, the structure of this T = 3, 280 Å diameter virus is currently being determined. The immediate observation presented by the APCF-grown TYMV crystals produced in microgravity is the remarkable alteration in crystal morphology. Hundreds of TYMV crystals were grown in APCF cells 205 and 222. The indentation creasing the center of each triangular face and the subtle scalloping of each edge led to a significantly more polygonal, multifaceted shape for the crystals. This is the result of growth limited by diffusive transport at the most active points of unit addition.

X-ray diffraction analysis of the TYMV could only be carried out using our laboratory apparatus because no synchrotron source was available. Using this system we could not accurately record a representative intensity set over a broad resolution range and no comparative Wilson plot was possible. We estimated the resolution limit of several crystals, but we did not observe a significant extension of their diffraction pattern.

The only crystals observed in the APCF cells for the SPMV samples were a few very small microcrystals. No meaningful observations or X-ray diffraction data were collected from these. The failure of SPMV to produce any meaningful crystals is probably attributable to experimental conditions. The SPMV trials were the only liquid-liquid diffusion experiments reported here that employed PEG as the precipitating agent. Our impression, shared by other colleagues on this mission who also used PEG in their experiments, is that the diffusion rate of PEG is so slow that only a long-duration experiment in space using free interface diffusion would be successful. Thus we would predict that

optimization of conditions for PEG-based liquid-liquid diffusion will be hard to achieve on the ground. While PEG may be suitable for vapor diffusion and batch crystallization in microgravity, it might be wise to minimize its use in liquid-liquid diffusion trials on short-duration flights until its fluid properties are better understood.

Conclusion

Three kinds of IML-2 data suggest changes in the phenomena of macromolecular crystal growth as it occurs in microgravity compared with that in conventional laboratories. These include alteration in average or maximum size of crystals, morphological modifications, and changes in the diffraction properties.

The most straightforward of these to explain are the morphological changes observed in the canavalin hexagonal crystals and those in the TYMV crystals. Both the deep conical occlusion seen in the former and the scalloping of the edges and faces of the latter are readily explained by conversion from the mass transport regime that is dominated by convection on Earth to a near purely diffusive regime that dominates transport in microgravity. Both occur as a consequence of the most rapidly growing points on the crystal creating quasi-stable, local environments of reduced supersaturation leading in turn to the retardation of growth at those points. The hexagonal canavalin crystals and the TYMV crystals grown in microgravity provide macromolecular versions, and examples, of a phenomenon long known and studied for conventional crystals.

The dramatic increase in size observed for the cubic STMV crystals is, we believe, again attributable to diffusive transport processes in the absence of convective mixing. Because of the low diffusivity of macromolecules, and particularly so for viruses because of the large size, regions of reduced supersaturation, or depletion zones, form in the immediate neighborhood of crystals growing in microgravity. This self regulation of local supersaturation near growing crystals promotes more ordered and controlled addition of growth units to the developing crystal surfaces. These quasi-stable depletion zones have the further effect of limiting the transport of aggregates and larger molecular weight impurities having even lower diffusivity that are the most likely sources of imperfections and dislocations to the growing crystal. Since growth termination likely occurs because of the accumulation of defects, reducing their number would tend to promote greater ultimate size.

The IML-2 results suggest that the particular technique one employs in microgravity experiments may be of substantial consequence. The IML-2 results are consistent with IML-1 findings, and those reported by a number of other investigators from other missions. In many cases some dramatic alterations in crystal morphology were observed, nearly all explicable in terms of the diffusive transport processes that dominate in microgravity. In addition, some remarkable increases in crystal size were also seen (cubic STMV). Similar results for orthorhombic crystals of STMV were seen on IML-1. Finally, and most encouraging, unequivocal improvements in the quality and resolution of the diffraction patterns for some types of crystals (rhombohedral and hexagonal canavalin, cubic STMV) were clearly evident. While we cannot explain precisely why such improvements were obtained, we again believe them to be a function of the altered kinetics and mechanisms of presentation of molecules to the growing crystal surfaces that exist in microgravity.

References

Ban, N. and McPherson, A., "The three-dimensional structure of satellite panicum mosaic virus (SPMV)," *Virology,* vol. 215, pp. 571-583, (1996).

Canady, M. A., Day, J., and McPherson, A., "Preliminary X-ray diffraction analysis of crystals of Turnip Yellow Mosaic Virus (TYMV)," *PROTEINS,* vol. 21, pp. 78-81, (1995).

Day, J. and McPherson, A., "Macromolecular crystal growth experiments on International Microgravity Laboratory-1," *Protein Science,* vol. 1, pp. 254-1268, (1992).

Koszelak, S., Day, J., Leja, C., Cudney, R., and McPherson, A., "Protein and virus crystal growth on International Microgravity Laboratory-2," *Biophysical Journal,* vol., 69, pp. 13-19, (1995).

Crystal Growth of Ribonuclease S

Dr. L. Sjolin, Chalmers University of Technology and Göteborg University, Göteborg, Sweden

The structure of biological macromolecules, especially those of proteins, have been used in a variety of industrial studies that have led to new products. Industrial applications include protein engineering to tailor the properties of proteins for specific uses, molecular design of new pharmaceuticals, development of synthetic vaccines, and the development of biosensor technology. In many cases, crystals with increased size and superior diffraction properties would facilitate the determination of new structures and produce more accurate data for those structures already solved. The possibility of producing crystals under microgravity conditions has fueled studies supported by most of the world's space agencies. We used a variety of statistical methods to assess the differences between the X-ray diffraction data sets collected from Earth- and space-grown crystals.

Flight Activities

Ribonuclease S (RNase S) was crystallized in the Advanced Protein Crystallization Facility (APCF) using the vapor diffusion technique. A 10 mg/mL protein solution was prepared by dissolving 10 mg of the enzyme in 1 mL of 0.1 M sodium acetate, pH 5.0. The reservoir solution was 0.1 M sodium acetate, pH 5.0, 25% ammonium sulfate and 60% sodium chloride. The 6 RNase hanging drop reactors were divided into 3 groups, one with larger droplets. Crystallization occurred during unattended growth in the APCF. Two control experiments were performed with identical equipment on Earth concurrently with the flight experiments; after the mission, three of the flight reactors were used for further ground-control experiments.

Postflight Analysis

After the mission, the reactors were photographed and then opened for further photography and harvesting of the crystals. Crystals were harvested into a salt solution equivalent to the reservoir. The crystal content of each reactor was inventoried and photographed, and crystals of sufficient size were mounted for X-ray diffraction.

Highlights

- Crystals grown in microgravity had increased perfection, as measured by reduced mosaicity, and concordance, as measured by the agreement between diffraction data sets.
- Space-grown crystals had more uniform morphologies than Earth-grown crystals.

Five of the six RNase reactors, including all three of the larger-drop experiments, produced crystals. In the chamber with no growth, the protein solution had apparently been ejected from the crystallization cylinder, possibly as a result of disturbances around the time of launch. The results from Earth and space are similar. In both situations, a typical drop contains 2 or 3 large (longest dimension 0.8 - 12 mm) crystals, several medium size crystals (longest dimension 0.4 - 0.8 mm), numerous small crystals, and a quantity of crusty crystalline aggregate. In 0-g and 1-g, crystals grew on all surfaces inside the cylinders. Close inspection showed that the Earth crystals have rounder surfaces, while the space crystals have flatter faces. Also, a few crystals from two of the ground-control reactors contain ingrown cracks; such cracks were not seen in the space-grown crystals.

The space-grown crystals of ribonuclease S had a smaller mosaic spread and were larger or displayed more uniform morphologies than crystals obtained under comparable conditions on Earth. Analysis of the three-dimensional X-ray diffraction intensity data set from all 10 crystals of RNase S from both space and Earth clearly showed that the agreement of the intensity distributions for the crystals grown in space was superior to that of Earth-grown crystals. This indicates that the probability of finding a crystal that has better internal order is higher when crystals are grown in space.

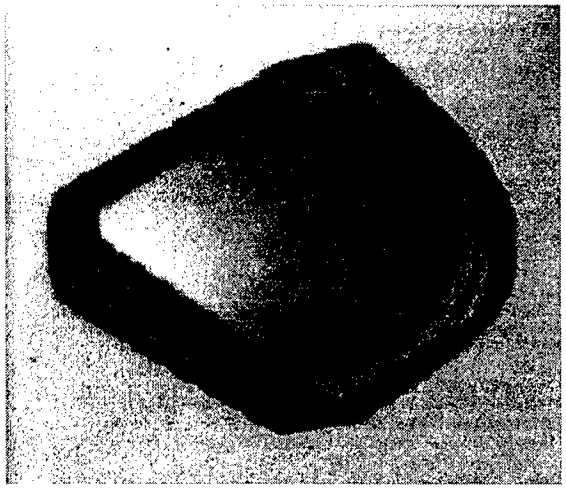

Figure 1: Close inspection showed that the Earth crystals had more rounded surfaces, while the space crystals had more flat faces.

The perfection of a protein crystal (determined by a reduced mosaicity, pronounced homology and symmetry, and higher diffraction data reproducibility) is an important indication of its potential usefulness in structure determination. This investigation proved that better methods of crystal growth (microgravity) directly affect the perfection of most protein crystals, which leads to smaller rocking widths. To fully use the plausibly enhanced perfection of these crystals, synchrotron data collection procedures are recommended for future experiments, especially if the rocking width of the reflections are thought to be smaller than the local data collection equipment can resolve in terms of beam divergence and/or detector resolution elements.

Conclusion

Crystals of ribonuclease S were successfully grown in space using the APCF. Five crystals of the enzyme grown in microgravity experiments were compared with five crystals grown on the ground under identical conditions. X-ray diffraction data were compared and analyzed.

The statistical results comparing X-ray data indicate that crystals grown in microgravity have increased crystal perfection, measured by reduced mosaicity, and concordance, as measured by the agreement between diffraction data sets from crystals grown in the same environment, Earth or space. The reduced mosaicity of the crystals necessitates the optimization of the experiment design for X-ray data collection for individual crystals to insure critical evaluation and comparison.

References

DeLucas, L.J., Suddath, F.L., Snyder, R., Naumann, R., Broon, M.B, Pusey, M., Yost, V., Herren, B., Carter, D., Nelson, B., Meehan, E.J., McPherson, A., and Bugg, C.E., "Preliminary investigations of protein crystal growth using the space shuttle," *J. Cryst. Growth*, vol. 76, p. 681, (1986).

Helliwell, J.R., "Protein crystal perfection and the nature of radiation damage," *J. Cryst. Growth*, vol. 90, p. 259, (1988).

McPherson A., "Virus and protein crystal growth on Earth, and in microgravity," *J. Phys. D. Appl. Phys.*, vol. 26, p. B104, (1993).

Sjolin L., Wlodawer, A., Bergqvist, G., Holm, P., Loth, K., Malmstrom, H., Zaar, J., Svensson, L.A., and Gilliland, G.L., "Protein crystal growth of ribonuclease A and pancreatic trypsin inhibitor aboard the MASER 3 rocket," *J. Cryst. Growth*, vol. 90, p. 318, (1991).

Svensson, L.A., Dill, J., Sjolin, L., Wlodawer, A., Toner, M., Bacon, D., Moult, J., Veerapandian, B., and Gilliland, G.L., "The crystal packing interaction of two different crystal forms of bovine ribonuclease A.," *J. Cryst. Growth*, vol. 110, p. 119, (1991).

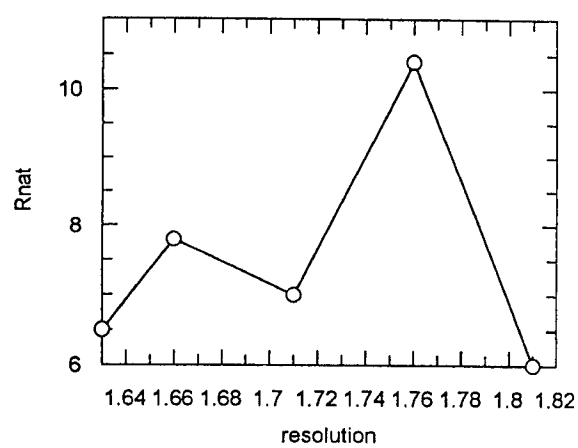

Figure 2: The multi-variate analysis showed there is no correlation between the overall resolution parameter and quality parameters such as R_{sym} and R_{nat}, regardless of the source of the crystal. A strong correlation was found between the R_{sym} and R_{nat} parameters possessing almost linear relationships in the performed experiments.

Crystallization of Ribosomal Particles in Space

Dr. A. Yonath, Max-Planck-Laboratory for Ribosomal Structure, Hamburg, Germany

Of all organelles in the living cell, only the ribosome has thus far been crystallized. The ribosome is the universal supramolecular assembly responsible for one of the most fundamental life-processes: the translation of the genetic code to proteins. Because of their importance in life sciences, ribosomes have been the target of numerous biochemical, genetic, and physical studies. Yet a full understanding of the molecular mechanism of the process of biosyntheses is still dependent on the availability of a molecular model for the ribosome.

All ribosomal particles display a marked tendency to form very thin crystals. Our best crystals, those that diffract to an almost atomic resolution, 2.9 Å, have a morphology that is most difficult to handle. Being fragile, thin plates (typical size of 0.2x0.2x0.001 mm), they tend to fracture, split, or crack upon handling, causing a lose of precious synchrotron radiation time and severe difficulties in data collection and evaluation.

We consistently observed that significantly better crystallographic data could be collected from thicker crystals grown occasionally in the laboratory. Therefore, we are investing considerable effort in obtaining them. We attempted to use microgravity for further improvement of crystal morphology and size.

Flight Activities

In preparation for the missions, we ran several test experiments, screening for the particular conditions that are most suitable for each of the ribosomal preparations. We used the method of vapor diffusion, attempting slow equilibration of small droplets with their reservoirs.

Highlights

- Grew crystals that had more isotropic shapes, which had never been observed on Earth.
- Growth of crystals without seeding indicates potential of microgravity.

The samples were prepared immediately before delivery to the KSC and inspected right after landing. The crystallization mixtures and reservoirs were prepared with the same compositions that have proved to be suitable on Earth.

Postflight Analysis

We have participated in seven missions. In all, regardless of the design of the crystallization chambers, almost every droplet yielded crystals even without seeding, which is a crucial requirement for the growth of quality crystals on Earth.

Although in most of the space experiments we had no control over the design of the crystallization chambers, it was possible to obtain crystals of intact ribosomal particles in space. In fact, crystals appeared in almost every chamber. Of special importance is the morphology of the crystals. A few crystals grown in space are of somewhat better proportions than those grown on Earth and have a more isotropic shape, indicating the potential of microgravity. In addition, almost all crystals grown in space are rather round, a property never observed on Earth.

Most of the fragile and delicate crystals did not break on returning to Earth, although we feel that some crystals did break during landing or on Earth while being transferred from the Shuttle to the laboratory. However, many others arrived at the laboratory intact, and crystals that had already formed (sent to space as a control experiment) remained intact after the mission was completed.

It is noteworthy that we attempted growing ribosomal crystals on Earth under conditions mimicking microgravity. We constructed

crystallization solutions with density similar to that of the crystals and attempted crystallization in these solutions, assuming that the crystals, once formed, would float rather than sink. In parallel, we tried to grow crystals within gels. None of these attempts were successful, presumably because the composition of the modified crystallization solutions was not suitable for crystal growth of ribosomal particles.

Conclusion

The significance and the uniqueness of our studies stem not only from the idea of growing crystals of giant, flexible, and unstable biological assemblies (ribosomes) under microgravity, but also from the expectations for the design of a tool for controlling specific properties in crystal morphology. The fact that a few years of constant effort were needed to reach our current resolution on Earth should not be overlooked. We believe that more screening for the exact conditions that promote better crystal growth will lead to desirable crystals.

We consider the mere growth of more isotropic ribosomal crystals under microgravity to be a remarkable achievement. Even on Earth, one has to search for proper crystallization conditions for each ribosomal batch. Since in individual space missions the possibility for exploration of conditions is limited, it is no wonder that refining the conditions for the growth of ribosomal crystals under microgravity requires participation in additional experiments. The objects for improving crystal quality will be the large (50S) subunits of *H. marismortui* and the small (30S) of *T. thermophilus.* The latter are important since they still do not diffract to a resolution comparable with that of the large (50S) subunits. We assumed that this is, in part, because of their small size and therefore attempted their growth in space (NASA: STS-42). Based on the encouraging results obtained in this mission (i.e., the production of a few small crystals of rather isotropic morphology), we plan to expand these experiments in future flights.

References

Erdmann, V.A., Lippmann, C., Betzel, C., Dauter, Z., Wilson, K., Hilgenfeld, R., Hoven, J., Liesum, A., Saenger, W., Muller-Fahrnow, A., Hinrichs, W., Duvel, M., Schulz, G.E., Muller, C.W., Wittmann, H.G., Yonath, A., Weber, G., and Plass-Link, A., "Crystallization of proteins under microgravity," *FEBS Letters*, vol. 259, p. 194, (1989).

Crystallization of Bacteriorhodopsin

Dr. G. Wagner, Justus-Liebig University of Giessen, Giessen, Germany

Small amphiphilic membrane proteins such as bacteriorhodopsin (BR), with little surface protruding the cell membrane, will be embedded in large numbers in the micelles after detergent solubilization, and the concept of small additives may not fundamentally change the situation. Detergent-solubilized BR molecules tend to form filamentous crystals such as micelles do in the hexagonal phase. The contacts that cause the BR filaments to pack together and to form a multicrystalline cluster are hydrophilic interactions between the loop regions of protruding BR molecules in aligned filaments. The hydrophilic interactions are weak and easily disturbed, resulting in considerable disorder in the BR crystalline array in the presence of convective turbulence and sedimentation. The lack of sedimentation and convection in microgravity may improve the growth of BR crystals using the liquid-liquid-diffusion technique.

Highlights

- Crystals were grown using two different techniques and varying ingredients.
- Crystals grown with liquid-liquid diffusion had sharp edges, smooth faces, and increased sizes, up to 200 μm in length.
- Adding benzamidine hydrochloride to crystals grown with liquid-liquid diffusion resulted in crystals with improved compact alignment of the crystalline filaments, increased crystal size, and higher resolution X-ray diffraction data.

Flight Activities

The liquid-liquid-diffusion technique of crystallogenesis predominantly was used in the Advanced Protein Crystallization Facility (APCF) throughout the experiments of the IML-2 mission. For one set of crystals, no benzamidine hydrochloride was added to the detergent-solubilized bacteriorhodopsin; for the other set, benzamidine hydrochloride was added to the growth chamber. As the ground control, the same ingredients were used for the same type of APCF growth reactors. As the laboratory control, the results in the liquid-liquid-diffusion technique were compared to those in the vapor diffusion technique performed using the same ingredients in laboratory hardware on Earth.

Postflight Analysis

After landing, the crystals were returned to the investigator for analysis and comparison to the ground and laboratory controls. Using the vapor diffusion technique, dimorphic three dimensional BR crystals were grown, i.e., pseudo-hexagonal needles and single cubic crystals. Crystals grown with liquid-liquid diffusion had a predominate cubic habit. In microgravity, the cubes with sharp edges and smooth faces considerably increased in size up to a length of 200 μm.

In the third set of crystals, in which benzamidine hydrochloride was added to the chambers, we verified both the compact alignment of the crystalline filaments of BR and the significant increase in crystal size under microgravity conditions. When subjected to X-ray diffraction analysis after the mission, these crystals had improved diffractional power, compared to the best crystals grown under the same conditions on Earth. Based on the iso-anisotropy of the unit cell in the crystalline array, a micellar type of bacteriorhodopsin crystal growth occurred.

Conclusion

Crystallographers are still exploring the best conditions for crystal growth in microgravity. For this experiment, the APCF made it possible for us to try two different growth techniques, varying the ingredients used to grow BR crystals. Compared to the ground and laboratory controls, cubic BR crystals of increased size were received in microgravity.

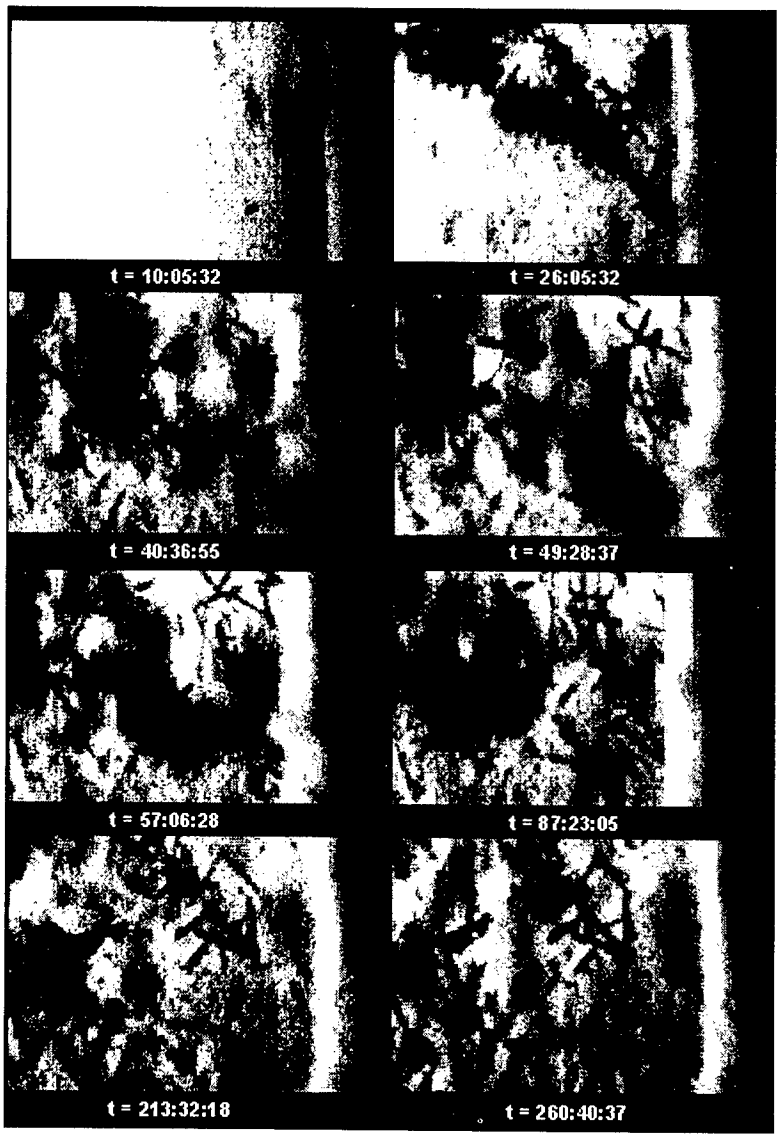

Figure 1: Sequence of video recordings of bacteriorhodopsin crystal growth in APCF during the IML-2 flight experiment in reactor #210-H, at the time points after reactor activation (t=h:min:s).

References

Wagner, G., "Bacteriorhodopsin crystal growth under microgravity - results of IML-1 and Spacelab-1 experiments," *ESA J.*, vol. 18, pp. 25-32, (1994).

Wagner, G., Rothärmel, T., and Betzel, Ch., "Crystallization and preliminary diffraction studies of baceriorhodopsin," *DESY-Yearbook,* (1995).

Wagner, G. and Rothärmel, T., "Dimorphic bacteriorhodopsin-mixed micelle crystal growth - results of IML-2 and USML-2 experiments," *Microgravity Science and Technology*, (1996), submitted.

Wagner, G., Rothärmel, T., and Briegleb, W., "The fast-rotating clinostat as a tool to mimic weightlessness for macromolecular crystal growth," *Internet:* http://www.hamptonresearch.com

FREE FLOW ELECTROPHORESIS UNIT (FFEU)

INVESTIGATIONS	PRINCIPAL INVESTIGATORS	RESULTS HIGHLIGHTS
Applications of Continuous Flow Electrophoresis to Rat Anterior Pituitary Particles (Part 1) Feeding Frequency Affects Cultured Rat Pituitary Cells in Low-Gravity (Part 2)	Dr. W.C. Hymer Pennsylvania State University University Park, Pennsylvania United States	A microgravity-feeding interactive effect occurred and affected hormone output and cell surface charge. Microgravity-processed samples had increases throughputs, greater bandspreads, and better discrimination of some growth hormone variants. Found differences in the quantity and quality (bioactivity) of growth hormone and prolactin released from primary rat pituitary cells *in vitro*. Changes were similar to those found in pituitary cells of space-flown rats after 7-14 days in microgravity.

INVESTIGATORS	PRINCIPAL INVESTIGATORS	RESULTS HIGHLIGHTS
Separation of a Nematode *C. elegans* Chromosome DNA by FFEU	Dr. H. Kobayashi Josai University Saitama, Japan	Used electrophoresis to collect DNA samples in space. Used a new computer program to monitor experiment in space from the ground.
Experiments of Separating Animal Cell Culturing Solution in High Concentration in Microgravity	Dr. T. Okusawa Hitachi, Ltd Ibaraki, Japan	Cells cultured in space produced twice as much protein as those cultured on Earth. Electrophoresis was much more stable in space than on Earth.

Applications of Continuous Flow Electrophoresis to Rat Anterior Pituitary Particles (Part 1)

Dr. W. C. Hymer, Pennsylvania State University, University Park, Pennsylvania, United States

During continuous flow processing, distortions of the sample stream occur; these are hydrodynamic, electrodynamic, and electrohydrodynamic in character. Some are limited by Earth's gravity. Gravitational effects on biological systems relevant to electrophoretic measurements include sedimentation of cells and organelles, flotation of some lipid materials, buoyant convection, segregation of components by density, and perhaps flows that originate from the interplay of density gradients and interfacial tension.

Our laboratory has applied electrophoresis technology to the separation of rat pituitary cells and their subcellular constituents. In a 1983 microgravity experiment, increased bandspread of recovered cells suggested enhanced resolution of the different hormone-containing cell types, but poor recoveries and biological contamination did not establish this point definitively.

Flight Activities

The availability of the Cell Culture Kits (CCK) and the Free Flow Electrophoresis Unit (FFEU) allowed us to use continuous flow electrophoresis to separate organelles contained in a rat pituitary cell lysate prepared from cultured cells during microgravity operations. Pituitary cells ($4x10^7$) in 3 CCKs were prepared 3 days before launch. Cells in one of the CCKs were not fed before preparation of the cell lysate on flight day 9. Fifty percent of the flight lysate was processed during the mission; the remainder was processed later at our laboratory. The samples fractionated and frozen in space were returned to our laboratory for analysis.

Postflight Analysis

After landing, cells were removed from 1 cell chamber (fed 4 times in microgravity) and from another (not fed during the 14-day mission).

Highlights

- A microgravity-feeding interactive effect occurred and affected hormone output and cell surface charge.
- Microgravity-processed samples had increases throughputs, greater bandspreads, and better discrimination of some growth hormone variants.

Cell viabilities averaged 93 and 90% for fed and unfed cells, respectively. Both samples were processed by continuous flow electrophoresis (CFE). Sufficient cells were obtained after processing of the fed cells to do a 6-day culture of the separated cells.

The concentration of growth hormone (GH) in the flight lysate was 20% greater than that in the synchronous ground-control preparation, a result that is consistent with the finding that there were also greater amounts of GH released into the 9-day culture medium before lysate preparation. After continuous flow electrophoresis processing in microgravity, 9 out of 30 fractions contained detectable growth hormone; after synchronous ground processing, only 5 fractions contained detectable GH. Three GH peaks were found after flight processing, but only one was present in the ground trial. When frozen aliquots of these same concentrated lysates were subsequently processed on Earth, the distribution profiles of GH were essentially identical. Postflight tests indicate that while the general protein profiles of the starting lysates were similar, there was a tendency for the flight samples to contain higher molecular weight material (>29,000).

Hardware failure prevented us from doing an actual CFE separation trial in microgravity. Instead, cells from flight groups (fed and unfed) were processed individually by CFE at Kennedy Space Center within 8 h after Shuttle landing. After CFE separation, fed cells from both flight and synchronous ground controls were cultured for 6 days to determine if separated cells released GH and if the CFE process enriched

GH-producing cells equally well from both flight and ground samples. For an unknown reason, the microgravity-exposed cells that were fed during space flight released ~5 times more hormone than corresponding ground controls. Space-exposed cells showed greater bandspread. Most interestingly, high-producer GH cells had greater electrophoretic mobility (~7.2 x 10^{-4} cm^2/vs) than their ground control counterparts (~3.9 x 10^{-4} cm^2/vs).

The average electrophoretic mobility distribution profiles of unfed ground and flight cells were similar. These profiles add support to the concept that there may be specific microgravity-feeding interactions that affect cell electrophoretic mobility. The morphologies of growth hormone cells prepared from ground and flight cultures before and after continuous flow electrophoresis processing revealed the presence of intact cells that were typical of those seen in other studies.

Conclusion

Even though not all the original objectives were met, our results indicate that continuous flow electrophoresis processing in microgravity is advantageous. The flight sample had increased throughput, 5.6 times more concentrated than the ground sample. There was a greater bandspread of growth-hormone-containing particles in the lysate sample and better discrimination of some GH variants within different fractions. Since this same microgravity sample did not show a mobility difference when it was processed at 1-g, we conclude that microgravity exposure has little effect on the net surface charge of intracellular GH-containing particles. On the other hand, microgravity-exposed cells had markedly different mobilities. The idea that microgravity may effect the net cell surface charge density, depending upon the cell culture conditions, is to our knowledge entirely new. Our data also indicate that feeding pituitary cells in microgravity alters their net surface charge. It is unknown whether this reflects a gravisensing mechanism or is the result of one.

Our data established that high mobility growth-hormone-producing cells were recovered from flight (but not ground) cell containers and also that a microgravity-feeding interactive effect occurred that apparently affects not only hormone output but also cell surface charge. This experiment showed that the rat pituitary cell system lends itself well to microgravity experimentation involving the coupled technologies of cell culture and continuous flow electrophoresis.

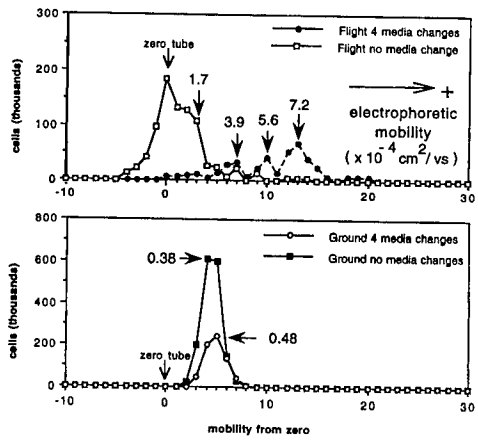

Figure 1: Electrophoretic mobility profiles for cells cultured in space and on the ground.

References

Hymer, W., Grindeland, R., Salada, T., Cenci, R., Krishnan, K., Mukai, C., and Nagaoka, S., "Feeding frequency affects cultured rat pituitary cells in low gravity," *J. Biotechnology,* vol. 47, pp. 289-312, (1996).

Hymer, W., Salada, T., Cenci, R., Krishnan, K., Seaman, G.V.F., Snyder, R., Matsumiya, H., and Nagaoka, S., "Bioprocessing in microgravity: applications of continuous flow electrophoresis to rat anterior pituitary particles," *J. Biotechnology,* vol. 47, pp. 353-365, (1996).

Hymer, W., Grindeland, R., Salada, T., Nye, P., Grossman, E., and Lane, P., "Experimental modification of rat pituitary growth hormone cell function during and after space flight," *J. Appl. Physiol.,* vol. 80, no. 3, pp. 955-970, (1996).

Hymer, W., Salada, T., Avery, L., and Grindeland, R., "Experimental modification of rat pituitary prolactin cell function during and after space flight," *J. Appl. Physiol.,* vol. 80, no. 3, pp. 971-980, (1996).

Hayes, D., Exton, C., Salada T., Shellenberger, K., Waddle, J., and Hymer, W., "Separation of rat pituitary secretory granules by continuous flow electrophoresis," *Electrophoresis,* vol. 11, pp 976-978, (1990).

Feeding Frequency Affects Cultured Rat Pituitary Cells in Low-Gravity (Part 2)

Dr. W.C. Hymer, Pennsylvania State University, University Park, Pennsylvania, United States

We have studied rat anterior pituitary gland cell structure and function during and after space flight. Investigators have focused on synthesis and release of growth hormone (GH) and prolactin (PRL) molecules because these two protein hormones are known to participate in the regulation of musculoskeletal, immune, vascular, metabolic, and endocrine systems, all of which are often changed in microgravity.

The unique design of the cell culture hardware permitted the first studies of possible effects of cell feeding on hormone release from each of 6 major hormone-containing cell types. The payload specialist was able to prepare fresh solutions from preweighted powders and use them to trypsinize the anchorage-dependent pituitary cells from their surface.

Flight Activities

Before launch $4x10^7$ cells were selected into each of 6 Cell Culture Kits (CCK). Three CCKs were maintained in an incubator in the Shuttle middeck, and three were kept under similar conditions in a ground laboratory. Constant real-time monitoring of operational parameters of this incubator in microgravity indicated that the temperature variance between the ground and flight units was ±0.1 °C; relative humidity ranged between 40-60% in both units. The crew changed culture medium four times in one CCK and once in another, while the cells in the third were left undisturbed for the entire mission.

The hardware permitted microscopic observations of cells attached to the pronectin-treated polycarbonate surface, removal of spent media and storage at -20 °C, addition of fresh culture media, and onboard preparation of 2 fresh solutions from preweighed powders stored in syringes.

Highlights

- Found differences in the quantity and quality (bioactivity) of growth hormone and prolactin released from primary rat pituitary cells *in vitro*.
- Changes were similar to those found in pituitary cells of space-flown rats after 7-14 days in microgravity.

Postflight Analysis

Within 3 h after landing, cells in each of the 6 CCKs were photographed, media was withdrawn, and cells were removed. The viabilities of cells removed from the CCKs were >90%. A portion of these cells were used for morphological analysis, and the remainder was subjected to separation by free flow electrophoresis.

The total amounts of immunoreactive hormones released from either ground or flight cells varied over a wide range, i.e. ~10 mg (LH, FSH, and TSH); 2-10 mg (PRL and GH), ~100 ng (ACTH). There was a 4x increase in GH released from unfed flight cells; slight to moderate reductions in LH released from fed cultures; small increases in GH and PRL release from cells fed 4 times; and 2-fold increases in total ACTH release.

When the same media from all 3 CCKs were assayed for their content of biologically active GH and PRL, interesting flight-related differences were found, both in total amounts of bioreactive hormone released and in the kinetics of that release. In terms of the total bGH release, there was a ~50% reduction from fed flight cells and a doubling of hormone from unfed flight cells. For total bPRL release, the opposite occurred. There was a 2.5x increase in total bPRL release from cells fed 4 times in microgravity while unfed PRL cells reduced bPRL output by one-half.

Microscopy revealed that live cells were present in all ground and flight chambers. Photographs

documented cell viability and growth patterns, which were sometimes different in microgravity.

Conclusion

Operations in biotechnology laboratories on Earth routinely couple one process with another. This experiment demonstrated the feasibility of several operations that will be required on a routine basis during the space station era.

We found complex microgravity-related interactions between the frequency of cell feeding and the quantity and quality (biological activity) of some of the six hormones released in flight. Analysis of growth hormone molecules released from cells into culture media on different mission days was measured using gel filtration and ion exchange chromatography and showed similar results for ground and flight cultures. Vigorous fibroblast growth occurred in both ground and flight cultures fed four times. These results are interpreted within the context of autocrine and/or paracrine feedback interactions.

The payload specialist prepared fresh trypsin solution in microgravity, detached cells from their surface, and reinserted them into the culture chamber. These cells reattached and continued to release hormone in microgravity.

Our data indicated that anterior pituitary gland function is affected in low gravity. Complete definition of the underlying cellular and molecular mechanisms will require extensive use of cell culture technology in microgravity. When the mechanisms are better understood, they should prove of use in studies aimed at defining countermeasures to physiological changes encountered during space flight. At the same time, the unique microgravity environment can help us learn about the function of this complex neuroendocrine system on Earth.

In summary, this experiment provided significant new information concerning the issue of direct microgravity effects on pituitary cell structure and function in microgravity. Some pituitary cell types directly sense the lack of gravity, regardless of whether they are present in their native condition. (i.e., in the rat) or in a cell culture system. In terms of secreting function, of the six major hormones producing cell types, GH, PRL, and ACTH cells appear to be the most sensitive to the microgravity environment.

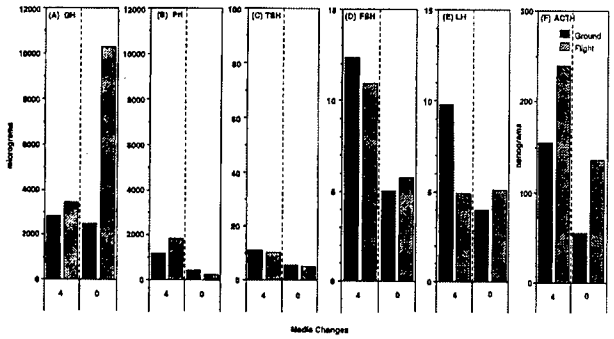

Figure 1: Release of immunoreactive (A) GH, (B) PRL, (C) TSH, (D) FSH, (E) LH, and (F) ACTH from cells cultured in microgravity and on the ground.

References

Hymer, W., Grindeland, R., Krasnov, I., Victor, I., Motter, K., Mukherjee, P., Shellenberger, K., and Vasques, M., "Effects of space flight on rat pituitary cell function," *J. Appl. Physiol.,* vol. 73, no. 2, pp 151S-157S, (1992).

Hymer, W., Grindeland R., Salada, T., Nye, P., Grossman, E., and Lane, P., "Experimental modification of rat pituitary growth hormone cell function during and after space flight," *J. Appl. Physiol.,* vol. 80, no. 3, pp. 955-970, (1996).

Hymer, W., Salada, T., Avery, L., and Grindeland, R., "Experimental modification of rat pituitary prolactin cell function during and after spaceflight," *J. Appl. Physiol.,* vol. 80, no. 3, pp. 971-980, (1996).

Grindeland, R., Hymer, W., Farrington, M., Fast, T., Hayes, C., Motter, K., Patil, L., and Vasques, M., "Chanes in pituitary growth hormone cells prepared from rats flown on Spacelab 3," *Am. J. Physiol.,* vol. 252, pp. R209-R215, (1987).

Hymer, W. and Hatfield, J., "Separation of cells from the rat anterior pituitary," *Methods in Enzymology,* Colowick, S. and Kaplan, N., eds., Academic Press, San Diego, vol. 103, part H, pp. 257-287, (1983).

Separation of a Nematode *C. elegans* Chromosome DNA by FFEU

Dr. H. Kobayashi, Josai University, Saitama, Japan

Free flow electrophoresis is an efficient method for the separation of cells, organelles, and any suspension of biological materials. Although DNA can be separated in a gel matrix by applying a pulse electric field, this method is not adequate to collect enough for a DNA sequencing study or a DNA reconstruction study. We tried to separate a macromolecule of DNA under formation of a pH gradient in the Free Flow Electrophoresis Unit (FFEU). In microgravity, the separation can be carried out efficiently using a high voltage without thermal convection.

We selected the DNA prepared from *Caenorhabditis elegans* (*C. elegans*). Since the Mendelian and molecular genetics and cell lineage have been established for the nematode, it is useful for studying the development and behavior by genetic analysis. The objectives of this experiment were to separate *C.elegans* DNA with the FFEU, to observe the migration profile of the two markers in real-time, and to collect the fractionated sample by judging the profile of the electrophoresis. After the flight, we planned to measure the pH gradient and the conductivity and to analyze the DNA of the fractionated sample. The analyses of the electropherogram, the pH gradient formation, the conductivity of separated sample, and the DNA contents elucidate a part of free flow electrophoresis. The separation experiment confirms that the technique works better in microgravity.

Flight Activities

The effective size of the FFEU separation chamber was 60 mm in width, 100 mm in height, and 4 mm in thickness. The maximum electric field of the separation chamber was 100 V/cm and 100 mA. The 60 separation tubes at the ports of the plunger pump could collect the fractionated fluid in a maximum of 5.0 ml each.

Highlights

- Used electrophoresis to collect DNA samples in space.
- Used a new computer program to monitor experiment in space from the ground.

The 30 separation tubes and the buffer tank were loaded on the Space Shuttle 17 h before launch. The experiment was performed on the tenth day of the mission. The time of the experiments was reduced by two-thirds because an In-Flight Maintenance procedure was performed to remove bubbles inside the FFEU's cooling water system. The success of the procedure allowed us to collect some samples.

Electrophoresis was performed at an applied electric field strength of 33.3 V/cm (the circuit voltage of 200) and on flow rates of the buffer in 3 cm/min and the sample in 2.5 cm/min, respectively. During the electrophoresis, the current value of the circuit increased gradually from 9 to 11 mA and reached a constant value, 12 mA, after 760 sec from charging the electric field. The fractions, 12 and between 22 and 50, were recovered in the 30 separation tubes and kept at -20 °C until the landing.

Postflight Analysis

After landing, we chose the fractions which contained more than 1 ml and then analyzed the DNA contents of these samples according to the PCR method with the two probes, sod-4 and unc-6 gene. The highest content of DNA was detected in fraction number 35, and the ratio of DNA component estimated by the sod-4 and unc-6 gene was around sevenfold. The fraction number 32, the second highest peak, contained almost all the same ratio of DNA component. Those peaks may have contained different contents of DNA and different kinds of DNA.

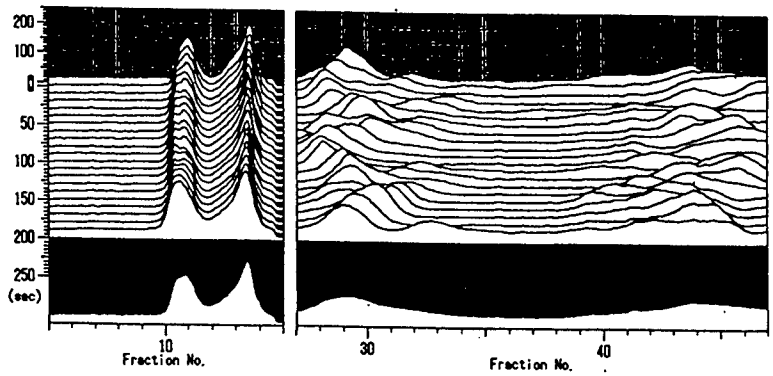

Figure 1: The 3 DEP of the DNA sample from space (left) and from the ground (right). Z-axis shows the time during 200 sec. The magnitude of X-axis is the same in both figures.

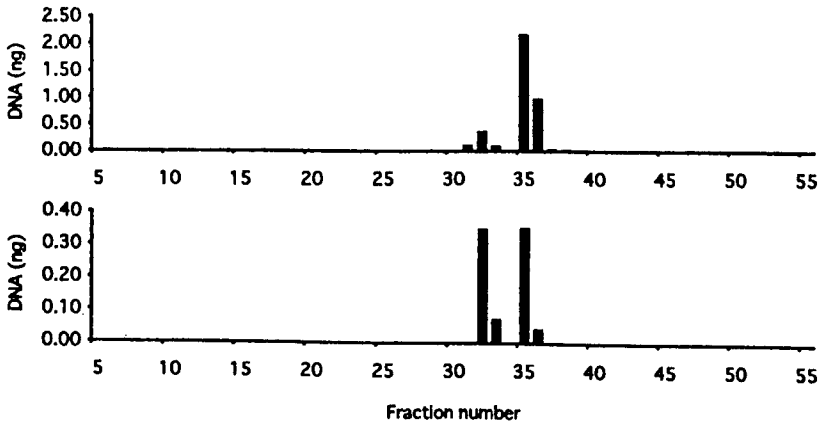

Figure 2: Relative DNA contents in the samples fractionated by electrophoresis in space.

Conclusion

Two specific types of DNA were separated effectively from the DNA mixture prepared from *C. elegans*. Because of the bubble in the separation chamber, the recovered volumes in the separation tubes were irregular, and the experiment of the comparison of electric field strength could not proceed. However, parts of the process were advanced: the real-time computer monitoring from the ground, the contamination-free solution, and the lack of thermal convection in the electrophoresis process.

References

Serafini, T., Kennedy, T.E., Galko, M.J., Mirzayan, C., Jessell, T.M., and Tessier-Lavigne, M., *Cell*, vol. 78, pp. 409-424, (1994).

Wilson, R., *et al.*, *Nature*, vol. 368, pp. 32-38, (1994).

Kobayashi, H., Ishii, N., and Hirokawa, T., *ISAS Space Utilization Symposium*, pp 151-154, (1992).

Ishii, N., Wadsworth, W.G., Stern, B.D., Culotti, J.G., and Hedgecock, E.M., *Neuron*, vol. 9, pp. 873-881, (1992).

Experiments of Separating Animal Cell Culturing Solution in High Concentration in Microgravity

Dr. T. Okusawa, Hitachi, Ltd, Ibaraki, Japan

Animal cells synthesize physiologically active substances, such as antibody proteins, growth and transfer factors, that have medicinal value. Recently, a method for culturing animal cells in high concentration has been put to practical use. The method yields pharmaceutical products such as interferon, interleukin, and monoclonal antibodies, which are secreted by the cells cultured continuously in solution when supplied with nutrients and oxygen. But since only very small quantities of these useful substances are produced by the cells, efficient purification technology is critical. Purification is, at present, carried out through a series of ultrafiltrations combined with a final chromatographic separation, but the following problems remain: limited resolution and difficulty in recycling cells because of physical damage in the ultrafiltration processes.

We expect space electrophoresis to provide an answer to the problems because it can purify substances in large quantity with high resolution. Space electrophoresis has been expected to improve separation resolution remarkably because of the absence of gravity-induced thermal convection. A cell suspension at high concentration is directly fractionated with an electrophoretic unit to get the trace biological substance. The first aim of this study was to develop an efficient separation technology using the advantage of the microgravity condition in space. Our second aim was to investigate the feasibility of the continuous purification process of cell suspension in high concentration. Since space-cultured cells have been reported to produce more secretion than those cultured on Earth, we expected space electrophoresis combined with space cultures to be very effective.

Space electrophoresis is expected to provide excellent separation resolution and throughput due to the absence of gravity, especially for cells because of higher density than the electrophoretic buffer. Our sample was a mixture of cells and culture medium. The cell, STK1, secretes an antibody or IgG (Immunoglobulin G) that has potential uses in cancer treatment and diagnosis.

Highlights

- Cells cultured in space produced twice as much protein as those cultured on Earth.
- Electrophoresis was much more stable in space than on Earth.

Flight Activities

After launch, cells multiplied in a culture to a saturated concentration so that cell secretion might attain its maximum. Using a microscope equipped with a camera, the crew recorded cell growth status in a cell culture kit (CCK) before electrophoresis; this was also done with ground control samples. The cell concentration and viability in the ground control experiment were found to be 1.9x106/cm^3 and 15%. The space-cultured and ground-cultured cells produced about 50 μg/cm^3 and 26 μg/cm^3 of IgG respectively. That is, the space-cultured cells were found to have double the secretion of the ground-cultured cells.

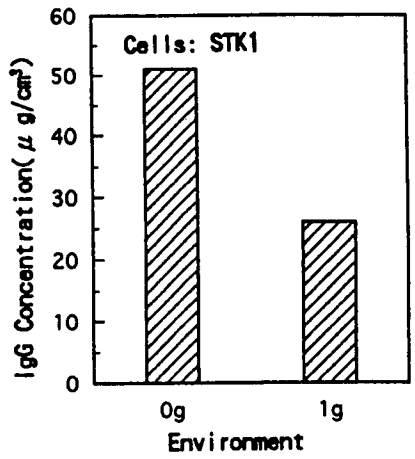

Figure 1: Environmental effect on cell secretion

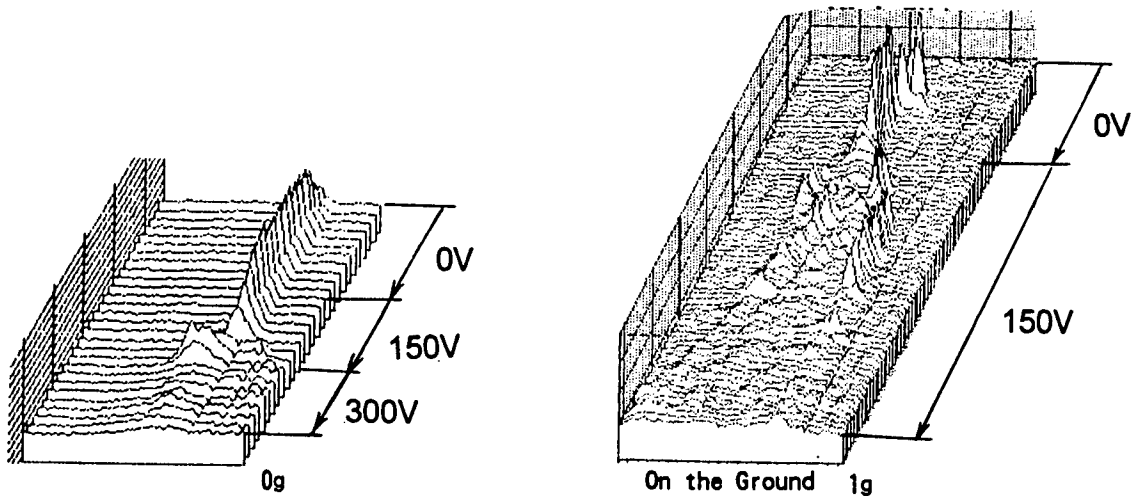

Figure 2: Comparison of electrophoretic behavior (Sample detector outputs)

Next, the cell suspension liquid was injected into the Free Flow Electrophoresis Unit (FFEU) to be separated. Although the FFEU had 60 fractionating outlets, only 30 fractionating tubes were available because of the stowage limit. Therefore, selection of the fractionating outlets depended critically on the sample detector outputs. Electrophoretic separation was detected with a sample detector. By taking advantage of the fact that 254 nm light is well absorbed by a protein such as the cell or IgG, positions and relative concentration of separated components were detected in a sample. The crew and ground monitored the data in real time, and data were downlinked for postflight analysis.

Postflight Analysis

Cell-secreted IgG content was measured after the flight on the basis of antigen-antibody reaction. Channels 1 to 17 were the part of the electrophoretic field in which electrophoresis could occur in spite of the air bubble contamination. Except at 0V, there were 2 main peaks: one was IgG, and the other was cell debris. On the ground, at 150V, the IgG was tagged and dissipated abruptly because of thermal convection initiation. In space, at 150V, the IgG was near fraction channel 17, and at 300V, it went into the air bubble region, that is, it was driven out of the electrophoretic field. However, by comparison, we found that the output peak in space was much more stable than that on the ground, especially at 0V. This indicated that space

electrophoresis could improve the separation resolution remarkably.

Conclusion

Cells cultured in space produced double the secretion of cells cultured on Earth. Although it was hampered by bubble penetration, space electrophoresis appeared to give a much more stable performance than ground-based electrophoresis. The investigator recommends the use of In-Flight Maintenance procedures for future space experiments, since it saved this IML-2 experiment.

References

Okusawa, T., *et al.*, "Electrophoretic separation of animal cell culturing solution," *Japanese Society of Mechanical Engineers, 72nd Conventional General Meeting, Wading Technology Forum 15, Learned Lessons of Mechanical Engineers from IML-2,* (1995) (in Japanese).

Hitachi, Ltd., "System for culturing animal cells in high concentration," *Free-flow Electrophoresis,* JETRO, 88-10-004-254, Hannig, K., et *al.*, eds., GIT Verlag (1990).

Okusawa, T., *et al.*, "Investigation on electrophoretic separation of cell culturing suspension for IML-2," *Proceeding of 18th International Symposium on Space Technology and Science*, pp. 2229-2234, (1992).

APPLIED RESEARCH ON SEPARATION METHODS USING SPACE ELECTROPHORESIS (RAMSES)

INVESTIGATIONS	PRINCIPAL INVESTIGATORS	RESULTS HIGHLIGHTS
Purification of Biological Molecules by Continuous-Flow Electrophoresis in a Microgravity Environment	Dr. V. Sanchez, Université Paul Sabatier, Toulouse France and Dr. B. Schoot, Roussel Uclaf, Romainville, France	Stable flows were obtained in microgravity under all conditions studied, showing that certain problems encountered on Earth are related to instabilities of gravitational origin that arise from either within the carrier buffer or around the sample filament. For the purification of biologically active substances, the use of microgravity and concentrated samples allowed the throughput to be increased by a factor of about 5, while rendering a product equally pure and biologically active.
Electrohydrodynamic Sample Distortion During Electrophoresis	Dr. R.S. Snyder NASA Marshall Space Flight Center, Alabama, United States	Disturbances by phenomena such as electrohydrodynamics, must be characterized to examine their effects on space electrophoresis. The experiment was not completed because of a power failure, but some parts may be done on a MAXUS sounding rocket.

SLOW ROTATING CENTRIFUGE MICROSCOPE (NIZEMI) MATERIALS SCIENCE EXPERIMENT

INVESTIGATIONS	PRINCIPAL INVESTIGATORS	RESULTS HIGHLIGHTS
Convective Stability of Solidification Fronts (Moni)	Dr. K. Leonartz Engineering, Aachen, Germany (formerly with ACCESS e.V.)	First observation of the growth transition from near diffusive to convective mass transport in a melt as a function of increasing g-level. First use of NIZEMI for directional solidification.

Purification of Biological Molecules by Continuous-Flow Electrophoresis in a Microgravity Environment

Dr. V. Sanchez, Université Paul Sabatier, Toulouse France and Dr. B. Schoot, Roussel Uclaf, Romainville, France

When electrophoresis is performed on Earth in a free liquid, the electrophoretic separation is very sensitive to natural convection in the medium that can in certain cases cause remixing of the substances as they separate, thus making the system inoperative. The Recherche Appliquee sur les Methodes de Separation en Electrophorese Spatiale/Applied Research on Separation Methods Using Space Electrophoresis (RAMSES) facility was part of the Physical Sciences in Microgravity program of the Centre National d'Etudes Spatiales (CNES) and was built to study the separation of biological substances by continuous-flow zone electrophoresis. With the investigators and CNES, the facility was built in collaboration with several French, Belgian, and Spanish industrial partners.

In using weightlessness, the aim was to stabilize the liquid so as to emulate gel electrophoresis and thus obtain the best resolution for this process. From the technological point of view, it was essential to qualify the designs and technologies involved in the subsystems of the facility operating in microgravity.

Scientifically, the goals were (1) to determine the optimum conditions for separating biological species from a given mixture, (2) to evaluate the quality of the separation (the resolution and the yield in purified substance, (3) to verify and validate the theoretical model of the process, (4) to demonstrate the relevance of microgravity to the performance of the process (both in terms of quality and quantity), and (5) to study the possibility of applying the results obtained to the case of purifying biologically useful substances.

Highlights

- Stable flows were obtained in microgravity under all conditions studied, showing that certain problems encountered on Earth are related to instabilities of gravitational origin that arise from either within the carrier buffer or around the sample filament.
- For the purification of biologically active substances, the use of microgravity and concentrated samples allowed the throughput to be increased by a factor of about 5, while rendering a product equally pure and biologically active.

Flight Activities

Five experiments were planned. The first was a "reference" separation that contained two colored proteins (hemoglobin and dyed BSA) using the same operating conditions as on Earth.

The next two experiments, E2 and E3, devised by the Laboratoire de Génie Chimique at the Université Paul Sabatier, were concerned with the separation of two proteins of know physicochemical properties. The final two experiments were concerned with purifying a protein of therapeutic interest from a crude bacterial extract.

Postflight Analysis

The first experiment confirmed that migration distances in space were the same as observed on Earth. The next two experiments showed the dependence of sample displacement and resolution on the concentration of the two proteins. Although the dilute samples were separable, it was not possible to distinguish the two peaks in the concentrated profile. However, up to 26% was still recoverable as pure protein from the distribution "tails".

The commercial protein mixture from Rossel-Uclaf showed broad bands with enrichment of the desired protein obtained from collected samples. A better purification was obtained with the longer residence time since the spreading did not increase proportionally.

These flight results were supported by an extensive model development that was confirmed by several operational measurements.

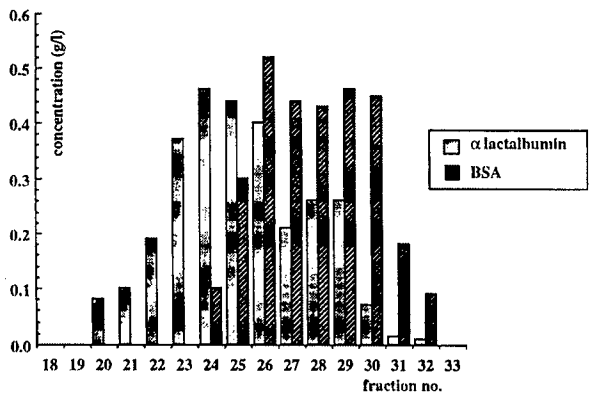

Figure 1: RAMSES Experiment E3: Protein concentration profiles in the collected fractions. With no electric field applied, the proteins were in fraction No. 8.

Conclusion

From a scientific point of view, several conclusions can be drawn. The first concerns the advantage offered by microgravity, which from Earth-based research had been expected to allow a much broader range of useful operating conditions. Stable flows were obtained in microgravity under all the conditions studied; this shows unequivocally that certain problems encountered on Earth are truly related, as had been thought, to instabilities of gravitational origin, arising either within the carrier buffer or around the sample filament.

The comparison of results obtained with samples of different concentrations, made possible by microgravity, showed that under the physicochemical conditions chosen (i.e., for proteins far from their isoelectric points) an increase in concentration (by a factor of 10) leads to a definite decrease in the quality of the separation. The use of a numerical model representing the behavior of the sample filament during its passage through the chamber has shown that the phenomenon responsible for this experimental observation is electrohydrodynamics. This phenomenon is related to the conductivity difference between the sample and the carrier buffer.

Finally, particularly interesting results were obtained in the purification by continuous-flow electrophoresis of biologically active substances. In this case microgravity, with the use of more concentrated samples, allowed the throughput to be increased by a factor of about 5, while giving a product equally pure and biological active.

References

Clifton, M.J., Roux-de Balmann, H., Sanchez, V., Bleuzen-Mariotte, V., and Schoot, B.M., "Purification of biological molecules by continuous-flow electrophoresis in the second international microgravity laboratory," *J. Biotechnology,* vol. 47, pp. 341-352, (1996).

Clifton, M.J., Roux-de-Balmann, H., and Sanchez, V., "Protein separation by continuous-flow electrophoresis in microgravity," *AIChE J.,* vol. 42, no. 7, pp. 2069-2079m (1996).

Clifton, M.J., "Numerical simulation of protein separation by continuous-flow electrophoresis," *Electrophoresis,* vol. 14, no. 12, pp. 1284-1291, (1993).

Clifton, M.J., Roux-de Balmann, H., and Sanchez, V., "Electrohydrodynamic deformation of the sample stream in continuous-flow electrophoresis with an AC electric field," *Can. J. Chem. Eng.,* vol. 70, pp. 1055-1062, (1992).

Electrohydrodynamic Sample Distortion During Electrophoresis

Dr. R.S. Snyder, NASA Marshall Space Flight Center, Alabama, United States

The specific objectives of this investigation were two-fold: to study the effects of sample concentration on sample stream distortion and to determine the limits of electrohydrodynamic (EHD) stability of the sample stream in the absence of shear flow. Analysis of previous flight experiments has depended entirely on photography of separated sample bands and evaluation of collected fractions. Although this data has demonstrated the magnitude of the problem and the importance of the interaction between the electrical and the fluid forces, complete resolution of the numerous interactions involved will require variation of the forces and operating conditions as well as a three-dimensional view of the sample bands being distorted by these forces.

Electrokinetic and EHD effects will be selectively evaluated by the appropriate use of AC or DC electric fields. Sample stream distortions resulting from specified experimental conditions can be determined from concentration profiles obtained using the UV spectrophotometer and from visible analysis using the cross-sectional illuminator and traditional frontal photography.

Highlights

- Disturbances by phenomena such as electrohydrodynamics, must be characterized to examine their effects on space electrophoresis.
- The experiment was not completed because of a power failure, but some parts may be done on a MAXUS sounding rocket.

Flight Activities

The experiments were to be done in the RAMSES (Recherche Appliqué sur les Methodes de Separation en Electrophoreses Spatiale/ Applied Research on Separation Methods Using Space Electrophoresis), a multipurpose facility for the study of electrokinetic phenomena in microgravity, proposed by the Centre National d'Etudes Spatiales (CNES) as part of the French contribution to the scientific efforts of the IML-2 mission.

The system, consisting of an electrophoretic separation chamber, used a cross-flow illumination system to allow the study of the shape of the injected sample. At the upper (collection) end of the electrokinetic chamber, there was an Ultraviolet (UV) spectrophotometer that measured the optical densities of the sample, which can be correlated to concentration profiles. The chamber was transparent, so photographs could be taken through the front face. RAMSES had the capability of applying AC or DC electric fields and could be used to study electrohydrodynamic effects.

Two types of tests were planned. One set intended to investigate the role of sample stream concentration by injecting polystyrene latex of two different concentrations and comparing the results in space with preflight measurements in the laboratory. The second set intended to compare the sample stream configuration during normal flow and with the carrier buffer immobile (stop flow). Alternating voltage of either 2 or 1000 Hz applied during these sets observed the EHD influence on the sample stream in the absence of electroosmosis. Photographs and video recordings were to be the only data returned from orbit.

Postflight Analysis

This experiment was not done because of a power failure in the RAMSES facility. Therefore, there was no data available for postflight analysis.

Conclusion

The investigators hoped to gain knowledge into EHD forces that affect electrophoretic separations in space as well as on Earth. The effects of

these phenomena are masked on Earth due to buoyancy-induced convection and sedimentation. This experiment focused specifically on two such phenomena: (1) the effect of high sample concentration and (2) EHD instabilities in the absence of shear flow.

In a reduced gravity environment where sedimentation is not a factor, throughputs many times greater than these achievable on Earth can be potentially obtained by increasing the concentration of the sample. However, there is a good reason to believe that a "concentration effort" exists that degrades resolution by causing the sample stream to distort under the action of an electric field. Alternatively, there is also data and analysis, which shows high concentrations of particles act independently during electrophoresis and do not interact with each other in concentrations far in excess of 20%. This implies that a concentration effect may not exist. However, if a concentration effect does exist for EHD, it will significantly influence the rationale for designing separation devices for space operation and for selecting samples appropriate for space-based purification.

Although it has been demonstrated that flow distortions resulting from buoyancy-induced convection are eliminated by operating in space, other phenomena such as EHD, which result in only second order disturbances on Earth, may produce intolerable effects in reduced gravity. Severe fluid disturbances noted in separation experiments flown on early Shuttle missions are being attributed to these second order effects. In conventional ground-based operations, these disturbances are not critical since they are attenuated by fluid flows necessary to control thermal convection. These disturbances must be adequately characterized and evaluated since they will greatly affect the operation of similar devices in space. It is now planned to do the essential parts of this experiment on a MAXUS sounding rocket.

References

Rhodes, P.H., Snyder, R.S., and Roberts, G.O., "Electrohydrodynamic distortion of sample streams in continuous flow electrophoresis, *J. Coll. and Interface Science,* vol. 129, p. 78, (1989).

Convective Stability of Solidification Fronts (Moni)

Dr. K. Leonartz, Engineering, Aachen, Germany (formerly with ACCESS e.V.)

For today's technology, solidification processing is of major importance and widely used. Nevertheless, the formation of micro- and macrostructure during solidification of metals and semiconductors is not yet completely understood. The knowledge gained by scientific work with transparent model systems and reduced gravity applied to manufacturing will have impact on the properties and quality of materials and products and thus on the achievable increase in value.

The MONI project is dedicated to the investigation of the fluid flow in solidifying and not solidifying melts. On Earth the parameters temperature gradient, solidification velocity, and melt composition control the transition from liquid to solid. Since gravity is the driving force for convection, we varied it for these experiments. In space experiments that were exposed to 0.001-g, 0.01-g and 0.1-g were performed using the NIZEMI facility, a slow rotating centrifuge. Additional experiments were performed on Earth. For the investigations, binary alloys of Succinonitrile-Acetone and Succinonitrile-Ethanol were used. The transparency of this materials allows *in situ* observation of convection and solidification. Our primary goal was to determine g-level boundaries for the onset of thermosolutal convection as predicted by S.R. Coriell, *et al.* (1980).

Flight Activities

Two different alloys were processed, Succinonitrile-0.33wt% Ethanol with latex spheres (∅ 15.8 μm) and Succinonitrile-0.45wt% Acetone. Latex spheres are used for flow visualization. Their density is similar to that of Succinonitrile.

The samples were enclosed in chemically neutral quartz glass cells 30 mm wide, 2 mm high, and 30 mm solidification length. The sample was melted and directionally solidified in a gradient freeze furnace that we developed. The maximum outer dimensions of the gradient freeze furnace are 93 mm x 82 mm x 19.4 mm. It was mounted on the NIZEMI turntable, which enables the stepwise variation of the g-level from 0.001-g to 1-g by changing the rotational speed.

Four different directional solidification experiments were performed during the IML-2 mission with varied g-levels and solidification velocities. We observed the solidification process with a video system. The astronaut could control the experiment or the investigator could control it via telescience. In parallel, the video data were stored on tapes.

Highlights

- First observation of the growth transition from near diffusive to convective mass transport in a melt as a function of increasing g-level.
- First use of NIZEMI for directional solidification.

Postflight Analysis

After the space experiments, the samples were homogenized on Earth and processed in the NIZEMI without use of the centrifuge. Thus additional data under 1-g conditions were achieved.

We used the videotapes of the experiments to evaluate the real solidification velocity, the macroscopic and microscopic structure, and the convective motion of the melt visualized by the latex tracers. From the housekeeping data the temperature gradient inside the sample and the gravity level were determined.

First we investigated the fluid flow behavior in the melt caused by a residual temperature gradient resulting from the geometrical and thermal boundary conditions of the sample. The fluid flow scales as expected with the acceleration

level. It was demonstrated that the flow velocity is extremely small and below or in the order of the solidification velocity up to 0.01-g. An effect of this convection on the solid/liquid interface could not be determined.

The main phenomenon, the g-level dependence of convection due to superimposed thermal and solutal gradients (thermosolutal convection) was investigated in spite of the described additional effects. Up to 0.01-g, no thermosolutal effects can be determined (Fig.1a-b). Discontinuous curvature of the solid/liquid interface can be observed for 0.1-g in space with running centrifuge (Fig 1c), and 1-g on Earth (Fig 1d).

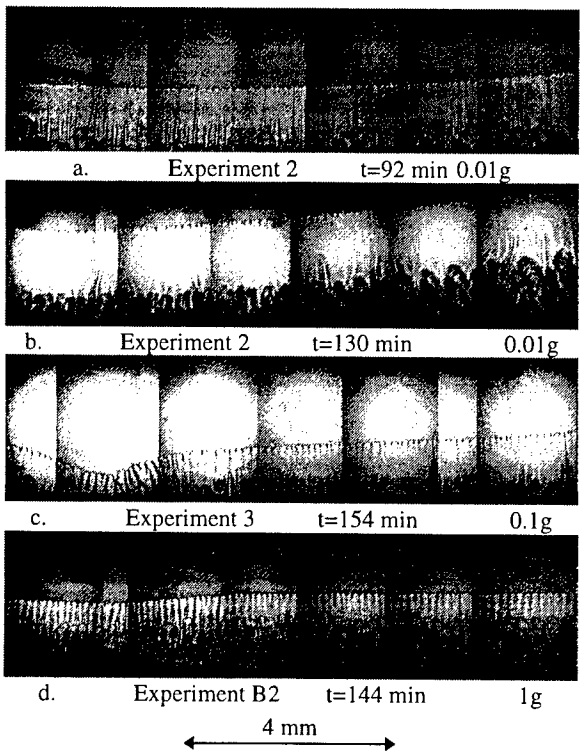

Figure 1: Solid/liquid interface of the Succinonitrile-0.45wt% Acetone alloy.

The correlation of the experiment to theoretical predictions was important. The model of S.R. Coriell, *et al.* (1980) describes the case of uncoupled morphological and convective instability (Fig. 2). A coupled model still does not exist. The model predicts thermosolutal instability at 0.001-g acceleration level for the Succinonitrile-0.45wt% Acetone alloy and the solidification parameters temperature gradient 1K/mm and solidification velocities smaller than 2μm/s. Experimentally we detected instability for 0.1-g and more. The model's predictions are too conservative. The gain in stability can be correlated to the friction at the side walls of the sample and the lack of interaction between convective flow and solid/liquid interface.

Conclusion

The NIZEMI facility was an efficient tool for the Moni project and would be useful for other materials sciences studies of gravity's impact. For the first time the reaction of a solidifying melt to g-levels of 0.001-g, 0.01-g and 0.1-g was observed. The space environment allowed parameter constellations that enabled us to observe the change from near diffusive mass transport during solidification to convective mass transport. A theoretical model was confirmed quantitatively over a variety of growth parameters.

References

Coriell, S.R., Cordes, M.R., Boettinger, W.J., and Sekerka, R.F., "Convective and interfacial instabilities during unidirectional solidification of a binary alloy," *J. Crystal Growth,* vol. 49, pp. 13-28, (1980).

Leonartz, K, "Konvektive Stabilität erstarrender schmelzen," *VDI Verlag,* (1996).

Leonartz, K., Sahm, P.R., and Coriell S.R., "Konvektion in schmelzen unter variablem schwerkrafteinfluß von 0.001g-1g," *Zeitschrift Metallkunde*, accepted.

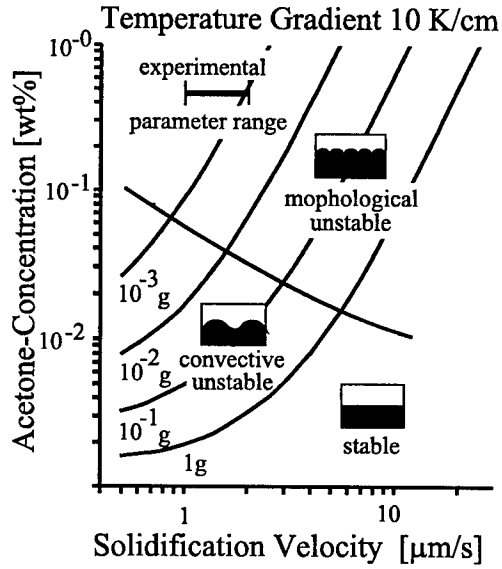

Figure 2: Stability diagram for the Succinonitrile-Acetone alloy.

AQUATIC ANIMAL EXPERIMENT UNIT (AAEU)

INVESTIGATIONS	PRINCIPAL INVESTIGATORS	RESULTS HIGHLIGHTS
Mechanism of Vestibular Adaptation of Fish under Microgravity	Dr. A. Takabayashi Fujita Health University Tokyo, Japan	Observed unusual behavior and posture of fish in microgravity. Fish with different vestibular functions on the ground behaved differently in microgravity. The fish visual system did not provide cues to stabilize posture.
Early Development of a Gravity-Receptor Organ in Microgravity	Dr. M.L. Wiederhold University of Texas Health Science Center, San Antonio, Texas, United States	Newt eggs developed normally and survived well during flight. After return to Earth, otoconia increased.

INVESTIGATIONS	PRINCIPAL INVESTIGATORS	RESULTS HIGHLIGHTS
Fertilization and Embryonic Development of Japanese Newt in Space	Dr. M. Yamashita Institute for Space and Astronomical Science Kanagawa, Japan	Newt eggs were laid in space. Early development of newts proceeded normally. Space flight caused pathological damage to adult newts' livers, stomachs, and lungs.
Mating Behavior of the Fish (Medaka) and Development of their Eggs in Space	Dr. K. Ijiri University of Tokyo Tokyo, Japan	First time fish mated and laid eggs in space. First offspring (8 fry) of a vertebrate ever born in space. Confirmed microgravity had no genetic, behavioral, or developmental effect on the offspring of fish flown or hatched in space.

Mechanism of Vestibular Adaptation of Fish under Microgravity

Dr. A. Takabayashi, Fujita Health University, Tokyo, Japan

This experiment investigates the adaptation of goldfish during flight and their readaptation after landing. Six goldfish (1 normal, 1 with otoliths removed on both sides, 4 with otoliths removed on one side) were flown in the Aquatic Animal Experiment Unit (AAEU), a small aquarium with a water temperature of 23 ± 1 °C.

The goldfish (*Carassius auratus*), 7-8 cm in length and 7.5 - 11 g in body weight, were suited for vestibular function studies since their postural motor output does not involve head-neck-body reflexes. A fish swimming has few gravitational cues from tactile input or from proprioceptors. The major sensory input for postural control comes from vestibular organs.

Highlights

- Observed unusual behavior and posture of fish in microgravity.
- Fish with different vestibular functions on the ground behaved differently in microgravity.
- The fish visual system did not provide cues to stabilize posture.

Flight Activities

Fish behavior was recorded on video on flight days 1, 3, 4, 7, and 11. On the first day, two fish with otoliths removed on one side showed flexion of their bodies toward the operated side. These fish also rolled toward the operated side. However, the body flexion disappeared by either the fourth day or the eighth day, and no more rolling was observed. Five fish showed backward looping behaviors. Although the frequency of looping decreased after the seventh day of the mission, five fish still showed looping behavior on the eleventh day, the last day of video recording on orbit. In microgravity, the visual system did not provide sufficient cues to prevent looping or rolling.

Because the fish without otoliths, the most important gravity-sensing organ in the inner ear on both sides, still looped in microgravity, the utlicular otolith may not induce looping behavior. In microgravity, sensory input through the somatosensory system may be altered in addition to otolith input. There is a possibility that the disappearance of buoyancy by the swimming bladder could induce looping behavior combined with the loss of body weight and/or water pressure.

Another unusual behavior observed in microgravity was rolling. Three out of four fish with the otolith removed on one side rolled toward the operated side. The rolling behavior continued for a long time within a 30-minute recording. In normal fish, the frequency of looping increased gradually and reached a maximum 1 week after launch and then decreased but did not became zero on flight day 11. Other fish that looped had the same tendency during the mission. These results implied that the looping behavior was not dependent on whether the otolith was intact or not and either the period of adaptation on the ground after labyrinthectomy was longer or shorter. It was noted that the frequency of looping episodes depended not only on microgravity but also on the period of exposure to microgravity.

Although the looping behavior tended to decrease in microgravity, 2 weeks was not long enough for complete adaptation. However, the fish only rolled until the middle of the mission and not in the latter half, so all fish adapted their rolling behavior in microgravity.

No clear dorsal light responses (DLRs) were observed during the mission. All fish that were showing looping or rolling behavior indicated that they could not maintain their body equilibrium with their back toward light source. Even while swimming forward most of the time, fish

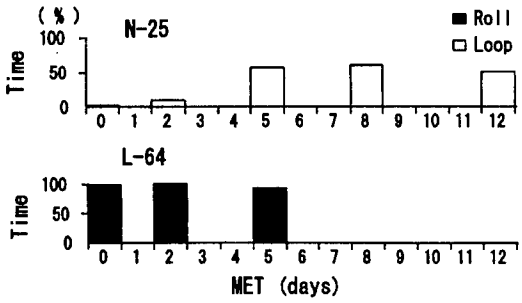

Figure 1: Percentage of time that fish spent looping and rolling during the mission

did not orient with their backs toward the light source. These results suggested that the visual system of fish did not provide sufficient cues to prevent them from looping or rolling. Although the intensity of light must be considered, it was suggested that microgravity might induce sensory conflict between the visual and vestibular system.

Postflight Analysis

After landing, no looping and rolling behavior was observed. However, the tilt angle of the dorsal light response increased in the fish with the otolith removed 5 months before launch but not in normal fish and those with otoliths removed 2 weeks before launch. This suggests that behavioral dysfunction and adaptation in space are dependent on vestibular inputs.

In the tests performed 6 h after landing, no looping, rolling, and body flexion were observed in any fish. The DLRs were video recorded in each fish for 7 days after landing. In normal fish, the maximum tilt angle of the DLR after landing was not changed compared with that before launch. In the fish with the otolith removed 5 months before launch, the maximum tilt angle of the DLR increased gradually for about 3 to 4 days and then decreased. The fish with the otolith removed 2 weeks before launch did not show an increase of tilt angle of the DLR. On the first day after landing, the maximum tilt angle of the DLR in all of the fish flown was not changed or slightly decreased. An increase of tilt angle of the DLR appeared in the fish with the otolith removed 5 months before launch and not in the fish with the otolith removed 2 weeks before launch. These results suggested that sensitivity to microgravity might depend on vestibular function on the ground.

Conclusion

In microgravity, we observed unusual behavior and postures that might be induced by the disappearance of inputs to gravity-sensing organs. Fish behavior was different, depending on the fish's vestibular function on the ground. Flexion of body and rolling behavior appeared in fish with the otolith removed on one side and disappeared in microgravity, which might indicate adaptation during space flight. Looping behavior appeared in five fish but did not disappear during the mission. The fish visual system did not provide sufficient cues to stabilize posture.

Swimming readaptation to the ground was very fast. However, the change of the DLR after landing depended on the functional difference of each fish's vestibular system. The period of vestibular compensation on the ground may be related to readaptation after landing.

These results raise new questions that can be studied in a follow-up experiment. For instance, would looping behavior disappear in prolonged microgravity? Can visual input provide sufficient cues for the body equilibrium system after prolonged stays in space?

References

Takabayashi, A., Watanabe, S., Mori, S., Tanaka, M., Sakuragi, S., and von Baumgarten, R., "Effects of sensory input changes on postural control of fish in microgravity," *8th Space Utilization Symposium*, pp. 96-100, (1991).

von Baumgarten, R.J., Simmonds, R.C., Boyd, J.F., and Garriott, O.K, "Effects of prolonged weightlessness on the swimming pattern of fish aboard Skylab 3," *Aviat. Space Environ. Med.*, vol. 46, pp. 902-906, (1975).

von Baumgarten, R.J., Baldrighi, G, and Shllinger, G.L. Jr., "Vestibular behavior of fish during diminished G-force and weightlessness," *Aerospace Med.*, pp. 626-632, (1972).

Early Development of a Gravity-Receptor Organ in Microgravity

Dr. M.L. Wiederhold, University of Texas Health Science Center, San Antonio, Texas, United States

This experiment aimed to determine what role the gravitational field might have on the initial development of the gravity-sensing portions of the inner ear. Particular emphasis was placed on the formation of the otoliths, test masses on which gravitational and linear-acceleration forces act. If the growth of the otoliths is somehow regulated by their weight, their mass should be increased in reduced gravity.

The Japanese red-bellied newt, *Cynops pyrrhogaster*, is a favorable model system in which to study inner-ear development because fertilized eggs of any desired developmental stage can be readily obtained and the major development of the inner ear occurs from 4 to 20 days after eggs are laid. Thus, viable fertilized eggs that either have not yet begun to form the inner ear, or in which no otoconia have yet been formed, can be launched and will develop nearly adult inner ears during a Shuttle mission. Upon return, the anatomy of the inner ear as well as its function can be studied and compared to ground-reared control specimens.

Flight Activities

Pre-fertilized eggs of the Japanese red-bellied newt, some at developmental stages before any portion of the inner ear had formed and others just before the otoliths are formed, were flown in the Aquatic Animal Experiment Unit (AAEU). Approximately 36 h before launch, 148 eggs at stages 10 to 25 were loaded into individual egg holes (6 mm diameter, approximately 12 mm deep) in an egg container in each of three cassettes of the AAEU. One or two adult newts were also loaded in each cassette. This unit circulated fresh, aerated water at 24 °C continuously. A similar unit was maintained at KSC Hangar L as a ground-control facility.

Two adult newts died, resulting in the loss of some eggs when the adults were removed from the AAEU. Sixty-two of the original eggs survived to the end of the flight. The progression through the developmental stages was assessed from high-magnification, downlinked video and videotapes reviewed after the flight. Similar observations were made on the ground-control equipment. For cassette A3, the flight and ground-control specimens developed at rates that were indistinguishable from one another by external morphological criteria. If temperature is well controlled and identical between ground- and space-reared newts, they appear to develop at the same rate. By extrapolation between the stages at loading and the first inflight observations, the flight larvae were divided into 2 groups, 1 from stages 17 to 27 and the other from stages 29 to 30 at launch, whereas the ground larvae were in groups from stages 19 to 23 and from 28 to 31. Since the otic vesicle is first seen at stage 25, all but 1 larva in the 2 younger groups were in μ-g before any of the otic vesicle formed. In the older groups, the larvae were all in μ-g before any otoconia were formed (otoconia are first seen at stage 33).

Highlights

- Newt eggs developed normally and survived well during flight.
- After return to Earth, otoconia increased.

Postflight Analysis

The flight cassettes were retrieved about 6 h after landing. Some larvae were fixed and preserved for analysis, and some were tested to estimate the gain of the otolith-ocular reflex. These larvae were restrained in a device that allowed rotation about the longitudinal body axis, and counter-rotation of the eyes was measured using high-magnification video records. Six flight and 6 ground-control larvae were studied on postflight days 1, 3, and 5 by X-ray microfocus imaging of the otoliths. Otolith volumes and areas of associated sensory epithelia were calculated from three-dimensional reconstructions of serial sections through the inner ears at the stages available.

During the 15-day flight, these eggs reached larval stages in which the inner ear neared its adult form. The otoliths of the saccule and utricle, the two gravity-sensing portions of the inner ear, were not of significantly different volumes when prepared for histological study within the week after landing. The endolymphatic duct and sac extend dorsally from the saccule and, in the adult newt, cover the brain stem and portions of the spinal cord. In the adult, these structures are filled with a different form of otoconia. This system develops earlier and is significantly larger in the flight-reared larvae, compared to ground-controls (See Figure 1). At the stages the larvae reached at the end of the flight, endolymphatic otoconia begin to appear in the saccule and contribute to the saccular otolith.

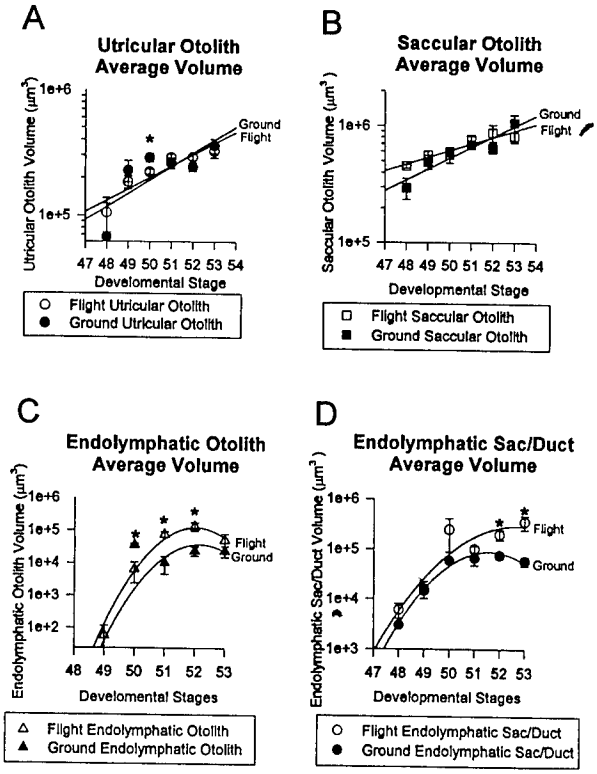

Figure 1: Plots of volumes of utricular (A) and saccular (B) otoliths at different development stages in flight- and ground-based research newt larvae fixed within 5 days of return from orbit. Total volume of otoconia in the endolymphatic sac (C) and of the lumen of the endolymphatic sac (D) for same animals. Each point represents mean +/- standard error for measurements from 2 to 8 reconstructed inner ears. Asterisks indicate cases in which difference between flight and ground- control measurements are statistically significant with $0.0006 < p < 0.05$. Linear regression lines for A and B; second-order polynomial regression for C and D.

In X-ray micofocus studies performed by our Japanese collaborators, the saccular otolith and endolymphatic otoconial mass are seen to be significantly larger in one flight-reared larva maintained in Japan for several months post-flight. Thus the system of otoconia formed in the endolymphatic sac (ES) is accelerated in the flight-reared animals and leads to a long-lasting increase in the saccular otolith in the one specimen maintained for months after landing. However, the endolymphatic system is clearly larger in the flight-reared larvae, and the saccular and utricular otoliths are also larger at 2 and 3 months after return, compared to lab-reared controls from the same original stock of eggs. Otolith-ocular reflexes were measured in the week after return, but those data are still being analyzed.

Conclusion

The newt eggs developed normally and survived well during flight. Fertilized newt eggs appear to be excellent specimens in which to study development in µ-g. Data indicate that the increase in ES otoconia began after return to Earth. Determining whether this is a response to entering 1-g conditions after development in µ-g, or might be even greater with continued development in µ-g, will require much longer flight experiments. These could be accomplished in the Aquatic Habitat on the space station.

References

Wiederhold, M.L., Gilpatric, K.D., Hejl, R.J., Koike, H., and Nakamura, K., "Development of otoliths and endolymphatic otoconia in newt larvae reared in microgravity," *Abstract for the Eighteenth Midwinter Meeting of the Association for Research in Otolaryngology*, St. Petersburg Beach, Florida, (1996).

Mogami, I., Imamizo, M., Yamashita, M., Izumi-Kurotani A., Wiederhold, M.L., Koike, H., and Asashima, M., "Astronewt: early development of newt in space," *Adv. Space Res., vol.* 17, no. 6/7, pp. 257-263, (1995).

Fertilization and Embryonic Development of Japanese Newt in Space

Dr. M. Yamashita, Institute for Space and Astronomical Science, Kanagawa, Japan

Gravity is believed to have a role on amphibian development. Early stages of development, especially before the first cleavage of a single egg cell to two cells, are sensitive to gravity. The newt egg is a large, single cell. The heavier vegetal hemisphere orienting downward by gravity gives a fixed reference of morphogenesis with respect to gravity. Effects of gravity on the early development of the Japanese red-bellied newt were studied. In this experiment, four female newts were sent to space. They were treated with a hormone to ensure egg laying in space and fertilization with sperm stored in their body cavities.

Flight Activities

Four female newts lived in the Aquatic Animal Experiment Unit (AAEU). The newt cassette A-3 in the Aquarium Package housed 2 newts, (A-3a and A-3b), who were treated before launch with a suprathreshold dosage of hormone for egg laying. Newts in the other 2 cassettes, A-l and A-2, were given about half of the dosage. To ensure egg laying, an additional injection was made on orbit.

During the mission, two newts were lost, one on the fourth day and one on the eighth day of the mission. In contrast to the flight group, all four ground-control newts were kept healthy and laid many eggs. Based on the AAEU water pressure log, water circulation seemed to be blocked in the cassette after winding the egg laying tape on the third day, a day before the newt in it expired. In orbit, close-up video images of eggs and embryos were taken by the crew and recorded to analyze the morphology of embryos and trace their time course of development.

Highlights

- Newt eggs were laid in space.
- Early development of newts proceeded normally.
- Space flight caused pathological damage to adult newts' livers, stomachs, and lungs.

Development of newt eggs in the Flt A-3 cassette was video recorded on flight days 1, 4, and 11. Close-up images showed 3 embryos at stage 26 (tail bud) on the fifth flight day. These eggs might have been laid between flight days 1 and 3. This estimation is based on crew observations 9 h after launch and video images of the Flt A-3 cassette on flight day 1. The embryos were at stage 36 on day 11. However, 2 developed embryos recorded on video at that time were not seen when the cassette was opened after its recovery at the ground laboratory 6 h after landing. The time course of development was 3 to 5 days from spawning to stage 26 and 7 days from stage 26 to 36.

In the Flt A-2 cassette, most of the eggs were spawned between the first and second day of flight. Eggs laid in Flt A-2 were videotaped on the fourth day after the adult newt died. Among 37 eggs in the cassette, 2 or 3 were at stage 8 or 9 (late morula or early blastula). Since the number of eggs recovered to the ground was more than the number reported for Flt A-2 on the second day, those developed eggs were probably laid after that observation time. Therefore, the eggs developed to stage 8 or 9 in no more than 2 days.

Based on the recorded video of the embryos in cassettes A-2 and A-3, their morphology can be judged to be normal. The time course of their development did not deviate from those of eggs grown under Earth's gravity in the same temperature range. It was shown that the fundamental process of early development occurs normally without gravity. Because of the small size of the sample and the lack of histological survey on the embryos, we cannot generalize any further.

Postflight Analysis

Soon after sample recovery, we made X-ray images of the adult newts and dissected them to examine the effects of space flight. The specimens fixed or frozen for analysis were: the brain, eye, lower jaw, vertebral column, heart, lung, liver, stomach, intestine, ovary, abdominal muscle, blood, skin, limb, and tail.

The expired newts were returned frozen. They were dissected to examine the cause of death. The newt that died on flight day 8 had features associated with death while egg spawning in a submerged condition. The newt found dead on the fourth day showed a quite different posture: stretching four limbs and bending its head upward; the diameter of the oviduct was 2-3 mm, twice larger than normal. No injury caused by hormone injection was seen in the abdominal organs of either newt.

By visual inspection at dissection, no abnormality was found in the body surfaces and abdominal organs of the 2 flight newts, A-3a and A-3b, or the ground controls. It should be noted that 2 newts enclosed in the A-3 cassette presented astonishingly active movement when they were released from the cassette. Microscopic examination of the two newts that were recovered alive from orbit revealed many biological effects of space flight. The livers, stomachs, and lungs of the flight samples showed pathological changes that were not found in the ground controls. An additional postflight control experiment confirmed that space flight probably caused the pathological changes in the two newts.

Conclusion

Newt eggs were spawned on orbit and exposed to space from their early stage of development. The early developmental process was found to proceed normally without gravity. Neither the morphology of embryos nor the time course of their development differed from those on the ground. The basic steps of development such as determination of embryonic axis does not require the presence of gravity.

Space flight affected the adult newts. The survival rate was low for the flight group. Severe pathological damages was observed in the livers, stomachs, and lungs of the two newts that were recovered alive from orbit. An independent observation on the liver of a frog showed certain similarities with the results obtained in this study. It strongly suggests that space flight influences protein synthesis in the liver.

References

Mogami, Y., Imamizo, M., Yamashita, M., Izumi-Kurotani, A., Wiederhold, M.L., Koike, H., and Asashima, M., "Astro newt: early development of newt in space," *Adv. Space Res.*, vol. 17, no. 6/7, pp. 257-263, (1996).

Imamizo, M., Mitsutaka, Y., Fujioka, K, Takada, Y., Hisada, A., Izumi-Kurotani, A., and Yamashita, M., "Sustained release of hCG minipellet for newt experiment in space," *Biol. Sci. in Space*, vol. 8, no. 4, pp. 226-230, (1994).

Yamashita, M., Izumi-Kurotani, A., and Nagaoka, S., "Air bubble under microgravity: astro newt experiment onboard IML-2," *J. Jpn Soc. Microgravity Appl.*, vol. 12, no. 3, pp. 150-156, (1995).

Pfeiffer, C.J., Yamashita, M., and Asashima, M., "Cytopathologic observation of the lung of adult newts (*Cynops pyrrhogaster*) onboard the Space Shuttle, during the Second International Microgravity Laboratory experiments," *J. Submicroscopic Cytol. Pathol.*, (1995).

Mating Behavior of the Fish (Medaka) and Development of their Eggs in Space

Dr. K. Ijiri, University of Tokyo, Tokyo, Japan

Previous experiments have shown that fish swim in a looping pattern when exposed to microgravity. They cannot mate while swimming in this pattern. Through parabolic flights, the investigator found a strain of Medaka fish that do not exhibit this looping behavior; this ccT strain was selected as the fish best suited for reproducing in microgravity.

The adult fish *Oryzias latipes* weighs ~0.7 g and is 3 cm in length. Female and males can be distinguished by the shape of their dorsal and anal fins. Four fish (2 males and 2 females) were put in an aquarium (the Aquatic Animal Experiment Unit), which was placed inside the Space Shuttle about 30 h before launch. They were kept under specific temperature- and light-controlled conditions (24 °C, 14 h of light and 10 h of dark).

On Earth, the fish use gravity to orient their posture for mating behavior. In space, the investigator substituted oriented light to help the fish obtain the correct posture for mating. Since mating was triggered by exposure to light, it was anticipated to be completed within 2 h after the transition from dark to light.

Flight Activities

Each day, the payload crew visually checked the aquarium for eggs. On the third day of the mission, Japanese payload specialist Chiaki Mukai reported three newly laid eggs.

Spawning continued, and by the next day the total egg count reached 10. Airflow in the aquarium moved the eggs to a separate hatching area where they could not be disturbed by the adult fish. Video recordings of the eggs showed the embryos' large, black-pigmented eyes and allowed investigators to compare embryonic development in space with similar development on the ground. At the end of the twelfth day, the payload specialist detected a baby fish and recorded video of the swimming baby.

Highlights

- First time fish mated and laid eggs in space.
- First offspring (8 fry) of a vertebrate ever born in space.
- Confirmed microgravity had no genetic, behavioral, or developmental effect on the offspring of fish flown or hatched in space.

Postflight Analysis

After launch, all the adult fish, fry, and embryos were returned safely to the investigators. At first the adult fish rested almost lifeless on the bottom of the aquarium. Finally, they tried to swim upward, but after a 1 to 2 sec, they would drop back to the bottom of the tank. By the fourth day back on Earth, the fish had recalled how to swim under 1-g conditions. Video revealed that the stresses of living in microgravity made mating more difficult and increased aggressive behavior.

The adult fish were returned to the laboratory in Japan, where the investigator obtained data on eggs laid after the flight. The adult fish resumed mating and egg laying on the seventh day after the mission and continued every day for 40 days. Data were obtained for the number of eggs laid, the percent of fertilized eggs, and the percent of embryos surviving until hatching. For the four adult fish, no effects of space flight have been detected on their germ cells when offspring studies were carried out on the eggs laid in space or the eggs laid upon return to Earth. Approximately 1,300 adult fish were obtained and distributed to more than 300 locations in Japan for use in educational programs.

Eight baby fish were also returned to Earth. These space-originated fry could swim normally, acting no differently than Earth-born fry. Four fry were preserved for histological

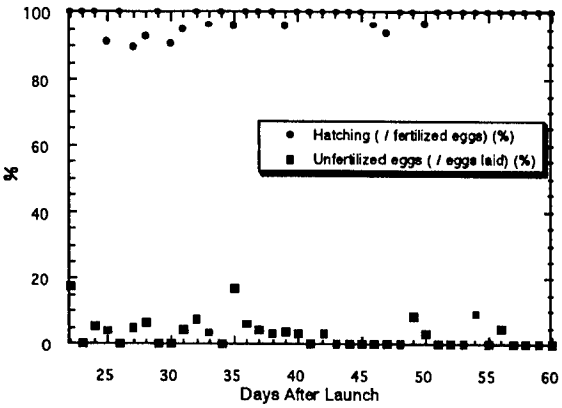

Figure 1: Fertilization (expressed in the percentage of unfertilized eggs) and hatchability of eggs laid by space-flown adult fish after return to Earth. The abscissa is expressed in days after launch, i.e. days after exposure to microgravity for the first time. Microgravity exposure ended on day 15.

observation with microscopes, two died of natural causes, and the other two were transferred to a new aquarium, where they were reared to adulthood and reproduced offspring.

By examining video, the investigator could also study the embryonic development inside the transparent egg envelop. This yielded information on the role gravity plays in egg development. A total of 43 eggs were laid: 8 babies hatched in space, 30 fry hatched after landing, and 5 eggs stopped development at early stages. This is a normal hatching rate when compared to ground-based laboratory data, and embryonic development in space seemed no different than on the ground. The dominant lethal mutation test detected no large-scale aberrations on chromosomes of the germs cells that could bring about non-fertilization or early death of the embryos before hatching.

Conclusion

The present experiment proved that fish can mate and lay eggs in space, and the eggs can develop normally (at least until hatching and coming out as fry) in microgravity. Among vertebrate species, this was the first successful mating and reproduction in space. The next step is a long-term experiment to breed multiple generations of this fish strain on the space station.

When humans begin to live and work in space for extended periods, fish can provide important protein for their sustenance. While the Medaka fish is small and not edible, it is an ideal fish for space experimentation because it is easy to breed and it has a short life cycle (eggs develop to mature fish in 3 months). The investigator believes that space studies using this fish may result in the evolution of a mutant fish with genes responsible for better adaptation to microgravity. These genes could then be transferred to the DNA of edible fish such as plaice, trout, or cod.

References

Ijiri, K., *The First Vertebrate Mating in Space - A Fish Story*,. RICUT, Tokyo. (1995).

Ijiri, K., *Biological Science in Space*, vol. 9, pp. 3-16, (1995).

Ijiri, L., *Proc. V. Congr. Europ. Ichthyologists*, Stockholm, Kullander, S.O. and Fernholm, B., eds.), Dept. Vertbr. Zool., Swedish Museum of Natural History, Stockholm, pp. 227-284, (1987).

Ijiri, K. and Egami, N., *Radiation Research*, vol. 72, pp. 164-173, (1977).

von Baumgarten, R.J., *etal.*, *Aviation Space Environment Medicine*, vol. 46, pp. 902-906, (1975).

BIORACK (BR)

INVESTIGATIONS	PRINCIPAL INVESTIGATORS	RESULTS HIGHLIGHTS
Activation Signals of T Lymphocytes in Microgravity (Adhesion)	Dr. A. Cogoli Swiss Federal Institute of Technology, Zurich, Switzerland	Failure of T cells to proliferate in microgravity can be attributed to the reduction in the expression of IL-2 receptor and not the absence of IL-1. Activation in terms of DNA synthesis and genetic expression of specific cell products (IL-2R; IFN-γ) may be under a different control.
Movements and Interactions of Lymphocytes in Microgravity (Motion)	Dr. A. Cogoli Swiss Federal Institute of Technology, Zurich, Switzerland	Cell-cell contacts occur in microgravity. Cells are not transferring through the complete cell cycle, resulting in a dramatic decrease in activation.
Effect of Microgravity on Cellular Activation in Lymphocytes: Protein Kinase C Signal Transduction (Phorbol) and Cytokine Synthesis (Cytokine)	Dr. D.A. Schmitt and Mr. J.P. Hatton, Laboratory of Immunology, CHU Rangueil, Toulouse, France	Results indicated a moderate suppression in the concentration of cells associated with cytokines in microgravity. Distribution of protein kinase C inside the cell varies in proportion to gravity level. Differences in basal levels of cytokine synthesis may mean even unstimulated cells may be sensitive to microgravity.

INVESTIGATIONS	PRINCIPAL INVESTIGATORS	RESULTS HIGHLIGHTS
Cell Microenvironment and Membrane Signal Transduction in Microgravity (Signal)	Dr. P. Bouloc University of Paris-Sud Orsay, France	Observed possible reduced growth lag period of a non-motile culture of *E. coli* in microgravity. Efficient induction of one two-component system regulating the osmoregulation in *E. coli* in microgravity.
Effect of Stirring and Mixing in a Bioreactor Experiment in Microgravity (Bioreactor)	Dr. A. Cogoli Space Biology Group of ETH Zurich, Switzerland	Bioreactor performed well. Higher percentage of randomly distributed bud scars in flight cells (17%) than in ground control cells (5%). Found no remarkable differences in the cell cycle, ultrastructure, cell proliferation and volume, ethanol production, and glucose consumption.

BIORACK (BR)

INVESTIGATIONS	PRINCIPAL INVESTIGATORS	RESULTS HIGHLIGHTS
Biological Investigations of Animal Multi-Cell Aggregates Reconstituted under Microgravity Conditions (Aggregates)	Dr. U.A.O. Heinlein Heinrich-Heine-Universität Düsseldorf, Germany	Results indicate the initial adhesion among cells is not disturbed in microgravity. Formation of interconnecting cables (a prerequisite to cell migration between aggregates under normal gravity) did not occur in the flight samples.
Replication of Cell Growth and Differentiation by Microgravity: Retinoic Acid-Induced Cell Differentiation (Mouse)	Dr. S.W. de Laat Netherlands Institute for Developmental Biology Utrecht, The Netherlands	The RA-induced reporter gene expression is impaired by microgravity. Need more experiments to demonstrate the effect of microgravity on DNA synthesis.
The Sea Urchin Larva, A Suitable Model for Biomineralization Studies in Space (Urchin)	Dr. H.-J. Marthy CNRS, Observatoire Océanologique Banyuls sur mer, France	Basic biomineralization occurred in microgravity, and no pronounced demineralization was observed. Developmental processes such as the proliferation and specific differentiation of the skeletogenic cells occurred; however the process of their positioning appears to be more sensitive to environmental factors, possibly including microgravity.

INVESTIGATIONS	PRINCIPAL INVESTIGATORS	RESULTS HIGHLIGHTS
The Effect of Microgravity and Varying Periods of 1-g Exposure on Growth, Mineralization, and Resorption in Isolated Fetal Mouse Long Bones (Bones)	Dr. J.P. Veldhuijzen Amsterdam Academic Center for Dentistry Amsterdam, The Netherlands	Confirmed IML-1 results: microgravity did not affect overall growth but did decrease mineralization. A decrease in mineralization was not found in long bones placed for 6 h daily on the 1-g centrifuge. Initial effects were found after 3 h daily 1-g exposure.
Investigation of the Mechanics Involved in the Effects of Space Microgravity on *Drosophila* Development, Behavior, and Aging (Drosophila)	Dr. R. Marco Universidad Autónoma de Madrid, Madrid, Spain	Confirmed accelerated aging of male fruit flies exposed to microgravity. Linked increased aging to increased activity and mitochondrial processes. Verified normal development of fruit flies (from single cells to adulthood) in space.
The Role of Gravity in the Establishment of the Dorso-Ventral Axis in the Amphibian Embryo (Eggs)	Dr. G.A. Ubbels Hubrecht Laboratory Utrecht, The Netherlands	Found rate of cell divisions unchanged in actual and simulated microgravity. Microgravity perturbs blastocoel formation.

BIORACK (BR)

INVESTIGATIONS	PRINCIPAL INVESTIGATORS	RESULTS HIGHLIGHTS
Regulation of Cell Differentiation by Gravity in the Lentil Root (Lentil)	Dr. G. Perbal and Dr. D. Driss-Ecole Pierre and Marie Curie University, Paris, France	Gravity did not affect the elongation of roots growing in the vertical position. Cell cycle in the meristem is regulated by gravity.
Root Orientation, Growth Regulation, Adaptation, and Agravitropic Behavior of Genetically Transformed Roots (Transform)	Dr. T.-H. Iversen Norwegian University of Science and Technology, Dragvoll, Norway	Similar distribution of amyloplasts in WT and transgenic root cap cells both in orbit and on the ground. Total growth was higher for roots grown on the ground than for roots grown in space. Space-grown transgenic root tips were kept alive under sterile conditions. The roots have been propagated *in vitro* since August 1994 and are undergoing further analysis
Plant Growth and Random Walk (Random)	Dr. A. Johnsson University of Trondheim Dragvoll, Norway	Average bending direction of the plants stayed constant equal to zero despite the spontaneous movements performed in weightlessness. The average squared deviation of the root movements increased linerly with time during the first period of growth, a pattern characteristic for random processes. Growth of roots in weightlessness was smaller than on the ground.

INVESTIGATIONS	PRINCIPAL INVESTIGATOR	RESULTS HIGHLIGHTS
Dosimetric Mapping in Biorack (Dosimetry)	Dr. G. Reitz DLR Institute for Aerospace Medicine, Cologne, Germany	Total doses differ up to a factor of 1.5 and heavy ion fluxes by more than a factor of 6 in the different locations. The mission equivalent dose for the astronauts was calculated from the measurement to be 3.8 mSv.
The Influence of Microgravity on Repair of Radiation-Induced DNA Damage in Bacteria and Human Fibroblasts (Repair & Kinetics)	Dr. G. Horneck DLR, Institute for Aerospace Medicine, Cologne, Germany	Both prokaryotes and human cells had normal repair pathways in microgravity. The synergistic effects of microgravity and radiation are not a result of a disturbance of intracellular repair. Results indicate that repair processes function normally and are not disturbed by microgravity conditions.

Activation Signals of T Lymphocytes in Microgravity (Adhesion)

Dr. A. Cogoli, Swiss Federal Institute of Technology, Zurich, Switzerland

Prior experiments revealed a dramatic depression of the *in vitro* activation of T lymphocytes in suspension by the mitogen concanavalin A (Con A). The results suggested that the major reason for the depression was the failure of the monocytes (acting as accessory cells) to provide the second signal, interleukin 1 (IL-1), required for activation of T cells. Our IML-2 experiment could not confirm this hypothesis, as activation could not be restored by exogenous IL-1, nor by IL-1 produced by the monocytes themselves. The lack of expression of the interleukin 2 receptor (IL-2R) is more likely the cause for the impaired proliferation of T lymphocytes in microgravity. We concluded that signal transduction is markedly changed in microgravity.

Flight Activities

Four cylindrical cell culture chambers of 5.4 ml capacity each were carved in a cell culture block. A mixed population of lymphocytes (82.5 %), monocytes (6.5 %) and granulocytes (11 %) was prepared, and 4.5 ml of cell culture were sealed in each culture chamber. A total of 32 chambers in 8 culture blocks (4 flight blocks, 4 ground blocks) were flown; each block was sealed in one Type 1 container. The same batch of cells was used in the Motion experiment.

The cultures were stored at ambient temperature until activation by a crew member who injected 0.15 ml of solution in PBS of either Con A, Con A + IL-1, Con A + IL-1 + IL-2, or PBS alone, in all the cultures at 0-g and at 1-g, respectively. All the cultures were incubated for 71 h at 37 °C, 2 Type 1 containers at 0-g and 2 on the 1-g centrifuge. After injection of 0.15 ml [^{3}H]thymidine, incubation continued for another 1.5 h. Half of the 0-g cultures were fixed by injection of glutaraldehyde and stored at 4 °C, and the rest were cryopreserved with DMSO and stored at -10 °C until landing.

Highlights

- Failure of T cells to proliferate in microgravity can be attributed to the reduction in the expression of IL-2 receptor and not the absence of IL-1.
- Activation in terms of DNA synthesis and genetic expression of specific cell products (IL-2R; IFN-γ) may be under a different control.

Postflight Analysis

Activation, i.e. incorporation of labeled thymidine into the DNA, was measured by autoradiography. IL-1β, IL-2, s-IL-2R, IFNγ, TNF-α were determined in aliquots of the supernatants of the cultures, and glucose, lactate, ammonia, and urea were analyzed.

The 1-g centrifuge failed when the experiment was activated by the injection of Con A. The inflight 1-g samples were kept for about 1 h at 0-g. It is known that a series of events (e.g. the expression of oncogenes like c-fos and c-myc) is triggered within seconds after addition of the mitogen. Other important events are taking place within the following 30 min. Most likely the exposure to 0-g during this critical phase of the stimulation influenced the results of this control. Moreover, the centrifuge had to be stopped for a total of 60 min during the 3 d incubation to process other experiments.

The most important results are shown in Fig.1. Fig. 1A shows the percent of cells with labeled nuclei, i.e. activated cells. The control samples without Con A show, as expected that neither 0-g nor 1.4-g have a stimulatory effect.

This is true also for IL-2R and IFN-γ, but not for the monocyte products IL-1 and TNF (Fig.1 B-E). All samples with Con A alone or in combination with exogenous IL-1 or IL-1+IL-2 confirm the well known inhibition of activation at 0-g. The difference between the cultures at 1-g in space and at 1-g on the ground can be

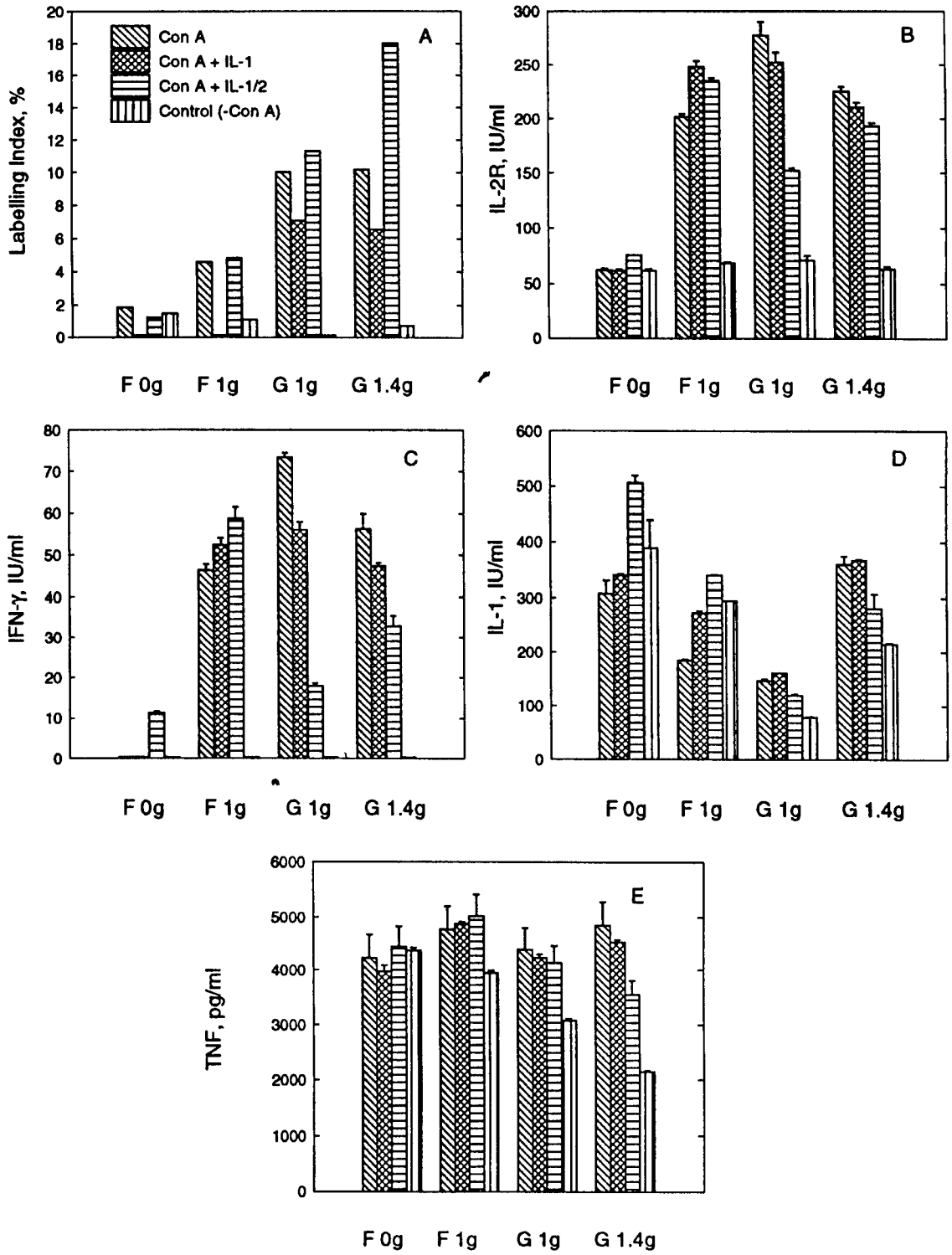

Figure 1: Analysis of cultures of lymphocytes on IML-2. (A) Mitotic index; (B) IL-2 receptor in supernantant; (C) IFNγ, (D) IL-1; (E) TNF-α. Cultures were kept in space at 0-g and 1-g and on the ground at 1-g and 1.4-g, respectively. F=flight samples; G= ground samples. SEM values are given.

attributed to the stops of the inflight centrifuge (see above). The loss of activation at 0-g cannot be attributed to a lack of cell-cell contacts between lymphocytes in suspension and monocytes adhering to the wall of the culture vessel. T-cell proliferation can be observed in the inflight 1-g control, although the gravity vector on the rotating centrifuge was opposite to the vector on the launch pad, where the monocytes have time to attach to the surface of the culture vessel. Furthermore, it was found that leukocytes are able to move in microgravity even in the absence of the mitogen. In the presence of Con A, the formation of aggregates could be observed.

Early production of IL-2 is required to activate the secretion of IL-1 by monocytes. After activation of PKC in T cells by IL-1, larger amounts of IL-2 are secreted. At a later stage IL-2R is expressed in the cell membrane and in part released in the supernatant. Nearly all newly synthesized IL-2 is bound to the IL-2R within 3 d after the beginning of the activation and, therefore, not found in the supernatant. This is confirmed by our data. Fig. 1B gives the concentrations of IL-2R found in the supernatants. The inhibition at 0-g, observed in a prior experiment, is confirmed. The data from the 1-g cultures in space correspond well with those at 1-g on the ground. The contradiction with the labeling index data (reduced at 1-g in space) is only apparent. The expression of IL-2R is a late event in T cell activation and is not affected by the early exposure of the flight 1-g samples to 0-g at the beginning of the incubation. If this is true, the expression of IL-2R is under a different control than DNA proliferation.

IFN-γ is an important cytokine produced by activated T lymphocytes. In microgravity, the expression of IFN-γ is completely depressed in the presence of Con A or Con A+IL-1. (Fig. 1C) Exogenous combination of IL-1 and IL-2 partially restores the inhibition observed at 0-g.

Fig. 1D gives the content of IL-1 after 3 d of incubation. As expected IL-1 is produced also in the absence of Con A by monocytes adhering to the wall of the culture flask. Spontaneous monocyte IL-1 expression can be induced also by the isolation procedure. What was totally unexpected is the production of IL-1 by monocytes at 0-g. This is in contrast with what we found previously in a similar experiment and contradicts our hypothesis that a malfunction of the monocytes and therefore the lack of IL-1 as second signal of T cell activation is the cause of the inhibition at 0-g. In this respect this is the most important result of our investigation. Further studies are required to clarify this aspect. Moreover, it appears that the IL-1 production is enhanced at 0-g, including the 1-g samples in flight that experienced 0-g at the beginning of and during the incubation. This is in agreement with previous studies conducted with a monocyte cell line in space showing increase of IL-1 production at 0-g.

Fig. 1E shows the data on TNF secretion. TNF has a great pharmacological importance in tumor therapy. Our data do not point to particular influence of microgravity on this cytokine and agree with our previous results.

Conclusion

We confirmed that there is a strong inhibition of mitogenic activation of resuspended cells in microgravity (-80% compared to the ground). The addition of exogenous IL-1 alone or IL-1+IL-2 is not capable to prevent the loss of activity at 0-g. This is the most important result of the experiment: the hypothesis based on prior results was not confirmed. It is more likely that the failure of the T cells to proliferate in microgravity can be attributed to the reduction in the expression of the IL-2R and not to the absence of IL-1 as postulated earlier.

Interestingly enough, exogenous IL-1+IL-2 restore slightly but significantly the production of INF-γ at 0-g. This indicates that activation in terms of DNA synthesis and of genetic expression of a specific cell product are under different control.

References

Pippia, P., Sciola, L., Cogoli-Greuter, M., Meloni, M.A., Spano, A., and Cogoli, A., "Activation signals of T lymphocytes in microgravity," *J. Biotechnol.*, vol. 47, pp. 215-222, (1996).

Cogoli, A., "The effect of hypogravity and hypergravity on cells of the immune system," *J. Leukoc. Biol.* , vol. 54, pp. 259-268, (1993).

Movements and Interactions of Lymphocytes in Microgravity (Motion)

Dr. A. Cogoli, Swiss Federal Institute of Technology, Zurich, Switzerland

Cell-cell interactions and aggregate formation are important for cell communication and signal delivery in T lymphocyte activation. The fact that the formation of cell aggregates is only slightly reduced in microgravity suggests that cells are also moving and interacting in space. Direct evidence was obtained for the first time in an experiment performed on a sounding rocket flight, where the motions and interactions of free-floating, non-activated cells were observed in microgravity for 12 min.

The objective of this investigation was to provide direct evidence that lymphocytes are capable of autonomous movements and of cell-cell contacts in microgravity. Such evidence would disprove the argument that the loss of activation of T lymphocytes in microgravity is caused by the lack of contacts between cells resuspended in a weightless environment.

Flight Activities

The cuvettes were stored at ambient temperature until activation 13 h after launch. Activation was carried out manually by a crew member who pulled the towing strip of the cuvette, thus allowing the transfer of the mitogen (0.5 ml Con A) into the culture chamber. The final concentration of the cells was 2.25 x 10^6/ml, and that of Con A was 15 µg/ml. The Type 1 containers were stored in the Biorack incubator at 37 °C. At 12, 46, and 78 h, respectively, after the addition of the mitogen, one of the cuvettes was transferred to the NIZEMI microscope.

The astronaut selected viewing fields containing an aggregate during a 5-min downlink period allowing the investigator to give advice to the crew member. Observation was done with a 32x objective with brightfield illumination. The behavior of the cells was recorded on board with a video camera during two 25-min observations, first at 0-g and then at 0.01-g. For the third observation both recordings were at 0-g. Then the cuvette was returned to the Biorack incubator.

Highlights

- Cell-cell contacts occur in microgravity.
- Cells are not transferring through the complete cell cycle, resulting in a dramatic decrease in activation.

Postflight Analysis

Analysis of the behavior of single cells and aggregates was performed on printouts of the videotapes. The velocity of the moving cells was analyzed by measuring the position of the cells on the video-printouts in intervals of 30 s. For each observation, the locomotion of 6 to 9 cells was analyzed. Statistical analysis was performed with the one-tailed U-test of Wilcoxon, Mann, and Whitney. For morphological analysis, the cells from the Adhesion experiment were fixed in flight and prepared for observations with a scanning electron microscope at 25 kV.

The video reveals that lymphocytes resuspended in microgravity in the presence of the mitogen Con A moved autonomously in random directions and formed cell aggregates. Aggregates were observed at 1-g and in microgravity 12 h after the addition of the mitogen. Both samples of space aggregates observed 78 h after the addition of Con A were larger (i.e., consisted of more cells) than the ones observed after 12 and 48 h. For the second and third observations, the ground aggregates were mostly larger than the corresponding space aggregates. Aggregates of similar size to those in space or even smaller ones were also found in the ground control samples. Because a limited number of space aggregates were observed, we could not determine the statistical significance of the size difference.

The aggregates, both in space as well as on ground, changed their shape throughout the observation period. Cells within the aggregate

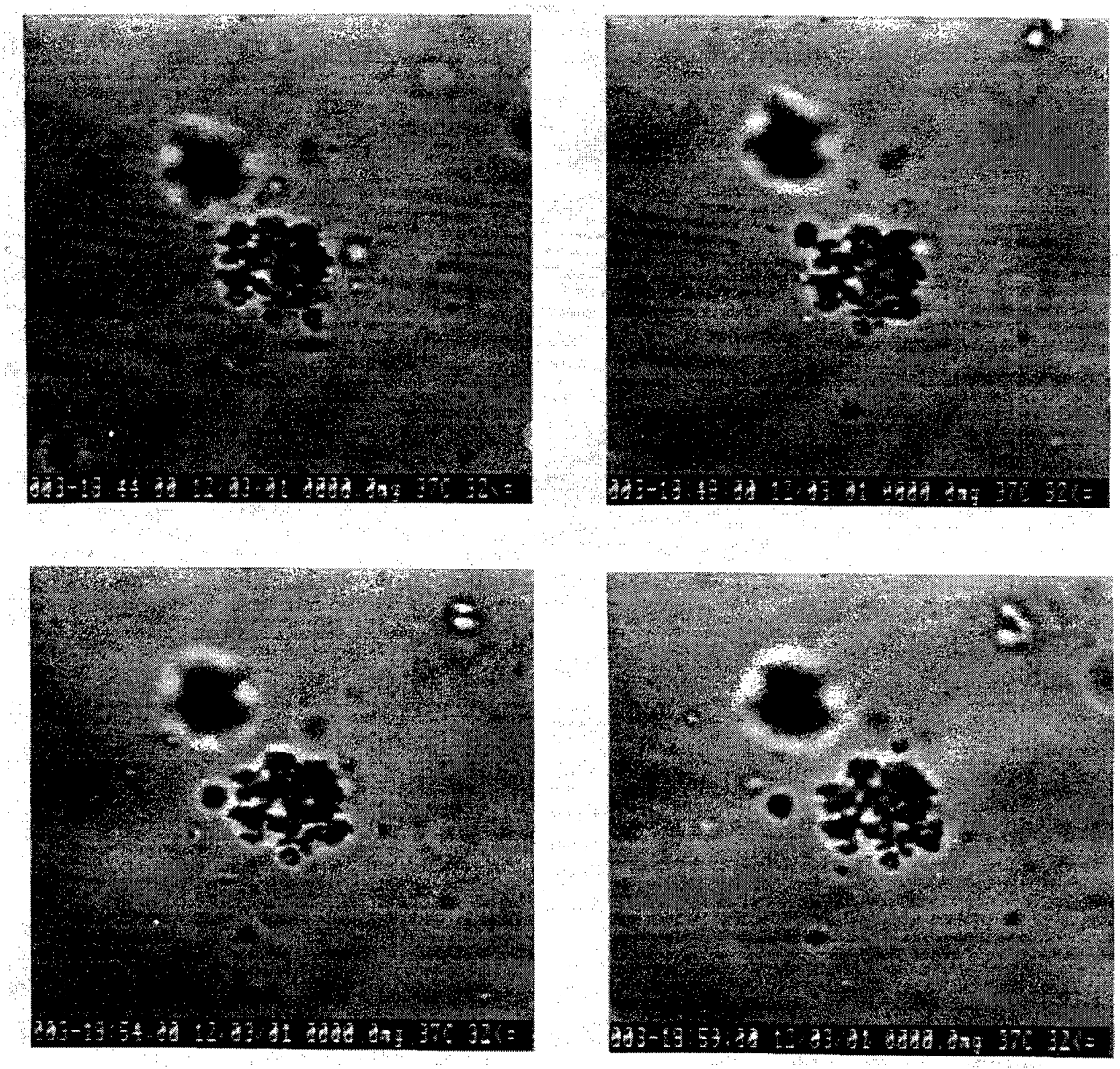

Figure 1: Aggregate of cells 78 h after the addition of Con A. The time given in the status bar corresponds to the mission elapsed time on the fourth day.

changed their location and shape. This is most clearly observed at the periphery where they often exhibit rapid movements (rocking and twisting). Single cells migrated into or out of an aggregate. (Figure 1)

The observation of aggregate formation at 0-g demonstrates that cell-cell contacts that are crucial in lymphocyte activation also occur in microgravity. Nevertheless, the activation is nearly abolished at 0-g.

Although it might be argued that the quality of the contact itself may be changed in microgravity, we have strong evidence that lack of cell contacts is not the primary cause of the inhibition of activation. Moreover, the aggregates confirm that the binding of Con A to the cell membrane is not affected at 0-g.

Single cells in suspension (not attached to an aggregate) as well as cells at the periphery of the aggregate show motion similar to that previously observed in non-activated cells on a

sounding rocket flight. The motion velocity varies considerably from one 30 s interval to the other. In microgravity, the mean velocity of the free lymphocytes is significantly higher than at 1-g ($\alpha = 0.01$) and does not change with increasing incubation time. (Figure 2)

Since the flight centrifuge failed, we compared the morphology of the cells cultured at 0-g with that of the cells kept on ground at 1-g. No difference is found between cultures without Con A, either at 0-g or 1-g. Two types of morphologies appear in both cultures: one with a smooth surface, the other with the surface covered by small blebs.

In the presence of Con A, larger aggregates of cells are seen after 3 d in culture at 1-g than at 0-g, thus confirming the data from NIZEMI. The surface of the cells in the aggregate show a great heterogeneity. Con A alone and combined with IL-1 and IL-2 causes in some cells the appearance of microbilli and lamellar expansions of the membrane. Such cells are also larger. A polarization of the microvilli are seen at 0-g in Con A activated cells. This morphology is typical for moving lymphocytes.

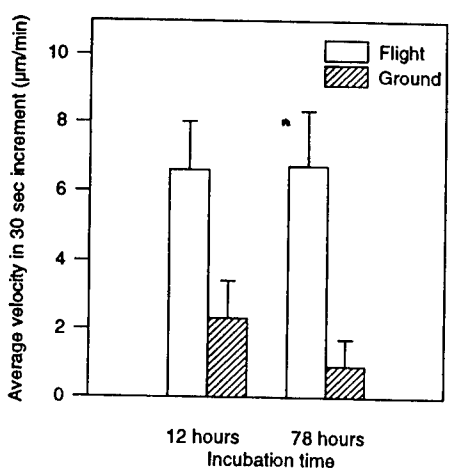

Figure 2: Locomotion velocity of leukocytes during in vitro activation with Con A

Conclusion

The observation in real time of the formation of aggregates during the mitogen-induced activation of lymphocytes in microgravity confirms the indirect evidence obtained earlier from samples fixed in microgravity and analyzed on ground. Therefore cell-cell contacts are occurring in microgravity.

The locomotor capability of lymphocytes in the presence of a mitogen at 0-g is significantly increased compared to the 1-g control on ground. The fact that it is not decreasing with prolonged incubation time confirms our observation that the cells are not transferring through the complete cell cycle, resulting in a dramatically decreased activation.

References

Cogoli-Greuter, M., Meloni, M.A., Sciola, L., Spano, A., Pippia P., Monaco, G., and Cogoli, A., "Movements and interactions of lymphocytes in microgravity," *J. Biotechnol.*, vol. 47, pp. 279-287, (1996).

Cogoli-Greuter, M., Sciola, L., Pippia, P., and Cogoli, A., "Lymphocytes on sounding rocket flights," *J. Gravit. Physiol.*, pp. *90-91*, (1994).

Cogoli-Greuter, M., Sciola, L., Spano, A., Meloni, M.A., Pippia, P., and Cogoli, A., "Lymphocyte movements and interactions in microgravity," *J. Gravit. Physiol.*, pp. *117-118*, (1995).

Effect of Microgravity on Cellular Activation in Lymphocytes: Protein Kinase C Signal Transduction (Phorbol) and Cytokine Synthesis (Cytokine)

Dr. D.A. Schmitt and Mr. J.P. Hatton, Laboratory of Immunology, CHU Rangueil, Toulouse, France

In the Cytokine experiment, white blood cells were activated in three different conditions: (1) by cellular interaction between monocytes and T-lymphocytes, (2) activation of monocytes by phorbol esters, which directly activate Protein Kinase C (PKC), and (3) activation of T-cells by phorbol esters and calcium ionophore. The Phorbol investigation examined the ability of phorbol esters to bind to Protein Kinase C (PKC) and subcellular localization of PKC.

Flight Activities

In the Cytokine experiment, the efficiency of T-cell and monocyte activation was quantified by measuring the synthesis and secretion of cytokines. Cytokines are extracellular signaling molecules that are produced in response to cell stimulation, and they act as useful markers of cell activation. For T-cells, interleukin 2 (IL2) was measured, and for monocytes, IL-1 beta production was measured.

In the Phorbol experiment, we investigated the subcellular localization of PKC and the binding of phorbol esters to PKC. In a number of previous space flights, a decrease in the response of cells to phorbol esters in microgravity has been observed. Therefore, in this experiment, we tried to determine whether this effect was caused by an alteration in the distribution of PKC or in the binding of phorbol esters to PKC.

Highlights

- Results indicated a moderate suppression in the concentration of cells associated with cytokines in microgravity.
- Distribution of protein kinase C inside the cell varies in proportion to gravity level.
- Differences in basal levels of cytokine synthesis may mean even unstimulated cells may be sensitive to microgravity.

In both U937 (monocyte) and Jurkat (T-cell), cytokine synthesis in response to stimulation with the phorbol ester, Phorbol-12, 13, Di-butyrate (PDBu), was suppressed in microgravity, whereas no significant differences were observed for stimulation with Phorbal-12-Myristate-13-Acetate (PMA) at the level of sensitivity of the experiment.

Although both PDBu and PMA stimulate PKC, they have different physical properties and affinities for different PKC isoforms. This suggests that different subsets or localizations of PKC molecules may be more sensitive to the microgravity environment. Interestingly, a difference in the basal level of cytokine synthesis was noted, indicating that even the unstimulated cell is sensitive to microgravity.

In the Phorbol experiment, radio-labeled phorbol ester was used as a marker for PKC localization. The percentage of total radioactively labeled phorbol ester in the membrane, cytosolic, and nuclear fractions revealed a trend in both Jurkat and U937 cell lines. In microgravity, the total percentage of the cytosolic fraction was lowest, increased in both the 1-g samples, and was highest in the 1.4-g sample. This increase in the cytosolic percentage was at the expense of the nuclear fraction, which decreased from the microgravity sample to the 1.4-g sample. (See the first reference).

The combined total percentage of nuclear and cytosolic fractions was constant in all samples between 75% and 80%. In comparison, the per-

centage of the membrane fraction was similar in all samples. Additionally, the total labeling was approximately two times higher in the microgravity samples compared to the 1-g centrifuge samples.

For both cell types, the data suggested that both the subcellular localization and regulation of PKC synthesis was modified in microgravity. Translocation of PKC to the nucleus appeared to increase in microgravity at the expense of the translocation to the cytosol, and synthesis was enhanced in microgravity.

Conclusion

The Cytokine experiment results indicated a moderate suppression in the synthesis of cytokines in microgravity compared to the on-board centrifuge control. Results on basal cytokine synthesis showed that even the unstimulated cell was sensitive to microgravity.

The Phorbol experiment results suggested that both the localization and regulation of PKC synthesis is modified by microgravity. Translocation of PKC to the nucleus appeared to increase in microgravity at the expense of translocation to the cytosol. These results have important implications for understanding the effect of microgravity on cellular activation processes.

References

Schmitt, D.A., Hatton, J.P., Emond, C., Chaput, D., Paris, H., Levade, T., Cazenave, J., and Schaffar, L., "The distribution of protein kinase C in human leukocytes is altered in microgravity," *FASEB J,* vol. 10, pp. 1627-1634, (1996).

Limouse, M., Manie, S., Konstantinova, I., Ferrua, B., and Schaffar, L., "Inhibition of phorbol ester-induced cell activation in microgravity," *Experimental Cell Research,* vol. 197, pp. 82-86, (1991).

Schmitt, D., Ohlmann, P., Gachet, C., and Cazenave, J., "Platelet shape change and protein phosphorylation induced by ADP and thrombin are not sensitive to short periods of microgravity," *Journal of Cell Science,* vol. 104, pp. 805-810, (1993).

Cell Microenvironment and Membrane Signal Transduction in Microgravity (Signal)

Dr. P. Bouloc, University of Paris-Sud, Orsay, France

A space cabin is subject (1) to the near absence of gravity forces, microgravity, and (2) to the presence of heavy particle (cosmic) radiation. As a consequence, living organisms may exhibit different behavior in space. Several experiments suggest an effect of gravity on single eukaryotic cells through alteration of Signal transduction pathways. Results on prokaryotes are often controversial. We concluded that the growth yield and the average cell mass of the bacterium *Escherichia coli* were not affected by growth in space. However, *E. coli* seems less sensitive to antibiotics in space, suggesting that biological processes could be affected. Since convection movements are decreased by weightlessness, we speculated that the microenvironment of a cell could be affected. Surface tension, modified by microgravity, could also affect the structure of a membrane. The goal of the Signal experiment was to examine the effects of microgravity on microenvironment and signal transduction using *E. coli*.

A specific instrument was designed to treat timepoints simultaneously, with easy handling by astronauts. Containers house chambers of 3 rows of 6 wells of 1 ml. Chambers are sealed by septa through which multi-injectors to inject either glucose, NaCl, or an antibiotic can be inserted.

Flight Activities

When saturated cultures of *E. coli* are diluted to extremely low density, they are unable to grow unless the medium contains carbonate. This reflects a requirement for carbon dioxide that diffuses freely across membranes, resulting in a very low cytoplasmic concentration. We speculated that the absence of convection in microgravity might permit the accumulation of carbon dioxide around the cell, thereby shortening the growth lag.

Highlights

- Observed possible reduced growth lag period of a non-motile culture of *E.coli* in microgravity.
- Efficient induction of one two-component system regulating the osmoregulation in *E.coli* in microgravity.

To evaluate the lag, we prepared dilute suspensions of motile and non-motile *E. coli* cultures in medium lacking glucose with or without sodium carbonate. The containers maintained at 4 °C, shortly before the experiment were transferred to 37 °C. At time zero, glucose was injected by the astronaut into all the wells. After 9 h, growth was stopped by the injection of an antibiotic and the container was stored at 4 °C. The same protocol was followed for flight, ground, and 1-g centrifuge (flight and ground) samples. On recovery, all samples were assayed for viable bacteria. For the motile strain, no significant difference was observed. The situation was rather different for the non-motile strain. A fraction of the inoculum of this mutant failed to form colonies, complicating the interpretation of the results. Taken at face value, the growth lag appears shorter in microgravity than at 1-g, whether in the flight centrifuge or on the ground. Surprisingly, the apparent lag under 1-g conditions was not abolished by sodium carbonate.

Postflight Analysis

Signal transduction pathways across membranes ensure communication between the cell and its environment, allowing the cell to adjust its metabolism with changes in the surrounding medium. Several results have suggested that this type of communication may be reduced or abolished in microgravity. This led us to test a bacterial transduction pathway. We chose the response to osmotic shock in *E. coli* that we monitor by the expression of a *ompC::lacZ* operon fusion. Its induction depends on a two-component regulatory system.

The microenvironment experiment was started by injecting glucose into the wells. After 9 h, NaCl was injected. After one more hour, growth was stopped by the injection of an antibiotic. The *ompC::lacZ* fusion expression was assayed on Earth; the results show clear induction after hyperosmotic shock in conditions of microgravity. The bacterial system transducing osmotic information from the external medium to the cytoplasm is functional in microgravity.

Conclusion

The constraints to perform experiments in space impose a certain degree of caution in drawing conclusions. Our experiments (1) suggest that non-motile *E. coli* cells in microgravity have less of a lag period before resuming growth than at 1-g, and (2) that one system of signal transduction across the *E. coli* envelope is functional in microgravity conditions.

References

Bouloc P. and D'Ari R., "*Escherichia coli* metabolism in space," *Microbiol.* (formerly *J. Gen. Microbiol.*), vol. 104, pp. 2839-2843, (1991).

Gasset G., Tixador R., Eche B., Lapchine L., Moatti N., Toorop P., and Woldringh, C., "Growth and division of *Escherichia coli* under microgravity conditions," *Res. Microbiol.*, vol. 145, pp. 111-120, (1994).

Gmünder F.K. and Cogoli A., "Cultivation of single cells in space," *Applied Microgravity Technology*, vol. 1, pp. 115-122, (1988).

Thévenet D., D'Ari R. and Bouloc P., "The Signal experiment in BIORACK: *Escherichia coli* in microgravity," *J. Biotech.*, vol. 47, pp. 89-98, (1996).

Effect of Stirring and Mixing in a Bioreactor Experiment in Microgravity (Bioreactor)

Dr. A. Cogoli, Space Biology Group of ETH, Zurich, Switzerland

On Earth, nutrients and/or waste macroscopic gradients can be formed when non-motile cells sediment in static cultures or, at 0-g, when cell uptake is quicker than the diffusion rate. Microscopic gradients may also appear in the close environment of the cells when no convection occurs (0-g). Such gradients have an influence on the metabolism of the cells. In microgravity, the physico-chemical environment changes may play an important role in the reaction of the cells to weightlessness. Gradient formation is avoided when the culture is correctly stirred. The comparison of mixed or non-mixed cultures in microgravity with the ground controls will elucidate the role of the physico-chemical environment on the cells and the effect of stirring on cells at 0-g.

Highlights

- Bioreactor performed well.
- Higher percentage of randomly distributed bud scars in flight cells (17%) than in ground control cells (5%).
- Found no remarkable differences in the cell cycle, ultrastructure, cell proliferation and volume, ethanol production, and glucose consumption.

Flight Activities

We developed a miniaturized Bioreactor for continuous cultivation of cells in space. The organism we used was the baker's yeast *Saccharomyces cerevisiae* LBGH1022 (ATCC 32167). Four identical Bioreactors were used, two in flight and two on the ground as controls. The flight Bioreactors were either stirred (400 rpm) or unstirred to investigate the effect of mixing in microgravity. One ground Bioreactor was stirred at 400 rpm; the other one was slowly stirred at 100 rpm to avoid total sedimentation of the cells in 1-g conditions. The need for fresh medium was approximately 100 ml per unit (8 d at dilution rates varying between 0.07 and 0.35 h^{-1}). The data on pH, pH-regulation, redox potential, and temperature were transmitted real-time to the ground during the experiment.

Seventy-two hours after launch, the Bioreactors were transferred from the storage at 5 °C to the Biorack incubator at 22 °C. Sampling took place 72 h, 120 h, 144 h, 168 h, and 192 h after beginning of the incubation. The astronauts drew the samples manually (1 ml each). Two aliquots of 500 µl each were injected in small flasks sealed with a rubber septum. One set of samples was stored at -20 °C, and the other was fixed and stored at 5 °C.

Postflight Activities

The samples and the Bioreactors were recovered 6 h after landing. The exhaust bags and the cultivation chambers were emptied in separated flasks and frozen. The fixed samples were processed and stored at 5 °C. The samples were carried to our laboratory and stored in containers at 5 °C and -20 °C, respectively. The frozen samples were used for the biochemical analyses.

Adverse laboratory conditions during mounting and filling of the Bioreactors before the mission caused the formation of air bubbles in the micropump and in the Bioreactor liquid circuitry. This greatly reduced the capacity of the pump. Because of inconsistent pumping rates, most of the data from the four cultures cannot be compared. However, we demonstrated the potential of the Bioreactor, and the morphological analysis of the cells is interesting.

Cell growth was measured by two methods, i.e. by determination of the optical density of the culture and by counting the cells. Both methods gave corresponding results. The cells grew well, both in space and on the ground and in the unstirred and stirred Bioreactors.

The supernatant of the frozen samples was analyzed for the glucose that was not consumed and

for the ethanol produced by the cells. The cells were able to consume glucose and to produce ethanol in space and on the ground. This shows, together with the results of the cell counts, that the Bioreactor is a suitable instrument for continuous culture of single cells in space. The scanning and the transmission electron micrographs show that the cells grown in space are morphologically similar to those grown on Earth. The numerous small mitochondria indicate that the cells were not limited in oxygen.

The duration of the cell cycle of *S. cerevisiae* depends on the growth rate. Analysis of the DNA by flow cytometry showed that the variations in the cell cycle duration are mainly due to the differences in the length of the G1 phase. The reduction or even absence of a G2+M phase in certain samples (flight stirred and ground slow stirred) cannot be explained yet and needs further clarification.

Two aspects were considered in the analysis of the bud scars, first, their positioning and second, their number per cells. *S. cerevisiae* cells multiply by cell division (budding). During budding, a chitin ring is formed at the bud site. The ring leaves a scar on the mother cell after separation of the daughter cell. The scars are distributed polarly. The P-value ($P<0.001$) of the percentage random versus bipolar distributed scars shows that the difference between ground and flight samples is very strongly significant. No significant difference was observed between the samples taken at the beginning and the end of the experiment. The spindle body and the microtubules machinery play an important role in the localization of bud emergence. Therefore, we may speculate that alterations of the cytoskeleton (which followed exposure to microgravity) may have influenced the positioning of the scars. Morphological changes in microgravity strongly suggest a direct effect of gravity on the cytoskeleton.

Conclusion

This experiment shows that the miniaturized Bioreactor is an instrument suitable for continuous cultivation of single cells under controlled conditions. A significant morphological difference has been detected between cells grown in microgravity and at 1-g at the level of budding scars. Further experiments in space and on Earth in the clinostat will clarify whether such changes are a direct effect of gravitational variations (e.g., on the cytoskeleton) and therefore, have an impact on important cellular mechanisms. Bioreactors will be required for long-duration exposure of single cells to microgravity (bacteria, plants, protozoa, and animals) in satellites and on space stations.

References

Moore, D. and Cogoli A., "Gravitational and space biology at the cellular level," *Biological and medical research in space*, Moore, D., Bie, P., and Oser, H., eds., Springer Verlag, pp. 1- 106, (1996).

Walther, Z., Bechler, B., Mueller, O., Hunzinger, E., and Cogoli, A., "Cultivation of *Sacchoromyces cerevisiae* in a bioreactor in microgravity," *J. Biotechnol.*, vol. 47, pp. 113-127, (1996).

Visser ,W., van Spronsen, E.A., Nanninga, N., Pronk, J.T., Kuenen, J.G., and van, Dijken J.P.; "Effects of growth conditions on mitochondrial morphology in *Saccharomyces cerevisiae," Antonie van Leeuwenhoek*, vol. 67, pp. 243-253, (1995).

Cogoli-Greuter, M., Pippia, P., Sciola, L., and Cogoli, A., "Lymphocytes on sounding rocket flights," *J. Gravitational Physiol.*, vol. 1, p. 90, (1994).

Walther, I., van der Schoot, B., Jeanneret, S., Arquint, P., de Rooij, N.F., Gass, V., Bechler, B., Lorenzi, G., and Cogoli, A., "Development of a miniature bioreactor for continuous culture in a space laboratory," *J. Biotechnol.*, vol. 38, pp. 21-32, (1994).

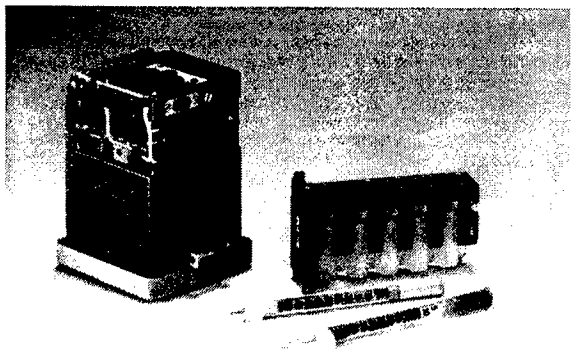

Figure 1: Bioreactor, sampling bottles, and syringes

Biological Investigations of Animal Multi-Cell Aggregates Reconstituted under Microgravity Conditions (Aggregates)

Dr. U.A.O. Heinlein, Heinrich-Heine-Universität, Düsseldorf, Germany

Primary cells obtained from dissociated neonatal mouse tissues like cerebellum and testis are convenient model systems to study the reaggregation and reorganization of cells into multicellular objects. Both starting tissues are capable of forming three-dimensional aggregates mimicking the *in vivo* situation by beginning cell layering, formation of interconnecting cables, and cellular migration along supporting cells.

A number of molecular parameters are known to influence not only the aggregation properties, including general cell surface components like glycoconjugates but also special cell surface molecules that have been identified and shown to be involved in cell adhesion. One of these molecules is the neural cell adhesion molecule, NCAM, which has been shown to exert influence on the *in vitro* reaggregation properties of primary cerebellum cells.

In an attempt to analyze the importance of the cell surface information, primary cultures of dissociated cerebellum and testis cells have been performed under microgravity conditions. To achieve this, novel cell culturing hardware (the C5 Unit) had to be developed, allowing semi-automatic medium exchange and fixation without the use of syringes and septa.

Flight Activities

The 10 samples in the incubation unit of the "C5 Unit" included 4 aliquots of primary neonatal cerebellar cells, 4 aliquots of primary neonatal testis cells, and 2 co-cultures of cerebellum cells and NCAM-transfected mouse L cells. The cells in the incubation unit were kept at 4 °C during the launch phase. Total time at 4 °C, from preparation to Biorack activation, was 27 h. Using the medium exchange unit of the C5 Unit, fresh medium was supplied every 48 h. The cells were finally processed by the addition of fixative, and the incubation unit stored at ambient temperature until mission completion. Each medium exchange/fixation step required approximately 15 min of crew time.

Highlights

- Results indicate the initial adhesion among cells is not disturbed in microgravity.
- Formation of interconnecting cables (a prerequisite to cell migration between aggregates under normal gravity) did not occur in the flight samples.

Postflight Analysis

Fixed samples were processed for light, fluorescence, and electron microscopy. To achieve best conservation of the samples, the entire Accurel™ membrane cylinders containing the cells were infiltrated with low-melting agarose. The agarose plugs were then either observed by light microscopy or embedded for sectioning.

Aggregates recovered from the "C5 Unit" flight hardware showed differences from those obtained during ground-control experiments. Dissociated cerebellum cells reaggregated to smaller aggregates than the respective ground samples. The number of aggregates, however, was considerably higher in the flight samples (see Table 1).

Neonatal testis cells, when plated under appropriate conditions on the ground, form extended structures with beginning cell sorting and layering. These cell aggregations, called nodules, were not detectable in the flight samples examined. The testis microgravity aggregates displayed loose adhesion and random branching. This overall structures made it impossible to collect any statistical data.

Two of the 10 flight samples contained co-cultures of cerebellum cells and mitomycin-treated mouse L cell fibroblasts transfected with recombinant NCAM cDNAs. There was no

significant difference between flight and ground samples with respect to the aggregation and integration properties of these cells. Integration of NCAM-expressing fibroblasts into newly forming cerebellar aggregates occurred as well as initial adhesion among the L cells.

	Number (n/mm^2)	Length (mm)	Shape (d_1d_2)
Ground 1-g	40	43	1.33
Flight 1-g	45	40	1.26
Flight 0-g	82	28	1.07

Table 1: Aggregate number and dimensions compared between Biorack ground and flight samples.

Conclusion

In vitro reaggregation of dissociated primary cells is a process including four major steps: (1) initial adhesion, (2) agglomeration to larger aggregates, (3) formation of cable-like interconnections, (4) cell migration. Our results indicate that the initial adhesion among cells is not disturbed in microgravity, i.e. the cell surface parameters are sufficient to support initial interactions. This is supported by ground and inflight data on the adhesion and integration properties of NCAM-transfected heterologous L cells. Subsequent formation of interconnecting cables, however, which is a prerequisite to cell migration between aggregates under normal gravity, did not occur in the flight samples. This is presumably due to the nearly perfect spherical shape of the aggregates and a configuration of the cytoskeleton not capable of supporting normal cable outgrowth. The failure to response properly to the initial adhesion events might also be due to an altered capability to respond to external stimuli, i.e. signal transmission from surface to nucleus and adequate response. Further experiments are necessary to gain more and detailed knowledge.

References

Hartmann, U., Vens, C., Vopper, G, Wille, W., . Heinlein, U.A.O., "Ectopic expression of NCAM in mouse fibroblasts stimulates self-aggregation, and promotes integration into primary cerebellum cell aggregates," *Cell Adhes. Comm.*, vol. 2, pp. 287-298, (1994).

Vens, C., Kump, B., Münstermann, B., Heinlein, U.A.O., "The C5 Unit: a semi-automatic cell culture device suitable for experiments under microgravity," *J. Biotechnol.*, vol. 47, pp. 203-214, (1996).

Replication of Cell Growth and Differentiation by Microgravity: Retinoic Acid-Induced Cell Differentiation (Mouse)

Dr. S.W. de Laat, Netherlands Institute for Developmental Biology, Utrecht, The Netherlands

Experiments have shown that microgravity causes impairment of the signal transduction pathway by EGF in A431 cells as induction of the AP1 is lowered, while some other steps in the process (e.g. EGF binding to its receptors and receptor clustering) are not affected. At the same time changes in the (actin) microfilament cytoskeleton have been observed. We do not know if microgravity affects long-term processes such as DNA synthesis (and subsequent cell division) in adherent cells.

The vitamin A derivative, retinoic acid (RA) is a potent inducer of cell differentiation usually accompanied by growth inhibition and cell cycle arrest. Lipophilic molecules such as RA (and steroids) have free access to the cell and will bind to nuclear receptors that act as ligand-activatable transcription factors at the level of the DNA. This experiment aimed to obtain the first evidence of microgravity effects on signal transduction by growth factors and a natural growth inhibitory agent retinoic acid, on long-term processes such as DNA synthesis (induction by growth factors and inhibition by RA) and gene induction by RA.

Flight Activities

We selected a permanent mouse fibroblast cell line, C3H/10T1/2 cells, which can be kept in a quiescent, non-growing state for weeks upon serum starvation. Upon addition of growth factors, these cells are re-activated and re-enter the cell cycle, whereas RA will inhibit this process. To study the effects of microgravity on growth factor-induced DNA synthesis, C3H/10T1/2 cells were stimulated by growth factors in the presence of BrdU, a marker for DNA synthesis that is incorporated into DNA when cells enter the S-phase of the cell-cycle.

Highlights

- The RA-induced reporter gene expression is impaired in microgravity.
- Need more experiments to demonstrate the effect of microgravity on DNA synthesis.

To study gene induction by RA, we have genetically engineered C3H/10T1/2 cells by introducing a reporter DNA construct in which RA-sensitive sequences are connected to the β-galactosidase (*LacZ*) gene. Upon addition of RA, cells will accumulate LacZ protein that can be visualized by X-gal (blue) staining. The samples of the experiment in which the effect of microgravity on growth factor-induced DNA synthesis is studied will be referred to as the **BrdU-experiment**, while the samples of the experiment in which the effect of microgravity on RA-induced RARβ expression will be referred to as the **LacZ-experiment**.

The AECs were placed into Biorack Type I/E containers, which were equipped with a connector for electrical activation and recording of temperature and housekeeping signals. The I/E containers were stored at room temperature until they were inserted into Biorack, for 32 and 58 h respectively (LacZ and BrdU experiments), after launch. Half of the AECs were incubated at microgravity, while the other half were in a 1-g reference centrifuge. The temperature of the AEC remained at 37 °C during the whole experiment. The unstimulated controls for both the BrdU and LacZ experiments, were fixed 1 min after initiation of the experiment. For the LacZ experiment, the cells were stimulated for 16 h with growth factors after which the cells were fixed. For the BrdU experiment the cells were stimulated with growth factors in the presence of BrdU. After 30 and 48 h the cells were fixed, and the AECs were transferred to 4 °C.

Postflight Analysis

After the mission, the samples were stained. Since there are differences between the samples

26-NL MOUSE
Results

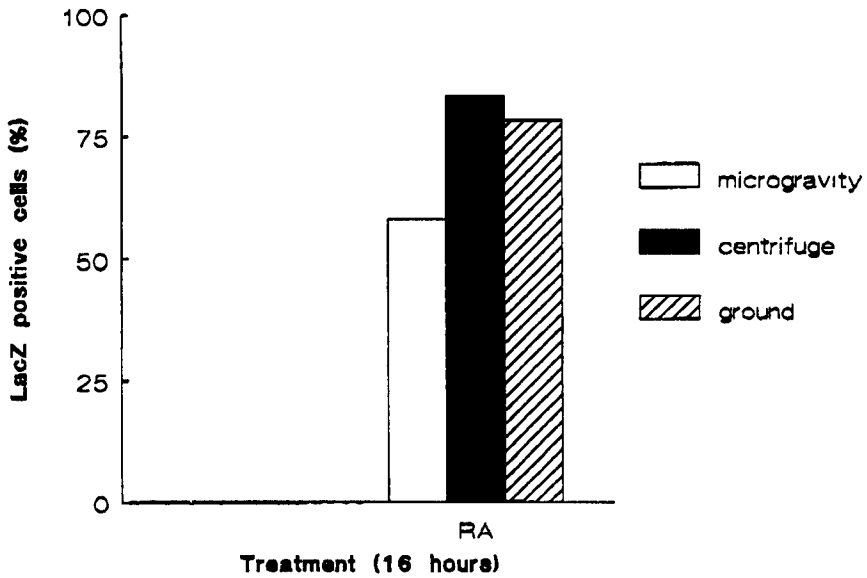

Figure 1: The effect of microgravity on RA-induced RARβ expression in C3H/10T1/2 c18-1.8-c3 cells.

with respect to cell morphology and cell viability, only the viable cells were evaluated for the outcome of the experiment. There is a tendency that the RA-induced RARβ expression is repressed to some extent under microgravity, since less nuclei of the samples incubated under microgravity (58%) were stained in comparison with the samples of the 1-g reference (83%) centrifuge and ground control (78%). In the controls, samples that were immediately fixed after initiation of the experiment without stimulation, no blue staining could be detected. No results were obtained with the samples which were incubated with both RA (105 M) and insulin (10 μg/ml)/EGF (25 ng/ml) since practically all cells died.

The major part of the results from the BrdU experiment are not suitable for detailed analysis and can be considered lost. Viable cells could only be found in the ground control untreated samples or 30 h treated with insulin/EGF and in one flight sample treated for 30 h with insulin/EGF/RA. Moreover in the untreated ground control sample, we observed that not all the cells were in the quiescent state since a significant percentage (16%) of the cells had incorporated BrdU. Nevertheless cells could still be driven into S-phase, since the ground control sample treated for 30 h with insulin/EGF contained more BrdU-stained nuclei (39%).

Conclusion

In conclusion, the outcome of the LacZ experiment is promising, as the RA-induced reporter expression seems to be impaired considerably. However, definitive conclusions are hard to draw because no intact duplicate samples were available. Although no firm conclusions can be drawn from these experiments, the results indicate that the RA-induced reporter gene expression is impaired under microgravity conditions. Similar experiments have to be performed to demonstrate the precise effect of microgravity on the regulation of DNA synthesis.

The Sea Urchin Larva, A Suitable Model for Biomineralization Studies in Space (Urchin)

Dr. H.-J. Marthy, CNRS Observatoire Océanologique, Banyuls sur mer, France

The sea urchin larva (pluteus) is morphologically well characterized by an internal skeleton, a transient, essentially calcarous structure ($CaCO_3$). It differentiates from the primary mesenchyme cells (a cell population derived from the micromeres), which proliferate in the blastocoelic cavity of the embryo from the blastula stage onward. Originating as 2 small granules, skeletogenesis in *Sphaerechinus granularis* larvae is completed within about 5 days (at ±20 °C).

The first objective of the experiment was to determine whether under microgravity conditions the process of mineralization (the formation of skeletal structures in the growing embryo/larva of sea urchins) does occur correctly. The second goal was to determine whether larvae with skeletons fully differentiated on the ground will demineralize in microgravity. Since normal embryogenesis and larval development is the prerequisite for the formation of a completely normal skeleton, persisting skeletal structures recovered from space not only show if the mineralization process can occur but also show (by their normal or abnormal skeleton architecture and by comparison to ground controls) to what extent the mineralization process is "normal" or disturbed in microgravity. Inversely, a demineralization process under conditions of microgravity would show up by reduced or "ghost" skeletons.

Flight Activities

Adult sea urchins (*Sphaerechinus granularis*) from the Mediterranean Sea were maintained in Florida. Blastula embryos (prior to the onset of skeleton formation) and pluteus larvae (skeleton formation accomplished) were sealed into small, double-wall plastic bags, packed into Type 1 Biorack containers and kept at +5 °C until activation of the experiment in microgravity and on the ground. Except for one container kept at +5 °C, all others were transferred to +22 °C. After 2, 4 and 9 days, respectively, containers were put in the +37 °C incubator for 2 h (destroying the embryonic tissues, without effect on skeletons or skeletal spicules) and then stored at ambient temperature (except one container, transferred at day 9 directly from +22 °C back to +5 °C) until landing.

Highlights

- Basic biomineralization occurred in microgravity, and no pronounced demineralization was observed.
- Developmental processes such as the proliferation and specific differentiation of the skeletogenic cells occurred; however the process of their positioning appears to be more sensitive to environmental factors, possibly including microgravity.

Postflight Analysis

Analysis started immediately after recovery of the flight and ground containers. First, a polarization microscope was used to search through the plastic bags for skeletal structures. The main analysis was done at our laboratory. The experiment plastic bags were opened, the content recovered, photographed, and prepared for Scanning Electron Microscopy studies and X-ray microprobe analyses. For statistical analyses, we used diameters of simple spicules.

The material was good enough for all analyses. Skeletons with a fairly normal architecture and skeletal spicules with simple and fenestrated parts of the skeletons were recovered from all experiments started with blastulae. From the experiments started with plutei, intact skeletons and individual spicules were also recovered.

Since skeletons and spicules were recovered from the flight experiments, it is evident that the basic biomineralization process actually occurs in microgravity. No pronounced demineralization phenomena appear to occur in microgravity

in larvae with skeletons that had differentiated already on Earth.

X-ray microprobes on the mineral composition of the different spicules revealed no significant qualitative and quantitative differences. Measurements of spicule thickness show a somewhat lower value in samples cultured for 2 days on the on-board centrifuge (Figure 1). Extensive Scanning Electron Microscope studies on recovered skeleton and spicule forms reveal a great heterogenity (architecture, size, and length) in 0-g in flight and 1-g on the ground (Figure 2) and 1-g in flight and 1.4-g on the ground.

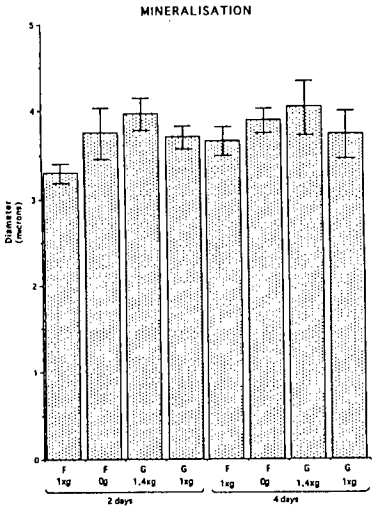

Figure 1: Mineralization state in pluteus larvae after 2 and 4 days, respectively, in culture (at +22 °C) at different g-levels from blastula stage onward as revealed from spicule thickness. After 4 days in culture, no significant difference between samples is observed. After 2 days in culture, however, samples on the on-board centrifuge (F 1-g) show some delay in the mineralization process, possibly a gravity-related adaptation phenomenon.

Conclusion

This experiment showed that sea urchin larvae under conditions of microgravity are capable of differentiating skeletal structures. This means that developmental processes such as the proliferation of the skeletogenic cells (primary mesenchyme cells), the positioning of these cells in

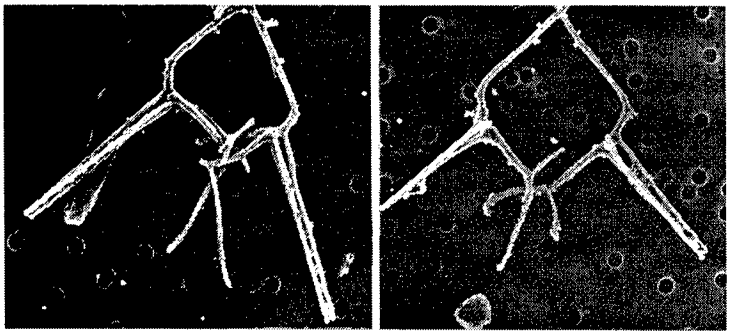

Figure 2: Skeletons developed in ESA Bioracks under 0-g conditions in flight (left) and under 1-g conditions (right). Note the bilateral architecture of the skeletons, built by simple and fenestrated spicules, in both samples.

the blastocoelic cavity at blastula and gastrula stages, and their capacity of specific differentiation (capacity of mineral apposition) do occur. Differences in spicule diameters are interpreted as some delay in the mineral apposition on the organic matrix of the skeletogenic cells. The great variety of abnormal skeletal forms and spicules in all samples is confusing. There may be microgravity effects; if so, they are masked by unidentified factors. From an embryological point of view, studies on the phase-specific behavior of the skeletogenic primary mesenchyme cells, essentially their positioning process, are needed.

The experiment also showed that sea urchin larvae under conditions of microgravity maintain their previously formed skeletons and mineral composition. If microgravity produced any demineralization, the effect must be weak and was not perceived.

References

Marthy, H.-J., Gasset, G., Tixador, R., Schatt, P., Eche, B., Dessommes, A., Giacomini, T., Tap, G., and Gorand, D., "The sea urchin larva, a suitable model for biomineralisation studies in space (IML-2 ESA Biorack experiment '24-F urchin')," *J. Biotechnology,* vol. 47, pp. 167-177, (1996).

Marthy, H.-J., Gasset, G., Tixador, R., Eche, B., Schatt, P., Dessommes, A., Marthy, U., Bacchieri, R., "Skeletogenesis in sea urchin larva under varied gravity conditions," *31st Scientific Assembly of COSPAR,* Birmingham, Abstracts, p. 312, (1996).

Marthy, H.-J., Gasset, G., Tixador, R., Schatt, P., Eche, B., Dessommes, A., "Skeletogenesis in urchin larvae in space (IML-2 ESA Biorack experiment)," *ASGSB Bull.*, abstract, vol. 9, no. 1, p. 88, (1995).

Marthy, H.-J., Schatt, P., Santella, L., "Fertilization of sea urchin eggs in space and subsequent development under normal conditions," *Adv. Space Res.*, vol. 14, pp. 197-208, (1994).

The Effect of Microgravity and Varying Periods of 1-g Exposure on Growth, Mineralization, and Resorption in Isolated Fetal Mouse Long Bones (Bones)

Dr. J.P. Veldhuijzen, Amsterdam Academic Center for Dentistry, Amsterdam, The Netherlands

Their responsiveness to mechanical loading make isolated mouse fetal long bone a useful model for studying the effects of microgravity on growth, mineralization, and resorption. These developing bones consist of cartilage that mineralizes during culture. Bone-forming cells (osteoblasts), which are responsible for the formation of the bony shaft, are also present. Depending on the embryonic age of the long bones, mineralized cartilage is removed by the action of osteoclasts (mineral- or bone-resorbing cells). In this model of isolated developing mouse long bones, we have demonstrated that under intermittent hydrostatic compression, the activity of chondrocytes and osteoblasts in relation to matrix mineralization is stimulated, while osteoclastic mineral resorption is decreased.

An IML-1 experiment demonstrated that microgravity did not change the growth (length increase) of the bone, but matrix mineralization was significantly reduced. On the other hand, osteoclastic mineral resorption was significantly enhanced in microgravity. The first objective of the IML-2 experiment was to verify results from IML-1 and other prior experiments. The second objective was to see if varying periods of 1-g exposure would counteract the effects of microgravity on bone mineralization and resorption.

Flight Activities

We used mouse long bones of one embryonic age (17-day stage). The experiment was housed in 10 Type 1 containers, 5 flight and 5 ground control. In addition, long bones in an extra ground control Type 1 container were fixed at the moment when the flight experiment started. Analyses of this group were used for baseline data. Two flight containers were used to verify IML-1 results: one container remained on the static rack exposed to microgravity for 4 days, and the other stayed on the 1-g centrifuge. Of the 3 remaining containers, 1 was placed daily for 3 h on the 1-g centrifuge, the second for 6 h, and the third for 12 h. These containers were compared with the 2 other containers (microgravity and 1-g continuous exposure) to study the threshold value of 1-g exposure needed as a countermeasure to microgravity.

The experiment was initiated when the containers were placed in the 37 °C incubator. After 4 days, the experiment was stopped with chemical fixation of the bones. The cultures were stored at 4 °C until landing. They remained at this temperature during transportation to our laboratory for analysis.

Highlights

- Confirmed IML-1 results: microgravity did not affect overall growth but did decrease mineralization.
- A decrease in mineralization was not found in long bones placed for 6 h daily on the 1-g centrifuge. Initial effects were found after 3 h daily 1-g exposure.

Postflight Analysis

Of the 16 long bones in each experiment container, 10 were prelabeled with ^{45}Ca to study mineral resorption (measured as ^{45}Ca release). The release of the labeled calcium is a measure of the mineral resorption by osteoclasts. After mineral extraction, the long bones were used for normal histology (such as morphology), enzyme histochemistry (staining for osteoclasts), and immunocytochemistry (collagen typing).

The 6 long bones in each container that were not labeled with ^{45}Ca were used to study mineralization. Photomicrographs of the bones taken before and after the experiment were used to measure overall length increase (growth) and the length increase of the mineralized diaphysis (mineralization).

Analyses revealed that the cultures were healthy, and no dead cells were found. No morphological differences were observed between the flight groups and ground controls. Some osteoclasts were present in the mineralized diaphysis of the bones; however resorption phenomena were not seen in all bones. In general, mineral resorption in all groups was much less than expected. When present, measurements of the number and localization of osteoclasts indicated that in the diaphysis of the microgravity group, more mineral resorbing osteoclasts were present than in the bones of the 1-g group. This finding may suggest an increased mineral resorption under microgravity. In addition, the ^{45}Ca-release measurements in another group of ^{45}Ca-prelabeled long bones revealed very little or no osteoclastic activity. These histological and biochemical observations indicate that perhaps the mice were slightly too young for the resorption studies.

Overall growth of the long bones was calculated from measurements of the pre- and postflight photomicrographs and was expressed as a percentage increase in overall length. The length increase of the long bones cultured continuously

In microgravity and in the 1-g centrifuge did not differ. The values (50-60%) are well in the range of those found during IML-1. Microgravity did not affect the overall growth of the long bones.

Mineralization in the long bones decreased (29%), which verifies prior findings. The results from all experiments to date strongly suggest that the loss of mineral from the skeleton during space flight is a direct effect of microgravity on the skeletal tissue cells. A new finding was that under *in vitro* conditions a daily exposure of the long bones to only 6 h of 1-g was sufficient to fully counteract the microgravity-induced mineral loss. Multiple regression analysis of the data showed a significant relation between the time of 1-g exposure and the mineralization. This analysis demonstrated that from a 3 h period on, 1-g exposure is effective in counteracting the influence of microgravity on mineralization. (See Figure 1.) At 24 h exposure, the effects leveled off and even decreased.

We were not able to draw any conclusion from these data about the effect of microgravity or varying 1-g exposure on mineral resorption. The ^{45}Ca measurements revealed very little or no osteoclastic activity, perhaps indicating that the mice used for the resorption studies were too young. We are performing an histological evaluation using a special staining for osteoclasts to determine if this was the case.

Conclusion

The data from prior space experiments was validated. Under *in vitro* conditions, microgravity had direct effects on skeletal tissue cells, which resulted in reduced mineralization, but no effect on overall growth. This may explain the loss of calcium from the skeleton and the reduction in bone mass reported after space flights in humans and other animals. From a daily 1-g exposure period as short as 3 h on, 1-g exposure was effective in counteracting the negative effect of microgravity on mineralization. The next step in microgravity and bone cell research should be to use isolated cells (osteoblasts and chondrocytes) and study the mechanisms that the cells use to translate the loss of gravity stimulation into a cellular response.

References

van Loon, J.J.W.A., Veldhuijzen, J.P., and Burger, E.H., "Bones and space flight: an overview," In: *Biological and Medical Research in Space,* (An overview of Life Sciences Research in Microgravity), Chapter 5, Moore, Bie, and Oser, eds., Springer-Verlag, Heidelberg, p. 259, (1996).

Veldhuijzen, J.P., Bervoets, T.J.M., Blaauboer, C.W., Dieudonné, S.C., Haaijman, A., Hagen, J.W., Semeins, S.M., and Zandieh-Doulabi, B., "Isolated skeletal tissues cultured under microgravity," COSPAR, 31st Scientific Assembly, Birmingham, England, p. 307, (1996).

Veldhuijzen, J.P., van loon, J.J.W.A., Haaijman, A., Semeins, C.M., and Bervoets, T.J.M., "Reduced mineralization under microgravity is counteracted by short-term exposure to 1xg conditions," *Calcif. Tissue Int.*, vol. 56(5), p. 458, (1995).

Veldhuijzen, J.P. and van loon, J.J.W.A., "Effects of microgravity on mineralization and resorption in isolated fetal mouse long bones," *Congress of European Developmental Biology Satellite Symposium*, Toulouse, France, (1995).

van Loon, J.J.W.A., Bervoets, D.J., Burger, E.H., Dieudonné, S.C., Hagen, J.W., Semeins, C.M., Zandieh-Doulabi, B., and Veldhuijzen, J.P., "Decrease mineralization and increased calcium release in isolated fetal mouse long bones under near weightlessness," *J. Bone Min. Res.*, vol. 10, p. 550, (1995).

Investigation of the Mechanisms Involved in the Effects of Space Microgravity on *Drosophila* Development, Behavior, and Aging (Drosophila)

Dr. R. Marco, Universidad Autónoma de Madrid, Madrid, Spain

One experiment objective was to confirm earlier findings that young male *Drosophila* fruit flies exposed to microgravity showed an acceleration in aging. A second objective was to study fruit fly reproduction and development in space.
A main challenge of current biological research is to understand the aging process in complex, multicellar organisms. The idea that an enhanced metabolism (the rate-of-living theory) accelerates the rate of aging was one of the explanations of this phenomena, which was further refined by linking an increase in mitochondrial function to increased metabolism. Prior space experiments indicated that the male fruit fly life span did decrease in microgravity. This experiment confirmed this result and provided information on the link to mitochondrial function.

Female fruit flies were used to study a second aspect of living in space: reproduction and development. *Drosophila* has many advantages for space experimentation: it is small and resilient, scientists understand its development well, and it develops very quickly, providing the opportunity to study all phases of development.

Flight Activities

Two hundred male flies were housed in the Biorack's static containers for continuous exposure to microgravity, while 100 were in an in-flight 1-g centrifuge. Every 2 days, the crew recorded the flies on video, revealing a marked increase in fruit fly locomotor activity in 0-g

For the developmental experiments, 160 females produced several thousand embryos during the mission. The experiment was performed in 2 containers installed in the Biorack's microgravity static position and 2 installed in the 1-g centrifuge. Before launch, 40 females and 10 males were loaded in each container; the flies were young, hatched from the pupae cases the night before loading. An identical experiment with sibling flies was performed in parallel on the ground. In flight, the crew collected and froze embryos and larvae at predesignated times, allowing some of the eggs laid at defined times to continue development in space.

Highlights

- Confirmed accelerated aging of male fruit flies exposed to microgravity.
- Linked increased aging to increased activity and mitochondrial processes.
- Verified normal development of fruit flies (from single cells to adulthood) in space.

Postflight Analysis

The male flies used for the aging study were returned to the laboratory. Tests, including physiological vitality assays (mating and negative geotaxis) and life span curves, showed an accelerated aging response. The involvement of mitochondrial metabolism was suggested by the finding of a greater decrease in mitochondrial 16S ribosomal RNA in the microgravity-exposed flies than in the ground controls. The amount of food consumed by the flies supported the concept that acceleration in activity is associated with increased metabolism.

For the development experiment, all the embryos, larvae, pupae, and imagoes recovered were normal in morphology and function. Representative samples of the frozen embryos and larvae were examined microscopically and hatched imagoes were individually visually inspected. In the live samples, the male/female ratios were calculated, and no significant mutagenic effects were indicted.

The number of fruit flies recovered was quite large, demonstrating that fruit flies can develop normally in space. As frozen samples 2,155

embryos and larvae were collected from microgravity samples and 1,752 were collected from ground-control samples. Thus, 20% more were collected in microgravity, confirming the increase in number of viable progeny in microgravity found in earlier space experiments. Results from earlier experiments were reproduced on IML-2 with a better experiment design. In space, we confirmed that oogenesis is stimulated and that development is slightly delayed when compared to that of synchronous parallel ground controls. It is clear from the 1-g flight control centrifuge and from the ground centrifuge samples that centrifugation can produce similar effects. The effects of development are small and more the consequences of a reaction to the abnormal space environment in general than a specific effect of microgravity.

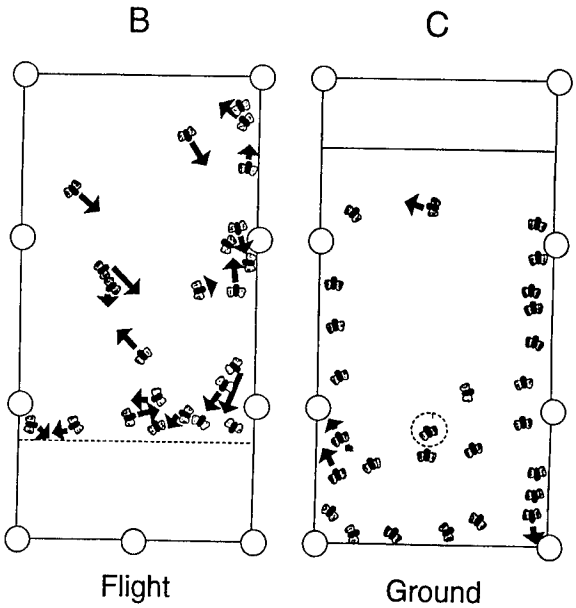

Figure 1: Snapshots of the video recordings of Drosophila male imagoes. Each point corresponds to a male fly and the arrows indicate the movement of the flies in the subsequent 1/6 of a second, i.e., during the next 5 video frames. B. corresponds to a flight container recorded at day 10 (T9) during the flight. C. corresponds to a ground container recorded at day 10 (T9) during the experiment. Most of the flies in C. are immobile. The point circled by a broken line, corresponds to a fly that is initiating a jump.

Conclusion

Any modification of *Drosophila* aging by exposure to microgravity has potentially important implications for our understanding of the aging process. For the IML-2 experiment, the increase in fly metabolism was measured by an increase in locomotor activity and an increase in food consumption. Future experiments should study male and female fruit flies to see if the shortened life span effect is more or less pronounced over longer periods of exposure to microgravity.

We have again confirmed that *Drosophila* development can occur normally under microgravity conditions. In microgravity, several hundred embryos reached pupation, a very advanced stage of development. Normal imagoes hatched from these pupae during the days immediately after landing.

References

Marco, R., Benguria, Al, Sánchez, J., and de Juan, E., "Effects of the space environment on *Drosophilia melangaster* development. Implications of the IML-2 experiment," *J. Biotechnol.*, vol. 47, pp. 179-190, (1996).

Anothony, P., Ausseil, J., Bechler, B., Benguria, A., Blackhall, N., Briarty, L.G., Cogoli, A., Davey, M.R., Garesse, R., Hager, R., Loddenkemper, R., Marchant, R., Marco, R., Marthy, H.-J., Perry, M., Power, J.B., Schiller, P., Ugalde, C., Volkmann, D., and Wardrop, J., Preservation of viable biological samples for experiments in space laboratories," *J. Biotechnol.*, vol. 47, pp. 377-393, (1996).

Benguria, A., Grande, E., de Juan, E., Uglade, C., Garesse, R., "Microgravity effects on *Drosophila melangaster* behavior and aging. Implications of the IML-2 experiment," *J. Biotechnol.*, vol. 47, pp. 191-202, (1996).

Chapes, S.K., Morrison, D.R., Guikema, J.A., Lewis, M.L., and Spooner, B.S., "Production and action of cytokines in space," *Adv. Space Res.*, vol. 14, no. 8, pp. 5-8, (1994).

Claasen, D.E. and Spooner, B.S., "Impact of altered gravity on aspects of cell biology," *Int. Rev. Cytol.*, vol. 156, pp. 301-373, (1994).

Agarwal, S. and Sohal, R.S., "DNA oxidative damage and life expectancy in houseflies," *Proc. Natl. Acad. Sci.*, vol. 91, pp. 12332-12335, (1994).

The Role of Gravity in the Establishment of the Dorso-Ventral Axis in the Amphibian Embryo (Eggs)

Dr. G.A. Ubbels, Hubrecht Laboratory, Utrecht, The Netherlands

In microgravity, the tempo of cell divisions is perturbed in some biological systems. On Earth, in normal embryos of the South African clawed toad (*Xenopus laevis)*, the first 8 egg divisions are synchronous. Only at the mid-blastula transition, i.e., at the onset of transcription in the zygote, the cleavage divisions become progressively asynchronous. During the IML-1 mission, we showed that automated (even 24 h delayed) fertilization in microgravity was successful and initiated embryonic development. This experiment also revealed that gravity was not required for axis formation since gastrulae were fixed at the programmed normal time. These results were confirmed by Souza, *et.al.*, on the Spacelab J mission.

In embryos from both these Shuttle missions, the formation of the blastocoel was perturbed, but this was regulated from gastrulation onward, so normal tadpoles were retrieved from Spacelab J. Sounding rocket and clinostat experiments also confirmed that simulated and actual microgravity may perturb blastocoel formation, but these anomalies do not interfere with normal development later on. Neither of the two previous Spacelab experiments gave relevant information regarding the role of the sperm in determination of the dorsal-ventral polarity in microgravity.

Our objectives were to (1) determine the cell cycle length and cleavage pattern during the fourth and eighth cleavage, (2) analyze the blastocoel formation and distribution of various yolk components under microgravity, and (3) identify the position of the sperm entry point in relation to the blastopore at gastrulation in microgravity. All space-grown embryos were compared to ground controls that developed at 1-g.

Highlights

- Found rate of cell divisions unchanged in actual and simulated microgravity.
- Microgravity perturbs blastocoel formation.

Flight Activities

The Automated Experiment Container (AEC) was used in the Biorack on IML-1 for fertilization and embryo culture. It was fully automated for IML-2, requiring no crew activities; housekeeping signals and temperatures were recorded and downlinked to the ground in real time. Structural modifications improved the fluid circulation in the blocks of the modified AEC (m-AEC) as well as visibility of the developing embryos, which could only be videotaped on Earth.

Before the mission, *Xenopus laevis* eggs and testes, salt solutions, and fixatives were loaded into 6 m-AECs, within 2 h after stripping eggs from adult female toads. The m-AECs were inserted in Biorack Type 1E containers and kept at 10 °C. Seven hours after reaching microgravity, the experiment was activated. The histological fixations were scheduled at the times of the fourth and eighth cleavage and at the gastrula stage.

Unfortunately, the relatively long period between manufacture and use of the m-AECs resulted in the testis plungers sticking in 4 out of the 6 flight m-AECs and in the m-AEC recorded on Earth. Thus, in those m-AECs, sperm was not released, and only in 2 out of the 6 flight m-AECs, eggs were successfully fertilized. One flight microgravity sample was fixed at the eighth cleavage and one flight sample under simulated 1-g on the centrifuge was fixed at the fourth cleavage. No flight samples were fixed at the fourth cleavage and the gastrula stage. The eggs in the 4 m-AECs in the Biorack ground experiment were fertilized successfully and fixed nominally. These embryos were used as 1-g references.

Postflight Analysis

We developed a staining method for the nuclei in the blastomeres of the embryos. Using a specific fluorescent nuclear dye and through an analysis by Confocal Laser Scanning Microscopy (CSLM), we determined the number of nuclei in the relatively few eighth cleavage embryos retrieved from microgravity and in the eighth cleavage embryos developed in m-AECs on Earth. The numbers of nuclei in the blastulae of these groups were similar and not significantly different.

As suggested by the IML-1 results, the development of the blastocoel was abnormal in microgravity. Its volume was significantly smaller in the embryos from IML-2 in microgravity as well as in the embryos from eggs fertilized and developed under simulated microgravity in the clinostat. The roof of the blastocoel was also thicker in the microgravity eggs than in the 1-g embryos.

Newly laid eggs fertilized in the clinostat, which simulates microgravity, had slightly but significantly smaller blastocoels than those developed simultaneously in the non-rotating tubes. After 24 h delayed fertilization, i.e., as in the IML-1 and IML-2 flights, the effect of simulated microgravity on the blastocoel formation in the rotating clinostat tubes was much greater.

Conclusion

Cell counts in *Xenopus* blastulae in the period of synchronous cleavages retrieved from the IML-2 mission after fixation in microgravity at the eighth cleavage did not significantly differ from those in 1-g control embryos. Similar results were obtained from experiments on the fast-rotating clinostat. Thus, in *Xenopus laevis* early embryos, microgravity does not perturb the tempo of cleavage divisions.

Although the roof of the blastocoel was significantly thicker in embryos from actual microgravity as well as from simulated microgravity, the number of the nuclei in a selected central area of the roof did not significantly differ from that in a similar area in 1-g control embryos. We assume that the thicker roof is not due to an increase in cell number but to an increase in cell size. The size of the whole microgravity embryos was identical to that of the 1-g embryos.

In normal development, water accumulates in the blastocoel, probably because of an osmotic effect. The volume of the blastocoel may be controlled by water exchange with the medium since the ion-impermeability of the old egg membrane and tight junctions between the surface cells prevent the loss of ions, while the inner membranes are actively pumping ions. Volume differences between blastocoels in microgravity embryos, compared to 1-g embryos, could be caused by ion-pumping differences.

For different reasons, neither our previous attempt on IML-1, nor a similar one by Souza, *et. al* on Spacelab J, and the present results, enabled us to identify the position of the sperm entry point in relation to the blastopore at gastrulation in microgravity.

References

De Mazière, A., Gonzalez-Jurado, J., Reijnen, M., Narraway, J., and Ubbels, G.A., "Transient effects of microgravity on early embryos of *Xenopus laevis*," in: [Cospar Hamburg, July 1994], *Adv. Sp. Res.*, vol. 17, no. 6/7, pp. 219-223, (©. 1995), Cospar, (1996).

Ubbels, G.A., "Establishment of polarities in the oocyte of *Xenopus laevis*; the provisional axial symmetry of the full-grown oocyte of *Xenopus laevis*," *CMLS, Cellular and Molecular Life Sciences* (formerly *Experienta*), vol. 1, accepted 1995, in press. Birkhäuser Verlag Basel, Boston, Berlin, (Review article written on invitation, containing all our data from microgravity studies and studies on Earth.)

Xenopus laevis embryos developed a significantly smaller blastocoel in microgravity (left) than in 1-g (right); average volumes: 22 ± 6 nl (n=7), resp. 36 ± 4 nl (n=9), P≤ 0.05. Average volumes of the whole embryos were identical in μ-g and at 1-g.

Regulation of Cell Differentiation by Gravity in the Lentil Root (Lentil)

Dr. G. Perbal and Dr. D. Driss-Ecole, Pierre and Marie Curie University, Paris, France

Plant morphogenesis is dependent upon gravity, which represents a reference for the direction of growth of the organs. In roots, it is well known that the cap is the source of at least one growth inhibitor that continuously regulates root growth. Whether or not gravity acts on the regulation of the growth of roots when these organs are strictly vertically oriented remains to be analyzed. In space experiments, we can analyze this by comparing plants grown in microgravity or on the 1-g centrifuge.

In our first space experiment, lentil seedlings were grown in microgravity and on a 1-g centrifuge for 25 h. Root length was not statistically different in the two samples. In the second space experiment, root length was less in microgravity than on the 1-g centrifuge after 29 h. It was necessary to determine the reason that root elongation seemed to be changed after 29 h in microgravity.

Flight Activities

Four sets of seedlings were grown (1) on a 1-g centrifuge in space for 29 h (F1-g sample), (2) in μ-g for 29 h (Fμ-g sample), (3) on the 1-g centrifuge for 25 h and placed in microgravity for 4 h (F1-g + μ-g sample) and (4) in microgravity for 29 h and placed on the 1-g centrifuge for 4 h (Fμ-g + 1-g sample).

After hydration, 2 mini-containers (with a total of 24 seeds) were placed together on a metal holder and inserted in an ESA Type 1 container. The seedlings were grown in microgravity or on the 1-g centrifuge for 25 h. They were then photographed by the crew. The seedlings that were grown in microgravity were put back in near weightlessness (Fμ-g) or placed on the 1-g centrifuge (Fμ-g + 1-g) for 4 h.

Highlights

- Gravity did not affect the elongation of roots growing in the vertical position.
- Cell cycle in the meristem is regulated by gravity.

Those which were grown first on the 1-g centrifuge were put back on the centrifuge (F1-g) or placed in microgravity (F1-g + μ-g) for 4 h. The seedlings were fixed in space. Orientation of the root tip and root length was determined on color prints with a specific program that we developed. The angle of deviation in the different samples was counted negatively when the root grew away from the cotyledons.

Postflight Analysis

In microgravity, there were strong oscillations of the root tip, even when the seedlings were grown first on the 1-g centrifuge (F1-g +μ-g). In the Fμ-g + 1-g sample, the roots grown in microgravity were oblique with respect to the 1-g acceleration when the seedlings were placed on the centrifuge. They were therefore gravistimulated. However, root length was similar in the 4 samples after 29 h of growth, and growth rate of the root was the same between 25 h and 29 h although it appeared to be slightly greater in the Fμ-g + 1-g sample.

Cell elongation was analyzed as a function of the distance from the root cap junction. Cell length was similar in the seedlings grown in microgravity or on the 1-g centrifuge. The transfer from the 1-g centrifuge to microgravity (F1-g + μ-g) did not modify cell elongation in the roots. Cell length in the microgravity-grown roots and gravistimulated (Fμ-g + 1-g) was different from that seen in microgravity, but this was only caused by gravistimulation. Thus, gravity does not have an effect on cell elongation when the roots are strictly oriented in the vertical position, but it does as soon as the root tip deviates from this orientation. However, the cell cycle is affected by the position of the root with respect to gravity.

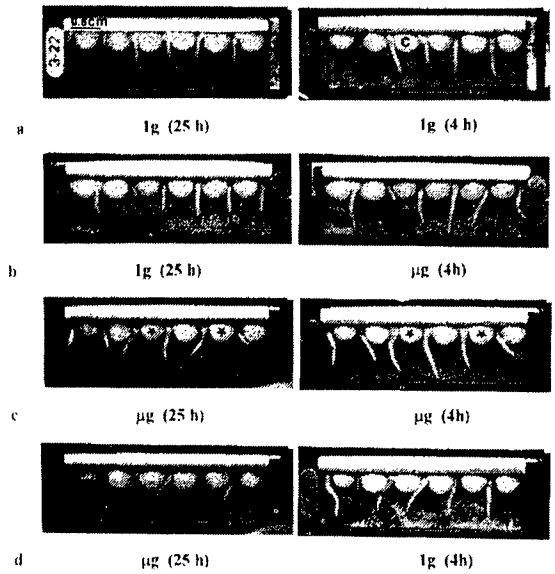

Figure 1: These images show root orientation for roots exposed to µg and 1-g.

Conclusion

The absence of gravity does not perturb root growth. Cell elongation is not regulated by gravity as long as the root tip remains vertical. However, as soon as it deviates from the vertical, an asymmetrical growth occurs.

The orientation of the root is strongly dependent upon gravity. On the 1-g centrifuge, the deviation of the root tip from the direction of the centrifugal acceleration is very slight. On the contrary, the deviation of the root tip from its initial orientation is stronger in microgravity.

When the seedlings are grown on the 1-g centrifuge and placed in microgravity for 4 h, strong oscillations occur, indicating that there is no memory of the former direction of growth.
It is accepted that the cap is the source of at least one inhibitor that regulates root growth. The results we obtained show that the symmetrical release of this inhibitor is not dependent upon gravity. However, its lateral transport is stimulated by gravity. These results are consistent with the hypothesis that, in the statocytes, the sedimentation of the amyloplasts on the endoplasmic reticulum should not induce any signal of cell elongation, since the separation of these organelles in microgravity does not change cell elongation. On the contrary, the movement of the statoliths toward the longitudinal wall of the statocytes induces a gravistimulation and a differential growth of the flanks of the root, i.e., a lateral transport of the inhibitor.

These results do not mean that there is no effect of gravity on root morphogenesis, since we observed a significant difference in the cell cycle in the meristem. However, its action on root development cannot be observed in short-term experiments. (In our experiment, the lentil seedling roots were about 7 mm long.)

References

Darbelley, N., Perbal, P., and Perbal, G., "Which cells respond to gravitropic stimulus in the lentil root?" *Physiol. Plant.*, vol. 67, pp. 460-464, (1986).

Driss-Ecole, D., Schoëvaërt, D., Noin, M., and Perbal, G., "Densitometric analysis of nuclear DNA content in lentil roots grown in space," *Biol. Cell,* 81, pp. 59-64, (1994).

Halstead, T.W. and Dutcher, F.R., "Plants in space,"*Amer. Rev. Plant Physiol,* vol. 38, pp. 317-345, (1978).

Perbal, G., Driss-Ecole, D., Rutin, J., and Sallé, G., "Graviperception of lentil seedling roots grown in space (Spacelab D1 Mission)," *Physiol. Plant*, vol. 70, pp. 119-126, (1987).

Selker, J.M. and Sievers, A., "Analysis of extension and curvature during the graviresponse in *Lepidium* roots," *Amer. J. Bot.*, vol. 74, pp. 1863-1871, (1987).

Root Orientation, Growth Regulation, Adaptation, and Agravitropic Behavior of Genetically Transformed Roots (Transform)

Dr. T.-H. Iversen, Norwegian University of Science and Technology, Dragvoll, Norway

The main aim of the experiment was to clarify if wild- type (WT) roots behaved differently in growth, morphology, gravitropical sensitivity, and organelle appearance and distribution from genetically transformed agravitropic rapeseed roots. Another goal was to keep the root material from the flight under sterile conditions to regenerate new plants from space root material.

Flight Activities

The roots were growing on agar in small plant chambers (type C) placed in a holder, 2 of which fit into an ESA Type 1 container. The design and dimensions of the C-chambers made it possible to orient the chambers in different positions on the 1-g control centrifuge in the Biorack. A photobox recorded root growth.

The holders were cooled down to 4 °C for 2 h until transfer to the Shuttle 17 h before launch. After launch, the root tips were kept at 5 °C. Initiation of the experiment took place after 52 h (L+52), when the containers were transferred to the nominal temperature (23 °C). The photographic recording of the root development started immediately after the 60 min, 1-g stimulation period and lasted from L+65 up to L+100, i.e., for 36 h. A computer imaging program helped measure the lengths and curvatures of the root tips. After 37 h in the photobox the root tips were fixed, and the chambers were kept at 4 °C.

Postflight Analysis

At our laboratory, we started postfixation 25 days after fixation in orbit. The statoliths were randomly distributed in the statocytes of both WT and transgenic roots that had been kept under micro-g for 37 h after a 14 h longitudinal stimulation at 1-g.

Highlights

- Similar distribution of amyloplasts in WT and transgenic root cap cells both in orbit and on the ground.
- Total growth was higher for roots grown on the ground than for roots grown in space.
- Space-grown transgenic root tips were kept alive under sterile conditions. The roots have been propagated *in vitro* since August 1994 and are undergoing further analysis.

Also the root cap morphology was similar in the roots exposed to micro-g and those grown on the ground, with the characteristic V-shaped root cap of the transformed roots unchanged. The analysis of the statocyte ultrastructure in roots exposed to micro-g did not reveal any dramatic difference between the transgenic root cells and the cells of the WT. TEM analysis of transgenic roots that had been kept at micro-g conditions for the entire orbital period up to fixation demonstrates that there are no significant changes at the ultrastructural level. Both the amyloplasts with their starch content and the mitochondria, endoplasmic reticulum, ribosomes, and plasmodesmata appear normal and unaffected by the micro-g environment.

No significant difference in elongation rates was found between WT and transgenic roots exposed to 1-g stimulation in orbit or kept under micro-g conditions. In the ground control, highly significant differences ($P < 0.05$) were found between the 2 types of roots. The respective mean elongation rates were 0.11 mm/h for the WT and 0.30 mm/h for the transgenic roots, while the statistical analysis did not demonstrate significant differences under flight conditions.

The general impression was that total growth, both in the WT and the transgenic roots, was higher in the ground control than for roots grown in orbit. Compared to the average values

for WT and the transgenic roots in orbit, the increase in total length after 24 h was 31% and 38 % higher, respectively.

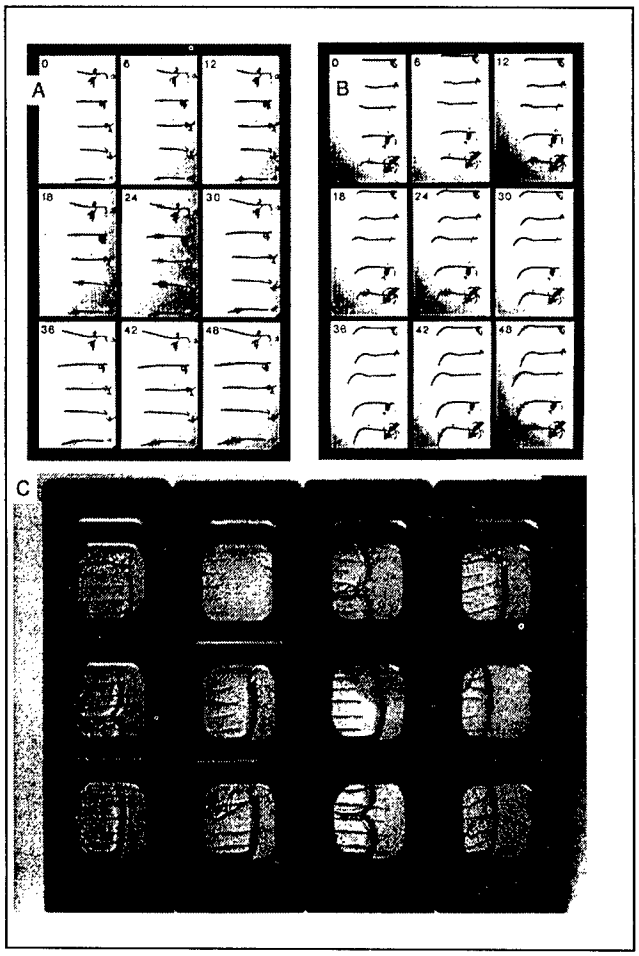

Figure 1: Growth pattern of WT and transgenic root tips on the ground and in orbit.

A. Transgenic root tips on the ground stimulated at 135° to the g-axis for 48 h

B. WT root tips on the ground stimulated at 135° to the g-axis for 48 h

C. Space-grown root tips after retrieval to Trondheim, Norway. Four holders for plant chambers type C are shown. From the left: plant chamber holder 3A: C-chambers with transgenic roots; 3B: WT roots; 4A: transgenic roots; and 4B: WT roots.

Conclusion

The roots were successfully kept under aseptic conditions during the entire orbital period and during transport back to the laboratories. Since August 1994, a considerable number of flight roots have been established as *in vitro* root organ culture, both on solidified media and in suspension. So far regeneration of the roots has not been successful, but it is hoped that mature plants will be regenerated in due time.

We are still performing the statolith movements and root ultrastructure analysis, e.g., attempting to make a 3-D reconstruction of the statocytes in the 2 root types exposed to micro-g and in the ground controls. A more detailed analysis of DNA will be performed as soon as regenerated plants have been obtained to see if the 14-day orbital period had an effect on the genetic stability of the transformed roots.

The root material from IML-2 was used as a source for protoplast production from roots in the PROTO experiment on S/MM-03, which was performed on the Space Shuttle Atlantis in March 1996.

References

Iversen, T-H., Oedegaard, E., Beisvåg, T., Johnsson, A., and Rasmussen, O., "The behavior of normal and agravitropic transgenic roots of rapeseed *(Brassica napus L.)* under microgravity conditions, *J. Biotechn.*, vol. 47, pp. 137-154, (1996).

Briarty, L.G., Maher, E.P., and Iversen, T.-H., " Growth, differentiation and development of *Arabidopsis thaliana* under microgravity conditions (15-UK SHOOTS)", In: *Biorack on Spacelab IML-1*, ESA SP-1162, pp. 141-154, (1995).

Oedegaard, E., Iversen, T-H., Nielsen, K.M., Beisvåg, T., Evjen, K., Johnsson, A., and Rasmussen O., "Agravitropic behavior of roots of rapeseed *(Brassica napus L.)* transformed by Agrobacterium rhizogenes," *J. Grav. Physiol.* (submitted 1995).

Rasmussen, O., Baggerud, C., Larsen, H.C., Evjen, K., and Iversen, T-H., "The effect of 8 days microgravity on regeneration of intact plants from protoplasts," *Physiol. Plant*, vol. 92, pp. 404-411, (1994).

Rasmussen, O., Bondar, R.L., Baggerud, C., and Iversen, T-H., "Development of plant protoplasts during the IML-1 mission," *Adv. Space Res.*, vol. 14, no. 8, pp. 189-196, (1994).

Plant Growth and Random Walk (Random)

Dr. A. Johnsson, University of Trondheim, Dragvoll, Norway

The gravitropic system of plants is designed to handle deviations of plant organs from a reference direction set by gravity. In weightlessness the reference direction as well as the stimulus for the gravitropic system is not present. The experiment studied the root growth dynamics in weightlessness. Root length as well as root curvatures were mapped as function of time. The plant material chosen for the experiment was roots of garden cress (*Lepidium sativum L.*).

We tested an hypothesis based on the assumption that a root devoid of its reference direction for the gravitropic system (balance system) in weightlessness should move totally randomly. In more detail, it was hypothesized that the root, once protruded from the seed, might show random growth processes, which could lead to curvatures and deviations that are not compensated in weightlessness.

If the root showed growth movements by pointing in randomly determined direction during its growth, random walk mathematics should be adequate to describe the random growth directions. The random walk is characterized by two mathematical expressions: the first one simply stating that the average growth direction should stay constant (and by definition called zero). The second one says that the averaged squared deviation from the starting direction should increase linearly with time.

Flight Activities

The plants were grown in plant chambers: A-chambers (39 x 62 x 19 mm^3) and B-chambers (19 x 62 x 19 mm)^3. The design of the B-chambers was necessary to fit the 1-g centrifuges in Biorack which provided facilities for the 1-g onboard control experiment. In the experiment three A-chambers and eight B-chambers were used.

Highlights

- Average bending direction of the plants stayed constant equal to zero despite the spontaneous movements performed in weightlessness.
- The average squared deviation of the root movements increased linearly with time during the first period of growth, a pattern characteristic for random processes.
- Growth of roots in weightlessness was smaller than on the ground.

Photographs of the seedlings were taken by an automatic preprogrammed camera in the photobox, producing a time-lapse sequence (1 picture per hour) of images of root growth. A flash with a green filter provided safe light (560 nm). The bending angles of the roots were measured manually from the films. The standard deviations of the measurements indicated that the error in the angle determinations was about 3.9° when the roots just protruded and 2.3° after an additional 8 h growth.

Some samples were fixed to preserve cells for further study. The extended fixation period in glutaraldehyde, necessary to use in the experiment, decreased the quality of the cell preparations and caused ultrastructural changes. The major effect was higher degree of vacuolization and destruction of tonoplast in statocytes. Such vacuolization may cause disturbances in the organelle distribution, and fixation period must be evaluated in space experiments to preserve root cap ultrastructure.

Postflight Analysis

We used the photographs to determine cress root length, bending of root tips, curvatures of roots, etc., as a function of time. All but 2 of the 42 seeds produced measurable roots. Plants grown under 1-g control conditions appeared to grow in the normal, straight fashion characteristic for cress roots under the influence of 1-g. The roots that grew in weightlessness seemed to diverge

more in their growth direction. The length of the roots in weightlessness was significantly smaller than in the ground controls.

The measurements of the root tip bending direction produced one series of data (a time series) for each plant in the chambers. The angles of the roots in the first measured photo are all defined as zero deviation and all subsequent angles are then referenced to this baseline position. The average bending deviates slightly from 0 in both cases but not to a significant extent; the maximum average deviation value was about 15.7° in the vertical direction with a standard deviation of 47.7° for flight plants and -6.6° with a standard deviation of 10.0° for ground plants. The same conclusion could be found for the corresponding B-chambers (grown on flight 1-g centrifuges). In contrast to the roots growing in weightlessness, the ground-control roots did not show an increase at all in the average square bending data.

The consecutive changes in the bending of the roots were studied, and it was found that the changes were more vigorous at the start of the recordings and diminished toward the end of it. Therefore, the roots performed spontaneous curvatures to a greater extent during the first hours of the recordings and decreased their spontaneous activity toward the end of it. The bending behavior should be further studied.

The averaged squared deviations of the plants increased linearly with time during the first 8 h of the experiment. This pattern was as expected for a random growth and the positive test of this functional relationship was an important outcome from the experiment. This growth pattern was not characteristic for the growth toward the end of the experiment.

Autocorrelation functions were determined for the individual time series for changes of bending. The correlation between the bending directions in consecutive 1 h measurements was about 0.4. If bending directions were totally uncorrelated, the autocorrelation function would have been zero. The bending changes 1 h apart were, therefore, slightly correlated, but data 2 h or more apart were uncorrelated.

Conclusion

Our predictions on root bending patterns were correct for the initial growth period of the roots. The random walk type growth seemed to last for about 8-10 h, and then the mean square deviation increased much more slowly. A simultaneous decrease in the hourly changes of the bendings occurred. These features could indicate that the growth patterns as well as the spontaneous nature of the bendings did change at this time of the experiment. Such changes may be initiated by weightlessness or by other influences from the chamber climate.

This experiment generated new questions. It would be valuable to perform extended space experiments, e.g., to cultivate roots under 1-g and then transfer them to weightlessness to study how soon the random bendings start. This could give clues to the lengths of the memory of normal gravity conditions, i.e., the time required for adaptation to weightlessness.

References

Johnsson, A., Karlsson, C., Iversen, T.-H., and Chapman, D. K. , "Random root movements in weightlessness," *Physiol. Plant.*, vol. 96, pp. 169-178, (1996).

Johnsson, A., Antonsen, F., Iversen, T.-H., Chapman, D.K., and Karlsson, C., "Curvatures of cress roots growing in weightlessness," *Proceedings from the 6th European Symposium on Life Sciences Research in Space,* ESA, accepted.

Johnsson, A., Karlsson, C., Chapman, D.K., Braseth, J., and Iversen, T.-H., "Dynamics of root growth in microgravity," *J. Biotechnology,* vol. 47, pp. 155-165, (1996).

Braseth, J. D., Iversen, T.-H., Johnsson, A., and Karlsson, C., "Influence of an extended prefixation period on the ultrastructure of root cap cells in garden cress (*Lepidium sativum L.), Proceedings 47th Ann. Meeting Scand. Soc. Electron Micr.,* Beisvåg,T., Iversen T.-H., and Solberg, J.K., eds., ISBN 82-993546-0-9, pp. 32-33, (1995).

Johnsson, A., Karlsson, C., Iversen, T.-H., Chapman, D. K. & Braseth, J., "Plant growth and random walk - an experiment for IML-2," *Proceedings ESA SP-366, Fifth European Symposium on Life Sciences Research in Space,.* ISBN 92-9092-306-7, pp. 121-125, (1994).

Johnsson, A. , "Introduction of noise in the gravity compensating system in *Helianthus annuus,*" *Stud. Biophys.* vol. 11, pp. 149-154, (1968).

Dosimetric Mapping in Biorack (Dosimetry)

Dr. G. Reitz, DLR, Institute for Aerospace Medicine, Cologne, Germany

Radiation is an acknowledged primary concern for manned space flight and is a potentially limiting factor for long orbital missions. Although in several space flight experiments a considerable amount of data has been accumulated, so far, it is not possible to provide a quantitative description of the highly complex radiation field in space. The necessity of monitoring fluxes and doses of each single component is therefore an indispensable part of each mission. Special attention has to be given to the densely ionizing component of the radiation field due to its unique radiobiological properties. This component is constituted of the heavy ions of cosmic radiation, neutrons, and nuclear disintegration stars produced by protons and neutrons in irradiated tissue, whereas the sparsely ionizing component consists of photons, electrons, muons, pions, and protons.

The contribution to the dose of the later component was measured with lithium fluoride thermoluminescence detectors (TLDs). Plastic nuclear track detectors, such as diallylglycol carbonate (CR39), cellulose nitrate-Kodak (CNK), cellulose nitrate-Daicel (CND), and polycarbonate (Lexan) were used to determine the heavy ion fluxes and their linear energy transfer (LET) spectra. The absorbed doses deposited by neutrons has been estimated from the differences between doses recorded in lithium fluoride detectors TLD600 and TLD700 from Harshaw, which differ in their relative content of the isotopes 6Li and 7Li. The data were used to determine dose equivalents.

Flight Activities

For the measurements, 7 track detectors (Meter-1 through Meter-7) were used. The stacks were flown inside Biorack Type 1 containers. Crew members placed Meter-1 in incubator C, Meter-2 in the cooler, Meter-4 in incubator A (after being located in the middeck for about 4 days), and Meter-7 in the overhead storage container OH-7. Meter-3 remained inside a stowage container in the middeck and Meter-5 in a middeck stowage that was moved to Spacelab.

Highlights

- Total doses differ up to a factor of 1.5 and heavy ion fluxes by more than a factor of 6 in the different locations.
- The mission equivalent dose for the astronauts was calculated from the measurement to be 3.8 mSv.

Postflight Analysis

After landing, the stacks were disassembled. The plastic nuclear track detectors were etched in sodium hydroxide. The submicroscopic latent tracks were developed into conically shaped, microscopically visible etch tracks. The nuclear emulsions were developed similarly to photographic films. The TLD chips were heated, the number of photons emitted during the heating being a measure of the absorbed dose.

To obtain the dose equivalent contributed by the different radiation types, we had to multiply the absorbed dose by a weighting or quality factor. Since the quality factor is related to LET, the determination of the contribution of the densely ionizing radiation to the equivalent dose requires a measurement of the fluence rate in dependent of LET. This was done only for heavy charged particles. For the other components, the absorbed dose was converted into dose equivalent by means of mean quality factors determined as spectral averages from known or postulated energy spectra of the constituents.

The mean total dose measured with TLD 700 varies from about 1.7 mGy to 1.1 mGy. The daily dose rate was 114 ± 11 μGy d^{-1} as maximum and 73 ± 3 μGy d^{-1} as minimum. This is calculated with a mission duration of 353 h. The measured doses are mainly caused by the protons of the South Atlantic Anomaly (SAA) in the radiation belt.

Dosimeter	Number of Particles cm^{-2}	Number of Particles $cm^{-2} sr^{-1} s^{-1}$
M1	4.2 ± 0.4	$2.2 \pm 0.2 \cdot 10^{-6}$
M2	2.1 ± 0.2	$1.1 \pm 0.1 \cdot 10^{-6}$
M3	1.5 ± 0.2	$8.2 \pm 1.3 \cdot 10^{-6}$
M4	2.9 ± 0.3	$1.6 \pm 0.2 \cdot 10^{-6}$
M5	7.4 ± 0.5	$4.0 \pm 0.3 \cdot 10^{-6}$
M6	9.5 ± 0.5	$5.0 \pm 0.3 \cdot 10^{-6}$
M7	7.7 ± 0.5	$4.2 \pm 0.3 \cdot 10^{-6}$

Table 1: Number of particles recorded in the plastic detector cellulose nitrate-Kodak during IML-2

The difference between the mean TLD 600 and TLD 700 readings amounts to 129 ± 32 μGy. Taking the maximum dose induced per neutron in TLD 600 as 1.6×10^{-9} Gy cm^{-2}, this dose corresponds to a thermal neutron flux of about 0.65 neutrons cm^{-2} s^{-1}. Assuming that this flux can be used as a lower estimate for the fast neutron flux, a dose rate of 3.4 μGy d^{-1} in tissue can be calculated.

Heavy ion flux was determined in the detector CN-Kodak, CN-Daicel and Lexan. The observed heavy ion fluence varies in CN-Kodak between 9.5 ± 0.5 cm^{-2} and 1.5 + 0.2 cm^{-2}. No particles were detected in CN-Daicel and Lexan.

Mission	Dose Equivalent Rates [μSv d^{-1}]	Mission Dose Equivalent [mSv]
SL1	459	4.7
D1	478	3.3
IML-1	362	2.9
MIR92	613	4.9
EUROMIR94	767	24.2
D2	200	2
IML-2	360	3.8

Table 2: Dose equivalent rate and mission dose equivalent in manned missions

Conclusion

During IML-1 and IML-2, there were attitude changes only at the beginnings and the ends of the missions. Both flights were gravity-gradient stabilized throughout the mission. When comparing the dosimetric results of both IML missions, we observed a higher heavy ion flux variation for the different locations in IML-2, a factor of more than 6 compared to a factor of 2 in IML-1. In IML-1, there was nearly no variation in the absorbed dose for the different locations; in IML-2, a factor of 1.5 was measured. The high differences in fluxes for the single locations clearly indicate that actual measurements are the only way to obtain confident information about the types and intensities of radiation present and are therefore indispensable as baseline data for all other biological experiments in space and for radiation protection measures.

The radiation exposure of the astronaut during the IML-2 mission is twice the mean annual public exposure but is still far below the annual limit of exposure for radiation workers on Earth. For comparison, a compilation of radiation exposures during other manned missions is given in Table 2.

References

Reitz, G., Beaujean, R., Heckeley, N., and Obe, G., "Dosimetry in the space radiation field," *Clin. Investig.*, vol. 71, pp. 710-717, (1993).

Heinrich, W., Wiegel, B., Ohrndorf, T., Bucker, H., Reitz, G., and Schott, U., "LET spectra of cosmic-ray nuclei for near earth orbits," *Radiation Research*, vol. 118, pp. 63-82, (1989).

Reitz, G., "Space radiation dosimetry," *Acta Astronautica*, vol. 32, no. 11, pp. 715-720, (1994).

Reitz, G., Facius, R., Beaujean, R., and Heilmann, C., *Dosimetric Mapping in Biorack*, ESA SP-1162, pp. 35-40 (1995).

Reitz, G., Beaujean, R., Leicher, M., and "Dosimetric measurements in manned missions," *Acta Astronautica*, vol. 36, No. 8-12, pp. 517-526, (1995).

The Influence of Microgravity on Repair of Radiation-Induced DNA Damage in Bacteria and Human Fibroblasts (Repair & Kinetics)

Dr. G. Horneck, DLR, Institute of Aerospace Medicine, Cologne, Germany

In radiobiological experiments in space, a synergistic interaction of microgravity and radiation has been reported in several cases. Although the observation of a synergism between the action of radiation and microgravity are important for the evaluation of hazards to humans in space, little research has been done to understand the mechanisms of these interactions. One possible explanation conjectured is that microgravity might interfere with the operation of some cellular repair processes, which results in an augmentation of the radiation response.

With the different cellular systems, the influence of microgravity was tested on the efficiency and kinetics of different repair systems: repair Kinetics of radiation-induced DNA strand breaks (1) in procaryotic (*E. coli* B/r) cells and (2) in eukaryotic cells (human skin fibroblasts); (3) induction of SOS repair system in *E. coli* (strain PQ37) cells, and (4) efficiency of Repair in *B. subtilis* cells.

Flight Activities

All cells (*E. coli* B/r, *E. coli* PQ37, and human fibroblasts) were irradiated about 1 month before the mission. For the Kinetics experiment, all samples were kept frozen to prevent repair processes. Repair was only allowed for defined time periods and conditions (repair under microgravity and on the 1-g centrifuge) during the active phase of incubation. Immediately after incubation, cells were frozen again until analysis. Sample holders that fit into Biorack Type 1 containers held the following samples: 10 culture vessels of 0.6 ml with human fibroblasts and 12 culture vessels of 0.25 ml with *E. coli* cells. Each experimental point was represented in duplicate or triplicate in each set.

Highlights

- Results indicate that repair processes function normally and are not disturbed by microgravity conditions.
- The synergistic effects of microgravity and radiation are not a result of a disturbance of intracellular repair.
- Both prokaryotes and human cells had normal repair pathways in microgravity.

For repair of DNA damages, the cells in the Type 1 containers were then incubated at 36.5 °C either in microgravity or under 1-g. The incubation of different duration (50 min, 105 min, 164 min, and 269 min) was terminated by transfer into the -24 °C freezer, where the samples were stored until the end of the mission. For the Repair experiment, the efficiency of repair was studied in cells of *Bacillus subtilis*, grown from ultraviolet-irradiated (254 nm) spores. Before launch, the spore-coated filter membranes were placed on top of dry nutrient disks. The samples were stored on board at room temperature. On mission day 10, the nutrient disks were humidified by injection of 0.2 ml of distilled water in each incubation compartment. Culture chambers in Type 1 containers were incubated at 36.5 °C, allowing germination of the spores and growth of the colonies. After 24 h of incubation, the colonies (which were red because of the reduction of TTC by the cells) were photographed. Then the samples were stored at room temperature. Ground control experiments were also performed.

Postflight Analysis

The Kinetics data points reflect the fraction of intact DNA of irradiated samples relative to that of unirradiated controls that received the same treatment. For DNA strand break measurements in *E. coli*, the rejoining kinetics of the flight samples under microgravity are identical with those of the centrifuge as well as with

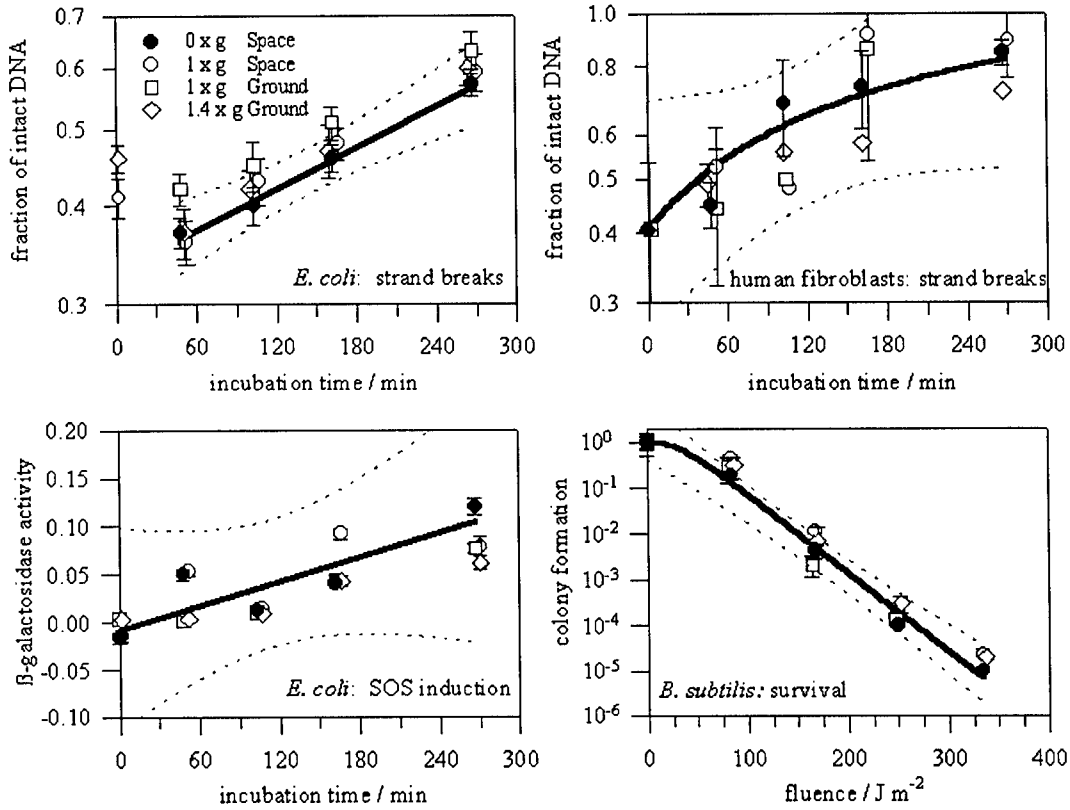

those of the ground controls, within experimental errors. The data points for 0 min incubation results from samples differ in their treatment to the incubated samples. They were kept frozen all the time and did not receive the additional step of warming and freezing that induces additional breakage of the DNA. During incubation of irradiated fibroblasts at growth temperature, the relative fraction of intact cellular DNA increases at microgravity as well as on the centrifuge. Within experimental errors, the rejoining kinetics for human fibroblasts are similar for both flight and ground conditions. Fibroblasts irradiated with 5 and 10 Gy X-rays gave comparable results.

In the irradiated samples, the β-galactosidase activity increases during incubation, whereas it is nearly constantly low in unirradiated samples. While the rate of SOS response is identical in the two ground controls, the data are somewhat scattered for the flight samples. After 164 min of incubation, the SOS response is higher in the centrifuge samples than in the static samples, whereas after 269 min of incubation the static samples have a higher SOS response than the centrifuge samples.

For the Repair experiment, cellular survival, which is the consequence of efficient cellular repair, was measured after UV-irradiation. Hence spores of *B. subtilis* were allowed to germinate and to form colonies in space under static and centrifuge conditions. Within experimental errors, the curve characteristics (i.e., threshold value, extrapolation number, and slope of the exponential part of the curve) do not differ significantly for the two conditions in flight and on the ground. For all experiments performed, the different repair conditions (repair

under microgravity or on the 1-g centrifuge in space and on the ground) show no significant differences using the T-test.

Conclusion

Although the experiments had different constraints, the results from all four experiments provide evidence that repair processes function normally and are not disturbed in microgravity compared to that on ground. The synergistic effects of microgravity and radiation in biological systems, which have been observed in several instances, can probably not be explained by a disturbance of intracellular repair in microgravity.

In all cell types tested, prokaryotes as well as human cells, the corresponding repair pathways function close to normal in the microgravity environment. On the other hand, even if the rejoining of DNA strand breaks is not affected by microgravity, we do not know whether the probability of disrepair may be augmented. Further studies in space are required to shed light into the phenomenon of combined action of radiation and microgravity in biological systems.

References

Baltschukat, K. and Horneck, G., "Responses to accelerated heavy ions of spores of *Bacillus subtilis* of different repair capacity," *Radiat. Environm. Biophysics*, vol. 30, pp. 87-103, (1991)

Baumstark-Khan, C., " Effect of aphidicolin on DNA synthesis, PLD-recovery and DNA repair of human diploid fibroblasts," *Internat. J. Radiat. Biol.*, vol. 61, pp. 191-197, (1992 a).

Baumstark-Khan, C., Griesenbach, U., and Rink, H., "Comparison of DNA strand break induction in CHO cells measured by alkaline elution and by fluorometric analysis of DNA unwinding (FADU)," *Free Radicals Res. Comm.*, vol. 16, pp. 381-386, (1992 b).

Baumstark-Khan, C., "Alkaline elution versus fluorescence analysis of DNA unwinding," *Methods Enzymology*, vol. 234, pp. 88-102, (1994).

Schäfer, M., Schmitz, C., and Bücker, H., "Heavy ion induced DNA double strand breaks in cells of *E. coli*," *Adv. Space Res.*, vol. 14, pp. (10)203-(10)206, (1994).

SLOW ROTATING CENTRIFUGE MICROSCOPE: LIFE SCIENCES EXPERIMENTS

INVESTIGATIONS	PRINCIPAL INVESTIGATORS	RESULTS HIGHLIGHTS
Gravisensitivity and Gravi(Geo)taxis of the Slime Mold *Physarum polycephalum* (Slime mold)	Dr. I. Block, DLR, Institute for Aerospace Medicine, Cologne, Germany	The lowest acceleration capable of inducing a response is 0.1-g. The gravity response is based on direct effects of gravity. The low acceleration-sensitivity threshold favors rather large and dense cell organelles as gravi-receptor candidates in *Physarum.*
Influence of Accelerations on the Spatial Orientation of *Loxodes* and *Paramecium* (Loxodes)	Dr. R. Hemmersbach DLR, Institute for Space Medicine, Cologne, Germany	The threshold for gravitaxis of *Paramecium* was >0.16-g and 0.3-g, and the unicellular organism did not adapt to weightlessness. *Loxodes* showed no gravi-responses to increasing accelerations in space but did demonstrate gravitaxis upon return to Earth. Prolonged cultivation in space did not change the size and content of the barium sulfate of the statocyst organelles of *Loxodes.*

SLOW ROTATING CENTRIFUGE MICROSCOPE: LIFE SCIENCES EXPERIMENTS

INVESTIGATIONS	PRINCIPAL INVESTIGATORS	RESULTS HIGHLIGHTS
Gravitaxis in the Flagellate *Euglena gracilis* is Controlled by an Active Gravireceptor (Euglena)	D.-P. Häder, Friedrich-Alexander-University, Erlangen, Germany	Random orientation of flagellates at accelerations at and below 0.08-g confirmed prior results. Threshold for orientation $\leq$ 0.16-g Observed no adaptation during the extended duration of the mission.
Effects of Micro-g on *Aurelia* Ephyra Behavior and Development (Jellyfish)	Dr. D.B. Spangenberg Eastern Virginia Medical School Norfolk, Virginia, United States	Confirmed SLS-1 findings that ephyrae form in microgravity and can pulse and swim. Ephyrae that developed in space had more arm abnormalities.

INVESTIGATIONS	PRINCIPAL INVESTIGATORS	RESULTS HIGHLIGHTS
Chara rhizoids: Studies during a Long Period of Microgravity (Chara)	Dr. A. Sievers, Dr. M. Braun, and Dr. B. Buchen, University of Bonn, Bonn, Germany	Demonstrated tip-growing single cells develop normally in microgravity. Growing rhizoids maintained their structural polarity and grew straight. Distribution of statoliths was similar to that found in sounding rocket experiments.
Graviresponse of Cress Roots under Varying Gravitational Forces below Earth Acceleration (1-g) (Cress)	Dr. D. Volkmann University of Bonn Bonn, Germany	Roots cultivated under micro-gravity had a higher sensitivity than those grown on the 1-g centrifuge. These results and those from prior missions suggest the non-validity of the reciprocity rule. Transformation of the gravi-stimulus occurs near the statoliths.

Gravisensitivity and Gravi(Geo)taxis of the Slime Mold *Physarum polycephalum* (Slime mold)

Dr. I. Block, DLR Institute for Aerospace Medicine, Cologne, Germany

Free-living cells often use the gravity vector for their spatial orientation and also show distinct gravisensitivities. Plasmodia of the ameboid *Myxomycete* (acellular slime mold) *Physarum polycephalum* offer, with the rhythmic contractions of their protoplasmic strands, a sensitive parameter that can be modified by external stimuli. Space experiments and ground-based 0-g simulation studies have established that the contraction period transiently decreases after a transition from 1-g to 0-g with a back-regulating process starting after 30 min.

The perception mechanism underlying the gravity responses of cells is currently a prime target of investigations in space biology. Information on the gravireceptor itself can be obtained by the determination of the threshold for the cell's acceleration sensitivity. Information on the gravireceptor can also be obtained by comparing the responses to different acceleration changes: the greater the response to a defined acceleration change is, the greater/denser is the g-receptor.

Flight Activities

Physarum polycephalum were transferred to special culture/observation chambers of about 20 mm diameter and allowed to grow on agar to small plasmodia. During the mission, the cells were kept at 10 °C to keep their metabolism at a low level. Only a few hours before the actual experiment they were activated by transferring them to 20 °C in the Biorack incubator. The experiments were performed on the slow-rotating centrifuge microscope (NIZEMI). The NIZEMI provided varying accelerations ranging from 0-g to 1.5-g. Subjecting a cell to various accelerations below 1-g allows the determination of its acceleration-sensitivity threshold.

Highlights

- The lowest acceleration capable of inducing a response is 0.1-g.
- The gravity response is based on direct effects of gravity.
- The low acceleration-sensitivity threshold favors rather large and dense cell organelles as gravireceptor candidates in *Physarum*.

NIZEMI also offered the opportunity of simultaneous sample observation. Using the low magnification of the NIZEMI MACROscope, whole plasmodia of about 1 cm diameter were tested. In each of the 4 MACRO experiments *Physarum* was subjected to another profile of acceleration levels, with each acceleration level lasting 15 min. Using a higher magnification, allowed the observation of both the contraction rhythm and the internal cytoplasmic shuttle streaming. In each of these 3 MICRO experiments, *Physarum* was subjected to the same profile of acceleration levels with each acceleration level lasting about 1 h (1-g, 0-g, 1.5-g, 0-g, and 1-g). Also, the plasmodia were immersed in water in order to eliminate any indirect acceleration effect on the cells.

In both the MICRO and MACRO experiments, the rhythmic contractions of the plasmodial strands were registered using the NIZEMI video camera and a video recorder to allow a post-mission computer-based evaluation. The BIOIMAGE computer program used allows the morphometric and photometric measurement of the contraction activity of *Physarum*.

Postflight Analysis

MACRO experiment runs demonstrate that the response of 0-g-adapted plasmodia to increasing accelerations consisted of an increase in contraction period. This shows that acceleration increase and the stimulus deprivation induce opposite responses. This is consistent with experiments conducted in the ground module of the NIZEMI, where accelerations exceeding 1-g induced a period increase in 1-g-adapted plas-

modia. In the flight experiment, it was found that different plasmodia displayed different acceleration sensitivities, with some individuals responding to lower acceleration levels than others.

As the main result, the experiments revealed that the lowest acceleration level capable of inducing a response was 0.1-g. In general, if the acceleration was higher, the response was stronger; that is, the response increased with increasing acceleration. (See Figure 1.)

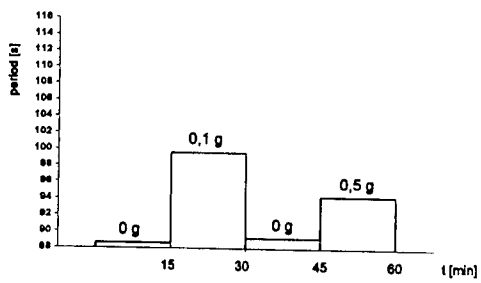

Figure 1: Contraction activity of a 0-g adapted plasmodium (4th MACRO experiment) is shown versus time. Note the prominent response to 0.1-g and the back-regulation after 30 min. The figure also demonstrates that any above-threshold acceleration is able to induce the complete response-regulation process so that a second and stronger stimulation, when applied during the back-regulation, only leads to a minor response.

In the experiments conducted on the MICROscope, the 1-g-adapted and immersed plasmodia showed, contrary to the expectation, a slow period increase during 0-g stimulation. However, the inverted and slow response is in accordance with geotaxis experiments performed in 1-g with plasmodia immersed for several hours and even days. They performed an inverted (negative) geotaxis to escape the water and the danger of oxygen depletion.

Upon 0-g stimulation the plasmodia in the MICRO experiments showed a slow period increase to almost 25% compared to the baseline. In the following hour of 1.5-g, the periods slowly returned to almost baseline values. The response to the second 0-g phase was an immediate strong period increase followed already after 20 min by the onset of the back-regulation. A short response is typically observed when a back-regulating process, following a previous stimulation, had not been completed before an additional stimulation. The experiment mainly demonstrates that immersed plasmodia were still able to respond to acceleration changes thus proving that the gravity response in *Physarum* is based on a direct effect of gravity.

Conclusion

A direct gravity effect is due to the density differences within the cell, relayed via primary gravity receptors. They must have a higher density than the rest of the cell. The low . acceleration-sensitivity threshold of 0.1-g in *Physarum* and the pronounced responses to small acceleration changes reflect a rather high g-sensitivity. This points to rather large and dense organelles as candidates for the g-receptor. With a diameter of 6 μm and a density of 1.35 g/cm^3, the nuclei represent good candidates for such a function. Moreover, they are present in high numbers in the cell (millions in larger plasmodia), and via a summation effect could be able to exert a pressure or tension in . 1-g large enough to affect membranes or the cytoskeleton in their vicinity.

Though very small (diameter 1.5 - 3.0 μm), the mitochondria in *Physarum* are also putative gravireceptor candidates, because of their high density (1.17 to 1.21 g/cm^3) and their presence in even higher numbers than the nuclei in the cell. Mitochondria are involved in the last steps of the acceleration signal-transduction chain.

References

Block, I., Wolke, A., Briegleb, W., and Ivanova, K., "Gravity perception and signal transduction in single cells," *Acta Astronautica,* vol. 36, No. 8-12, pp. 479-486, (1995).

Block, I., Wolke, A., and Briegleb, W., "Threshold of acceleration-sensitivity in *Physarum," Poster at European Cell Biology-Conference,* Heidelberg, Germany, (1995).

Block, I., Briegleb, W., and Wolke, A., "Acceleration-sensitivity threshold of *Physarum," J. Biotechnology,* vol. 47, pp. 239-244, (1996).

Block, I., Ivanova, K., Wolke, A., and Rabien, H., "Graviperception and signal transduction in *Physarum,*" ESA SP-390, pp. 199-202, (1996).

Influence of Accelerations on the Spatial Orientation of *Loxodes* and *Paramecium* (Loxodes)

Dr. R. Hemmersbach, DLR, Institute for Space Medicine, Cologne, Germany

Paramecium and *Loxodes* use gravity as a stimulus for their spatial orientation (gravitaxis) and for the control of their swimming velocity (gravikinesis). Both graviresponses increase under hypergravity conditions and disappear in microgravity. The ciliates can be regarded as swimming sensory cells because a direct correlation between membrane potential, second messenger levels, ciliary activity, and the fast swimming responses was manifested. Cellular organelles or the whole cell body are thought to serve the function of gravity perception in *Paramecium*. In contrast, *Loxodes* has "statocyst" organelles (Müller organelles), which were proved to be involved in the gravity signal transduction chain. A Müller organelle consists of a vacuole containing a granulum of barium sulfate, fixed to a modified ciliary complex. Demineralization in human bones is induced by a lack of tension forces in weightlessness. Mineralization processes also take place in *Loxodes* to build up the Müller organelles.

Flight Activities

To determine the threshold for graviperception of *Paramecium* and of *Loxodes*, their graviresponses were studied under different accelerations on the NIZEMI slow-rotating centrifuge microscope. The reaction was measured by the transition from oriented movement (gravitaxis) to random swimming or vice versa. The *Paramecium* plexiglass chambers consisted of two parts, one for cultivation, filled with cells, and one for observation, filled with sterile culture medium. Six hours before the experiments, an astronaut transferred the paramecia into the observation part by moving a piston. Two experiment runs on NIZEMI were performed with *Paramecium*, one in the beginning and one at the end of the mission. *Loxodes* was cultivated in a one-chamber system. At dedicated times, the astronauts transferred the cuvettes from the incubation places to the slow rotating centrifuge, where they were either accelerated to 1-g and subsequently in logarithmic steps back to μ-g (stop of the NIZEMI) or vice versa. Each acceleration step lasted for 5 min.

Evaluation was performed by computer image analysis in real time or using video-recorded sequences. Data about cell orientation, swimming velocities, and linearity of individual swimming tracks were obtained.

Highlights

- The threshold for gravitaxis of *Paramecium* was >0.16-g and 0.3-g, and the unicellular organism did not adapt to weightlessness.
- *Loxodes* showed no graviresponses to increasing accelerations in space but did demonstrate gravitaxis upon return to Earth.
- Prolonged cultivation in space did not change the size and content of the barium sulfate of the statocyst organelles of *Loxodes*.

Postflight Analysis

After landing, the cells were again observed in a horizontal microscope, where cell vitality and gravitaxis could be demonstrated. Later, cells were fixed for microprobe analysis.

Postflight video analysis revealed that the threshold for gravitaxis of *Paramecium* is below 0.3-g and above 0.16-g. The threshold was in the same range whether the cells had been cultivated on the 1-g reference centrifuge or in microgravity. In addition, there was no effect on the threshold value when the behavior of *Paramecium* was observed under increasing or decreasing accelerations.

In spite of the clear gravitactic responses in the ground experiments, no acceleration-dependent behavior *Loxodes* was registered in the NIZEMI runs. Three runs were performed with

different acceleration profiles with *Loxodes* cells that had been cultivated for different lengths time in weightlessness. During stepwise increasing acceleration, random distribution persisted, and no graviorientation was induced. The samples were also investigated after landing after 15 days in space, when *Loxodes* showed its characteristic gravitactic response, a positive gravitaxis with a high precision. Microprobe analysis revealed unchanged barium content of the "statocyst" organelles.

Figure 1: Circular histograms showing negative gravitaxis of Paramecium at 1-g (a) and random distribution at 0.16-g (b) during a NIZEMI run

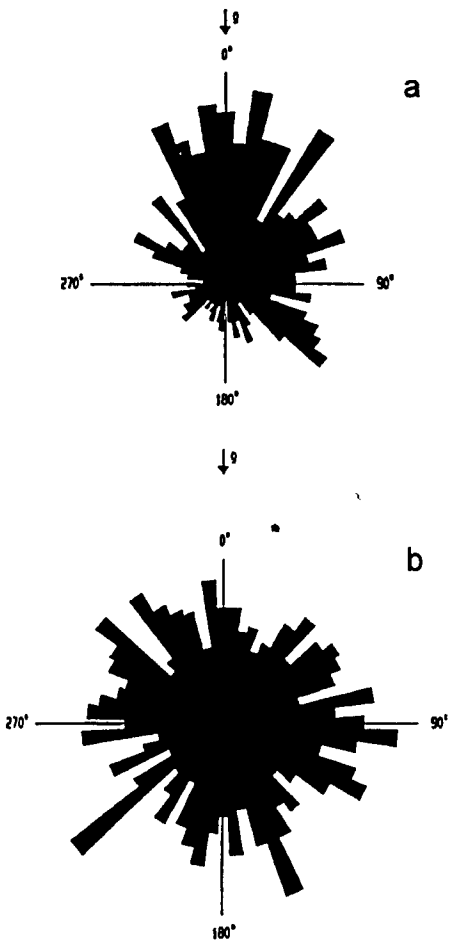

Conclusion

By using a centrifuge microscope in space, it was possible to determine the threshold for graviperception for the first time. The low threshold value of *Paramecium* between 0.16-g and 0.3-g is in the range of the values obtained for other species, e.g., *Euglena.* Because of the lack of gravitational responses, no threshold could be determined for *Loxodes.* Further experiments should clarify whether this unexpected behavior occurred because of an increase in temperature, a lack of oxygen, or other undiscovered factors or because *Loxodes* is more sensitive than *Paramecium* to deprivation of the gravity stimulus due to its "statocyst" organelles. Cultivation under gravity-free conditions did not change the barium sulfate content of the "statocyst" organelles of *Loxodes*, thus supporting findings on the unchanged calcium content and size of otoconia of hamster and frog after exposure to hypergravity or microgravity. The results, however, contradict the findings of decreased mineralization of bones in microgravity.

References

Häder, D-P., Rosum, A., Schäfer, J., and Hemmersbach, R., "Gravitaxis in the flagellate *Euglena gracilis* is controlled by an active gravireceptor," *J. Plant. Physiology*, vol. 146, pp. 474-480, (1995)

Hemmersbach, R., Voormanns, R., Briegleb, W., Rieder, N., Häder, D.-P., "Influence of accelerations on the spatial orientation of *Loxodes* and *Paramecium*, *J. Biotechnology*, vol. 47, pp. 271-278, (1996).

Hemmersbach, R., Voormanns, R., Häder, D.-P., "Graviresponses in *Paramecium* under different accelerations -- studies on the ground and in space," *J. Exp. Biol.*, vol. 199, pp. 2199-2205, (1996).

Hemmersbach, R., Voormanns, R., Rabien, H., Bromeis, B., and Ivanova, K., "Graviperception and signal transduction in unicellular organisms," *ESA-SP (Special Publication),* (1996), in press.

Hemmersbach, R., Voormanns, R., Bromeis, B., Schmidt, N., Rabien, H., and Ivanova, K., "Comparative studies of the graviresponses of *Paramecium* and *Loxodes*," *Advances in Space Res.*, in press.

Gravitaxis in the Flagellate *Euglena gracilis* is Controlled by an Active Gravireceptor (Euglena)

D.-P. Häder, Friedrich-Alexander-University, Erlangen, Germany

The gravireceptor of the unicellular flagellate *Euglena gracilis* has not yet been identified or isolated. An old hypothesis assumed that graviorientation is brought about by a passive alignment of the cells with the gravity vector caused by an asymmetry of their baricenters very much like a buoy. The alternative is that the cells possess an active physiological gravireceptor that stimulates the flagellum via a sensory transduction chain to reorient the cell. This experiment tested the hypothesis of an active gravireceptor under the conditions of prolonged microgravity.

Flight Activities

The experiments were carried out in custom-made cuvettes with 2 larger reservoirs that held about 1.5 ml cell suspension each; they were connected by a viewing window with a depth of 0.17 mm. In orbit, the astronauts transferred 2 cuvettes onto a 1-g reference centrifuge where they remained in darkness until the experiment commenced. The others were stored in microgravity and irradiated by red-light-emitting diodes. The temperature was kept constant at 22 °C ± 1 °C.

The astronauts transferred the cuvettes from the storage container to the slow rotating centrifuge microscope (NIZEMI). Each experiment cuvette was mounted flat on the vertical object table of the microscope off center from the rotation axis oriented radially. Temperature was kept constant by eight Peltier elements located around the cuvette holder. During rotation, images of the swimming cells were recorded by a CCD camera and stored on video. The investigator watched some of the video images during the mission and modified the area selection and focus.

Highlights

- Random orientation of flagellates at accelerations at and below 0.08-g confirmed prior results.
- Threshold for orientation ≤ 0.16-g
- Observed no adaptation during the extended duration of the mission.

Four runs lasted 60 min each. The first experiment was run on the second day of the mission using cells that had been stored in darkness on the 1-g reference centrifuge. During the experiment, the acceleration was increased in logarithmic steps from 0- to 1.5-g, each step lasting 5 min. The second run was performed on the sixth day on cells stored in microgravity. The third run on the following day also employed cells kept at microgravity, but the acceleration steps decreased from 1.5-g to 0-g. The final run on the eleventh day repeated the second run. For each run a new sample was used. We analyzed the tracks of the swimming cells with a real-time image analysis system.

Postflight Analysis

During the first run, the acceleration increased logarithmically from 0- to 1.5-g, with a 5-min recording time for each level. The videotape was evaluated in 1-min intervals so that changes in orientation could be observed. Because of the fast real-time image analysis, more than 1000 tracks could be recorded each minute, which yielded a high level of statistical significance. A significant orientation could not be observed below or at 0.08-g. This was proven by the Rayleigh test that showed r-values below 0.1, indicating a random orientation of the flagellates. For the following g-levels, the data were pooled again showing the orientation of the cells integrated over 5-min intervals. The r values measured here are similar to those observed at 1-g under terrestrial conditions. With a few exceptions (which can be explained by low organism numbers during that tracking period), the precision of orientation follows a sigmoidal curve. Below the threshold at 0.16-g, there is a

random orientation of the cells. At and above the threshold there is an increase in precision up to a saturation value reached at 0.64-g.

A similar behavior was found for the second run, although the cells had been kept at microgravity conditions for 6 days. Again the threshold was found at 0.16-g and a saturation of the precision of orientation at 0.32-g. At the end of this run, acceleration was reduced to 0, and the orientation of the cells dropped to values characteristic for random movement within 1 min.

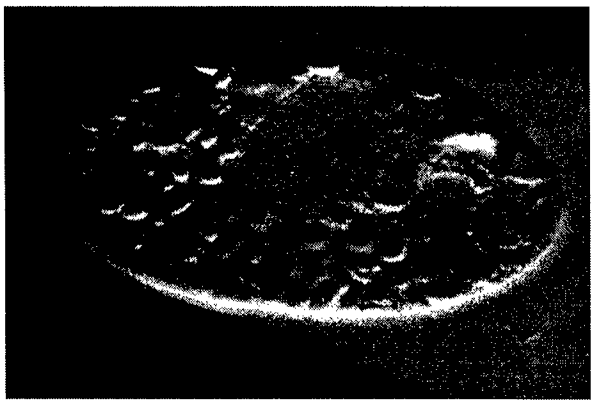

Euglena gracilis

The response of the cells to the new acceleration level can also be seen in run 3, which was performed on day 7 of the mission on cells adapted to microgravity. After the first 5 min at 0-g, the acceleration was suddenly increased to 1.5-g. The cells responded within 1 min and showed a very high precision of orientation (r values above 0.8). During this experiment the acceleration values followed a sequence inverse of that for the second run. The same saturation and threshold values were found as in the first and second run. These results were basically confirmed during the final run on day 11, which had similar conditions to run 2. In all cases when the cells showed an oriented swimming, they moved against the gravity vector (negative gravitaxis).

Conclusion

The random orientation of the flagellates at accelerations at and below 0.08-g confirmed earlier results of experiments on sounding rockets. The threshold value for orientation in this flagellate is remarkably low. Why do the flagellates start to orient at ≤0.16-g when their evolution on Earth has always been in the presence of 1-g? Future experiments should try to determine the threshold more precisely.

The hypothesis of an active physiological receptor is further supported by the observation that the flagellates deviate from the acceleration vector. The deviation angle decreases with the acceleration force and with exposure time to a given acceleration. There was no adaptation during the extended duration of the mission. Even though the flagellates underwent several cell divisions during that time, neither the threshold nor the saturation values differed between the organisms studied at the beginning or at the end of the mission.

References

Häder, D.-P., Rosum, A., Schäfer, J., and Hemmersbach, R., "Gravitaxis in the flagellate *Euglena gracilis* is controlled by an active gravireceptor," *J. Plant Physiol.*, vol. 146, pp. 474 - 480, (1995).

Hemmersbach-Krause, R., Briegleb, W., Häder, D.-P., Vogel, K., Grothe, D., and Meyer, I., "Orientation of *Paramecium* under the conditions of weightlessness," *J. Euk. Microbiol.*, vol. *40*, pp. 439 - 446, (1993a).

Hemmersbach-Krause, R., Briegleb, W., Vogel, K, and Häder, D.-P., "Swimming velocity of *Paramecium* under the conditions of weightlessness," *Acta Protozool.*, vol. *32*, pp. 229 - 236, (1993b).

Kühnel-Kratz, C., Schäfer, J., and Häder, D.-P., "Phototaxis in the flagellate, *Euglena gracilis*, under the effect of microgravity," *Microgr. Sci. Technol.* vol. *4*, pp. 188-193, (1993).

Stallwitz, E. and D.-P. Häder, "Effects of heavy metals on motility and gravitactic orientation of the flagellate, *Euglena gracilis," Europ. J. Protistol.*, vol. 30, pp. 18-24 (1994).

Effects of Micro-g on *Aurelia* Ephyra Behavior and Development (Jellyfish)

Dr. D.B. Spangenberg, Eastern Virginia Medical School, Norfolk, Virginia, United States

Jellyfish flown on the SLS-1 mission had ephyrae that were able to pulse and swim. Postflight, pulsing abnormalities were found in greater numbers (18.3%) in ephyrae that developed in space than in the ground-based controls (2.9%). In space, the behavior of the ephyrae was different from that of Earth-maintained ephyrae. On Earth, ephyrae tend to swim upward while pulsing and then when not pulsing to drift downward along the g-vector with their mouths pointing downward. In space, ephyrae from Earth tended to hang in place when not pulsing and to swim in circles or arcs when they were pulsing. The difference in the behavior of these organisms in space and on Earth was used during the IML-2 flight to determine the g-threshold for Earth-type behavior.

Highlights

- Confirmed SLS-1 findings that ephyrae form in microgravity and can pulse and swim.
- Ephyrae that developed in space had more arm abnormalities.

Flight Activities

Jellyfish polyps and ephyrae with and without statoliths were housed in Type 1 Biorack containers. The jellyfish were maintained at 22 °C in the Biorack incubator and on the 1-g centrifuge and were exposed to 28 °C while on the NIZEMI to facilitate swimming activity.

The g-threshold is defined as that amount of g required for more than 50% of the organisms to convert from space-type behavior to Earth-type behavior. To determine the g-threshold for the swimming behavior of the ephyrae, the NIZEMI was preprogrammed during the first video session to provide 15 levels of g. The ephyra samples had been videotaped on Earth prior to the flight. On approximately MET 16 h, the first video session was begun, and the investigator determined visually that the g-threshold range is between 0.312 and 0.412-g. The NIZEMI was reprogrammed with five levels, 0.3123, 0.339, 0.3639, 0.3907, and 0.412 plus 0.00 for the micro-g ephyrae and 1.0 for the 1-g ephyrae. Following a review of the videotapes of the first session, the g-threshold lower range was changed to 0.255 for the last session.

Four groups of 6 polyps each were given iodine in artificial saltwater (ASW) 24 h preflight to induce strobilation of the polyps, which results in ephyra formation. Two samples were selected to be videotaped on MET 4, 5, 6, and 12 days. The other 2 groups were fixed in flight on MET day 12. Ephyrae from Earth with statoliths, which were videotaped beginning at MET 16 h and approximately 48 h later, were fixed on MET day 4, as were ground controls.

Postflight Analysis

Living jellyfish were counted, coded, and photographed beginning 5 h postflight. Ephyrae developed in all of the groups that were given iodine, and they were able to swim. The pulse rate, numbers of arms, rhopalia, and statoliths were counted and recorded. Ephyrae with abnormal pulsing were videotaped postflight on landing day and again approximately 24 h later. Bottom pieces from the strobilae of space animals and controls as well as buds from both groups were isolated and fed brine shrimp or a liquid nutrient. Some of these jellyfish were allowed to form clones through isolation of a single organism and retention of their buds. After sufficient numbers of buds grew to polyps, members of some clones have been and are being tested to determine whether their arm numbers and other structures resemble those of the flight experiment ephyrae.

Postflight examination of the videotapes of strobilating jellyfish revealed that strobilation

occurred, and ephyrae formed in all of the groups. Considerable variation of developmental stages was present in all the animals in all the cuvettes. Most notable, however, was the presence of pulsing ephyrae on MET 6 in both the space-developed ephyrae groups, whereas ephyrae developing on strobilae of Earth controls did not pulse at this time. This result indicates that some of the micro-g developed ephyrae were developmentally ahead of the ground-based controls at that time. Further tests are needed using more animals to determine whether development of ephyrae proceeds at a faster rate in space than on Earth.

The micro-g groups, which had a significantly higher number of arms per ephyra, also had a significantly higher number of rhopalia. There was no statistically significant difference between the three groups of ephyrae tested with regard to statolith numbers.

Swimming ability was determined by observing the ephyrae's ability to swim for 1 min in ASW in a test-tube on day 1 postflight. Significantly more ephyrae that developed in space in micro-g did not swim upon return to Earth as compared with the 1-g controls. It is noteworthy that more of the animals maintained at 1-g in space controls swam than the ground-based controls.

Although the swimming behavior of ephyrae that developed in space in micro-g was significantly different from that of ephyrae in 1-g, there were no statistically significant differences in the pulsing ability of the animals postflight. Using the videotaped results and observations made during testing of organisms not videotaped, we found a 22.5% pulsing abnormality rate in the space-developed ephyrae as compared with 23% in the ground controls and 13% in the ephyrae that developed at 1-g in space.

The ultrastructure of the hair cells and statocysts of space-developed ephyrae from the SLS-1 and IML-2 missions were compared with 1-g controls using approximately 600 electron micrographs. The statocysts and hair cells were not significantly different from controls except that ephyrae that developed in microgravity had hair cells with fewer lipid droplets near their bases. Behavioral differences in swimming and orienting of ephyrae in microgravity and controls were not explained by morphological differences in their hair cells or statocysts, although functional differences apparently occurred.

Conclusion

This experiment confirmed that ephyrae form in micro-g, and they can pulse and swim. The ephyrae that developed in micro-g had statistically significantly more arm abnormality (especially regarding more than 8 arms) than ephyrae of the control groups. Microgravity may interfere with pattern formation or with the genetic programming for arm formation which may involve the activity of the Jf-T4 hormone. Some of the results may be explained through a greater understanding of the role that this hormone plays in the development and behavior of the jellyfish on Earth and in space.

References

Spangenberg, D.B., Coccaro, E., Schwarte, R., and Lowe, B., "Touch-plate and statolith formation in graviceptors of ephyrae which developed while weightless in space," *Scanning Microscopy,* vol. 10, no. 3, (1996).

Spangenberg, D.B., Lattanzio, F.A., Jr., Philput, C., Schwarte, R., Coccaro, E., Lowe, B., and Philput, J., "Effects of weightlessness on *Aurelia* budding and ephyra development," *6th International Conference on Coelenterate Biology*, Noordwijhout, The Netherlands, (1996).

Spangenberg, D.B., Jernigan, T., McCombs, R., Lowe, B.T., Sampson, M., and Slusser, J., "Developmental studies of *Aurelia* (Jellyfish) ephyrae which developed during the SLS-1 mission," *Adv. Space Res.*, vol. 14, no. 8, pp. 239-247, (1994).

Spangenberg, D.B., Jernigan, T., Philput, C. and Lowe, B., "Graviceptor development in jellyfish ephyrae in space and on Earth," *Adv. Space Res.*, vol. 14, no. 8, pp. 317-325, (1994).

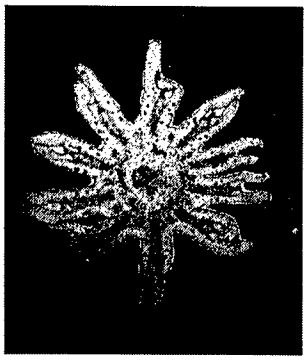

Ephyra that developed in microgravity during the IML-2 mission

Chara rhizoids: Studies during a Long Period of Microgravity (Chara)

Dr. A. Sievers, Dr. M. Braun, and Dr. B. Buchen, University of Bonn, Bonn, Germany

Gravity tells a plant where up and down are and thus the direction of root and shoot growth. To understand how gravity is perceived and how the stimulus results in an oriented-growth response, studies with rhizoids of the green alga *Chara* have been performed on Earth. They have provided insights into the behavior and mechanism of graviperception in single cells.

In Earth's gravity, we cannot determine the minimum threshold value of sensitivity to gravity. This mission provided the first chance to study (1) the development, growth, and expression of the structural polarity of rhizoids under a long period of microgravity, (2) the spatial distribution of statoliths and the velocity of their displacement, (3) the first approximation of the determination of threshold values of force and duration of the gravity stimulus, and (4) the role of actin filaments in the stimulus-response.

Flight Activities

Rhizoids in cuvettes were stowed in a Biorack Type 2 container. To determine threshold values for force and duration of accelerations, cuvettes with rhizoids grown for at least 30 h under microgravity at ambient Spacelab temperature (23-27 °C) were mounted on the stage of the microscope in the NIZEMI so that a definite acceleration force for a definite time period could be applied perpendicularly to the length axis of the rhizoid. To obtain data on the ultrastructure of rhizoids that had developed under 1-g on Earth and had grown for at least 30 h in microgravity, rhizoids in special culture chambers were fixed and processed for electron microscopy on the ground.

Highlights

- Demonstrated tip-growing single cells develop normally in microgravity.
- Growing rhizoids maintained their structural polarity and grew straight.
- Distribution of statoliths was similar to that found in sounding rocket experiments.

Postflight Analysis

For the first time, we documented the development of rhizoids in microgravity. Without gravity, the rhizoids radiate from the nodal cells of the thallus segment in different directions and grow straight on. The typical polarity of the rhizoids is present in those exclusively developed and grown under microgravity conditions. This proves that the inherent genetic program of the tip-growing cells is expressed under microgravity. The rhizoids that had already grown out on Earth also grew during exposure to a long period of microgravity and maintained their structural polarity.

The distribution of statoliths differs from that of 1-g controls. In both rhizoids formed previously in 1-g and those first developed in microgravity, the statoliths are spread over an area of about 50 μm basal to the apical cell wall. A similar displacement of statoliths has been found after 6-min of microgravity during sounding rocket flights. This demonstrates that a new balance of forces has been established in the rhizoids within short time. When NIZEMI applies an acceleration of 1-g in axial, apical direction (toward the tip of the rhizoid), the statoliths are relocated to the position they normally keep in vertical orientation of the rhizoid on ground. After 10 min, the distance of the basal border of the statoliths complex from the apical cell wall starts to diminish to ~20 μm, whereas the distance of the apical border remains nearly constant. Changing to microgravity induces a basipetal shift of the basal border of the statoliths complex, again.

Only rhizoids grown on ground plus 30 h under microgravity were fixed. Organelles like mitochondria, plastids, and dictyosomes can clearly be identified by their typical structural organization and distinct membranes. There is no obvious difference in the ultrastructural features of the rhizoids grown under microgravity compared to ground controls, and changing the gravity conditions does not disturb or destroy the cellular organization, the structure of organelles, or of cytoskeletal elements like microtubules.

To obtain first insights into the sensitivity of the rhizoids for the gravity stimulus, NIZEMI applied different acceleration forces for different times. We could only make first approximations on the sensitivity of the rhizoids, but the data look promising. For the analysis, photographs of the rhizoid tip with statoliths were taken from the videotapes before the experiment run, immediately at the end of the acceleration period, and after 30 min in microgravity. Application of 1-g for 1 min does not result in a visible displacement of statoliths. In spite of normal and typical movements of single statoliths, no asymmetrical distribution can be seen, and the statoliths complex as a whole remains in a stable position. Consequently, the rhizoid grows straight on without showing any curvature. The same situation holds for the dose of 0.1-g for 30 min. However, when either 1-g for 4 min or 0.5-g for 30 min have been applied, some changes and dislocations of the statoliths occur.

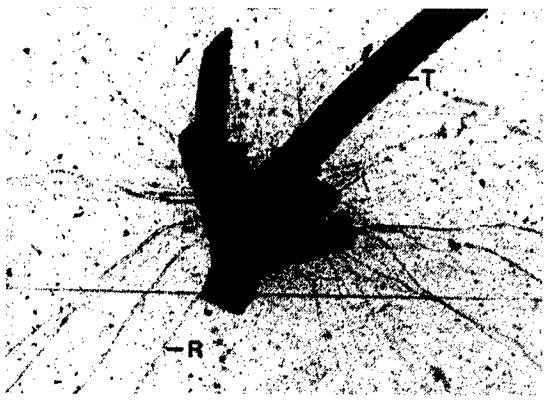

Figure 1: Rhizoids* (R) *exclusively originated under MG and radiating from nodal cells of the Chara thallus (T) segment

Conclusion

During exposure to a long period of microgravity, the growing rhizoids maintained their typical structural polarity. After only short periods of microgravity, a dynamically stable, new balance of forces exerted on statoliths by gravity and by actin filaments was established. After exposure to 1-g for 4 min or 0.5-g for 30 min perpendicular to the length axis of the rhizoid, the statoliths shifted slightly to one flank of the rhizoid according to the direction of the acceleration.

There was no obvious difference in the ultrastructural features of the rhizoids grown under microgravity compared with ground controls; therefore changing the gravity conditions does not disturb or destroy the cellular organization. In addition, for the first time rhizoids have developed exclusively under microgravity. Without gravity, the rhizoids grew straight. They did not develop in the form of bundles, but they radiated randomly in different directions.

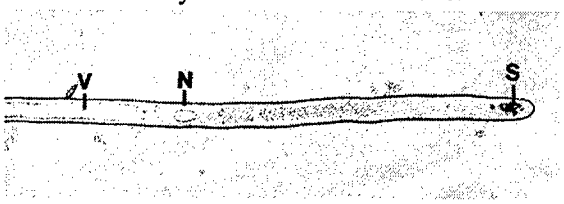

Figure 2: Light microscope image of a Chara rhizoid developed in MG with the characteristic organization of the apical zone with statoliths (S) and the basal zone with streaming cytoplasm, N = nucleus, V= vacuole; rhizoid diameter = ~ 25 μm.

References

Braun, M., Buchen, B., Sievers, A., "Fixation procedure for transmission electron microscopy of *Chara* rhizoids under microgravity in a Spacelab (IML-2)," *J. Biotechnol.*, vol. 47, pp. 245-251, (1996).

Sievers, A., Buchen, B., Hodick, D., "Gravity sensing in tip-growing cells," *Trends in Plant Science*, vol. 1, pp. 273-279, (1996).

Häder, D.-P., Rosum, A., Schäfer, J., Hemmersbach, R., "Gravitaxis in the flagellate *Euglena gracilis* is controlled by an active gravireceptor," *J. Plant Physiol.*, vol. 146, pp. 474-480, (1995).

Braun, M., Sievers, A., "Centrifugation causes adaptation of microfilaments - Studies on the transport of statoliths in gravity sensing *Chara* rhizoids," *Protoplasma*, vol. 174, pp. 50-61, (1993).

Graviresponse of Cress Roots under Varying Gravitational Forces below Earth Acceleration (1-g) (Cress)

Dr. D. Volkmann, University of Bonn, Bonn, Germany

The reciprocity rule (dose = stimulus x time = constant) is one of the most important rules of classical sensor physiology. For the first time, microgravity offers the possibility of testing this rule concerning gravity-controlled growth processes in plants under exact physiological conditions. For this purpose, three prerequisites have to be fulfilled: (1) the applied doses have to be in the range of the minimum dose, one of the most important threshold values, (2) stimulation by fractions of 1-g must be possible, and (3) the resulting gravitropic growth response has to occur in a stimulus-free environment, i.e., under microgravity conditions.

The D-2 gravisensitivity experiment estimated the minimum dose for cress roots cultivated in orbit on a 1-g-centrifuge for 50 to 60 g • s (i.e., stimulation of roots to 1-g for approximately 50 s) resulted in visible root curvature. This result did not confirm the threshold value of 12 g • s, which was determined by the use of clinostats on Earth. On the other hand, roots grown under microgravity conditions showed remarkable graviresponses after application of doses between 20 and 30 g • s, which indicated a higher gravisensitivity of microgravity-grown seedlings. NIZEMI, the slow rotating centrifuge microscope, allowed us to apply stimuli between 10^{-2}-g and 1-g in orbit. For the first time, we tested the reciprocity rule under precise physiological conditions. The results will enable us to draw conclusions on the very early steps of stimulus transformation.

Flight Activities

The astronauts added tap water to dry cress seeds in plant culture chambers, 4 chambers in one Biorack Type 1 container. Inside the Biorack incubator, at 22 °C, one group of roots was cultivated in a microgravity compartment whereas another group grew on the Biorack 1-g-centrifuge. Thirty hours after growth initiation, acceleration experiments were performed in the NIZEMI. Using lateral stimulation, different doses between 12 and 60 g • s were applied to the seedlings. Root curvature was tracked by a 60-min video recording.

Highlights

- Roots cultivated under microgravity had a higher sensitivity than those grown on the 1-g centrifuge.
- These results and those from prior missions suggest the nonvalidity of the reciprocity rule.
- Transformation of the gravistimulus occurs near the statoliths.

Postflight Analysis

On the ground, growth responses were estimated by image analysis. Curvature degrees were measured by superposition of video pictures of each root from the beginning and the end of the observation time. In corresponding experiments, chemical fixations were performed immediately after stimulation. Further processing for light and electron microscopy corresponded to conventional procedures. Calculations of statolith complex positions were performed from serial sections by estimating the focal point of complexes within a coordinate system depending on the cell shape.

In general, roots that were cultivated under microgravity conditions responded within a shorter time after stimulation than roots from the 1-g-centrifuge. Additionally, these microgravity roots showed a larger degree of curvature. The largest degree of curvature, however, was observed with roots from ground controls when gravitropic responses developed during rotation on clinostats. For testing the reciprocity rule, it is necessary to consider the same dose at different accelerations and different time intervals. Comparing results from IML-2 and D-2, roots

stimulated by 10^{-1}-g showed obviously smaller degrees of curvature than those stimulated by 1-g. These data indicate that the resulting gravitropic curvatures are not constant in spite of equal doses applied to the seedlings, i.e., the reciprocity rule validity under these conditions is questionable.

Corresponding structural investigations of gravity-perceiving cells showed no correlation between acceleration and statolith displacement. Displacement of the statoliths was very small for the different treatments, mainly less than 1μm, which is approximately one-third of a statolith's diameter.

Conclusion

We conclude that the first steps of stimulus transformation are related more to biochemical than biophysical processes. Several reports from experiments under microgravity and on clinostats indicate remarkably smaller threshold values in the range between 10^{-4}-g and 10^{-3}-g for roots and coleoptiles. However, for these experiments, the applied doses were higher than the minimum dose.

Accepting the statolith theory, we conclude that stimulus transformation has to occur in the vicinity of statoliths, i.e., stimulus transformation is probably mediated by the ground cytoplasm and the cytoskeleton suspended therein.

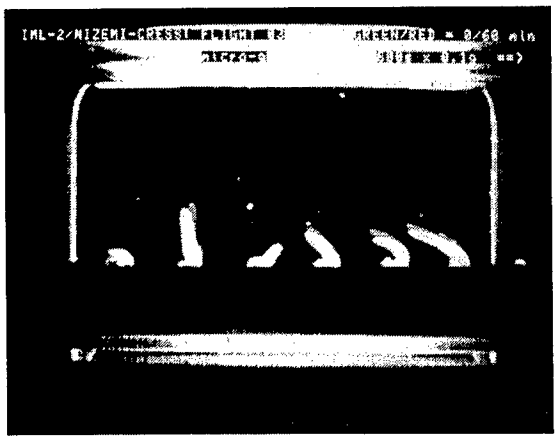

Figure 1: Inflight experiment: Cress roots cultivated under microgravity, stimulated for 600 s at 0.1-g (dose = 60 g• s, arrow indicates stimulus direction), after stimulation video recorded for 60 min in microgravity. Superposition of roots at 0 min and 60 min of video recording.

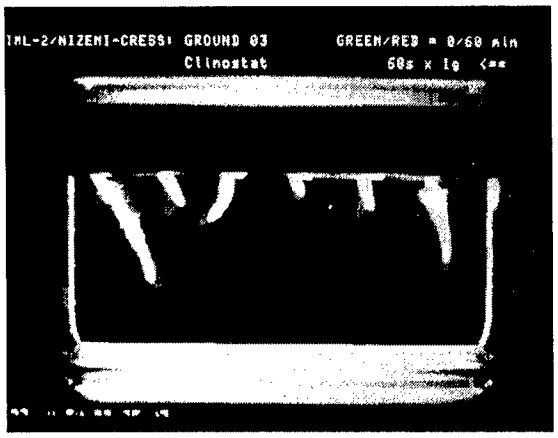

Figure 2: Ground control experiment on clinostat: Cress roots cultivated on clinostat, stimulated for 60 s at 1-g (dose = 60 g• s, arrow indicates stimulus direction), after stimulation video recorded for 60 min on clinostat. Superposition as in Figure 1.

References

Johnsson, A. Karlsson, C., Iversen, T.-H., and Chapman, D.K., "Random root movements in weightlessness," *Physiologia Plantarum 96,* pp. 169-178, (1996).

Volkmann, D. and Tewinkel, M., "Gravisensitivity of cress roots: investigations of threshold values under specific conditions of sensor physiology in microgravity," *Plant Cell and Environment,* vol. 19, pp. 1195-1202, (1996).

Volkmann, D. and Tewinkel, M., "Graviresponse of cress roots under varying gravitational forces," *Journal of Biotechnology,* vol. 47, pp. 253-259, (1996).

Iversen, T.-H. and Larsen, P., "Movement of amyloplasts in the statocytes of geotropically stimulated roots. The pre-inversion effect," *Physiologia Plantorum,* vol. 28, pp. 172-184, (1973).

THERMOELECTRIC INCUBATOR (TEI) AND CELL CULTURE KITS (CCK)

INVESTIGATIONS	PRINCIPAL INVESTIGATORS	RESULTS HIGHLIGHTS
Gravity and the Stability of the Differentiated State of Plant Somatic Embryos	Dr. A.D. Krikorian State University of New York at Stony Brook, Stony Brook, New York, United States	Flight samples had chromosomal damage whereas ground controls did not. Epidermal development of flight samples was poorer than ground controls. Perturbation is real and not an artifact of reentry or postflight adaptation.

INVESTIGATIONS	PRINCIPAL INVESTIGATORS	RESULTS HIGHLIGHTS
Microgravity Effects on the Growth and Function of Rat Normal Osteoblasts	Dr. Y. Kumei Tokyo Medical and Dental University, Tokyo, Japan	Microgravity affected the gene expression of osteoblast functions important for bone formation and metabolism. Observed cellular and molecular effects of bone demineralization. Obtained data to help prevent osteoporosis on Earth and in space.
Differentiation of *Dictyostelium discoideum* in Space	Dr. T. Ohnishi and Dr. K. Okaichi, Nara Medical University, Nara, Japan	Microgravity and cosmic radiation did not affect the NC4 spores. Cosmic radiation may have prevented germination of the gs13 spores.

Gravity and the Stability of the Differentiated State of Plant Somatic Embryos

Dr. A.D. Krikorian, State University of New York at Stony Brook, Stony Brook, New York, United States

This experiment evaluates cell division and somatic embryo progression in space. Test materials comprised embryogenic cells of daylily (*Hemerocallis*), a system which has been well-characterized in this laboratory from a developmental cell biology, physiology, and chromosome structure perspective. A prior experiment suggests embryogenic cells of daylily are a good model system for studying how space effects cell division and development and chromosome structure in *in vitro* cultured cells. Cells with double nuclei and breaks were found in space samples but not in controls. For this experiment, we asked if mitosis and chromosome behavior in developing plant cells are modified by the space environment

Flight Activities

Prior experiments showed it might be easier to control experiment parameters by using cell cultures instead of plants. Totipotent cells cultures can provide all the advantages of a developing plant system. Cells from the various organs of the higher plant body can be nurtured and grown on nutrient media to elicit morphogenetic capacity and to stimulate cell divisions to get structures that can make organized growing regions of shoot, root and even to yield an entire embryo, a so-called somatic embryo. This works not only at the cellular level but also at the level of cells that are morphogenetically competent and able to express this competence provided the conditions are permissive.

Embryogenic suspensions of a diploid daylily clone (*Hemerocallis* cv. Autumn Blaze) were derived from vegetative shoot apex. Plant Cell Fixation Chambers were used as well. These chambers allow fixative to be introduced into the dish. A synchronous ground control was carried out in identical dishes; additional synchronous ground controls were performed using 100 x 15 mm presterilized plastic petri dishes with a final volume of about 45 ml of medium.

Highlights

- Flight samples had chromosomal damage whereas ground controls did not.
- Epidermal development of flight samples was poorer than ground controls.
- Perturbation is real and not an artifact of reentry or postflight adaptation.

Postflight Analysis

At our laboratory, the materials were photographed and fixed within 9 h of landing and we were able to catch cells well before their first division cycle was completed on Earth. Chromosome analysis was carried out by examining materials fixed with the mitotic arresting agent (a cytostatic) colchicine. Relevant fractions of unorganized cell suspensions were collected. Somatic embryos at various stages of development and plantlets generated from them but maintained *in vitro* were handled in the same way. Photographs of chromosomes were made, and counts of cells in division were carried out. Five to ten representative cells at metaphase with well spread and favorably condensed chromosomes were selected for measurement and comparison within and between cultures. Long arm, short arm, total chromosome length and centromeric index measurements were used to construct idiograms. Relative length was determined by dividing the length of the total haploid genome times 100.

The examination of material fixed in space demonstrated that the cytological changes and chromosomal aberrations encountered by us in previous space flight missions are real. That is they are not caused by events during reentry and landing. Since they are present in both ground-fixed and space-fixed material, they are not caused by fixation.

We observed a substantial number of binucleate cells in flight samples. These binucleate cells are not uniformly present throughout individual somatic embryos that were scored but were present among normal, uninucleate cells. The ground control samples are all uninucleate. Aberrations in chromosome structure such as breaks, micronuclei, and microchromosomes also have been encountered.

Serial sampling and examination of flight samples after recovery, beyond what we refer to as sampling 1 (i.e. the first sampling after recovery) indicates that the number of binucleate cells diminish in some samples but do not disappear in any. This could be interpreted as adaptation, and it may be that plant cells adapt to space. We are rearing some embryos into plantlets of both flight and controls to see the outcome. See Figure 1 for some details.

Conclusion

This experiment extended our earlier findings on atypical nuclear and chromosome behavior in space-grown plant materials. We demonstrated convincingly through tests of this sort that cultured, embryogenic cells can serve as models for the study of development in higher plants in space environments and in microgravity. This means it will be considerably easier to achieve the kind of control over the system necessary to separate direct from indirect effects and thus enable us to move toward resolving the still many outstanding questions. Space flight can significantly affect the level of cell division and chromosome partitioning in plant cells. Whether this is a manifestation of altered signal processing or is a "stress" response to reduced gravity remains to be tested. Since plant cells undergo virtually no movement during development and the plane of cell division and subsequent enlargement determine morphology, modification in either should have important consequences for plant development during protracted exposure to space.

References

Krikorian, A.D., "Strategies for minimal growth maintenance of cell cultures: a perspective on management for extended duration experimentation in the microgravity environment of a Space Station," *Botanical Review*, vol. 62, pp. 41-108, (1996).

Krikorian, A.D., "Embryogenic somatic cell cultures of daylily (*Hemerocallis*): A system to probe spaceflight-associated mitotic disturbances," *Plants in Space Biology*, Suge, H., ed., Institute of Genetic Ecology, Tohoku University, Sendai, Japan, pp. 111-126, (1996).

Krikorian, A.D., "Space stress and genome shock in developing plant cells," *Physiologia Plantarum*, vol. 98, in press.

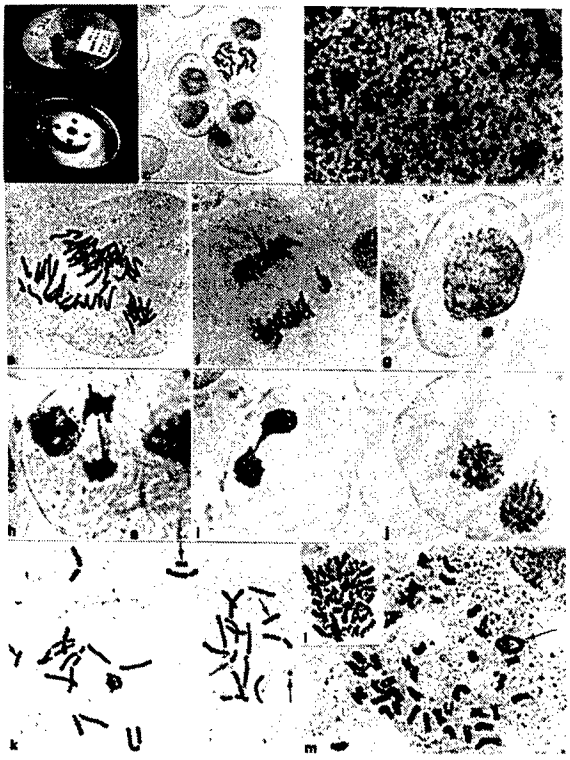

Figure 1: Observations of cells of squashed somatic daylily embryos that developed during IML-2. (a & b) outside and inside views, respectively, of a petri dish that allowed syringe attachment and fixation in space; (c) view of a typical squash of the 100-200 mesh fraction of embryogenic initials showing a diploid cell in division at "time zero," that is at the time of dish inoculation; (d) somatic embryo "units" at recovery, e.g., direct-fixed squashes; (e) a diploid cell at anaphase with a group of chromosomes that have remained outside the main spindle; (f) late anaphase, beginning of telophase, again a group of chromosomes outside the main spindle; (g) a cell in interphase with a prominent micronucleus; (h) telophase showing a bridge; (i) late telophase with persistent bridge (j) binucleate cell, with no evident wall separating the nuclei; (k) cell arrested in metaphase through prefixation with colchicine showing signs of fragmentation and diploid cell with fragments lacking centromeres; (l) direct-fixed squash with fragmented chromosomes; and (m) metaphase from a direct-fixed squash with rings.

Microgravity Effects on the Growth and Function of Rat Normal Osteoblasts

Dr. Y. Kumei, Tokyo Medical and Dental University, Tokyo, Japan

Bone demineralization and increases of renal stone-forming potential in space crews indicate the importance of understanding microgravity-induced changes in bone homeostasis. Rodent histological studies showed decreased bone formation and defects in bone maturation, suggesting inappropriate functioning of osteoblasts in microgravity. The purpose of this study was to cultivate normal rat osteoblast cells in microgravity and to investigate alterations in gene expression, concurrently with quantitation of known growth factors and cytokines produced and secreted by the osteoblasts.

Highlights

- Microgravity affected the gene expression of osteoblast functions important for bone formation and metabolism.
- Observed cellular and molecular effects of bone demineralization.
- Obtained data to help prevent osteoporosis on Earth and in space.

Flight Activities

Three days before launch, osteoblast-like cells grown in a primary femur marrow culture were suspended and inoculated in culture chambers. Four chambers were put in a middeck locker 15 h before launch, while 8 chambers became the ground controls. On orbit, the cells resumed incubation at 37 °C in an atmosphere of 95% air and 5% CO_2 with 60% humidity. On the third day of the mission, the crew reported the cell growth status, took phase-contrast microscopic photos, renewed the culture medium, and treated half of the chambers with vitamin D medium.

After 1 day of incubation, the vitamin D-containing medium was harvested, and cells were rinsed with phosphate-buffered saline solution, then fixed/extracted with guanidinethiocyanate (GTC) solution. The harvested medium and the chambers containing GTC solution were stored in a -20 °C freezer. This was repeated with the remaining chambers on the fourth day of the mission.

Postflight Analysis

The GTC solution containing cellular extracts was harvested completely, and RNA, DNA, and protein fractions were obtained. For gene expression analysis, a set of oligonucleotide primers, which recognized the forward and reverse sequence of a specific region of target gene cDNA, was used. The original mRNA level for each gene was compared quantitatively using high-sensitivity radioactivity counting coupled with image analysis. For cellular products analysis, the aliquots of the harvested medium that were kept in the 70 °C freezer were subjected to radioimmunoassay and enzymeimmunoassay to quantitate growth factors and cytokines.

The cells proliferated favorably in flight and ground cultures, and analysis indicated that total cell number and the condition of cell impairment was the same. Prostaglandin E2 (PGE2) content showed 20 pg/μg DNA in the harvested medium from the first 3 days of flight culture, which was 11-fold higher than the ground control. On the 4th day, the PGE2 productivity was 2.7 pg/μg DNA, which was 7-fold higher than the ground control. No effects of vitamin D addition were observed. In flight, the gene expression of cyclooxygenase-2, the rate-limiting key enzyme in the process of PGE2 synthesis, was increased by 2 to 20-fold compared to the ground control. PGE2 production by osteoblasts was greatly elevated in microgravity by the mechanism in which cyclooxygenase-2 induction was enhanced.

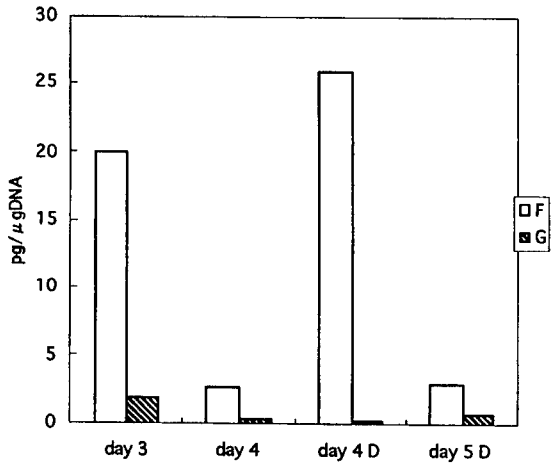

Figure 1: Prostaglandin E2 synthesis of rat normal osteoblasts. F=Flight, G=Ground

Osteocalcin production in the presence of vitamin D was 154 pg/day/μg DNA on the fourth day of flight, which was a decrease of 90% compared to the ground control. On the fifth day, osteocalcin productivity was increased to 583 pg/day/μg DNA but inhibited by 40% compared to the ground control. The osteocalcin gene expression was inhibited in the range of 60 to 90%. In microgravity, osteocalcin production by osteoblasts was inhibited at the level of osteocalcin gene expression.

Transforming growth factor-b1 (TGF-b1) production was 271 pg/day/μg DNA on the fourth day, which was 26% lower than the ground control. The TGF-b1 productivity was 45 pg/day/μg DNA on the fifth day of flight, which was inhibited by 80% compared to the ground control; vitamin D had no effect.

Transforming growth factor-b2 (TGF-b2) production was the same in flight and ground cultures on the fourth day. However, the TGF-b2 productivity was 3.8 pg/day/μg DNA on the fifth day, which was 90% inhibition of the ground control; vitamin D had no influence. Production of IGF-binding protein 3 (IGFBP-3) in osteoblasts was 30 pg/day/μg DNA in the presence of vitamin D, which was 10-fold higher than the ground control.

Conclusion

Both flight and ground cultures showed favorable growth of normal rat osteoblasts. Microgravity conditions enhanced the production of PGE2 and IGFBP-3, while inhibiting the production of osteocalcin, TGF-b1 and TGF-b2. These results were consistent with mRNA levels. Osteoblast functions that are important for bone formation and bone metabolism were seriously affected by microgravity at the level of gene expression. The mechanism of space flight-induced bone demineralization has been clarified at the cellular and molecular level. Our data will contribute to the prevention of osteoporosis on Earth as well as in astronauts.

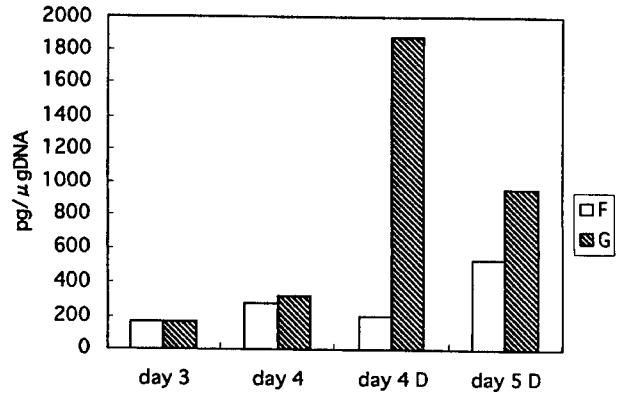

Figure 2: Osteocalcin synthesis of rat normal osteoblasts. F=Flight, G=Ground

References

Kaji, H., Sugimoto, T., Kanatani, M., Fukase, M., and Chihara, K., *Biochem. Biophys. Res. Comm.*, vol. 194, pp. 157- 162 (1993).

Togari, A., Arakawa, S., Arai, M., and Matsumoto, S., *Biochem. Pharmacol.*, vol. 46, pp. 1668-1670, (1993).

Kumei, Y., Whitson, P.A., Sato, A., and Cintron, N.M., *Exp. Cell Res.*, vol. 192, pp. 492-496, (1991).

DeGroot, R.P., Rijken, P.J., Hertog, J.D., Boonstra, J., Verkleij, A., de Laat, S.W., and Kruijer,*W., J. Cell Sci.*, vol. 97, pp. 33-38 (1990).

Chum, Y., Nakajima, T., Sato, A., Kamata, N., and Enomoto, S., *J. Cell Sci.*, vol. 93, pp. 221-226, (1989).

Differentiation of *Dictyostelium discoideum* in Space

Dr. T. Ohnishi and Dr. K. Okaichi, Nara Medical University, Nara, Japan

Two strains of the slime mold *Dictyostelium discoideum*, a wild-type strain (NC4) and a radiation-sensitive mutant (gs13), were used to investigate the effects of cosmic radiation and/or microgravity on cell morphology and cell differentiation over the whole life span. Dry spores of NC4 and gs13 were placed in a slime mold Cell Culture Kit (CCK) with *Escherichia coli* cells.

Flight Activities

On the seventh day after launch, the growth condition of the amoebae that developed from the spores were checked and feeding was not detected. We then investigated the growth condition of one control kit in the Biorack at KSC, and no growth of amoebae from the spores was evident. Since we could not complete the experiment, it was terminated and the kit was moved to a refrigerator.

After this we changed the purpose of the experiment to measure the effects of cosmic radiation on germination cell growth and mutation frequency of the spores. All the spores of the space sample and the NC4 controls germinated and the amoebae grew after the treatment. In the gs13 strain only the spores in one of the control samples germinated. We could not detect germination of spores in the space sample even after the germination treatment.

Postflight Analysis

Spores in the cell culture kits taken into space or left on Earth as controls germinated in Pi-buffer with *E. coli* cells. We measured the germination rate of the spores and the growth of the amoebae in NC4. All spores in the space sample and in the controls germinated to amoebae that grew in Pi-buffer with *E. coli* cells. To check the germination ability of the spores that did not germinate, we treated the rest of the spores with 0.4% Brij and heated them at 45 °C for 30 min. to force germination. All the spores of the space sample and the controls germinated, and the amoebae grew after the treatment. In gs13, only the spores in one of the control samples germinated. We could not detect germination of spores in the space sample even after the germination treatment.

Highlights

- Microgravity and cosmic radiation did not affect the NC4 spores.
- Cosmic radiation may have prevented germination of the gs13 spores.

The amoebae from three of the controls of NC4 were pooled into one sample. Both the amoebae that germinated before and after the germination treatment were pooled into one sample. The growth of NC4 amoebae from the spores in the space sample, the control NC4 samples, and the control gs13 samples was examined.

There was no difference in the growth rate of amoebae between the space and control NC4 samples. On the other hand, the amoebae from the control gs13 samples grew more slowly than the amoebae from the control NC4 samples. These conditions were almost the same as the usual experimental conditions at Nara Medical University.

The shapes of fruiting bodies formed by the amoebae were examined using spores sent into space or left on Earth as controls. There was no difference in abnormality of fruiting bodies between the space and the control NC4 samples. In addition no abnormal shape of fruiting bodies was detected in control gs13 samples.

The mutation rate of amoebae from the spores sent into space or left on Earth was examined. In NC4 there was no difference between the mutation rate for the space sample and that of the control. The mutation rate of the control for gs13 was lower than that of the control for NC4. This value was normal for gs13.

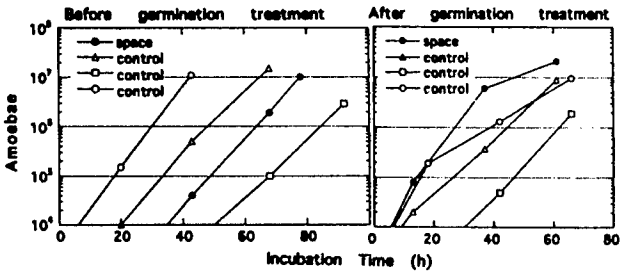

Figure 1: Germination and growth of NC4

We measured the dose of the cosmic radiation [consisting of low LET (X-rays) and high LET radiation such as neutron and heavy particles] by using dosimeter films that were attached to a culture kit for slime mold. We found that absorbed doses are 1.08 mGy and 1.55 mGy.

Conclusion

In NC4 there was no difference between spores that were sent into space and those that were left on Earth with regard to germination ability, growth rate, the formation of fruiting bodies, and mutation rate. These results indicate that there is no effect of microgravity and/or cosmic radiation in space on the spores of NC4. Because the spores of gs13 in the kit sent into space did not germinate, we conclude that either the spores of gs13 are sensitive to cosmic radiation or that the treatment of the spores was unsuitable.

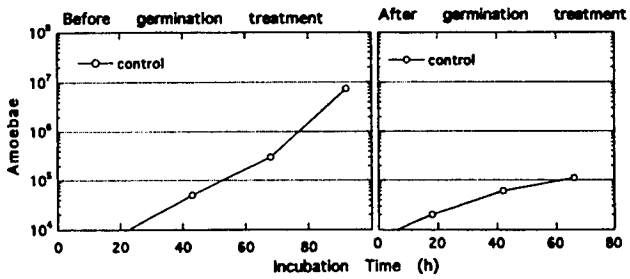

Figure 2: Germination and growth of gs13

References

Okaichi, K., Kajitani, N., Nakajima, K., Nozu, K., and Ohnishi, T., "DNA damage and its repair in *Dictyostelium discoideum* irradiated by a health lamp light (UV-B), *Photochem. Photobiol.*, vol. 50, pp 69-74 , (1989).

Ohnishi, T., "Possible induction of abnormal differentiation in *Dictyostelium discoideum* by cosmic radiation and low gravity," *J. Space Tech. Sci.*, vol. 4, pp. 29-34, (1988).

Ohnishi, T. and Deering, R.A., "Mechanism of strand breakage of DNA in UV-irradiated *Dictyostelium discoideum,"* *Coun. Sci. Res. Integr.*, vol. 7, pp. 15-18, (1988).

Ohnishi, T., Hazama, M., and Nozu, K., "Abnormal differentiation in *Dictyostelium discoideum* by furylfuramide, mitomycin C and methylmethanesulfonate," *Jpn. J. Genet.*, vol. 62, pp 265-269, (1987).

Tano, K., Ohnishi, T., Sato, S., and Nozu, K., "Characteristics of DNA repair of a UV-sensitive mutant (radC) of *Dictyostelium discoideum,"* *Mol. Gen. Genet.*, vol. 195, pp 385-389, (1985).

EXTENDED DURATION ORBITER MEDICAL PROJECT (EDOMP)

INVESTIGATIONS	PRINCIPAL INVESTIGATORS	RESULTS HIGHLIGHTS
Lower Body Negative Pressure (LBNP): Countermeasure Investigation for Reducing Postflight Orthostatic Intolerance	Dr. J. B. Charles Medical Sciences Division NASA Johnson Space Center Houston Texas	Orthostatic tolerance during LBNP was reduced in microgravity. The LBNP countermeasure (soak) lowered the heart rate response during the stress of reentry.

INVESTIGATIONS	PRINCIPAL INVESTIGATORS	RESULTS HIGHLIGHTS
Airborne Microbiological Contamination	Dr. D.L. Pierson Life Sciences Research Laboratories, NASA Johnson Space Center, Houston, Texas, United States	Airborne bacteria and fungi were within safe levels during the entire flight. Bacterial and fungal species recovered from the air were typical of those recovered from humans and outside environment. The air sampler designated for the Crew Health Care System of the International Space Station performed well within specifications.

Lower Body Negative Pressure (LBNP): Countermeasure Investigation for Reducing Postflight Orthostatic Intolerance

Dr. J. B. Charles, Medical Sciences Division, NASA Johnson Space Center, Houston Texas

During the IML-2 mission and on 6 other Space Shuttle flights, decompression of the legs and lower abdomen (lower body negative pressure, LBNP) was used (1) to apply a standardized stress to the cardiovascular system to document the loss of orthostatic function during an extended Shuttle flight in microgravity and (2) to test a countermeasure treatment to protect astronauts from gravitational-induced fainting during and after reentry. The loss of the crew's ability to tolerate LBNP occurred even earlier than indicated by similar testing on Skylab (1973-1974). The LBNP treatment was shown to be effective in reversing some of the effects of extended weightlessness on the cardiovascular system in the 2 crewmember participants on STS-65. The operational overhead of this activity may make it too expensive in crew time to be feasible as a full-time operational countermeasure for Shuttle missions. International Space Station (ISS) crew time may be more readily available near the end of a mission, so LBNP could serve as a useful countermeasure against orthostatic intolerance for long-duration crews prior to their return to Earth.

Highlights

- Orthostatic tolerance during LBNP was reduced in microgravity.
- The LBNP countermeasure (soak) lowered the heart rate response during the stress of reentry.

Flight Activities

Two IML-2 subjects participated in this investigation. Several LBNP tests were conducted on each subject before flight and during the mission. Two "ramps," a test consisting of a 10-min rest period, followed by five 5-min stages at each level of decompression (-10, -20, -30, -40, and -50 mmHg), and then completed with a 5-min recovery period after recompression to ambient pressure, were performed preflight, as well as 4 in flight. One countermeasure session ("soak") was performed on the flight day before the nominal landing day. This soak session consists of a standard "ramp" test followed by 3.5 h of continuous decompression at a level of 30 mmHg below ambient cabin pressure, ending with a 5-min recovery period. During the time spent at -30 mmHg, the crew member ingested the standard landing day fluid load of salt tablets and water. No postflight LBNP sessions were performed, however, orthostatic tolerance was assessed using stand tests on landing day and 3 days postflight.

Blood pressure, heart rate (HR) and Echocardiographic (2-D and Doppler blood flow) measurements were made during each LBNP session. These data were collected approximately every minute throughout the various stages of the tests, except that the Doppler measurements were collected every 30 min during the soak test. Blood pressure (auscultatory technique) was measured using a commercially available automatic blood pressure monitor (ABPM) modified for space flight. A set of ECG leads (three) were also attached to the subject via the ABPM to determine HR and document electrocardiographic activity. These data were telemetered to the ground in real-time to monitor the crew's responses to the LBNP tests. Echocardiography was performed using the American Echocardiographic Research Imaging System (AERIS), a commercial Ultrasound unit modified for flight at the NASA Johnson Space Center (JSC). These data were recorded onboard and returned to JSC for postflight analysis. From this we were able to determine cardiac dimensions, stroke volume (SV), cardiac output (CO), and total peripheral resistance (TPR). Preflight testing was performed with flight-like hardware and techniques for consistency of data with inflight measurements.

Postflight Analysis

Both subjects' response to the ramp tests indicated a loss of tolerance to this orthostatic stress early in flight, flight day (FD) 3, which progressed until the last ramp on FD13. Heart rate increases, measured at the maximal decompressive stress (-50 mmHg), ranged from 20 to 25% greater than preflight responses while drops in systolic blood pressure (SBP) were 25 mmHg in 1 subject and 15 mmHg in the other. Diastolic blood pressure (DBP) remained relatively stable in 1 individual yet showed an increase of more than 15 mmHg in the other. Narrowing of the pulse pressure in flight was more pronounced than that which occurred preflight. These changes suggest that orthostatic tolerance was compromised. A single test on one of the two subjects had to be terminated due to SBP dropping below our test termination criteria. This drop in arterial pressure was temporary and completely reversed itself upon release of negative pressure in the LBNP bag. No other incident of this nature was observed during subsequent LBNP tests.

Cardiac output (CO), as determined from continuous-wave Doppler flow measurements, was reduced at maximal stress compared to baseline, indicating a trend toward reduced orthostatic tolerance in flight. No significant changes in heart dimensions were found during the mission. Total peripheral resistance (TPR) response to the orthostatic stress of LBNP was higher in flight compared to preflight, perhaps suggesting a need for an increase in the compensatory mechanisms that are required during orthostatic stress. These findings agreed with results obtained on two other missions.

The two subjects' responses to standing after landing (during routine stand tests) were different, with one subject exhibiting larger increases in HR and greater decreases in arterial pressure (compared to preflight tests). These data indicate deconditioning of the cardiovascular system had occurred. The different responses in the two subjects could have been due to several factors including previous flight experience, anthropometrics, or other underlying differences such as gender. Heart Rate and BP response to entry and landing was measured as a DSO Shuttle experiment. Data from five subjects who

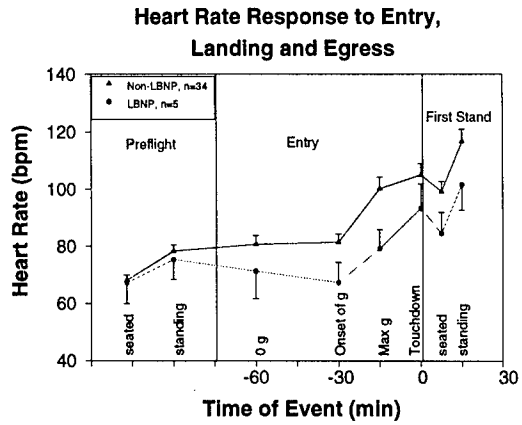

Figure 1: Heart rate measured preflight and during entry aboard the Space Shuttle on LBNP and non-LBNP crew members.

performed an LBNP soak in flight (including earlier missions) indicates a trend toward lower HR response to the stresses of entry, landing, and egress (Figure 1). Data from the postflight stand tests conducted in the landing site medical facility were also used in our analysis. Both subjects completed this test without incident.

Conclusion

Orthostatic tolerance shows some improvement with the application of an LBNP soak within 24 h of landing. LBNP as a countermeasure could be effective against orthostatic intolerance in the proper operational scenario. This scenario is not compatible with short-duration Shuttle missions but might be appropriate for Space Station operations.

References

Sawin, C. F., editor, *Results of Extended Duration Orbiter Medical Project 1989-1995*, in press.

Charles, J.B. and Collier, K., "DSO 623: In-flight LBNP Test of Countermeasures and End-of-Mission Countermeasure Trial," *Extended Duration Orbiter Medical Project, DSO Status Report*, pp. 46-47, July 1995.

Charles, J.B. and Lathers, C.M., "Summary of Lower Body Negative Pressure Experiments During Space Flight," *J. Clin. Pharmacol,* vol. 34, no. 6, pp. 571-583, (1994).

Airborne Microbiological Contamination

Dr. D.L. Pierson, Life Sciences Research Laboratories, NASA Johnson Space Center, Houston, Texas, United States

Airborne microorganisms can impact the air quality of spacecraft affecting the health and performance of the crew. Monitoring the microbial load is essential in assessing the habitability of spacecraft. A small, portable air sampler was used to sample the air from the middeck of the Space Shuttle and the Spacelab on four different days during the mission. This microbial air sampler was selected as candidate hardware for the Crew Health Care System of the International Space Station (ISS). Inflight air samples collected during the 15-day IML-2 mission resulted in the detection, identification, and quantitation of bacterial and fungal contaminants in the Space Shuttle and Spacelab. This investigation studied the effects of longer Space Shuttle missions on the types and levels of airborne microbial contaminants.

Flight Activities

The inflight plan for assessing the microbial contamination of the Space Shuttle/Spacelab required air sample collections from one location on the Orbiter middeck and one location in the Spacelab on flight days 4, 7, 11, and 12. An RCS Plus microbial air sampler (Biotest Diagnostics Corp., Denville, N.J.) was used. This sampler is a small, portable air sampler powered by a rechargeable nickel cadmium battery. Preflight calibration determined the air flow to be 50 liters/min, and the d_{50} value for the sampler was calculated to be 6 mm. Two air samples were collected at both sites (total of 4 samples) during each of the 4 sampling sessions for the mission. The sampler was set to collect 100 liters of air for bacteria and another 100 liters for fungi at each sample site during every sampling session. Agar strips with trypticase soy agar were used for bacterial recovery; rose bengal media was used for cultivation of fungi.

Highlights

- Airborne bacteria and fungi were within safe levels during the entire flight.
- Bacterial and fungal species recovered from the air were typical of those recovered from humans and outside environment.
- The air sampler designated for the Crew Health Care System of the International Space Station performed well within specifications.

The samples were collected at the designated times and stowed at ambient temperature until the completion of the mission.

Postflight Analysis

The samples were returned to the JSC Microbiology Laboratory for analysis. The quantitation of bacteria and fungi on each sampling day is shown in Figure 1. The sum of the bacterial and fungal levels were less than 1000 CFU/m^3 of air (acceptability limit of ISS) in both the Space Shuttle and the Spacelab during all sampling sessions. The results of the Orbiter middeck are given in Panel A. Unfortunately, air samples were taken from the Orbiter only three times during the nearly 15-day mission. Generally, the bacterial levels were less than 200 CFU/m^3 with a sharp increase on FD12, reaching a maximum of 925 CFU/m^3. Fungal levels were below 50 CFU/m^3 throughout the mission.

The results from the Spacelab are given in Panel B. The bacterial levels were characteristically low in Spacelab. Fungal levels were also very low in the Spacelab during the mission. Most probably the low levels (or absence) of airborne fungi in the Orbiter and the Spacelab were due to several factors: air filtration, the absence of an outside source of fungi after launch to add to the burden, and the humidity is usually 50% or less, which is not favorable for fungal growth.

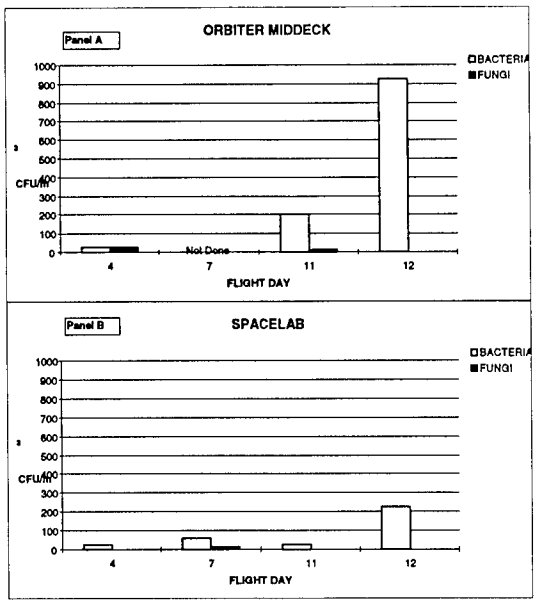

Figure 1: Quantitation of airborne bacteria and fungi

Table 1 lists the bacterial and fungal species recovered from both the Orbiter and the Spacelab. The bacterial species listed are commonly associated with humans. *Rhodotorula rubra*, a yeast, and some filamentous fungi were recovered. These microbial species were similar to those recovered on the Space Shuttle and the Spacelab during previous missions.

BACTERIA	FUNGI
Acinetobacter calcoaceticus biovar anitratus	**Hyphomycete**
Corynebacterium species	**Rhodotorula rubra**
Micrococcus species	**Aspergillus species**
Staphylococcus species	
Enterococcus faecalis	

Table 1: Airborne microorganisms recovered during the IML-2 mission (STS-65).

Conclusion

Microbial levels found in all air samples collected during the 15-day STS-65 mission were within the 1000 CFU/m^3 of air standard defined for the International Space Station. In the Orbiter, bacterial levels increased during the mission, approaching the acceptability limit. Fungal levels were low to absent during the mission. Airborne bacteria and fungi were characteristically low in the Spacelab. The bacteria generally were consistent with previous data and were mostly of human origin; fungal species were common indoor contaminants.

References

Pierson, D.L., "Monitoring airborne microorganisms in space," *American Society of Microbiology,* Washington, D.C. (1995).

Mehta, S.K., Mishra, S.K., and Pierson, D.L., "Evaluation of three portable samples for monitoring airborne fungi," *Applied and Environmental Microbiology,* vol. 62, pp. 1835-1838, (1996).

SPINAL CHANGES IN MICROGRAVITY (SCM)

INVESTIGATIONS	PRINCIPAL INVESTIGATORS	RESULTS HIGHLIGHTS
Spinal Changes in Microgravity	Dr. J. R. Ledsome University of British Columbia Vancouver, Canada	Subjects' heights increased in microgravity. First direct evidence of an increase in intervertebral distance. Evidence of a change in autonomic control.

PERFORMANCE ASSESSMENT WORKSTATION (PAWS)

INVESTIGATIONS	PRINCIPAL INVESTIGATORS	RESULTS HIGHLIGHTS
Microgravity Effects on Standardized Cognitive Performance Measures	Dr. S.G. Schiflett United States Air Force Armstrong Laboratory Brooks Air Force Base, Texas, United States	Reliably measured cognitive and psychomotor performance in microgravity. Performance decrements were related to fatigue. Databases on human performance in space need expansion.

Spinal Changes in Microgravity

Dr. J. R. Ledsome, University of British Columbia, Vancouver, Canada

Height changes in astronauts were first measured in flight on Skylab 4 and the Apollo-Soyuz flights and showed increases from 38 to 66 mm. Beginning in 1985, our group developed the hypothesis that lengthening of the vertebral column during exposure to microgravity would place traction on the muscles, ligaments, and nerves of the spine and could contribute to the back pain experienced by two-thirds of astronauts during and immediately after space flight. A series of measurements made on 3 astronauts on the IML-1 mission assessed changes in back pain, overall height, and spinal contour using stereophotogrammetry (Tsang et al. 1992). The increases in height in 3 subjects ranged from 48 to 74 mm. Two of 3 subjects experienced mild to moderate back pain during the first 2-5 days of the mission.

We postulated that the height increase in microgravity, which is 2-3 times greater than the normal diurnal variation in height might cause neuronal dysfunction contributing to some of the well known microgravity related physiological phenomena such as postflight orthostasis, ataxia, muscle weakness and altered reflexes. The measurements conducted on IML-2 extended our observations of the changes in the length and contour of the spinal cord and applied commonly used clinical tests to examine some of the functions of the sensory and autonomic nervous systems in 2 astronauts.

Flight Activities

Direct height measurements were made on the ground with the subject standing, with the back and heels against a wall on which a vertical scale had been placed. Height measurements were made daily during the flight. The scale was on the deck of the Spacelab and the height was measured by the second subject. Height changes were also measured stereophotographically on the ground and on 3 occasions in flight. Two cameras attached to a metal bar were triggered by the subject using a remote control with the subject standing with their back to the cameras.

Highlights

- Subjects' heights increased in microgravity.
- First direct evidence of an increase in intervertebral distance.
- Evidence of a change in autonomic control.

The two subjects each completed a daily pain questionnaire. The questionnaire was modified from a standard clinical questionnaire and included questions regarding the site and character of any pain as well as a diagram to help identify the site of the pain.

Subjects adopted a series of positions to provide information on the mobility of the spine. These included full flexion, full extension, left and right rotation, and left and right straight leg raising. The subject triggered the cameras when the required position had been adopted. Measurements were made from the stereophotographs using a digital plotting system which allowed reconstruction of the spinal contours.

A technique was developed to measure the distance between adjacent lumbar vertebrae using ultrasound (Ledsome et al., 1996). Briefly, the subjects were trained to obtain ultrasound images (on each other) of the tips of adjacent lumbar vertebrae. On the ground the subjects lay prone on a firm bed for the measurements; in flight the subject lay across the Spacelab in the neutral position and was steadied against the top of a locker in the middle of the Spacelab deck.

The latency between electrical stimulation of a sensory nerve at the ankle and the arrival of the excitatory impulse at the knee and at the vertex was measured using a repackaged commercially available system. The latency of the Somatosensory evoked potentials (SSEP) is proportional to the individuals height and remains stable over many months (Ledsome et al., 1995). The la-

tency of the SSEP was measured 3 times in flight.

Baseline and inflight measurements (4 tests on each subject) were made using an automatic blood pressure recording system. At the beginning of each test period, the subject rested quietly for 2 min. The electrocardiogram was recorded and the subject breathed to full inspiration and kept breathing in for 5 sec and then breathed fully out, and kept breathing out for 5 sec. The breathing pattern was repeated for 3 complete respiratory cycles. The subject then rested for 30 sec and then repeated the 3 respiratory cycles of deep breathing and 30 sec rest 5 more times. The maximum force subjects were able to generate on a hand grip dynamometer was determined. After a 2 min resting period, blood pressure and heart rate measurements were recorded. After a further 2 min interval, a second baseline measurement of blood pressure and heart rate was recorded. The subject was then asked to squeeze the hand grip dynamometer at 30% of the maximum force for 3 min, at which time a third measurement of blood pressure and heart rate was recorded. A final recording of blood pressure and heart rate was made at 3 min after the end of the isometric exercise.

The subjects were trained to obtain images of their bladder using the AERIS ultrasound system. Images were recorded on videotape before and as soon as possible after voiding. The baseline post-void images were obtained within 5 min of voiding. It had been expected that in flight there might have been some delay in obtaining the post-void images because of having to move from the middeck back to the Spacelab. In the event the delay was not significantly greater than for the baseline measurements. The bladder images were later analyzed using a digital measurement system which converted the traced circumference of the image into an area.

Postflight Analysis

Direct height measurements showed an increase in height in both subjects at the time of the first measurement, about 24 h after launch. The height increase did not change significantly during the 13 days when measurements were made. About half of the height increase was lost 2 h after landing and there was a further return to preflight values by 4 h after landing.

Stereophotographic measurements (Figure 1) confirmed this change and showed an increase in height of 42 mm in one subject and 39 mm in the other. This change was between 2 and 4 times the diurnal variation in these subjects; 17.8 and 11.2 mm, respectively. One subject reported mild back pain early in the mission.

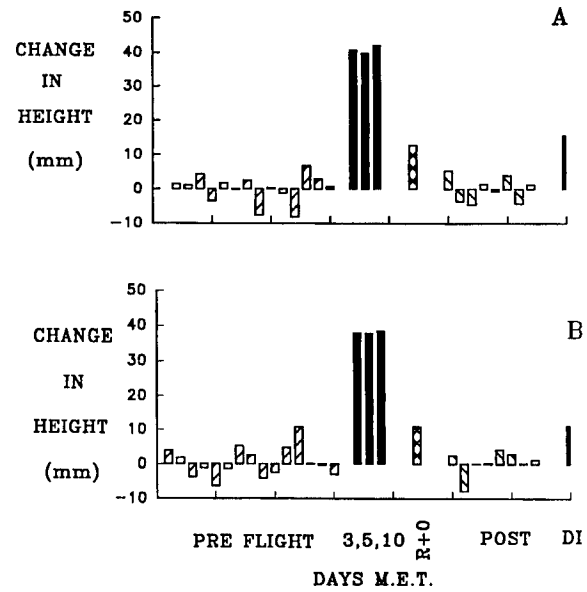

Figure 1: Height changes measured stereophotographically in 2 astronauts (A & B) expressed as a change from the average preflight value. Measurements were made between 120 and 15 days preflight, on flight days 3, 5, and 10, and between postflight days 0 to 90. The first postflight data point (R=0) was measured between 2 and 4 h after landing. DI refers to the change in height measured between morning and evening on 3 consecutive days.

The height increase in microgravity was partly due to a flattening of the lumbar lordosis and partly due to an increase in the length of the spine. There were no changes in microgravity in the angle of rotation of the trunk either to the left or to the right in either subject. Qualitative inspection of the plots during flexion and extension of the spine suggests that there was a decrease in flight, in the angle of flexion and extension in both subjects. The angle of straight leg raising was significantly increased in both subjects. The values, in 1 subject, increased

from 47.3 degrees preflight for each leg to 65.7 degrees for the right leg and 63.8 degrees for the left leg in flight. In the other subject the corresponding values were 59 degrees preflight and 79 degrees in flight for both legs.

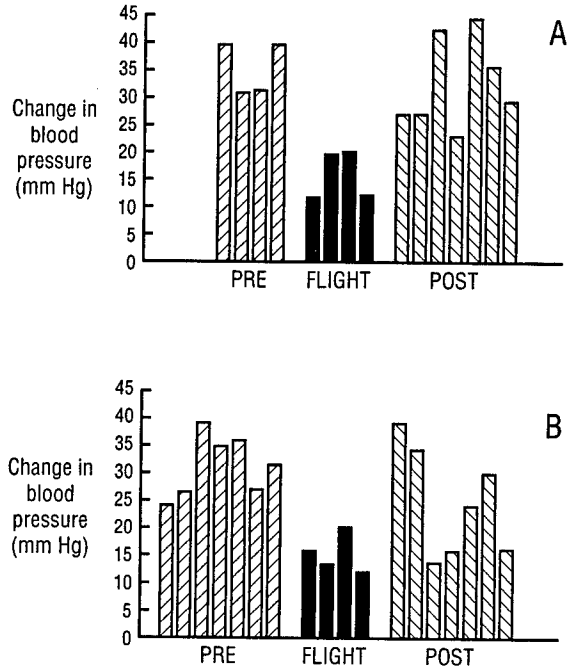

Figure 2: Changes in mean blood pressure induced by 3 min of isometric arm exercise in 2 astronauts. The inflight measurements were made on days 3, 5, 10, and 11. Conventions as in Figure 1. In both subjects the changes in flight were significantly smaller ($p<0.05$) than the preflight changes.

The distance between the lumbar vertebrae was significantly increased in flight in both subjects. The total distance between L1 and L5 (4 disc spaces) was increased by 6.7 ± 0.9 mm in one subject and 8.6 ± 0.9 mm in the other subject. There were no significant changes in the latency of the popliteal or cortical SSEPs in either subject in flight. Excellent recordings were obtained in microgravity indicating that the Spacelab provided a good environment for the recording of small bioelectric potentials.

There were no significant changes in the difference between the heart rate during inspiration and that during expiration (sinus arrhythmia) in either subject. The magnitude of the sinus arrhythmia was 18.2 ± 0.7 and 31.2 ± 2.5 beats/min in the 2 subjects, preflight. The corresponding in flight values were 20.8 ± 0.8 and 28.1 ± 2.8. There were no significant differences in resting heart rate or blood pressure in microgravity compared to pre and postflight measurements. The blood pressure and heart rate responses to isometric exercise were significantly reduced in both subjects in microgravity (Figure 2,3) compared to the preflight baseline. The changes in the response to isometric exercise could not be attributed to changes in hand grip strength in microgravity as hand grip strength was unchanged in flight.

In both subjects the post-void bladder area was significantly larger in flight than preflight. The residual urine volume, in flight was modest and was estimated to have been of the order of between 70-100 ml.

Conclusion

The increases in height observed in the two subjects were at the lower end of the range of changes previously reported. These changes in height were clearly present within the first 24 h of the flight and remained unchanged for the 14 days of the mission. There was a rapid return of the height after landing even though the subjects remained supine as much as possible. The changes in contour of the spine indicated that the increase in height was partly due to a flattening of the curvature of the spine. The ultrasound measurements of the intervertebral distance, as measured between the tips of the transverse processes of the lumbar vertebrae, proved that there was an increase in this distance.

The height changes were not associated with any changes in the angle of rotation of the spine. There was a significant increase in the angle of straight-leg raising similar to that observed on IML-1. The reasons for this change are not apparent, but we observed the same phenomenon during brief exposure to microgravity on the KC-135 and performing straight leg raising under water. One explanation would be that inhibitory reflexes arising from tendon receptors would not be activated in microgravity. The angle of straight-leg raising is often limited in the presence of spinal nerve traction and the observed increase in the angle of straight-leg rais-

ing would not be consistent with the presence of excessive traction on the spinal nerves.

The absence of any significant changes in the latency of the SSEPs indicates that the conduction velocity of the sensory nerve impulses between the ankle and the cerebral cortex was likely to be unchanged. Thus we have no evidence of any dysfunction of the sensory nervous system in microgravity in these subjects. Respiratory sinus arrhythmia, during controlled breathing at relatively slow rates, is largely dependent on changes in efferent parasympathetic (vagal) activity to the heart. Respiratory sinus arrhythmia was unaltered in microgravity suggesting that the parasympathetic efferent pathway to the heart was unaltered.

The blood pressure and heart rate responses to microgravity were significantly attenuated in microgravity. The reasons for this attenuation are unknown. Attenuation of this magnitude has been reported in patients with autonomic neuropathy. Changes in posture or long-term bed rest have not been found to attenuate the responses to isometric exercise. The reduction in the heart rate response to isometric exercise is not consistent with the interpretation from neck suction experiments that the carotid baroreceptor/heart rate reflex is attenuated due to reduced sensitivity of the baroreceptors. Such reduced baroreceptor sensitivity would be expected to be associated with an increase in the blood pressure and heart rate responses to isometric exercise. Further investigation is needed to identify the factors that caused the attenuation of the responses to isometric exercise in microgravity. It was of interest that within 2-4 h of landing the cardiovascular responses to isometric exercise had returned completely to their preflight values. Thus, whatever the mechanism for the changes it is unlikely that the factors that caused the attenuation of the response are present postflight and these factors are unlikely to contribute to postflight orthostatic hypotension.

The increase in the urinary residual volume in microgravity would be consistent with the presence of autonomic dysfunction. However, there may be other reasons for this finding; the precise time between voiding and measurement of the bladder area could not be controlled nor could the rate of urine formation. The

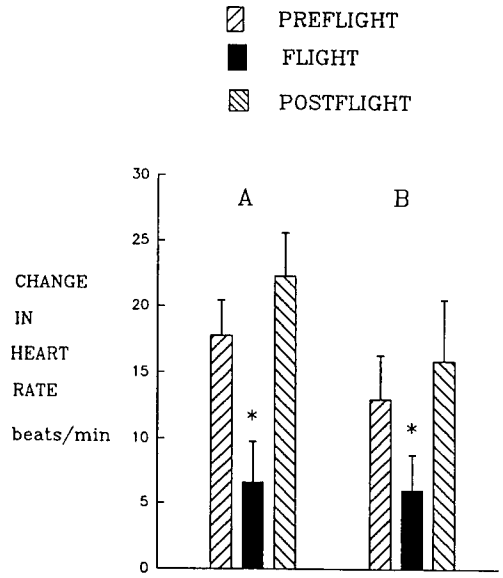

Figure 3: Changes in heart rate induced by 3 min of isometric exercise in 2 astronauts. Measurements were made at the same time as those in Figure 2. Summary data is shown to illustrate the statistical significance of the data. The inflight values were significantly less (p<0.001) than the pre- and postflight values.

contribution of gravity to the final emptying of the bladder at 1-g, or to the sensation of complete emptying is not known. The finding of an increased residual urine volume needs to be confirmed in additional subjects. A significant residual urine volume in microgravity could contribute to stone formation, especially in the presence of an increased calcium concentration in the urine.

References

Ledsome, J.R., Lessoway, V., Susak, L.E., Gagnon, F.A., Gagnon, R., Wing, P.C., "Diurnal changes in lumbar intervertebral distance measured using ultrasound," *Spine*, vol. 21, pp. 1671-1675, (1996).

Ledsome, J.R., Cole, C., Gagnon, F., Susak, L., Wing, P., "Long term stability of somatosensory evoked potentials and the effects of microgravity," *Aviat Space Environ Med.*, vol. 66, pp. 641-644, (1995).

Tsang, I.K.Y., Wing, P.C., Gagnon, F.A., Gagnon, R., "Changes in height and spinal contour at 0-G, Results of an IML-1 experiment," *Spacebound '92, Proc.*, pp. 146-49, (1992).

Microgravity Effects on Standardized Cognitive Performance Measures

Dr. S. G. Schiflett, United States Air Force Armstrong Laboratory, Brooks Air Force Base, Texas, United States

The experiment studied the interactive effects of microgravity and fatigue on the cognitive functioning of 3 astronauts before, during, and after a 13-day, dual-shift mission. A Performance Assessment Workstation (PAWS) was developed for space flight to collect cognitive performance test data. The performance tests were selected from the Department of Defense (DoD) Unified Tri-Service Cognitive Performance Assessment Battery (UTC-PAB). The tests measured short-term memory, spatial processing, attention, visual-motor tracking, and dual-task timesharing.

Flight Activities

Three astronauts completed forty 20-minute sessions of the test battery, which contained 6 cognitive performance tests and 2 subjective scales (mood and fatigue) on a laptop computer. Twenty-four sessions were preflight, 13 sessions were in orbit, and 3 sessions were postflight. A total of 958 data sets were recorded.

Non-linear, mathematical models were used to make predictions for the in-orbit data, providing a baseline for comparison with the actual data. Three families of equations (power, hyperbolic, and exponential) were fit to each subject's preflight data. Both R^2 and curve shape distortions were used to select the best model for each variable. The models allowed the assessment of the in-orbit effects while removing the expected, small effects of performance improvement. Expected values were generated from the best model for in-orbit performance. The model predictions and data were linearized according to the model used. The mean of the actual points was assessed against a 95% confidence interval for the mean of the in-orbit predicted values.

Highlights

- Reliably measured cognitive and psychomotor performance in microgravity.
- Performance decrements were related to fatigue.
- Databases on human performance in space need expansion.

If the mean of the in-orbit data points lay outside the confidence limit, it was judged significant for that subject and dependent measure.

Postflight Analysis

One subject's performance was not affected in orbit and appeared to improve on 4 measures in 2 of the tests. Another subject's performance was degraded in 9 of 11 measures (5 of 6 tests). The last subject's performance was degraded in 8 of 11 measures (5 of 6 tests).

The figure shows a dependent measure demonstrating an in-orbit effect: the number of manual tracking control losses in the dual task. This test requires the subject to keep a horizontally moving cursor centered using a trackball while performing a memory search task on previously memorized letters. Starting on session 10, tracking difficulty was increased for each subject based on previous tracking performance. Difficulty was higher for more skilled subjects and remained at that level throughout the remainder of the testing sessions. Although tracking performance was severely disrupted initially in orbit, the control losses appeared to be coming under control in sessions 33 and 34 until fatigue levels of 6 were reported in sessions 35 and 36. Higher subjective fatigue ratings indicate more fatigue. Performance appears to return to model-projected levels during the last day of in-orbit testing and after landing.

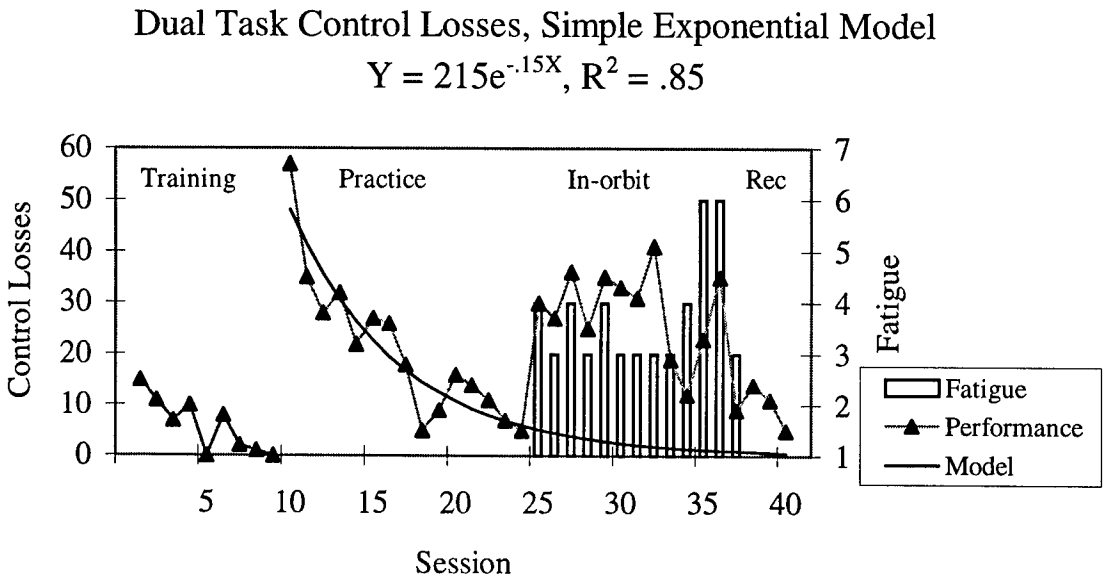

Figure 1: Dual Task tracking control losses are modeled with a simple exponential function for one subject. Both the slope and exponent for the constant e were significant, p<.05. The subjective fatigue ratings are represented with histogram bars.

Conclusion

The experiment demonstrated that cognitive and psychomotor performance can be reliably measured in microgravity. The performance measures were sensitive to the combined stressor effects of the microgravity environment. The performance patterns of the astronauts in orbit and during ground-based periods were comparable when the learning of the task had stabilized, with the exception of Memory Search for one subject and Unstable Tracking performance in another subject. Both of these performance decrements were related to fatigue.

Single-subject mathematical models of astronaut preflight performance revealed that predicted learning levels for two subjects were not achieved in tracking, short-term memory, and directed attention. Even if one considers the converging evidence from an extremely limited number of other in-flight experiments, the currently available database about human performance in space is too small to warrant final conclusions about cognition and visuomotor performance while living and working in microgravity. The isolation of microgravity as the single stressor causing the in-orbit performance deterioration can not be fully determined from these results. Therefore, additional ground-based control research studies and more in-orbit subjects are required before these results can be generalized to future space travelers.

References

Eddy, D.R., "In-orbit cognitive performance compared to model predictions based on preflight baseline learning," *Aerospace Medical Association Abstracts*, No. 504, 66th Annual Meeting, California, United States, (1995).

French, J., Schiflett, S.G., Eddy, D.R., Schlegel, R.E., and Shehab, R.L., "Shuttle crew subjective fatigue assessment during the IML-2 mission," *Aerospace Medical Association Abstracts,* No. 505, 66th Annual Meeting, California, United States, (1995 a).

Schlegel, R.E., Shehab, R.L., Gilliland, K., Eddy, D.R., and Schiflett, S.G., "Microgravity effects on cognitive performance measures: Practice schedules to acquire and maintain performance stability," AL/CF-TR-94-0040, Brooks Air Force Base, Texas, (1995).

Schiflett, S.G., "Cognitive performance assessment during sustained operations in unique environments," *103rd Convention American Psychological Association*, New York, United States, (1995 b).

Schiflett, S.G., Eddy, D.R., Schlegel, R.E., French, J., and Shehab, R.L., "Astronaut performance during preflight, in-orbit, and recovery," *Aerospace Medical Association Abstracts,* No. 503, 66th Annual Meeting, California, United States, (1995).

REAL-TIME RADIATION MONITORING DEVICE (RRMD)

INVESTIGATIONS	PRINCIPAL INVESTIGATORS	RESULTS HIGHLIGHTS
Measurement of LET Distribution and Dose Equivalent on Board the Space Shuttle STS-65 (IML-2) (RRMD, Part 1)	Dr. T. Doke Waseda University Tokyo, Japan	First real-time measurements of radiation dose and LET distribution. Attributed most radiation in the IML-2 orbit to galactic cosmic-ray particles. Good agreement between active and passive detector data.
Effect of Microgravity on DNA Repair of *Deinococcus Radiodurans* (RRMD, Part 2)		Results suggests that micro-gravity enhanced the DNA repair system. First use of radiation-resistant bacteria to examine relationship between microgravity and radiation.

Measurement of LET Distribution and Dose Equivalent on Board the Space Shuttle STS-65 (IML-2) (RRMD, Part 1)

Dr. T. Doke, Waseda University, Tokyo, Japan

Space radiation consists of protons and heavier nuclei of mainly helium through iron ions whose particles penetrate the human body and deposit energy in tissues. The radiation effects of particles depend on the deposited energy along the particle trajectory [the Linear Energy Transfer (LET)]. The LET distribution is given as a function of nuclear charge, energy, and the flux of the particles. These observable values allow us to evaluate space radiation effects coupled with various biological dose parameters.

Until this mission, detailed measurements of high LET particles have been made mainly by passive track detectors. Using this method, however, analysis of radiation effects have been done only after the mission. Therefore, for urgent radiation hazards such as big solar flare events, this method is not applicable. For long-duration manned space missions, radiation environments are governed mainly by galactic cosmic ray particles (GCRs), solar-flare particles, and protons trapped in Earth's radiation belts. To evaluate the radiation effects correctly in such a mixed field, accurate measurements of radiation must be made in a wide range of particle species from protons to ions and energies of ~MeV to relativistic (> GeV). Information on the time and orbital location of a spacecraft, that is, real-time radiation monitoring, is required.

Flight Activities

Three kinds of detectors were used: a newly developed active detector telescope, the Real-time Radiation Monitoring Device (RRMD), conventional detectors of thermoluminescence dosimeters (TLDs), and CR-39 plastic-track detectors. The RRMD has 8 layers of silicon detectors with 2 position detectors [PSD-1 and PSD-2 (62 mm x 62 mm) of a geometric factor 46.4 cm2sr)]. The RRMD instrument was installed at a corner of the Detector Unit, whose position and direction inside Spacelab were changed to investigate possible spatial and directional variations of space radiation about every 2 days.

Highlights

- First real-time measurements of radiation dose and LET distribution.
- Attributed most radiation in the IML-2 orbit to galactic cosmic-ray particles.
- Good agreement between active and passive detector data.

The RRMD measured the LET distribution and radiation dosimetry for LET > 75 keV/μm for a continuous period of 251.3 h giving the temporal variations of LET distribution, particle count rates, and rates of absorbed dose and dose equivalent. The RRMD results indicate that a clear enhancement of the number of trapped particles is seen at the South Atlantic Anomaly (SAA) without clear enhancement of dose equivalent, while some daily periodic enhancements of dose equivalent caused by high LET particles are seen at the lower geomagnetic cut-off regions for galactic cosmic ray particles (GCRs). Therefore, the main contribution to dose equivalent is seen to be caused by GCRs in this low-altitude mission (300 km).

The other conventional passive detectors, TLDs and CR-39 track detectors, included biological samples and were placed in various locations inside Spacelab. TLDs measured the total absorbed dose during flight for all values of LET > 0.2 keV/μm, although they could not give the LET distribution. CR-39 detectors measured the LET distribution for LET > 3.9 keV/μm, which is the detection threshold of the present CR-39. The dose equivalent rates obtained by TLDs and CR-39s ranged from 146.9 to 165.2 μSv/day and the average quality factors ranged from 1.45 to 1.57, depending on the locations and directions of detectors inside the Spacelab at this highly

protected orbit for space radiation with a small inclination (28.5°) and a low altitude (300 km).

Postflight Analysis

The RRMD instrument measured LET values of incident particles event by event in 8 individual silicon detectors, allowed construction of LET distribution, and allowed estimates of absorbed dose and dose equivalent rates in real time during the flight. There were temporal variations in the counting rate of particles with LET > 5 keV/μm obtained from the 8 individual silicon detectors (PSD-1 to D-6). Clear peaks in PSD-1 and PSD-2 are seen with a time interval of about 90 minutes corresponding to the passage of the Shuttle through the SAA. These particles were assigned to be mainly trapped protons of ~10 MeV at the detector position by the spectroscopy of energy loss and total energy in multi-layer silicon detectors. The contribution to dose equivalent from trapped protons at the SAA is not very large, while 1-day, periodic, small enhancements of dose equivalent rate are seen at the orbital position of the Shuttle corresponding to the lower cut-off rigidity region of geomagnetic field above Mexico and Australia, where the particle density of high-LET GCRs is considered to be enhanced.

Results revealed examples of differential LET distributions for trapped particles and GCRs, respectively, observed in eight silicon detectors. For trapped particles, the steeper LET distribution is seen with very few high-LET particles above 100 keV/μm, as expected. The main component of these particles were assigned to be low energy (~10 MeV) protons by the spectroscopy RRMD data. The differential LET distribution of GCRs indicates a clear peak at LET about 135 keV/μm for GCR Fe particles and several shoulders corresponding to the LET values of main components of relativistic GCRs.

Conclusion

The first real-time measurements of LET distribution and radiation dosimetry using the RRMD have been achieved successfully. The LET distributions by the RRMD and CR-39 in the LET region of 15 to 200 keV/μm are in good agreement. In this orbit (28.5° x 300 km), most of contribution to dose equivalent is caused by relativistic GCRs, and the values of dose equivalents (146.9 to 165.2 μSv/day) and mean quality factors (1.45 to 1.57) were obtained and are consistent with results obtained by others.

	1	2	3	4
TLDs (MS0):				
Average dose rate (μGy/day) in flight	91.4 ± 2.7	104.0 ± 2.5	110.6 ± 5.1	102.8 ± 5.9
CR-39:				
Average dose rate (μGy/day)	5.9	6.1	8.2	7.7
Average dose equivalent rate (μSv/day)	59.1	57.6	59.6	60.4
Total:				
Average dose rate (μGy/day)	93.7	106.4	113.8	105.8
Average dose equivalent rate (μSv/day)	146.9	157.8	165.2	158.5
Average quality factor	1.57	1.48	1.45	1.50

Table 1: A summary of results by TLDs and CR-39

The present RRMD could not detect particles of LET < 5 keV/μm. In the near future, detectors that can sense minimum ionizing particles will be modified, and then various applications of this detector type to real-time space dosimetry will be considered.

Effect of Microgravity on DNA Repair of *Deinococcus Radiodurans* (RRMD, Part 2)

Dr. T. Doke, Waseda University, Tokyo, Japan

Ionizing radiation and microgravity appear to be the main risk factors that astronauts are subjected to during their space flights, and these influences cannot be considered separately. We need to investigate the modifying influence of microgravity on the biological effects of cosmic radiation. This is the first examination of the influence of microgravity on the repair of radiation-induced damage using an extremely radioresistant bacterium, *Deinococcus radiodurans.*

The extraordinary radiation resistance of this bacterium has been ascribed to the ability to repair all DNA lesions, including double strand breaks induced with doses up to 5 kGy. This bacterium is also resistant to heavy-ion irradiation. Lyophilized cells of this strain can be kept stable at least several months after irradiation, until the repair processes are activated. This allows the evaluation of their ability to repair in microgravity, where the influence of cosmic radiation is negligible.

Flight Activities

Cells were lyophilized and exposed to 60Co g-rays with doses up to 12 kGy before the space flight. Ten sets of identical samples were prepared at the same time; one was used for space flight and the others were for ground controls. During the space flight the container of samples was attached to the RRMD, and ambient temperature was monitored. Almost at the end of the mission, the lyophilized cells were mixed on board with a liquid nutrient medium to activate the repair process by pushing the silicone rubber tubes with a bar to break the medium-filled glass capillary tubes inside. Then the cells were incubated at the room temperature of the Spacelab for 11 h to allow the repair of radiation-induced DNA damages. Afterwards the cells were stored at 4 °C to reduce metabolic activity until landing.

Highlights

- Results suggests that microgravity enhanced the DNA repair system.
- First use of radiation-resistant bacteria to examine relationship between microgravity and radiation.

Postflight Analysis

Two days and 5 h after the container was stored at 4 °C, the Shuttle landed. The samples were retrieved 3 h after landing and frozen immediately for transport to our laboratory. A parallel ground control experiment was carried out at KSC throughout the space flight according to the temperature data downlinked from the Shuttle. The other ground control experiments were carried out in our laboratory at a constant temperature of 24 °C.

We evaluated the cells' ability to repair by the survival (colony forming ability) of the ground controls compared with the flight samples in which the repair system was activated under microgravity condition in space. The cells recovered from the silicone rubber tubes were resuspended in 0.01 M phosphate buffer (pH 7.0). Diluted cell suspensions were plated on TGY agar and incubated at 30 °C for 3 days before we counted colonies.

The IML-2 flight samples show the statistically significant highest survival of all at doses above 6 kGy. The shoulder of the dose-effect curve of the flight samples was greater than those of ground controls; however, the slopes of the exponential part of the curves were almost the same. The flight sample and ground controls display decreased colony forming units compared with the non-incubation control. The decreased number of colony forming units is caused by the storage at 4 °C and freezing after incubation, but no significant differences were observed among the flight sample and ground controls, indicating that the number of living

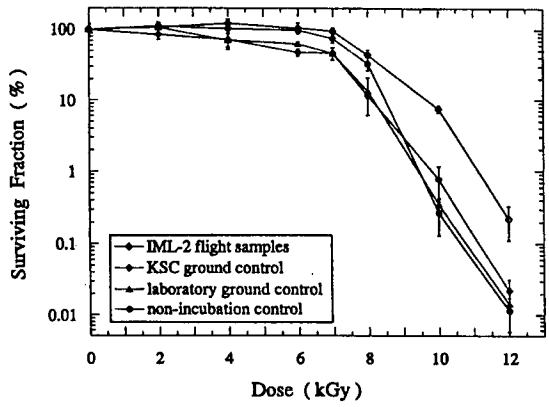

Figure 1: Surviving fractions of D. radiodurans cells as a function of dose of γ-ray irradiation prior to the space flight; incubated under microgravity conditions during space flight (flight samples: open diamonds), incubated on the ground simulating the temperature condition of the flight samples according to the data downlinked from the Space Shuttle (KSC ground control: closed diamonds), incubated on the ground at 24 °C (laboratory ground control: closed triangles), and laboratory control not incubated, not refrigerated at 4 °C and not frozen before counting colonies (non-incubation control: closed circles). The data show the mean value obtained from 2 sets of samples.

cells of the non-irradiated flight samples were not influenced throughout incubation in microgravity. The number of living cells in the lyophilized flight samples that were recovered from space without any incubation was also the same as that ground controls, suggesting that the lyophilized cells were stable in the space environment and not influenced by cosmic radiation and microgravity.

Conclusion

The survival of the cells activated in space increased significantly compared with the ground controls, suggesting that DNA repair system of this bacterium was enhanced under microgravity. Concerning the interactions of radiation and microgravity, many kinds of materials have been used in previous studies; however, almost no reports showed the tendency to antagonistic interaction or enhancement of radiation resistance under microgravity. Most of the biological objects used in previous studies might have been too sensitive to cosmic radiation to study the effect of microgravity.

We hypothesize the following:

(1) Larger amounts of repair enzymes were induced under microgravity than on the ground.

(2) The repair enzymes were induced in the same way as on the ground, but they worked more effectively under microgravity.

It is important to consider the possibility that cosmic background radiation is also causally involved in the enhancement observed in the flight samples. However, the estimated radiation intensities during the mission (ca. 100 μGy/day) were much lower than the dose of preflight irradiation to the samples. Furthermore, the repair system of *D. radiodurans* is not likely to be induced at such a low dose rate because the amount of repair enzymes is roughly proportional to the dose of pre-irradiation.

To understand the mechanism responsible for these possibilities, further studies in space are required. Especially, whether induction of repair enzymes are enhanced under microgravity needs to be investigated.

References

Kobayashi, Y., Shimizu, T., Tanaka, A., Kikuchi, M., Taucher-Scholz, G., and Watanabe, H., "Survival of dry cells of *Deinococcus radiodurans* after heavy ion irradiation," *JAERI TIARA Annual Report*, vol. 3, pp. 35-37 (1993).

Homeck, G., "Radiobiological experiments in space: a review," *Nucl. Tracks Radiat. Meas.*, vol. 20, pp. 185-205, (1992).

Kikuchi, M., Kobayashi, Y., Tanaka, A., Shimizu, T., and Watanabe, H., "DNA double-strand breaks and the repair in radioresistant bacterium, *Deinococcus radiodurans*, irradiated by heavy ion beams," *JAERI TIARA Annual Report*, vol. 2, pp. 34-37, (1992).

Kobayashi, Y., Kikuchi, M., Watanabe, H., and Taucher-Scholz, G., "Survival of dry cells of *D. radiodurans* after heavy ion irradiation," *GSI Scientific Report*, vol. 92-1, p. 286, (1991).

IML-2 RESULTS SUMMARY

LARGE ISOTHERMAL FURNACE

INVESTIGATIONS	PRINCIPAL INVESTIGATORS	RESULTS HIGHLIGHTS
Liquid Phase Sintering in a Microgravity Environment	Dr. R.M. German The Pennsylvania State University, University Park Pennsylvania, United States	Microstructural features were created that have never before been seen in tungsten-heavy alloys. Microgravity had a drastic impact on the samples' micro-structural development.
Mixing of a Melt of a Multicomponent Compound Semiconductor	Dr. A. Hirata Waseda University Tokyo, Japan	Samples were successfully processed in microgravity. Space-grown samples of In-Sb were almost spherical. Samples of In-GaSb-Sb were round, not quite spherical.
Effect of Weightlessness on Microstructure and Strength of Ordered TiAl Intermetallic Alloys	Dr. A. Sato National Research Institute for Metals Tokyo, Japan	TiB_2 particles were uniformly distributed in the alloy solidified in microgravity. Microgravity enhanced the uniformity of the microstructure.

ELECTROMAGNETIC CONTAINERLESS PROCESSING FACILITY (TEMPUS)

INVESTIGATIONS	PRINCIPAL INVESTIGATORS	RESULTS HIGHLIGHTS
Containerless Processing in Space: The TEMPUS Team Results	Dr. I. Egry DLR, Institute for Space Simulation, Cologne, Germany	First successful attempt to electromagnetically levitate samples in microgravity.
Effect of Nucleation by Containerless Processing	Dr. R. Bayuzick Vanderbilt University, Nashville, Tennessee, United States	Achieved 48 h of levitation time.
Thermodynamic and Glass Formation of Undercooled Metallic Melts	Dr. H. Fecht University of Augsburg Augsburg, Germany	Melted and heated Zr up to 2000 °C and subsequent undercooling by $\Delta T = 160$ °C.
Alloy Undercooling Experiments	Dr. M. Flemings Massachusetts Institute of Technology, Cambridge, Massachusetts, United States	Measured specific heat of NiNb and ZrNi in the undercooled state. Measured surface tension of Au, AuCu, and ZrNi.
Non-Equilibrium Solidification of Deeply Undercooled Melts	Dr. D.M. Herlach DLR, Institute for Space Simulation, Cologne, Germany	
Thermophysical Properties of Metallic Glasses and Undercooled Alloys	Dr. W. Johnson California Institute of Technology, Pasadena, California, United States	
Measurement of the Viscosity and Surface Tension of Undercooled Metallic Melts and Supporting MHD Calculations	Dr. J. Szekely Massachusetts Institute of Technology, Cambridge, Massachusetts, United States	
Structure and Solidification of Deeply Undercooled Melts of Quasicrystal-Forming Alloys	Dr. K. Urban Institute for Solid State Physics Research Center, Julich, Germany	

BUBBLE, DROP, AND PARTICLE UNIT (BDPU)

INVESTIGATIONS	PRINCIPAL INVESTIGATORS	RESULTS HIGHLIGHTS
Bubble Migration, Coalescence, and Interaction with the Solidification Front	Prof. R. Monti University of Napoli Napoli, Italy Dr. R. Fortezza MARS Center Napoli, Italy	Surfactant strongly affected the migration of bubbles in a liquid matrix formed by melted paraffin, preventing the development of the surface tension gradient. Further investigations need to study the interaction between planar and non-planar fronts with gas bubbles in low-gravity.
Thermocapillary Migration and Interactions of Bubbles and Drops	Dr. R.S. Subramanian Clarkson University Potsdam, New York United States	Confirmed the predictions of models for the migration velocities of bubbles and drops. Made unique observations of interactions between a small and large drop.
Bubble Behavior under Low Gravity	Dr. A. Viviani Seconda Università di Napoli Aversa, Italy	Achieved a milestone in thermocapillary research. First demonstration of thermocapillary migration of bubbles from hot to cold liquids.

BUBBLE, DROP, AND PARTICLE UNIT (BDPU) (cont.)

INVESTIGATIONS	PRINCIPAL INVESTIGATORS	RESULTS HIGHLIGHTS
Interfacial Phenomena in Multilayered Fluid Systems	Dr. J.N. Koster and Dr. S. Biringen, University of Colorado at Boulder Colorado, United States	Completed ground-based and theoretical research. Obtained a better understanding of the physics of coupling between convecting immiscible liquid layers. Need to verify pure thermo-capillary case with flight experiment.
Thermocapillary Convection in a Multilayer System	Dr. J.C. Legros and Dr. Ph. Georis, Universite Libre de Bruxelles, Brussels, Belgium	Built a mechanically stable, three-layer system that could be applicable for encapsulated floating zone crystal growth. Confirmed theoretical and numerical predictions, including that the heat diffusivity ratio of the liquids is the relevant parameter for the description of thermocapillary instability in multilayer systems.
Nucleation, Bubble Growth, Interfacial Phenomena, Evaporation, and Condensation Kinetics	Dr. J. Straub Technical University of Munich Munich, Germany	First measurements of the growth and collapse of bubbles in a homogenous supersaturated and subcooled liquid in microgravity over long periods, up to 300 sec. Determined the evaporation and condensation coefficients: $1{:}10^{-4}$ and $1{:}10^{-3}$ for R11.

BUBBLE, DROP, AND PARTICLE UNIT (BDPU) (cont.)

INVESTIGATIONS	PRINCIPAL INVESTIGATORS	RESULTS HIGHLIGHTS
Dynamics of Liquids in Edges and Corners	Dr. D. Langbein ZARM, University of Bremen, Bremen, Germany	Data revealed the dependence of the fluid-solid contact angle on temperature. Results posed questions regarding the role of hysteresis in critical-wetting phenomena.

CRITICAL POINT FACILITY (CPF)

INVESTIGATIONS	PRINCIPAL INVESTIGATORS	RESULTS HIGHLIGHTS
Critical Phenomena in SF_6 Observed under Reduced Gravity	Dr. D. Beysens Commissariat à l'Energie Atomique, Grenoble, France	First observation that thermalization by Piston Effect is dramatically disturbed by buoyancy-driven convection. First observation of two different regimes of phase separation in the same sample. Measurement of the state variables (P,ρ,T) and the key parameters $(\partial\rho/\partial T)_s$ and $(\partial T/\partial P)_s$.
Summary of Results from the Adiabatic Fast Equilibration (AFEQ) and Thermal Equilibration Bis (TEQB) Experiments	Dr. R.A. Ferrell University of Maryland College Park, Maryland United States	Measured the adiabatic response of fluid to a heat pulse and the late stages of density equilibrium. First measurements of the isothermal increase of the density of a near-critical sample as a function of the applied electric field.

CRITICAL POINT FACILITY (CPF) (cont.)

INVESTIGATIONS	PRINCIPAL INVESTIGATORS	RESULTS HIGHLIGHTS
Density Equilibration Time Scale	Dr. H. Klein DLR , Institute for Space Simulation, Cologne, Germany	The piston effect alone does not lead to short equilibration times. The times necessary for the sample to become homogeneous scale with the correlation length. Balloelectricity and surface tension convection have major influence on bubble and droplet distributions in phase separating fluids.
Heat Transport and Density Fluctuations in a Critical Fluid	Dr. A.C. Michels University of Amsterdam Amsterdam, The Netherlands	Isentropic heating offers a powerful tool for assessing equations of state in the vicinity of the critical point. Evaluation of the density fluctuations obtained by light-scattering measurements is promising.

MICROGRAVITY ENVIRONMENT AND COUNTERMEASURES

INVESTIGATIONS	PRINCIPAL INVESTIGATORS	RESULTS HIGHLIGHTS
Space Acceleration Measurement System (SAMS) and Orbital Acceleration Research Experiment (OARE)	Mr. R. DeLombard NASA Lewis Research Center Cleveland, Ohio, United States	Established a network to disseminate microgravity data to investigators. Recorded accelerations that helped investigators analyze their data.

MICROGRAVITY ENVIRONMENT AND COUNTERMEASURES (cont.)

INVESTIGATIONS	PRINCIPAL INVESTIGATORS	RESULTS HIGHLIGHTS
Quasi-Steady Acceleration Measurement (QSAM)	Dr. H. Hamacher DLR, Institute for Space Simulation, Cologne, Germany	Obtained data on accelerations in the g-jitter range. Demonstrated the role of microgravity measurement for controlling payload and facility operations.

VIBRATION ISOLATION BOX EXPERIMENT SYSTEM (VIBES)

INVESTIGATIONS	PRINCIPAL INVESTIGATORS	RESULTS HIGHLIGHTS
Influence of G-Jitter on Convection and Diffusion	Dr. H. Azuma National Aerospace Laboratory Chohu-shi, Japan	Observed enhanced diffusion caused by g-jitter. Recorded data indicating that convection caused g-jitter.
Thermally Driven Flow Experiments (TDFU)	Dr. M. Furukawa NASDA Tsukuba Space Center Ibaraki, Japan	Demonstrated a new type of thermal accumulator for two-phase fluid loop systems. Conducted experiments in liquid/vapor phase separation, liquid positioning, and liquid transfer.

ADVANCED PROTEIN CRYSTALLIZATION FACILITY (APCF)

INVESTIGATIONS	PRINCIPAL INVESTIGATORS	RESULTS HIGHLIGHTS
The Crystallization of Apocrustacyanin C_1	Dr. N.E. Chayen Blackett Laboratory, Imperial College of Science, Technology and Medicine London, United Kingdom	Space crystals were larger and of better quality than most of those grown on the ground. CCD images of the crystal growth during the flight display a motion of the crystals within the hanging drop (attributed to Marangoni convection effects) and provide the first evidence for depletion zones around the growing crystals, as would be expected in a microgravity environment.
Crystallization of Collagenase and Photoreaction Center under Microgravity	Dr. I. Broutin, Dr. M. Ries, and Dr. A. Ducruix, LEBS, CNRS, Gif sur Yvette, France	Collagenase space-grown crystals recorded on the wiggler beam line of LURE had stronger intensities and signal to noise ratio than ground controls. PRC space-grown crystals diffracted far less than ground crystals, probably because of aging of the protein. APCF was a versatile facility allowing good experimental control.
Crystallization of Rhodopsin in Microgravity	Dr. W. J. de Grip University of Nijmegen Nijmegen, The Netherlands	Microgravity seemed to enhance rhodospin crystallization. Longer growing periods (>1 month) are needed to obtain crystals suitable for X-ray diffraction.

ADVANCED PROTEIN CRYSTALLIZATION FACILITY (APCF) (cont.)

INVESTIGATIONS	PRINCIPAL INVESTIGATORS	RESULTS HIGHLIGHTS
Crystallization of RNA Molecules	Dr. V.A. Erdmann and S. Lorenz Institut für Biochemie, Freie Universität Berlin, Berlin, Germany	Space crystals were about 3 times larger in volume than ground grown crystals. The amount of crystals grown in space were lower than in the ground control experiments.
Studies of Lysozyme Protein Crystal Perfection from Microgravity Crystallization	Dr. J. R. Helliwell University of Manchester Manchester, United Kingdom	Rocking width data showed microgravity-grown crystals displayed intensity levels three to four times that of their Earth-grown counterparts. Large perfect regions were visible within the microgravity grown crystals while Earth controls had a crumbly network.
Crystallization of Octarellins and Copper Oxalate	Dr. J. Martial Université de Liège Belgique (U.Lg.), Brussels, Belgium Dr. L. Wyns Université de Bruxelles Brussels, Belgium	Obtained first crystals for a *de novo* protein of the size of Octarellin. Small crystals were obtained, which allowed us to finally approach the conditions required for crystallizing these artificial proteins.
Microgravity Effects on Macromolecule and Virus Crystallization	Dr. A. McPherson University of California Riverside, California, United States	Observed alterations in the average or maximum size of crystals. Crystals grown in space had morphological modifications. Changes in the diffraction properties were observed.

ADVANCED PROTEIN CRYSTALLIZATION FACILITY (APCF) (cont.)

INVESTIGATIONS	PRINCIPAL INVESTIGATORS	RESULTS HIGHLIGHTS
Crystal Growth of Ribonuclease S	Dr. L. Sjolin Chalmers University of Technology and Göteborg University, Göteborg, Sweden	Crystals grown in microgravity had increased perfection, as measured by reduced mosaicity, and concordance, as measured by the agreement between diffraction data sets. Space-grown crystals had more uniform morphologies than Earth-grown crystals.
Crystallization of Ribosomal Particles in Space	Dr. A. Yonath Max-Planck-Laboratory for Ribosomal Structure Hamburg, Germany	Grew crystals that had more isotropic shapes, which had never been observed on Earth. Growth of crystals without seeding indicated potential of microgravity.
Crystallization of Bacteriorhodopsin	Dr. G. Wagner Justus-Liebig University of Giessen, Giessen, Germany	Crystals were grown using two different techniques and varying ingredients. Crystals grown with liquid-liquid diffusion had sharp edges, smooth faces, and increased sizes, up to 200 μm in length. Adding benzamidine hydrochloride to crystals grown with liquid-liquid diffusion resulted in crystals with improved compact alignment of the crystalline filaments, increased crystal size, and higher resolution X-ray diffraction data.

FREE FLOW ELECTROPHORESIS UNIT (FFEU)

INVESTIGATIONS	PRINCIPAL INVESTIGATORS	RESULTS HIGHLIGHTS
Applications of Continuous Flow Electrophoresis to Rat Anterior Pituitary Particles (Part 1) Feeding Frequency Affects Cultured Rat Pituitary Cells in Low-Gravity (Part 2)	Dr. W.C. Hymer Pennsylvania State University University Park, Pennsylvania United States	A microgravity-feeding interactive effect occurred and affected hormone output and cell surface charge. Microgravity-processed samples had increases throughputs, greater bandspreads, and better discrimination of some growth hormone variants. Found differences in the quantity and quality (bioactivity) of growth hormone and prolactin released from primary rat pituitary cells *in vitro.* Changes were similar to those found in pituitary cells of space-flown rats after 7-14 days in microgravity.
Separation of a Nematode *C. elegans* Chromosome DNA by FFEU	Dr. H. Kobayashi Josai University Saitama, Japan	Used electrophoresis to collect DNA samples in space. Used a new computer program to monitor experiment in space from the ground.
Experiments of Separating Animal Cell Culturing Solution in High Concentration in Microgravity	Dr. T. Okusawa Hitachi, Ltd Ibaraki, Japan	Cells cultured in space produced twice as much protein as those cultured on Earth. Electrophoresis was much more stable in space than on Earth.

APPLIED RESEARCH ON SEPARATION METHODS USING SPACE ELECTROPHORESIS (RAMSES)

INVESTIGATIONS	PRINCIPAL INVESTIGATORS	RESULTS HIGHLIGHTS
Purification of Biological Molecules by Continuous-Flow Electrophoresis in a Microgravity Environment	Dr. V. Sanchez, Université Paul Sabatier, Toulouse France and Dr. B. Schoot, Roussel Uclaf, Romainville, France	Stable flows were obtained in microgravity under all conditions studied, showing that certain problems encountered on Earth are related to instabilities of gravitational origin that arise from either within the carrier buffer or around the sample filament. For the purification of biologically active substances, the use of microgravity and concentrated samples allowed the throughput to be increased by a factor of about 5, while rendering a product equally pure and biologically active.
Electrohydrodynamic Sample Distortion During Electrophoresis	Dr. R.S. Snyder NASA Marshall Space Flight Center, Alabama, United States	Disturbances by phenomena such as electrohydrodynamics, must be characterized to examine their effects on space electrophoresis. The experiment was not completed because of a power failure, but some parts may be done on a MAXUS sounding rocket.

SLOW ROTATING CENTRIFUGE MICROSCOPE (NIZEMI) MATERIALS SCIENCE EXPERIMENT

INVESTIGATIONS	PRINCIPAL INVESTIGATORS	RESULTS HIGHLIGHTS
Convective Stability of Solidification Fronts (Moni)	Dr. K. Leonartz Engineering, Aachen, Germany (formerly with ACCESS e.V.)	First observation of the growth transition from near diffusive to convective mass transport in a melt as a function of increasing g-level. First use of NIZEMI for directional solidification.

AQUATIC ANIMAL EXPERIMENT UNIT (AAEU)

INVESTIGATIONS	PRINCIPAL INVESTIGATORS	RESULTS HIGHLIGHTS
Mechanism of Vestibular Adaptation of Fish under Microgravity	Dr. A. Takabayashi Fujita Health University Tokyo, Japan	Observed unusual behavior and posture of fish in microgravity. Fish with different vestibular functions on the ground behaved differently in microgravity. The fish visual system did not provide cues to stabilize posture.
Early Development of a Gravity-Receptor Organ in Microgravity	Dr. M.L. Wiederhold University of Texas Health Science Center, San Antonio, Texas, United States	Newt eggs developed normally and survived well during flight. After return to Earth, otoconia increased.

AQUATIC ANIMAL EXPERIMENT UNIT (AAEU) (cont.)

INVESTIGATIONS	PRINCIPAL INVESTIGATORS	RESULTS HIGHLIGHTS
Fertilization and Embryonic Development of Japanese Newt in Space	Dr. M. Yamashita Institute for Space and Astronomical Science Kanagawa, Japan	Newt eggs were laid in space. Early development of newts proceeded normally. Space flight caused pathological damage to adult newts' livers, stomachs, and lungs.
Mating Behavior of the Fish (Medaka) and Development of their Eggs in Space	Dr. K. Ijiri University of Tokyo Tokyo, Japan	First time fish mated and laid eggs in space. First offspring (8 fry) of a vertebrate ever born in space. Confirmed microgravity had no genetic, behavioral, or developmental effect on the offspring of fish flown or hatched in space.

BIORACK (BR)

INVESTIGATIONS	PRINCIPAL INVESTIGATORS	RESULTS HIGHLIGHTS
Activation Signals of T Lymphocytes in Microgravity (Adhesion)	Dr. A. Cogoli Swiss Federal Institute of Technology, Zurich, Switzerland	Failure of T cells to proliferate in microgravity can be attributed to the reduction in the expression of IL-2 receptor and not the absence of IL-1. Activation in terms of DNA synthesis and genetic expression of specific cell products (IL-2R; IFN-γ) may be under a different control.

BIORACK (BR)

INVESTIGATIONS	PRINCIPAL INVESTIGATORS	RESULTS HIGHLIGHTS
Movements and Interactions of Lymphocytes in Microgravity (Motion)	Dr. A. Cogoli Swiss Federal Institute of Technology, Zurich, Switzerland	Cell-cell contacts occur in microgravity. Cells are not transferring through the complete cell cycle, resulting in a dramatic decrease in activation.
Effect of Microgravity on Cellular Activation in Lymphocytes: Protein Kinase C Signal Transduction (Phorbol) and Cytokine Synthesis (Cytokine)	Dr. D.A. Schmitt and Mr. J.P. Hatton, Laboratory of Immunology, CHU Rangueil, Toulouse, France	Results indicated a moderate suppression in the concentration of cells associated with cytokines in microgravity. Distribution of protein kinase C inside the cell varies in proportion to gravity level. Differences in basal levels of cytokine synthesis may mean even unstimulated cells may be sensitive to microgravity.
Cell Microenvironment and Membrane Signal Transduction in Microgravity (Signal)	Dr. P. Bouloc University of Paris-Sud Orsay, France	Observed possible reduced growth lag period of a non-motile culture of *E. coli* in microgravity. Efficient induction of one two-component system regulating the osmoregulation in *E. coli* in microgravity.

BIORACK (BR)

INVESTIGATIONS	PRINCIPAL INVESTIGATORS	RESULTS HIGHLIGHTS
Effect of Stirring and Mixing in a Bioreactor Experiment in Microgravity (Bioreactor)	Dr. A. Cogoli Space Biology Group of ETH Zurich, Switzerland	Bioreactor performed well. Higher percentage of randomly distributed bud scars in flight cells (17%) than in ground control cells (5%). Found no remarkable differences in the cell cycle, ultrastructure, cell proliferation and volume, ethanol production, and glucose consumption.
Biological Investigations of Animal Multi-Cell Aggregates Reconstituted under Microgravity Conditions (Aggregates)	Dr. U.A.O. Heinlein Heinrich-Heine-Universität Düsseldorf, Germany	Results indicate the initial adhesion among cells is not disturbed in microgravity. Formation of interconnecting cables (a prerequisite to cell migration between aggregates under normal gravity) did not occur in the flight samples.
Replication of Cell Growth and Differentiation by Microgravity: Retinoic Acid-Induced Cell Differentiation (Mouse)	Dr. S.W. de Laat Netherlands Institute for Developmental Biology Utrecht, The Netherlands	The RA-induced reporter gene expression is impaired by microgravity. Need more experiments to demonstrate the effect of microgravity on DNA synthesis.

BIORACK (BR)

INVESTIGATIONS	PRINCIPAL INVESTIGATORS	RESULTS HIGHLIGHTS
The Sea Urchin Larva, A Suitable Model for Biomineralization Studies in Space (Urchin)	Dr. H.-J. Marthy CNRS, Observatoire Océanologique Banyuls sur mer, France	Basic biomineralization occurred in microgravity, and no pronounced demineralization was observed. Developmental processes such as the proliferation and specific differentiation of the skeletogenic cells occurred; however the process of their positioning appears to be more sensitive to environmental factors, possibly including microgravity.
The Effect of Microgravity and Varying Periods of 1-g Exposure on Growth, Mineralization, and Resorption in Isolated Fetal Mouse Long Bones (Bones)	Dr. J.P. Veldhuijzen Amsterdam Academic Center for Dentistry Amsterdam, The Netherlands	Confirmed IML-1 results: microgravity did not affect overall growth but did decrease mineralization. A decrease in mineralization was not found in long bones placed for 6 h daily on the 1-g centrifuge. Initial effects were found after 3 h daily 1-g exposure.
Investigation of the Mechanics Involved in the Effects of Space Microgravity on *Drosophila* Development, Behavior, and Aging (Drosophila)	Dr. R. Marco Universidad Autónoma de Madrid, Madrid, Spain	Confirmed accelerated aging of male fruit flies exposed to microgravity. Linked increased aging to increased activity and mitochondrial processes. Verified normal development of fruit flies (from single cells to adulthood) in space.

BIORACK (BR)

INVESTIGATIONS	PRINCIPAL INVESTIGATORS	RESULTS HIGHLIGHTS
The Role of Gravity in the Establishment of the Dorso-Ventral Axis in the Amphibian Embryo (Eggs)	Dr. G.A. Ubbels Hubrecht Laboratory Utrecht, The Netherlands	Found rate of cell divisions unchanged in actual and simulated microgravity. Microgravity perturbs blastocoel formation.
Regulation of Cell Differentiation by Gravity in the Lentil Root (Lentil)	Dr. G. Perbal and Dr. D. Driss-Ecole Pierre and Marie Curie University, Paris, France	Gravity did not affect the elongation of roots growing in the vertical position. Cell cycle in the meristem is regulated by gravity.
Root Orientation, Growth Regulation, Adaptation, and Agravitropic Behavior of Genetically Transformed Roots (Transform)	Dr. T.-H. Iversen Norwegian University of Science and Technology, Dragvoll, Norway	Similar distribution of amyloplasts in WT and transgenic root cap cells both in orbit and on the ground. Total growth was higher for roots grown on the ground than for roots grown in space. Space-grown transgenic root tips were kept alive under sterile conditions. The roots have been propagated *in vitro* since August 1994 and are undergoing further analysis

BIORACK (BR)

INVESTIGATIONS	PRINCIPAL INVESTIGATORS	RESULTS HIGHLIGHTS
Plant Growth and Random Walk (Random)	Dr. A. Johnsson University of Trondheim Dragvoll, Norway	Average bending direction of the plants stayed constant equal to zero despite the spontaneous movements performed in weightlessness. The average squared deviation of the root movements increased linerly with time during the first period of growth, a pattern characteristic for random processes. Growth of roots in weightlessness was smaller than on the ground.
Dosimetric Mapping in Biorack (Dosimetry)	Dr. G. Reitz DLR Institute for Aerospace Medicine, Cologne, Germany	Total doses differ up to a factor of 1.5 and heavy ion fluxes by more than a factor of 6 in the different locations. The mission equivalent dose for the astronauts was calculated from the measurement to be 3.8 mSv.
The Influence of Microgravity on Repair of Radiation-Induced DNA Damage in Bacteria and Human Fibroblasts (Repair & Kinetics)	Dr. G. Horneck DLR, Institute for Aerospace Medicine, Cologne, Germany	Both prokaryotes and human cells had normal repair pathways in microgravity. The synergistic effects of microgravity and radiation are not a result of a disturbance of intracellular repair. Results indicate that repair processes function normally and are not disturbed by microgravity conditions.

SLOW ROTATING CENTRIFUGE MICROSCOPE: LIFE SCIENCES EXPERIMENTS

INVESTIGATIONS	PRINCIPAL INVESTIGATORS	RESULTS HIGHLIGHTS
Gravisensitivity and Gravi(Geo)taxis of the Slime Mold *Physarum polycephalum* (Slime mold)	Dr. I. Block, DLR, Institute for Aerospace Medicine, Cologne, Germany	The lowest acceleration capable of inducing a response is 0.1-g. The gravity response is based on direct effects of gravity. The low acceleration-sensitivity threshold favors rather large and dense cell organelles as gravi-receptor candidates in *Physarum.*
Influence of Accelerations on the Spatial Orientation of *Loxodes* and *Paramecium* (Loxodes)	Dr. R. Hemmersbach DLR, Institute for Space Medicine, Cologne, Germany	The threshold for gravitaxis of *Paramecium* was >0.16-g and 0.3-g, and the unicellular organism did not adapt to weightlessness. *Loxodes* showed no gravi-responses to increasing accelerations in space but did demonstrate gravitaxis upon return to Earth. Prolonged cultivation in space did not change the size and content of the barium sulfate of the statocyst organelles of *Loxodes.*
Gravitaxis in the Flagellate *Euglena gracilis* is Controlled by an Active Gravireceptor (Euglena)	D.-P. Häder Friedrich-Alexander-University Erlangen, Germany	Random orientation of flagellates at accelerations at and below 0.08-g confirmed prior results. Threshold for orientation $\leq$ 0.16-g Observed no adaptation during the extended duration of the mission.

SLOW ROTATING CENTRIFUGE MICROSCOPE: LIFE SCIENCES EXPERIMENTS

INVESTIGATIONS	PRINCIPAL INVESTIGATORS	RESULTS HIGHLIGHTS
Effects of Micro-g on *Aurelia* Ephyra Behavior and Development (Jellyfish)	Dr. D.B. Spangenberg Eastern Virginia Medical School Norfolk, Virginia, United States	Confirmed SLS-1 findings that ephyrae form in microgravity and can pulse and swim. Ephyrae that developed in space had more arm abnormalities.
Chara rhizoids: Studies during a Long Period of Microgravity (Chara)	Dr. A. Sievers, Dr. M. Braun, and Dr. B. Buchen, University of Bonn, Bonn, Germany	Demonstrated tip-growing single cells develop normally in microgravity. Growing rhizoids maintained their structural polarity and grew straight. Distribution of statoliths was similar to that found in sounding rocket experiments.
Graviresponse of Cress Roots under Varying Gravitational Forces below Earth Acceleration (1-g) (Cress)	Dr. D. Volkmann University of Bonn Bonn, Germany	Roots cultivated under microgravity had a higher sensitivity than those grown on the 1-g centrifuge. These results and those from prior missions suggest the nonvalidity of the reciprocity rule. Transformation of the gravi-stimulus occurs near the statoliths.

THERMOELECTRIC INCUBATOR (TEI) AND CELL CULTURE KITS (CCK)

INVESTIGATIONS	PRINCIPAL INVESTIGATORS	RESULTS HIGHLIGHTS
Gravity and the Stability of the Differentiated State of Plant Somatic Embryos	Dr. A.D. Krikorian State University of New York at Stony Brook, Stony Brook, New York, United States	Flight samples had chromosomal damage whereas ground controls did not. Epidermal development of flight samples was poorer than ground controls. Perturbation is real and not an artifact of reentry or postflight adaptation.
Microgravity Effects on the Growth and Function of Rat Normal Osteoblasts	Dr. Y. Kumei Tokyo Medical and Dental University, Tokyo, Japan	Microgravity affected the gene expression of osteoblast functions important for bone formation and metabolism. Observed cellular and molecular effects of bone demineralization. Obtained data to help prevent osteoporosis on Earth and in space.
Differentiation of *Dictyostelium discoideum* in Space	Dr. T. Ohnishi and Dr. K. Okaichi, Nara Medical University, Nara, Japan	Microgravity and cosmic radiation did not affect the NC4 spores. Cosmic radiation may have prevented germination of the gs13 spores.

EXTENDED DURATION ORBITER MEDICAL PROJECT (EDOMP)

INVESTIGATIONS	PRINCIPAL INVESTIGATORS	RESULTS HIGHLIGHTS
Lower Body Negative Pressure (LBNP): Countermeasure Investigation for Reducing Postflight Orthostatic Intolerance	Dr. J. B. Charles Medical Sciences Division NASA Johnson Space Center Houston Texas	Orthostatic tolerance during LBNP was reduced in microgravity. The LBNP countermeasure (soak) lowered the heart rate response during the stress of reentry.
Airborne Microbiological Contamination	Dr. D.L. Pierson Life Sciences Research Laboratories, NASA Johnson Space Center, Houston, Texas, United States	Airborne bacteria and fungi were within safe levels during the entire flight. Bacterial and fungal species recovered from the air were typical of those recovered from humans and outside environment. The air sampler designated for the Crew Health Care System of the International Space Station performed well within specifications.

SPINAL CHANGES IN MICROGRAVITY (SCM)

INVESTIGATIONS	PRINCIPAL INVESTIGATORS	RESULTS HIGHLIGHTS
Spinal Changes in Microgravity	Dr. J. R. Ledsome University of British Columbia Vancouver, Canada	Subjects' heights increased in microgravity. First direct evidence of an increase in intervertebral distance. Evidence of a change in autonomic control.

PERFORMANCE ASSESSMENT WORKSTATION (PAWS)

INVESTIGATIONS	PRINCIPAL INVESTIGATORS	RESULTS HIGHLIGHTS
Microgravity Effects on Standardized Cognitive Performance Measures	Dr. S.G. Schiflett United States Air Force Armstrong Laboratory Brooks Air Force Base, Texas, United States	Reliably measured cognitive and psychomotor performance in microgravity. Performance decrements were related to fatigue. Databases on human performance in space need expansion.

REAL-TIME RADIATION MONITORING DEVICE (RRMD)

INVESTIGATIONS	PRINCIPAL INVESTIGATORS	RESULTS HIGHLIGHTS
Measurement of LET Distribution and Dose Equivalent on Board the Space Shuttle STS-65 (IML-2) (RRMD, Part 1)	Dr. T. Doke Waseda University Tokyo, Japan	First real-time measurements of radiation dose and LET distribution. Attributed most radiation in the IML-2 orbit to galactic cosmic-ray particles. Good agreement between active and passive detector data.
Effect of Microgravity on DNA Repair of *Deinococcus Radiodurans* (RRMD, Part 2)		Results suggests that micro-gravity enhanced the DNA repair system. First use of radiation-resistant bacteria to examine relationship between microgravity and radiation.

REPORT DOCUMENTATION PAGE

Form Approved
OMB No. 0704-0188

Public reporting burden for this collecton of information is estimated to average 1 hour per response, including the time for reviewing instructions, searching existing data sources, gathering and maintaining the data needed, and completing and reviewing the collection of information. Send comments regarding this burden estimate or any other aspect of this collection of information, including suggestions for reducing this burden, to Washington Headquarters Services, Directorate for Information Operations and Reports, 1215 Jefferson Davis Highway, Suite 1204, Arlington, Va 22202-4302, and to the Office of Management and Budget, Paperwork Reduction Project (0704-0188), Washington, DC 20503.

1. AGENCY USE ONLY (Leave Blank)	2. REPORT DATE	3. REPORT TYPE AND DATES COVERED
	July 1997	Reference Publication

4. TITLE AND SUBTITLE

Second International Microgravity Laboratory (IML-2) Final Report

5. FUNDING NUMBERS

6. AUTHOR(S)

* Dr. Robert S. Snyder, Compiler

7. PERFORMING ORGANIZATION NAME(S) AND ADDRESS(ES)

George C. Marshall Space Flight Center
Marshall Space Flight Center, Alabama 35812

8. PERFORMING ORGANIZATON REPORT NUMBERS

M-835

9. SPONSORING/MONITORING AGENCY NAME(S) AND ADDRESS(ES)

National Aeronautics and Space Administration
Washington, DC 20546-0001

10. SPONSORING/MONITORING AGENCY REPORT NUMBER

NASA RP-1405

11. SUPPLEMENTARY NOTES

Prepared by Space Sciences Laboratory, Science and Engineering Directorate
* Each experiment description was written by the principal investigator cited at the beginning of the description

12a. DISTRIBUTION/AVAILABILITY STATEMENT

Unclassified-Unlimited
Subject Category 99

12b. DISTRIBUTION CODE

13. ABSTRACT *(Maximum 200 words)*

This report highlights the scientific and engineering accomplishments achieved during the 14-day Second International Microgravity Laboratory (IML-2) mission. The mission, managed by the National Aeronautics and Space Administration's Marshall Space Flight Center in Huntsville, Alabama, laid the groundwork for broader international partnerships and scientific alliances. Five other space agencies joined NASA on the mission: the Canadian Space Agency (CSA), the European Space Agency (ESA), the French Space Agency (CNES), the German Space Agency (DARA), and the National Space Development Agency of Japan (NASDA).

For the mission, microgravity and life sciences investigations were completed inside Spacelab by a crew working around the clock. The report foreword and introduction describe the mission and the facilities used for IML-2. By the end of the mission, hundreds of primary and secondary experiments were completed. With the help of the principal investigators, most of the primary investigations and some of the co-investigations are described in this document. The lead report authors are cited at the beginning of each experiment description. The remainder of the description includes the experiment objectives, flight activities, postflight analysis, conclusions, illustrations, and references for further research. The major scientific accomplishments of each investigation are highlighted.

14. SUBJECT TERMS Second International Microgravity Laboratory, IML-2, materials science, microgravity science and applications, life sciences, fluid science, applications, life sciences, fluid science, microgravity

15. NUMBER OF PAGES
226

16. PRICE CODE
A11

17. SECURITY CLASSIFICATION	18. SECURITY CLASSIFICATION OF THIS PAGE	19. SECURITY CLASSIFICATION OF ABSTRACT	20. LIMITATION OF ABSTRACT
Unclassified	Unclassified	Unclassified	Unlimited